IDENTIFYING SOX2 INTERACTION PARTNERS IN THE DEVELOPING LUNG

Kim Albertina Adriana Schilders

Colophon
ISBN: 978-94-91602-58-0

This thesis was written within the department of Pediatric Surgery and Cell Biology at the Erasmus University Medical Center, Rotterdam.

The research described in this thesis was financially supported by the Sophia foundation for scientific research (SSWO), project number 641.

Cover design and layout by Kim Schilders.

Printed by Print Service Ede.

IDENTIFYING SOX2 INTERACTION PARTNERS IN THE DEVELOPING LUNG

Identificatie van Sox2 interactie partners tijdens de longontwikkeling

Proefschrift

ter verkrijging van de graad van doctor aan de
Erasmus Universiteit Rotterdam
op gezag van de
rector magnificus
Prof.dr. H.A.P. Pols
en volgens besluit van het College voor Promoties.

De openbare verdediging zal plaatsvinden op
woensdag 15 juni 2016 om 09.30 uur

door

Kim Albertina Adriana Schilders

geboren te Hoogeloon, Hapert en Casteren

Erasmus University Rotterdam

Erasmus

Promotiecommissie:

Promotor:	**Prof.dr. D. Tibboel**
Overige leden:	**Dr. J.E.M.M. de Klein** **Dr. R.A. Poot** **Dr. M.N. Hylkema**
Copromotor:	**Dr. R.J. Rottier**

Voor ons kleintje

Contents

List of abbreviations

ACD/MPV	Alveolar capillary dysplasia with misalignment of pulmonary veins
AEG syndrome	Anophthalmia-esophageal-genital syndrome
ALI	Air Liquid Interfase
AT-I	Alveolar type I cell
AT-II	Alveolar type II cell
BADJ	Broncho-alveolar duct junction
BASC	Bronchoalveolar stem cells
BLPC	Basal luminal precursor cell
BMP	Bone morphogenetic protein
BPD	Bronchopulmonary dysplasia
BSC	Basal stem cell
CCAM	Congential cystic adenomatoid malformation
CDH	Congenital diaphragmatic hernia
CHAOS	Congenital high airway obstruction syndrome
Charge	Coloboma, heart defects, atresia of the choanac, retarded growth, genital hypoplasia and ear abnormalities
Chd4	Chromodomain-Helicase-DNA-Binding Protein 4
Chd7	Chromodomain-Helicase-DNA-Binding Protein 7
ChIP	Chromatin immunoprecipitation
CLE	Congentital lobar emphysema
COPD	Chronic obstructive pulmonary disease
CPAM	Congenital pulmonary and airway malformations
Cux1	Cut-like homeobox 1
DASC	Distal alveolar stem cell
E	Embryonic day
EA/TEF	Esophageal atresia/tracheoesophageal fistula
ECFCs	Endothelial colony-forming cells
ECM	Extracellular matrix
ELS	Extralobular sequestrations
ESC	Embryonic stem cell
Fgf	Fibroblast growht factor
Fox	Forkhead box
Grhl2	Grainyhead-like 2
hiPSC	Human induced pluripotent stem cell
HMG	High Mobility Group
ICM	Inner cell mass
iPSC	Induced pluripotent stem cell
Krt	Cytokeratin
LNEP	Lineage negative epithelial precursor
MALDI-ToF MS	Matrix Assisted Laser Desorption/Ionization - Time of Flight Mass Spectrometry
MSC	Mesenchymal stem/stromal cell
NSC	Neural stem cell
NEB	Neuroendocrine body
NLS	Nuclear localization signals
NuRD complex	Nucleosome remodeling and deacetylase complex
RA	Retinoic acid
rtTA	Reverse tetracycline transactivator gene
Sca1	Stem cell antigen 1
Scgb1a1	Secretoglobin family 1a member 1
Sftpc	Surfactant protein C
Shh	Sonic Hedgehog
SO_2	Sulfur dioxide
Sox2	Sry related HMG box gene 2
Spc	Surfactant protein C
Sry	Seks determining region of Y chromosome
TBSC	Tracheal basal cell
Tcf3	Transcription factor 3
TEV	Tobacco Etch Virus
Tgfβ	Transforming growth factor β
Wdr5	WD repeat domain 5
Wk	Week
Xpo4	Exportin 4

Chapter 1.

The role of SOX2 in foregut development in relation to congenital abnormalities

Kim Schilders, Joshua K. Ochieng, Cornelis P van de Ven,

Cristina Gontan, Dick Tibboel, Robbert J. Rottier

Adapted from World Journal of Medical Genetics 2014; 4(4) : 94 - 104

1.1 Sox family

1.1.1 General

Transcription factors play an important role in the regulation of gene expression, thereby contributing to cell fate and proliferation during development and adult life. One of the families of transcription factors that are involved in embryonic development include members of the SRY-related High-Mobility Group (HMG) transcription factors. The Sex-determining region on the Y chromosome (*Sry*) gene was the first identified member of the SOX family of transcription factors (1, 2). SOX family members are highly conserved and identified in all animal species. They were originally identified by homology, as they contain an HMG box closely related to that of the *Sry* gene (3). Therefore, Sry gave the *SOX* gene family its name; Sry-related HMG box, hence "SOX", followed by a number corresponding to the order of discovery (1). SOX proteins have properties of both classical transcription factors and architectural proteins (4). They function as classical transcription factors, either activa ting or repressing specific target genes through interaction with different partner proteins.

All SOX factors bind DNA via their HMG domain and recognize the same historical consensus motif 5'-(A/T)(A/T)CAA(A/T)G-3' (5). With currently new developed techniques like chromatin immunoprecipitation - sequencing, more binding sites are getting identified. The transcriptional function of SOX proteins dependent on the cell type and the promoter context, and they often have functional redundancy among each other (4). In contrast to other transcription factors which mainly target the major groove, SOX proteins interact with the minor groove of the DNA helix and, as a consequence, induce a sharp bend in the DNA (4). The DNA bending capacity of SOX proteins can be functionally important for several reasons. The local changes in chromatin structure induced by SOX proteins may bring different regulatory regions in close proximity, which facilitates the recruitment of higher-order architectural factors (like polycomb or trithorax protein groups), the formation of enhanceosomes, *i.e*., functionally active complexes of transcription factors on different gene enhancer sequences, or the interaction of distant enhancer nucleoprotein complexes with the basal transcription machinery (6-9). Bending of DNA by SOX proteins could also act in a negative way by preventing or disrupting the binding of other factors to adjacent sites in the major groove (6).

SOX genes are expressed in diverse and dynamic patterns during embryogenesis. Throughout development members of the SOX family are expressed in almost every tissue of the embryo, and also in a number of adult tissues (10, 11). The expression of a specific SOX transcription factor is not necessarily restricted to a particular cell type or lineage and their expression patterns during development appear to correlate with early cell fate decisions. For example, Sry is expressed in the undifferentiated male gonad and is quickly down regulated once the decision is made to initiate male development (12-14). Mutations in several of the *SOX* genes have been implicated in the pathogenesis of human congenital anomalies and syndromes (Table 1).

1.1.2 SOX2

SOX2 plays crucial roles during different stages of vertebrate embryonic development and its expression is temporally and spatially regulated (15). Zygotic *Sox2* expression starts at the morula-stage of embryo development and becomes restricted to the cells of the inner

cell mass (ICM) of the blastocyst. Expression continues in the epiblast, the tissue that will give rise to the embryo and germ cells (16). During early gastrulation, SOX2 expression in the embryo is restricted to the anterior ectoderm, which gives rise to neuroectoderm and anterior surface ectoderm, while the extraembryonic expression becomes confined to the chorion (17, 18). At later stages of embryonic development, SOX2 is expressed in the brain, neural tube, eyes, sensory placodes, branchial arches, gut endoderm, and the germ cells (16, 19-24). When the branchial arches develop, SOX2 continues to be expressed in the primitive foregut endoderm. Postnatal, SOX2 is present in the epithelium of foregut-derived organs, including the tongue, esophagus, trachea, proximal lung and stomach (16, 19, 25-28).

Table 1. The role of *SOX* genes in diseases.

SOX gene	Chromosome location	Disease
SOX2	3q26.3-q27	Microphthalmia, syndromic 3 optic nerve hypoplasia, abnormalities of the central nervous system (114), CHARGE-syndrome (62), AEG-syndrome (27), EA/TEF (29), CPAM (25, 58)
SOX3	Xq27.1	Mental retardation,X-linked with isolated growth hormone deficiency, infundibular hypoplasia, hypopituitarism (114)
SOX9	17q23	Campomelic dysplasia with autonomic XY sex reversal (114), Pierre-Robin syndrome (115)
SOX10	22q13.1	Waardenburg-Shah syndrome, Yemenite deaf-blind hypopigmentation syndrome, peripheral demyelinating neuropathy, central dysmyelinating leukodystrophy, Waardenburgh syndrome, Hirschprung's disease (114)
SOX11	2p25	Unknown
SOX17	8q11.23	Unknown
SOX18	20q13.33	Hypotrichosis-lymphedema-telangiectasia syndrome (114)

The lack of Sox2 expression in mice results in early embryonic lethality (16). *Sox2* null mutant mouse embryos implant but fail to develop an egg cylinder or epiblast, and die before gastrulation because Sox2 is required in the ICM. This lack of Sox2 seems to become critical after 7.5 days postcoitum, suggesting a role for maternal Sox2 during early development (16). The use of two *SOX2* hypomorphic mutants showed a dose-dependent role of SOX2 in the development of the retina and the differentiation of the foregut endoderm (23, 29). Heterozygous mutations in *SOX2* have been associated in human with severe structural malformations of the eye, bilateral anophthalmia (absent eye) and microphthalmia (small eye), and anophthalmia-esophageal-genital (AEG) syndrome (27). In infants with AEG syndrome, the esophagus and trachea fail to separate normally and the trachea is connected to the stomach by an abnormal distal esophagus (27, 30, 31). These symptoms underwrite the developmental functions for SOX2, as described for mice hypomorphic for Sox2.

1.2 Lung development

1.2.1 Anatomy of the respiratory system

The lung is a complex organ consisting of the gas transporting system in close association with the blood circulatory system. The lung has a clear proximal to distal orientation, which is best exemplified by the gas transport system. This can be divided into a conducting part where inspired air is warmed, moistened and filtered, and a respiratory part where gas exchange with blood occurs. The conducting zone is made up by the nasal cavities, pharynx, larynx, bronchi and (terminal) bronchioles. The respiratory zone contains the respiratory bronchioles, alveolar ducts and alveolar saccule (32). The alveoli are surrounded by a network of capillaries to facilitate gas exchange (fig. 1).

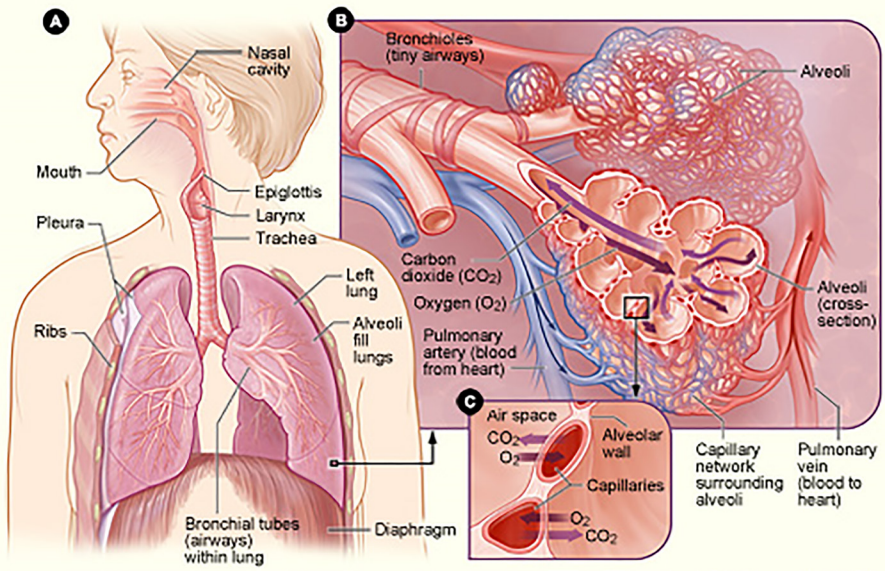

Figure 1. Respiratory system. (A) Location of the respiratory system in the human body. (B) Overview of the airways, alveoli and capillaries. (C) Gas exchange between capillaries and alveoli. From http://www.nhlbi.nih.gov/

Looking at the proximal-distal axis of the gas conducting regions of the lung, different subsets of epithelial cells can be found. The trachea and main stem bronchi are made up by basal cells, club cells, ciliated cells and a few scattered neuroendocrine cells. The intralobular airways consist of club cells, ciliated cells and neuroendocrine cells and in the alveoli, alveolar type I (AT-I) and alveolar type II (AT-II) cells are found (fig. 2) (33).

1.2.2 Embryonic lung development

Gastrulation is the process that adds complexity to the developing organism and results in a triploblastic animal by formation of the three germ layers, ectoderm, mesoderm and endoderm. At embryonic day 6 (E6.0) in mice (comparative to 3 wk in human), the sheet of endodermal cells starts to invaginate ventrally at the anterior and posterior intestinal portals, which subsequently migrate towards each other to form the primitive gut from the future mouth to anus (34). At E9.0, the notochord delaminates from the dorsal endoderm

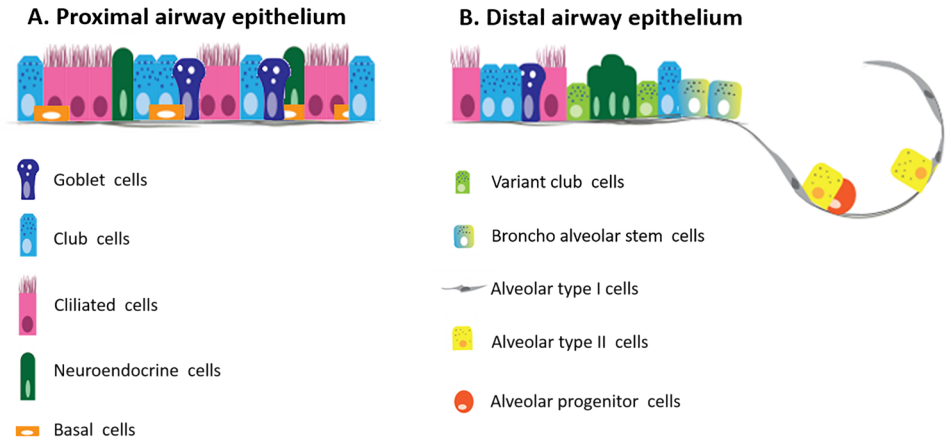

Figure 2. Epithelial cells in the lung. (A) The proximal airways are lined by a pseudostratified epithelium consisting of secretory cells (goblet and club cells), ciliated cells, neuroendocrine cells and basal cells. Goblet cells are abundant in the human epithelium, but are rare in mice. (B) The small airways lack basal cells and consist of cuboidal epithelium, containing secretory and ciliated cells, as well as clusters of neuroendocrine cells. The cuboidal epithelium passes into a broncho-alveolar duct junction which is the niche of broncho-alveolar stem cells. The alveolar epithelium consists of alveolar type I, type II cells and alveolar progenitor cells. (Modified from Schilders et al. Respiratory Research 2016)

and will eventually be situated between the primitive gut and the neural tube. The notochord serves in this phase of development as a strong signaling center, secreting morphogens like Sonic hedgehog (Shh) to pattern the endoderm as well as the neural tube (35). Another signaling center associated with the early patterning and morphogenesis of the foregut is the heart mesoderm, which secretes morphogens like Fibroblast growth factors (Fgf) 1 and 2. High levels of Fgf signals activate lung specific genes while lower levels of Fgf activate liver specific genes (36). The prospective lung field, the area which will eventually lead to the emergence of the primitive lung bud, is subsequently patterned by retinoic acid (RA) signaling. The RA receptor alpha (RARα) is required to maintain RA signaling and to assist the effects of RARβ, which induces the expression of Fgf10. RA signaling integrates the Wnt and transforming growth factor beta (Tgfβ) pathways by inhibiting the expression of the Wnt antagonist Dickkopf-1 and Tgfβ (37). Overall, the foregut becomes gradually regionalized as shown initially by the various dorsal-ventral gradients of morphogens and the subsequent spatially restricted expression of transcription factors. This pattern of expression is essential for proper development of the trachea, esophagus and lungs, and disturbances in these patterns result in various trachea-lung defects.

The lung primordium arises from the ventral foregut as a primary bud, just anterior to the developing stomach around embryonic day 9.5 in mice or week 4 in humans (38, 39). The lung bud splits in two buds, the future left and right bronchus, elongates and the proximal part, the trachea, is separated from the oesophagus, while distally the bronchial tree is formed through a repetitive process called branching morphogenesis (38).

Development of the lung can be divided into five distinct, but overlapping phases based on morphology (fig. 3) (40). During the earliest phase, the embryonic phase, the lung buds are formed from the primitive foregut, the mayor bronchi are formed and the tracheal-esophageal tube is dividing. Several signaling cascades direct the early embryonic morphogenetic events and cell fate decisions including Tgfβ, Bone Morphogenetic Proteins (BMPs), Shh, Wnt, and Fgf families (41, 42). The next phase, the pseudoglandular phase is characterized by the commencement of differentiation of epithelial cells. Also, the bronchial tree and all terminal bronchioles are formed. The pseudoglandular phase is followed by the canalicular phase and the saccular stage (38). During the canalicular phase, the conducting airways are completed and the respiratory portions of the lung as well as the capillary bed are formed, while during the saccular phase the terminal tubes narrow, giving rise to small saccules and the endoderm begins to differentiate into specialized alveolar type I and type II cells (38). The last phase, the alveolar phase, is characterized by the establishment of secondary septa resulting into alveolar formation, which mainly takes places after birth (40, 43). As development of the lung advances, the embryonic endoderm undergoes progressive fate decisions that generate epithelial progenitor cells with increasingly restricted developmental potential over time. During the branching program in lung development, three different branching modes can be distinguished: domain branching which forms the overall scaffold of the lobes, planar bifurcation which is responsible for the formation of the edges of the lobes and orthogonal bifurcation which forms the interior of the lobes. In this process, Sprouty 2 (Spry2) is responsible for initiation of the branching site and the number of branches (44). Formation of the proximal and distal airways occurs in two waves. During the first wave branching morphogenesis takes place, while during the second wave the conducting airways are differentiated (45).

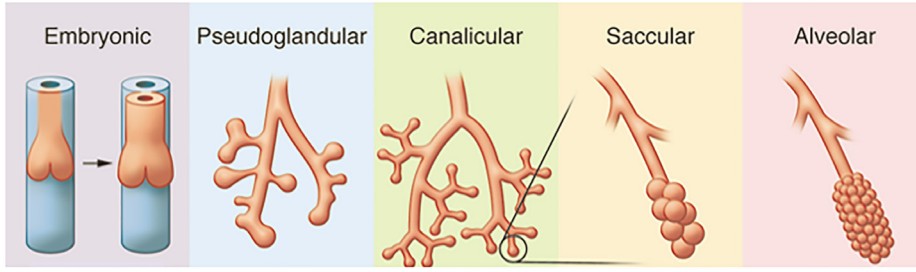

Phases of lung development	Gestational age	
	Human	Mouse
Embryonic phase	Wk3-7	E9-11.5
Pseudoglandular phase	Wk5-17	E11.5-16.6
Canalicular phase	Wk16-25	E16.6-17.4
Saccular phase	Wk24-38	E17.4-PN5
Alveolar phase	Wk36 to maturity	PN5-30

Figure 3. Gestational ages in human and mouse during the five stages of lung development. (Modified from Rackley and Strip, J. Clin. Invest. 2012 (42))

1.2.3 Sox genes and foregut development

To date, four members from the *SOX* gene family are known to be involved in lung organogenesis, *SOX2*, *SOX9*, *SOX11* and *SOX17* (25, 40, 46-50). *SOX9* was found throughout lung morphogenesis as a downstream target gene of Shh and modulated by BMP4 and Noggin. Using epithelial specific gain and loss of function mouse models, Sox9 has been shown to play a crucial role in branching morphogenesis through controlling a balance between proliferation and differentiation (51). In another study, knock out of Sox9 in the mesenchyme demonstrated that it plays a crucial role in differentiation of the lung tracheal epithelium (52). SOX9 is required for formation and patterning of tracheal cartilage by a mechanism mediated by Fgf18 (53, 54). SOX9 promotes proper branching morphogenesis by controlling the balance between proliferation and differentiation and regulating the extracellular matrix and can be used as a marker for the distal epithelium (51). SOX11 has been suggested to be involved in development and plays a key function in tissue remodeling, including the lung (47). Sox11 deficient mice die immediately after birth because of significant lung hypoplasia and other tissue defects (47). SOX17 was shown to be crucial early after gastrulation for the formation of definitive endoderm, which gives rise to the lung, liver, pancreas, stomach, and gastrointestinal tract (55). In the lung, SOX17 is expressed in the endothelial cells of the developing pulmonary vasculature and remains expressed in the pulmonary vascular endothelial cells in the adult lung (56). SOX17 has been shown to impair the expression of Tgfβ1 responsive inhibitors, p15, p21 and p57, while inhibiting Tgfβ1 and Smad3 transcriptional activity (48).

1.2.4 Sox2 in foregut and lung development

Sox2 is expressed throughout the early foregut epithelium, but becomes restricted to the dorsal epithelial cells at embryonic day 9.5, whereas Nkx2.1 is reciprocally expressed in the ventral epithelium (29, 57). Sox2 is expressed in the epithelial cells of the foregut at E9.5. From E11.5 until E14.5, Sox2 is exclusively expressed in the epithelial cells of the non-branching developing airways and it remains expressed in the epithelial cells of the conducting airways after birth. So, Sox2 is exclusively expressed at the non-branching airways (fig. 4).

Previously, it was shown that ectopic expression of Sox2 in epithelial cells of the lung result in abnormal alveolar formation, enlarged airspaces and a decrease in the number of airways, indicating that Sox2 modulates branching morphogenesis. Also, an increased number of neuroepithelial cells and (pre-) basal cells was observed. This indicates that Sox2 is important in cell fate choice and epithelial differentiation (fig. 5) (25). More recently it was shown that Sox2 regulates the emergence of lung basal cells by directly activating the transcription of the basal cell master gene Trp63, and ectopic expression of Sox2 results in the emergence of bronchioalveolar stem cells (25, 58).

The proper dorsal-ventral patterning of SOX2 and Nkx2.1 is critical for foregut morphogenesis. Down-regulation of SOX2 leads to the formation of esophageal atresia/tracheoesophageal fistula (EA/TEF) in SOX2 hypomorphic mutants (29), whereas deletion of Nkx2.1 leads to defects in foregut separation and the formation of EA/TEF associated with high SOX2 expression in the epithelium (29, 59). Similarly, the epithelial cells in the fistula of SOX2 hypomorphic mutants express high levels of Nkx2.1 suggesting that low level of SOX2 is required for Nkx2.1 expression to expand dorsally and reprogram the dorsal

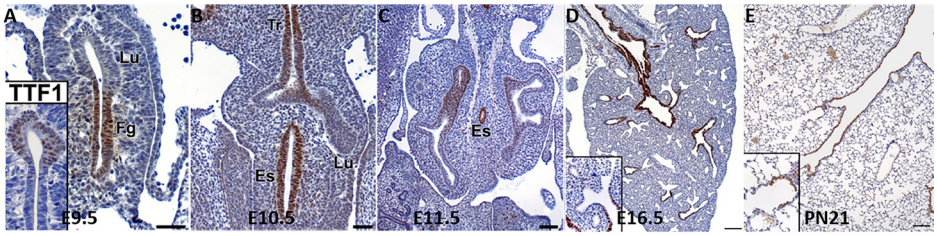

Figure 4. Endogenous Sox2 expression during lung development in mice. (A) At E9.5, Sox2 is expressed in the epithelial cells of the foregut. At E10.5 (B) and 11.5 (C), Sox2 is expressed in the epithelial cells of the on-branching developing airways, and it remains expressed in the epithelial cells of the proximal airways at E16.5 (D) and postnatally (E). (From Gontan et al.; Developmental Biology; 2008 (25))

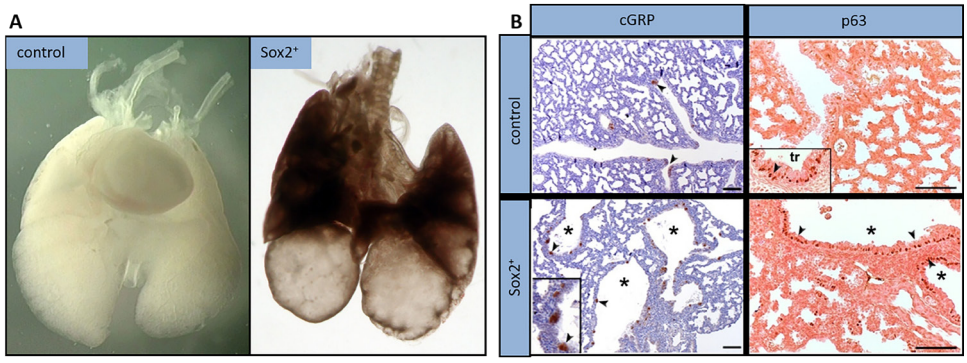

Figure 5. Ectopic expression of Sox2 in lung epithelium. (A) Ectopic Sox2 expression results in abnormal alveolar formation, enlarged airspaces and a decrease in number of airways. (B) In this abnormal epithelium, an increase in neuroepithelial cells (cGRP+) and basal cells (P63+) were detected, compared to control lung. (From Gontan et al.; Developmental Biology; 2008 (25))

epithelium to a respiratory fate (29). These findings suggested that the dorsal-ventral arrangement of SOX2 and Nkx2.1 is essential for foregut separation and the subsequent differentiation of epithelial progenitor cells into esophageal and tracheal epithelium and lung buds (60). Using Chromatin Immuno-Precipitation it was shown that SOX2 directly binds to the promoter region of the *NKX2.1* gene in human embryonic stem cells and this binding resulted in the inhibiton of NKX2.1 transcription (61). Other interesting SOX2 target genes that are involved in early lung morphogenesis are members of the Notch pathway (JAG1) and Shh pathway (GLI2, GLI3) (62). Since the activity of SOX2 depends on its interaction with other proteins, it is of high importance to reveal its interacting partners. Recently some of these partners were identified in embryonic and neural stem cells (62, 63). One of the partners identified is the Chromodomain-Helicase-DNA-Binding Protein7 (CHD7), which has been associated with CHARGE syndrome. CHARGE syndrome has several clinical features in common with AEG, a syndrome which, interestingly, has been linked with the CHD7 partner SOX2. Moreover, SOX2 and CHD7 co-regulate a number of genes, like *MYCN*, *JAG1* and *GLI2/3,* which have been linked to other, related syndromes themselves. Thus, gene networks like this *SOX2-CHD7*-regulated network can be used to better understand the

molecular basis of various human diseases and therefore associating partners in the lung epithelium could help us to reveal the mechanisms underlying lung-related abnormalities (62).

FGF SIGNALING

With *in vitro* organ cultures it was demonstrated that Fgf10 signaling inhibits Sox2 expression in the mouse foregut (29). Mesenchymal expression of Fgf10 around the distal ends of the lung epithelium functions as a chemoattractant by binding to the epithelial expressed Fgf receptor 2β (Fgfr2β) leading to branching and outgrowth of the epithelium (64, 65). Fgf10-null and Fgfr2β-null mouse mutants show high similarity, suggesting that Fgf10 could be a ligand of Fgfr2β (36, 66). Fgf10 knockout mice developed normal trachea, but completely lacked lung structures, whereas targeted deletion of Fgfr2β prevented branching, causing the trachea to terminate as a blind-ended sac (66-68). Conditional gene inactivation studies further demonstrate that both Fgf10 and Fgfr2β are required for a normal branching program and proper proximal-distal patterning of the lung (69). Recently, it was shown that ubiquitous overexpression of Fgf10 throughout the lung could rescue lung agenesis in Fgf10 knockout mice, suggesting that precise localization of Fgf10 expression is not required for lung branching morphogenesis (70). Rather, Fgf10 signaling prevents cells from expressing Sox2 by the activation of β-catenin. As the lung bud grows, the cells become more distant from the Fgf10 source and start to adopt a more proximal cell fate expressing Sox2. When Sox2 is ectopically expressed in the distal epithelial cells of the developing airways, these cells are no longer responsive to Fgf10 and differentiate into proximal cells, which results in reduced branching and formation of cyst-like structures (25, 58).

WNT SIGNALING

At embryonic day 9.5, Wnt signaling is active in the ventral side of the unseparated foregut tube, where the Wnt ligands Wnt2 and Wnt2b are highly expressed (57, 71). Wnt2 and Wnt2b are secreted by mesenchymal cells of the ventral foregut and signal through the canonical β-catenin pathway to specify lung progenitors in the foregut endoderm (57, 71). Conditional inactivation of β-catenin in the foregut endoderm results in the absence of both trachea and lung, whereas expression of a constitutively active β-catenin mutant results in the expansion of the earliest respiratory marker, Nkx2.1, and a loss of the SOX2 positive domain (57). Later in development, Wnt/β-catenin signaling is required for proper proximal-distal patterning of the lung (72). Wnt7b is expressed in the endoderm of the early foregut and its deletion does not disrupt foregut separation, but results in irregular lung branching morphogenesis and vasculature development (72). Mesenchymal Wnt2 and epithelial Wnt7b cooperate with Pdgf signaling to promote mesenchymal differentiation (73).

Receptor tyrosine kinases (RTKs) are able to activate Wnt/β-catenin through the Erk/MAPK mediated phosphorylation of the Wnt co-receptor Lrp6 on Ser1490 and Thr1572, leading to an increased cellular response to Wnt. Moreover, RTKs directly phosphorylate β-catenin on the Tyr142 residue, which causes its release from membrane bound cadherin complexes (74). In turn, in the absence β -catenin, ERK1/2 activity is drastically reduced (75). This regulation of distal epithelial progenitors by β-catenin suggests the progressive signaling cascade where Fgf10 regulates branching morphogenesis *via* Wnt signaling. When

β-catenin is deleted prior to E14.5 from the epithelial cells of the developing mouse lung, the lung mainly contains proximal epithelial cells, suggesting that by β-catenin is required for the formation of the distal airways by preventing cells to differentiate into proximal cells (76). Epithelial specific expression of Wntless, a cargo receptor protein important for directing Wnt ligands, has recently been shown to be important for lung differentiation and vasculature development probably by modulating the secretion of Wnt ligands (77).

Respiratory endodermal specific expression of a constitutive active β-catenin isoform showed that canonical Wnt signaling is not essential for the development of alveolar epithelium (76, 78). However, the formation of proximal epithelium was impaired, because ectopic Wnt signaling induced the expression of Tcf1 and Lef1 at the expense of SOX2 and Trp63 (76, 78). Also, when β-catenin is activated, there is ectopic differentiation of AT-II cells in the upper airways, air space enlargement and goblet cell hyperplasia (76). On the other hand, conditional deletion of β-catenin in respiratory epithelium resulted in the loss of alveolar structures. Selective loss of bronchiolar lineages with continued proliferation may result in cystic lesions of the lung resembling an anomaly known in humans as congenital pulmonary and airway malformations (CPAM) (76).

Ectopic expression of Wnt5a in the respiratory epithelium resulted in increased Fgf10 expression and a reduction in epithelial Shh expression (79). The precise dose and timing of Fgf and canonical Wnt signaling lead to the induction of Shh expression in the respiratory epithelium (36, 71). The paracrine effect of Shh on the surrounding mesenchyme results in the Foxf1 and Gli1/Gli3 mediated expression of BMP4.

BMP SIGNALING

BMP signaling plays prominent roles in foregut separation and lung development, however the molecular mechanisms controlling temporal-spatial BMP signaling dynamics in foregut organogenesis are poorly understood (80). In the unseparated foregut tube, BMP4 is expressed in the ventral mesenchyme, while BMP7 and the BMP antagonist Noggin are enriched in the dorsal endoderm (81). Ablation of Noggin resulted in increased BMP signaling in the foregut and the formation of EA/TEF (82). These embryos showed abnormal delamination of the notochord from the early definite endoderm epithelial sheet, resulting in epithelial cells of endodermal origin being present in the notochord (82). Subsequent deletion of either BMP4 or BMP7 in these Noggin null mice rescued the separation defects (81, 82). Recently, it was shown that Noggin is required to attenuate BMP signaling in order to allow the notochord to delaminate form the dorsal foregut endoderm (83). Tissue specific ablation of BMP4 in the early foregut endoderm resulted in tracheal agenesis accompanied by reduced cellular proliferation in the epithelial and mesenchymal compartments. However, the trachea does not separate from the foregut and Nkx2.1 expression is conserved in the ventral endodermal epithelium, suggesting that BMP4-mediated signaling is essential for separation but not for the initial specification of the tracheal epithelium (84). Similarly, conditional inactivation of BMPr1α and BMPr1β in the foregut leads to tracheal agenesis, a decrease of Nkx2.1 expression and a ventral expansion of SOX2 and Trp63 expression (85). Subsequent activation of Wnt signaling did not promote respiratory differentiation. Deletion of SOX2 in the BMPr1α/β deficient mouse rescued the foregut separation defect, showing that SOX2 is downstream of BMP signaling (85). Ectopic expression of Sox2 in the distal lung buds showed that Fgf-Erk signaling was

abrogated at the expense of BMP-Smad signaling (25).

1.3 Relationship between Sox2 and congenital defects of the foregut

Congenital malformations of the lung constitute a spectrum of lesions that originate during the embryonic period. Incidences of congenital defects of the foregut are in the range of 1:11.000-35.000 pregnancies (World Health Organization). Patients present a broad range of clinical manifestations ranging from intra uterine death to significant illnesses at birth with a variable severity of respiratory symptoms, and later in life distress and repeated chest infections. However a number may remain asymptomatic for long periods and significantly regress in the course of pregnancy, although they displayed impressive malformations at repeated prenatal ultrasound or magnetic resonance imaging. Congenital defects of the foregut occur either in isolated cases or as part of a complex syndrome (86). The causes of most of these malformations as well as their molecular genetic background are still unknown. Different types of congenital lung malformations can be distinguished, which will be briefly discussed.

CPAM

CPAM constitute a spectrum of lesions that originate during the embryonic period. The prevalence of congenital lung malformations has seemingly increased over the last decade probably due to better antenatal ultrasound screening and is estimated at 1 in 3000 pregnancies (87). Although most newborns with antenatally diagnosed congenital lung malformations are asymptomatic at birth, approximately 10% show respiratory insufficiency. Secondary infections of these lesions occur in approximately 5% of unoperated children.
The different types of congenital pulmonary and airway malformations are classified in bronchopulmonary malformations, pulmonary hyperplasia, congenital lobar overinflation and other cystic lesions (88).

Bronchogenic cyst

A bronchogenic cyst is often a solitary cyst in the mediastinum or in the lung parenchyma filled with fluid. Their structural lining resembles that of the bronchus, cartilage and bronchial-type glands included. Symptoms at birth are mostly due to compression of surrounding structures, especially bronchial structures resulting in hyperinflation of lung parenchyma distal to the obstruction. Symptoms at later age are mainly due to infection. Etiology is probably similar to other duplication cysts as aberrant bud formation from the foregut structures. The molecular biology has not been studied so far.

Bronchial atresia

Bronchial atresia, mostly asymptomatic often results in overinflation of a lobe, segment or even smaller part of the lung depending on the level of bronchus being atretic. Symptoms are rare. Etiology is unknown and may be similar to the reasons of bronchial blockage in congenital lobar overinflation.

Cystic adenomatoid malformation stocker type 1 and type 2

Although congenital cystic adenomatoid malformation (CCAM) pathogenesis is unknown, several authors have hypothesized that different types of CCAM originate at different stages of lung development. Abnormal airway development during branching morphogenesis probably results in specific areas of the lung where terminal bronchioles overgrow and

alveolar formations are absent (86). Another hypothesis postulates that CCAM originate as a result of imbalance between cell proliferation and apoptosis during airway branching (58, 89, 90). Type 1 CCAM consists of a few large cysts with bronchiolar configuration and a lining of respiratory epithelium overlying fibroelastic tissue and small amounts of smooth muscles. It may have a systemic arterial supply. Type 2 CCAM are multicystic lesions (cysts < 2 cm) often localized in one lobe, although multiple lobes can be affected.

Aberrant expression of genes involved in lung development has been shown to result in CCAM-like phenotypes. Transiently induced ectopic expression of SOX2, Fgf10, orthotopic overexpression of Fgf9 and heterotopic overexpression of Fgf7 show perturbations of lung morphogenesis some mimicking CCAM type 1 and 2 depending on the time of overexpression (25, 58, 91). In human resection specimens increased levels of the transcription factors HOXB5, TTF1, Fgf9 as well as changed expression patterns of the adhesion molecules a-2 integrins and E-cadherin, increased levels of Clara cell marker CC-10 and reduced expression of Fatty acid binding protein-7 have all been described (92-94). Moreover, microarray data revealed a 6 fold up-regulation of SOX2 in CCAM tissue compared with controls (94). These findings correspond with recently published data, describing the generation of CCAM-like phenotype by ectopic expression of SOX2 in mouse, and in a comparative study, expression of SOX2 in human CCAM tissue was identified (58). Moreover, TRP63 was co-expression in SOX2 positive cells, suggesting that the epithelium had proximal characteristics (58).

Extralobar sequestration

Extralobar sequestrations (ELS) are characterized by normal, non-functional lung tissue without connection to the bronchial tree and often receive blood supply from the systemic circulation. Mainly found in the left lower chest, these lesions can also be found in or below the diaphragm. In contrast to CCAM, associated anomalies like vertebral and chest wall deformities and congenital heart disease are described. In 5%-15% of patients with congenital diaphragmatic hernia an ELS is found at operation. Although often asymptomatic, antenatal diagnosis can be very helpful to detect congestive heart failure caused by the arteriovenous shunting through the anomalous systemic blood supply. Late symptoms are mainly infectious. One of the genes that is thought to be involved in the pathogenesis of this anomaly is the HOXB5 gene. It is previously shown that this gene is involved in airway branching (95).

Pulmonary hyperplasia and related lesions

Laryngeal atresia

Laryngeal atresia causes congenital high airway obstruction syndrome (CHAOS) at birth in the absence of a tracheoesophageal fistula. Prenatally, a polyhydramnios, large lung volume and inverted diaphragm are associated with fetal hydrops. Survivors are only described in those patients who have a tracheoesophageal fistula or a pinpoint laryngeal connection to relieve pressure from the lungs. Still, these patients may suffer from tracheobronchomalacia and diaphragmatic dysfunction due to increased lung extension during pregnancy. CHAOS can be associated with Fraser syndrome (96). If a bigger tracheoesophageal connection exists, prenatal diagnosis is difficult and diagnosis is only made at birth due to severe dyspnea. As a cause of laryngeal atresia, failure of recanalization of the laryngeal membrane is described. No detailed molecular analysis of

lungs of laryngeal atresia, either pre- or postnatally, has been reported.

Solid or cystic adenomatoid malformation, stocker type 3
The type 3 lesion, which accounts for 5%-10% of cases, occurs almost exclusively in males, and is associated with maternal polyhydramnios in nearly 80% of the cases. These are large, non-cystic bulky lesions, compressing the adjacent lung and mediastinum. Microscopically, randomly scattered bronchiolar/alveolar duct-like structures are lined by low cuboidal epithelium and surrounded by "alveoli" also lined by cuboidal epithelium. The virtual absence of any small, medium, or large pulmonary arteries in this type of lesion is remarkable.

Congenital Iobar overinflation
Congenital Iobar overinflation, or Congenital lobar emphysema (CLE), is a rare lung malformation with an incidence ranging from 1:20000 births to 1:30000 births (97-99). CLE is characterised by distended alveoli distal to the terminal bronchiole with destruction of the lining of the lobes, in contrast to a polyalveolar lobe where the number of alveoli is increased. CLE usually affects the left upper or right middle lobe (100). Prenatal diagnosis can be made when a hyperechogenic lung is seen, but discrimination with CCAM and ELS is difficult at that point. Although respiratory failure can be present at birth due to compression of normal lung and displacement of the heart, many patients are asymptomatic. As a cause of CLE, a disruption of normal bronchopulmonary tree development is described with dysplastic cartilage, mucosal overgrowth, main stem bronchial atresia or external compression from abnormal cardiovascular structures. No specific genetic anomalies have been linked to this anomaly so far.

Bochdalek type of Congenital diaphragmatic hernia
Bochdalek type of Congenital diaphragmatic hernia (CDH) is characterized by a posterolateral defect mostly in the left diaphragm, which results in herniation of the abdominal organs into the chest (101, 102). Subsequent pulmonary hypoplasia and pulmonary hypertension cause severe respiratory failure at birth. Lung hypoplasia is characterized by reduced alveolar air spaces lacking secondary septae, thickened alveolar walls and increased interstitial tissue. In the pulmonary vessels hyperplasia of the median and increased adventitial layer of the arterial wall is well described. The incidence of CDH is approximately one in 2500 births and the underlying cause of CDH is still unknown in a large number of patients.

Several links to gene loci have been found partly based on animal experiments and several members of the vitamin A-RA pathway have been implicated in the occurrence of CDH, such as vitamin A deficiency, STRA6 and RALDH2 (101-104). Moreover, some genes that are downstream of this pathway, like COUP-TFII, FOG2, GATA4 and GATA6, have also been found to be associated with CDH review (104, 105). Recent exome sequencing identified a novel candidate gene, PIGN, aside from the known FOG2 involvement (106, 107). A direct link of CDH and SOX2 has not been described.

Esophageal atresia
Esophageal atresia with or without TEF has an incidence ranging between one in 2500 to one in 4500 births. In EA, the proximal esophagus is blunt-ended, while the distal part is

connected to the trachea. This connection and the position of the atresia varies between patients and leads to the classification of five subtypes (108). In 85% of cases the esophageal atresia (EA) is accompanied by a distal tracheoesophageal fistula. Approximately half of the patients suffer from associated anomalies, as recently been reviewed (109).

The genetics of EA/TEF is complex, and several studies have indicated putative factors associated with either the multifactorial syndromes, or with EA/TEF. Based on murine models of this anomaly, several candidate genes and pathways have been identified, such as the receptors of the RARa/RARb, members of the SHH-PTC-GLI pathway (Shh, Gli2/3, Foxf1), BMP signaling (Noggin) and some transcription factors (Hoxc4, Ttf-1, Pcsk5, Tbx4, SOX2) (109).

Some of these candidate genes seem to be associated with human EA/TEF, such as FOXF1, PCSK5, SHH, NOG and SOX2. Moreover, other human genes have been associated with EA/TEF as part of several syndromes, such as Feingold (MYCN), Opitz G (MID1), Fanconi anemia (FANCA/C/D/G) and CHARGE (CHD7). Recently, CHD7 was shown to directly associate with SOX2, thereby linking CHARGE syndrome with AEG (62). Moreover, it was shown that these two proteins activated the transcription of a number of genes that are implicated in related syndromes, like *Shh*, *Gli2/3*, *Mycn*.

Alveolar capillary dysplasia

Although alveolar capillary dysplasia with misalignment of pulmonary veins (ACD/MPV) is a very rare condition without known incidence it has a dismal prognosis. The diagnosis is most likely underreported because it can only be made by histological examination of lung tissue. Newborn patients present with respiratory failure, hypoxemia, metabolic acidosis, pulmonary hypertension and right ventricular failure. Chest X-ray can be interpreted as normal but might show diffuse haziness or ground-glass opacities. Associated congenital anomalies may be present, especially of the genitourinary, gastrointestinal and cardiovascular system. Histologically, a decreased number of pulmonary capillaries is observed, distantly from the alveolar epithelium and thickened septae with a malposition of pulmonary veins close to pulmonary arteries. Often lymphangiectases are seen. Pulmonary arteries show medial hypertrophy with muscularization of distal arterioles. Although treatment response especially to therapy relieving pulmonary hypertension has been described, effects are transient. Late presenters and long-term survivors very rarely have been described and might be due to a lesser degree of histological changes. Deletions in chromosomal region 16q24.1q24.2 have been described. The smallest region of overlap in these deletions contains the FOX transcription factor gene cluster, including *FOXF1*, *FOXC2* and *FOXL1*. Findings in the mouse model with heterozygous deficiency of FOXF1 are similar to those in humans with ACD/MPV whereas mouse embryos with homozygous deficiency die at E9,5 due to pulmonary vascular abnormalities. A relationship with SOX2 never has been described (110-113).

1.4 Scope

SOX2 has only been found to be associated with a limited number of congenital anomalies. Modulating the expression levels of Sox2 during trachea and lung development in mice have led to abnormalities which relate to human conditions, such as CPAM and EA/TEF. Interestingly, CHD7, which is linked to CHARGE syndrome, was recently shown to be a binding partner of SOX2. SOX2 is linked to AEG syndrome, which is clinically related to CHARGE syndrome. In fact, some patients are incorrectly diagnosed with AEG or CHARGE, because the two syndromes are sometimes difficult to distinguish from each other. Thus, some of the congenital pulmonary abnormalities may be part of very complex syndromes, and it may be that the interactions between SOX2 and CHD7, or other proteins, may result in combinations of different clinical parameters. Therefore, mutations that change the interactions between SOX2 and other proteins, like CHD7, may result in the various clinical manifestations observed in syndromes.

Previously, our lab showed the importance of Sox2 in branching morphogenesis and epithelial differentiation during lung development. Because the transcriptional activity of Sox2 depends on its associating partners, the aim of this project was to identify these partners, and study their putative role during lung development

In chapter 2 we show that Sox2 directly regulates the transcription of Trp63, which is a marker for basal cells. We also show that Sox2 regulates Gata6, which is a transcription factor possibly involved in formation of bronchoalveolar stem cells. In chapter 3, we show the plasticity of terminally differentiated cells by ectopically expressing Sox2 in alveolar type II cells. This results in the gradual dedifferentiation of the type II cell and subsequently in the complete reversal into proximal, differentiated cells. In chapter 4 we will give an overview of the *in vivo* candidate partners that we identified, by performing affinity purifications using lungs from a mouse that expressed a biotinylatable form of Sox2 from the endogenous locus and in the chapter 5 we will highlight some of these partners. In chapter 6 we describe the different kind of stem cells in the lung, their regenerative capacity and how these cells could be used in the generation of lung mimics. Finally, in chapter 7 and 8 we discuss our findings in a broader perspective and summarize our results.

References

1. Gubbay J, Collignon J, Koopman P, Capel B, Economou A, Munsterberg A, et al. A gene mapping to the sex-determining region of the mouse Y chromosome is a member of a novel family of embryonically expressed genes. Nature. 1990;346(6281):245-50.
2. Sinclair AH, Berta P, Palmer MS, Hawkins JR, Griffiths BL, Smith MJ, et al. A gene from the human sex-determining region encodes a protein with homology to a conserved DNA-binding motif. Nature. 1990;346(6281):240-4.
3. Pevny L, Placzek M. SOX genes and neural progenitor identity. Curr Opin Neurobiol. 2005;15(1):7-13.
4. Wegner M. From head to toes: the multiple facets of Sox proteins. Nucleic Acids Res. 1999;Mar 15;27(6):1409-20.
5. Harley VR, Lovell-Badge R, Goodfellow PN. Definition of a consensus DNA binding site for SRY. Nucleic Acids Res. 1994;22(8):1500-1.
6. Pevny LH, Lovell-Badge R. Sox genes find their feet. Curr Opin Genet Dev. 1997;7(3):338-44.
7. Lefebvre V, Dumitriu B, Penzo-Mendez A, Han Y, Pallavi B. Control of cell fate and differentiation by Sry-related high-mobility-group box (Sox) transcription factors. Int J Biochem Cell Biol. 2007;39(12):2195-214.
8. Werner MH, Burley SK. Architectural transcription factors: proteins that remodel DNA. Cell. 1997;88(6):733-6.
9. Wolffe AP. Architectural transcription factors. Science. 1994;264(5162):1100-1.
10. Sarkar A, Hochedlinger K. The Sox Family of Transcription Factors: Versatile Regulators of Stem and Progenitor Cell Fate. Cell Stem Cell. 2013;12(1):15-30.
11. Kamachi Y, Kondoh H. Sox proteins: regulators of cell fate specification and differentiation. Development. 2013;140(20):4129-44.
12. Goodfellow PN, Lovell-Badge R. SRY and sex determination in mammals. Annu Rev Genet. 1993;27:71-92.
13. Hacker A, Capel B, Goodfellow P, Lovell-Badge R. Expression of Sry, the mouse sex determining gene. Development. 1995;121(6):1603-14.
14. Koopman P, Munsterberg A, Capel B, Vivian N, Lovell-Badge R. Expression of a candidate sex-determining gene during mouse testis differentiation. Nature. 1990;348(6300):450-2.
15. Liu K, Lin B, Zhao M, Yang X, Chen M, Gao A, et al. The multiple roles for Sox2 in stem cell maintenance and tumorigenesis. Cell Signal. 2013;25(5):1264-71.
16. Avilion AA, Nicolis SK, Pevny LH, Perez L, Vivian N, Lovell-Badge R. Multipotent cell lineages in early mouse development depend on SOX2 function. Genes Dev. 2003;17(1):126-40.
17. Wood HB, Episkopou V. Comparative expression of the mouse Sox1, Sox2 and Sox3 genes from pre-gastrulation to early somite stages. Mech Dev. 1999;86(1-2):197-201.
18. Papanayotou C, Mey A, Birot AM, Saka Y, Boast S, Smith JC, et al. A mechanism regulating the onset of Sox2 expression in the embryonic neural plate. Plos Biol. 2008;6(1):e2.
19. Ishii Y, Rex M, Scotting PJ, Yasugi S. Region-specific expression of chicken Sox2 in the developing gut and lung epithelium: regulation by epithelial-mesenchymal interactions. Dev Dyn. 1998;213(4):464-75.
20. Donner AL, Episkopou V, Maas RL. Sox2 and Pou2f1 interact to control lens and olfactory placode development. Dev Biol. 2007;303(2):784-99.
21. Schlosser G, Ahrens K. Molecular anatomy of placode development in Xenopus laevis. Dev Biol. 2004;271(2):439-66.
22. Uchikawa M, Ishida Y, Takemoto T, Kamachi Y, Kondoh H. Functional analysis of chicken Sox2 enhancers highlights an array of diverse regulatory elements that are conserved in mammals. Dev Cell. 2003;4(4):509-19.
23. Taranova OV, Magness ST, Fagan BM, Wu Y, Surzenko N, Hutton SR, et al. SOX2 is a dose-dependent regulator of retinal neural progenitor competence. Genes Dev. 2006;20(9):1187-202.
24. Pan W, Jin Y, Chen J, Rottier RJ, Steel KP, Kiernan AE. Ectopic expression of activated notch or SOX2 reveals similar and unique roles in the development of the sensory cell progenitors in the mammalian inner ear. J Neurosci. 2013;33(41):16146-57.
25. Gontan C, de Munck A, Vermeij M, Grosveld F, Tibboel D, Rottier R. Sox2 is important for two crucial processes in lung development: branching morphogenesis and epithelial cell differentiation. Dev Biol. 2008;317(1):296-309.
26. Okubo T, Pevny LH, Hogan BL. Sox2 is required for development of taste bud sensory cells. Genes Dev. 2006;20(19):2654-9.
27. Williamson KA, Hever AM, Rainger J, Rogers RC, Magee A, Fiedler Z, et al. Mutations in SOX2 cause anophthalmia-esophageal-genital (AEG) syndrome. Hum Mol Genet. 2006;15(9):1413-22.
28. Arnold K, Sarkar A, Yram MA, Polo JM, Bronson R, Sengupta S, et al. Sox2(+) Adult Stem and Progenitor Cells Are Important for Tissue Regeneration and Survival of Mice. Cell Stem Cell. 2011;9(4):317-29.
29. Que J, Okubo T, Goldenring JR, Nam KT, Kurotani R, Morrisey EE, et al. Multiple dose-dependent roles for Sox2 in the patterning and differentiation of anterior foregut endoderm. Development. 2007;134(13):2521-31.
30. Fantes J, Ragge NK, Lynch SA, McGill NI, Collin JR, Howard-Peebles PN, et al. Mutations in SOX2 cause

anophthalmia. Nat Genet. 2003;33(4):461-3.
31. Hagstrom SA, Pauer GJ, Reid J, Simpson E, Crowe S, Maumenee IH, et al. SOX2 mutation causes anophthalmia, hearing loss, and brain anomalies. Am J Med Genet A. 2005;138A(2):95-8.
32. www.embryology.ch. Developed by the universities of Fribourg, Lausanne and Bern (Switzerland) with the support of the Swiss Virtual Campus
33. Volckaert T, De Langhe S. Lung epithelial stem cells and their niches: Fgf10 takes center stage. Fibrogenesis Tissue Repair. 2014;7:8.
34. Wells JM, Melton DA. Vertebrate endoderm development. Annu Rev Cell Dev Biol. 1999;15:393-410.
35. Chamberlain CE, Jeong J, Guo C, Allen BL, McMahon AP. Notochord-derived Shh concentrates in close association with the apically positioned basal body in neural target cells and forms a dynamic gradient during neural patterning. Development. 2008;135(6):1097-106.
36. Serls AE, Doherty S, Parvatiyar P, Wells JM, Deutsch GH. Different thresholds of fibroblast growth factors pattern the ventral foregut into liver and lung. Development. 2005;132(1):35-47.
37. Desai TJ, Chen F, Lu JM, Qian J, Niederreither K, Dolle P, et al. Distinct roles for retinoic acid receptors alpha and beta in early lung morphogenesis. Dev Biol. 2006;291(1):12-24.
38. Morrisey EE, Hogan BL. Preparing for the first breath: genetic and cellular mechanisms in lung development. Dev Cell. 2010;18(1):8-23.
39. Herriges M, Morrisey EE. Lung development: orchestrating the generation and regeneration of a complex organ. Development. 2014;141(3):502-13.
40. Warburton D, El-Hashash A, Carraro G, Tiozzo C, Sala F, Rogers O, et al. Lung organogenesis. Curr Top Dev Biol. 2010;90:73-158.
41. Wells JM, Melton DA. Early mouse endoderm is patterned by soluble factors from adjacent germ layers. Development. 2000;127(8):1563-72.
42. Rackley CR, Stripp BR. Building and maintaining the epithelium of the lung. J Clin Invest. 2012;122(8):2724-30.
43. Burri PH. Structural aspects of postnatal lung development - alveolar formation and growth. Biol. Neonate. 2006;89(4):313-22.
44. Metzger RJ, Klein OD, Martin GR, Krasnow MA. The branching programme of mouse lung development. Nature. 2008;453(7196):745-50.
45. Alanis DM, Chang DR, Akiyama H, Krasnow MA, Chen JC. Two nested developmental waves demarcate a compartment boundary in the mouse lung. Nat Commun. 2014;5.
46. Kaplan F. Molecular determinants of fetal lung organogenesis. Mol Genet Metab. 2000; 71(1-2):321-41.
47. Sock E, Rettig SD, Enderich J, Bosl MR, Tamm ER, Wegner M. Gene targeting reveals a widespread role for the high-mobility-group transcription factor Sox11 in tissue remodeling. Mol Cell Biol. 2004;24(15):6635-44.
48. Lange AW, Keiser AR, Wells JM, Zorn AM, Whitsett JA. Sox17 promotes cell cycle progression and inhibits TGF-beta/Smad3 signaling to initiate progenitor cell behavior in the respiratory epithelium. Plos One. 2009;4(5):e5711.
49. Tompkins DH, Besnard V, Lange AW, Keiser AR, Wert SE, Bruno MD, et al. Sox2 activates cell proliferation and differentiation in the respiratory epithelium. Am J Respir Cell Mol Biol. 2011;45(1):101-10.
50. Park KS, Wells JM, Zorn AM, Wert SE, Whitsett JA. Sox17 influences the differentiation of respiratory epithelial cells. Dev Biol. 2006;294(1):192-202.
51. Rockich BE, Hrycaj SM, Shih HP, Nagy MS, Ferguson MA, Kopp JL, et al. Sox9 plays multiple roles in the lung epithelium during branching morphogenesis. Proc Natl Acad Sci U S A. 2013;110(47):E4456-64.
52. Turcatel G, Rubin N, Menke DB, Martin G, Shi W, Warburton D. Lung mesenchymal expression of Sox9 plays a critical role in tracheal development. BMC Biol. 2013;11(1):117.
53. Park J, Zhang JJ, Moro A, Kushida M, Wegner M, Kim PC. Regulation of Sox9 by Sonic Hedgehog (Shh) is essential for patterning and formation of tracheal cartilage. Dev Dyn. 2010;239(2):514-26.
54. Elluru RG, Thompson F, Reece A. Fibroblast growth factor 18 gives growth and directional cues to airway cartilage. Laryngoscope. 2009;119(6):1153-65.
55. Kanai-Azuma M, Kanai Y, Gad JM, Tajima Y, Taya C, Kurohmaru M, et al. Depletion of definitive gut endoderm in Sox17-null mutant mice. Development. 2002;129(10):2367-79.
56. Lange AW, Haitchi HM, LeCras TD, Sridharan A, Xu Y, Wert SE, et al. Sox17 is required for normal pulmonary vascular morphogenesis. Dev Biol. 2014;387(1):109-20.
57. Harris-Johnson KS, Domyan ET, Vezina CM, Sun X. beta-Catenin promotes respiratory progenitor identity in mouse foregut. Proc Natl Acad Sci U S A. 2009;106(38):16287-92.
58. Ochieng JK, Schilders K, Kool H, Boerema-de Munck A, Buscop-van Kempen M, Gontan C, et al. Sox2 Regulates the Emergence of Lung Basal Cells by Directly Activating the Transcription of Trp63. Am J Respir Cell Mol Biol. 2014.
59. Minoo P, Su G, Drum H, Bringas P, Kimura S. Defects in tracheoesophageal and lung morphogenesis in Nkx2.1(-/-) mouse embryos. Dev Biol. 1999;209(1):60-71.

60. Jacobs IJ, Ku WY, Que J. Genetic and cellular mechanisms regulating anterior foregut and esophageal development. Dev Biol. 2012;369(1):54-64.
61. Boyer LA, Lee TI, Cole MF, Johnstone SE, Levine SS, Zucker JP, et al. Core transcriptional regulatory circuitry in human embryonic stem cells. Cell. 2005;122(6):947-56.
62. Engelen E, Akinci U, Bryne JC, Hou J, Gontan C, Moen M, et al. Sox2 cooperates with Chd7 to regulate genes that are mutated in human syndromes. Nat Genet. 2011;43(6):607-U153.
63. Gontan C, Guttler T, Engelen E, Demmers J, Fornerod M, Grosveld FG, et al. Exportin 4 mediates a novel nuclear import pathway for Sox family transcription factors. J Cell Biol. 2009;185(1):27-34.
64. Bellusci S, Grindley J, Emoto H, Itoh N, Hogan BL. Fibroblast growth factor 10 (FGF10) and branching morphogenesis in the embryonic mouse lung. Development. 1997;124(23):4867-78.
65. Park WY, Miranda B, Lebeche D, Hashimoto G, Cardoso WV. FGF-10 is a chemotactic factor for distal epithelial buds during lung development. Dev Biol. 1998;201(2):125-34.
66. Sekine K, Ohuchi H, Fujiwara M, Yamasaki M, Yoshizawa T, Sato T, et al. Fgf10 is essential for limb and lung formation. Nat Genet. 1999;21(1):138-41.
67. Kato S, Sekine K. [FGF10, a key factor for limb and lung formation]. Seikagaku. 2000;72(4):288-91.
68. Colvin JS, White AC, Pratt SJ, Ornitz DM. Lung hypoplasia and neonatal death in Fgf9-null mice identify this gene as an essential regulator of lung mesenchyme. Development. 2001;128(11):2095-106.
69. Abler LL, Mansour SL, Sun X. Conditional gene inactivation reveals roles for Fgf10 and Fgfr2 in establishing a normal pattern of epithelial branching in the mouse lung. Dev Dyn. 2009;238(8):1999-2013.
70. Volckaert T, Campbell A, Dill E, Li C, Minoo P, De Langhe S. Localized Fgf10 expression is not required for lung branching morphogenesis but prevents differentiation of epithelial progenitors. Development. 2013;140(18):3731-42.
71. Goss AM, Tian Y, Tsukiyama T, Cohen ED, Zhou D, Lu MM, et al. Wnt2/2b and beta-catenin signaling are necessary and sufficient to specify lung progenitors in the foregut. Dev Cell. 2009;17(2):290-8.
72. Shu W, Guttentag S, Wang Z, Andl T, Ballard P, Lu MM, et al. Wnt/beta-catenin signaling acts upstream of N-myc, BMP4, and FGF signaling to regulate proximal-distal patterning in the lung. Dev Biol. 2005;283(1):226-39.
73. Miller MF, Cohen ED, Baggs JE, Lu MM, Hogenesch JB, Morrisey EE. Wnt ligands signal in a cooperative manner to promote foregut organogenesis. Proc Natl Acad Sci U S A. 2012;109(38):15348-53.
74. Krejci P, Aklian A, Kaucka M, Sevcikova E, Prochazkova J, Masek JK, et al. Receptor tyrosine kinases activate canonical WNT/beta-catenin signaling via MAP kinase/LRP6 pathway and direct beta-catenin phosphorylation. Plos One. 2012;7(4):e35826.
75. Shu W, Jiang YQ, Lu MM, Morrisey EE. Wnt7b regulates mesenchymal proliferation and vascular development in the lung. Development. 2002;129(20):4831-42.
76. Mucenski ML, Wert SE, Nation JM, Loudy DE, Huelsken J, Birchmeier W, et al. beta-Catenin is required for specification of proximal/distal cell fate during lung morphogenesis. J Biol Chem. 2003;278(41):40231-8.
77. Cornett B, Snowball J, Varisco BM, Lang R, Whitsett J, Sinner D. Wntless is required for peripheral lung differentiation and pulmonary vascular development. Dev Biol. 2013;379(1):38-52.
78. Hashimoto S, Chen H, Que J, Brockway BL, Drake JA, Snyder JC, et al. beta-Catenin-SOX2 signaling regulates the fate of developing airway epithelium. J Cell Sci. 2012;125(Pt 4):932-42.
79. Li C, Hu L, Xiao J, Chen H, Li JT, Bellusci S, et al. Wnt5a regulates Shh and Fgf10 signaling during lung development. Dev Biol. 2005;287(1):86-97.
80. Sountoulidis A, Stavropoulos A, Giaglis S, Apostolou E, Monteiro R, Chuva de Sousa Lopes SM, et al. Activation of the canonical bone morphogenetic protein (BMP) pathway during lung morphogenesis and adult lung tissue repair. Plos One. 2012;7(8):e41460.
81. Que J, Choi M, Ziel JW, Klingensmith J, Hogan BL. Morphogenesis of the trachea and esophagus: current players and new roles for noggin and Bmps. Differentiation. 2006;74(7):422-37.
82. Li Y, Litingtung Y, Ten Dijke P, Chiang C. Aberrant Bmp signaling and notochord delamination in the pathogenesis of esophageal atresia. Dev Dyn. 2007;236(3):746-54.
83. Fausett SR, Brunet LJ, Klingensmith J. BMP antagonism by Noggin is required in presumptive notochord cells for mammalian foregut morphogenesis. Dev Biol. 2014;391(1):111-24.
84. Li Y, Gordon J, Manley NR, Litingtung Y, Chiang C. Bmp4 is required for tracheal formation: a novel mouse model for tracheal agenesis. Dev Biol. 2008;322(1):145-55.
85. Domyan ET, Ferretti E, Throckmorton K, Mishina Y, Nicolis SK, Sun X. Signaling through BMP receptors promotes respiratory identity in the foregut via repression of Sox2. Development. 2011;138(5):971-81.
86. Correia-Pinto J, Gonzaga S, Huang Y, Rottier R. Congenital lung lesions--underlying molecular mechanisms. Semin Pediatr Surg. 2010;19(3):171-9.
87. Ng C, Stanwell J, Burge DM, Stanton MP. Conservative management of antenatally diagnosed cystic lung malformations. Arch Dis Child. 2014;99(5):432-7.

88. Langston C. New concepts in the pathology of congenital lung malformations. Semin Pediatr Surg. 2003;12(1):17-37.
89. Cass DL, Quinn TM, Yang EY, Liechty KW, Crombleholme TM, Flake AW, et al. Increased cell proliferation and decreased apoptosis characterize congenital cystic adenomatoid malformation of the lung. J Pediatr Surg. 1998;33(7):1043-6; discussion 7.
90. Fromont-Hankard G, Philippe-Chomette P, Delezoide AL, Nessmann C, Aigrain Y, Peuchmaur M. Glial cell-derived neurotrophic factor expression in normal human lung and congenital cystic adenomatoid malformation. Arch Pathol Lab Med. 2002;126(4):432-6.
91. Gonzaga S, Henriques-Coelho T, Davey M, Zoltick PW, Leite-Moreira AF, Correia-Pinto J, et al. Cystic adenomatoid malformations are induced by localized FGF10 overexpression in fetal rat lung. Am J Respir Cell Mol Biol. 2008;39(3):346-55.
92. Volpe MV, Wang KTW, Nielsen HC, Chinoy MR. Unique spatial and cellular expression patterns of Hoxa5, Hoxb4, and Hoxb6 proteins in normal developing murine lung are modified in pulmonary hypoplasia. Birth Defects Res A. 2008;82(8):571-84.
93. Jancelewicz T, Nobuhara K, Hawgood S. Laser microdissection allows detection of abnormal gene expression in cystic adenomatoid malformation of the lung. J Pediatr Surg. 2008;43(6):1044-51.
94. Wagner AJ, Stumbaugh A, Tigue Z, Edmondson J, Paquet AC, Farmer DL, et al. Genetic analysis of congenital cystic adenomatoid malformation reveals a novel pulmonary gene: fatty acid binding protein-7 (brain type). Pediatr Res. 2008;64(1):11-6.
95. Volpe MV, Archavachotikul K, Bhan I, Lessin MS, Nielsen HC. Association of bronchopulmonary sequestration with expression of the homeobox protein Hoxb-5. J Pediatr Surg. 2000;35(12):1817-9.
96. Berg C, Geipel A, Germer U, Pertersen-Hansen A, Koch-Dorfler M, Gembruch U. Prenatal detection of Fraser syndrome without cryptophthalmos: case report and review of the literature. Ultrasound Obstet Gynecol. 2001;18(1):76-80.
97. Epelman M, Kreiger PA, Servaes S, Victoria T, Hellinger JC. Current imaging of prenatally diagnosed congenital lung lesions. Semin Ultrasound CT MR. 2010;31(2):141-57.
98. Mei-Zahav M, Konen O, Manson D, Langer JC. Is congenital lobar emphysema a surgical disease? J Pediatr Surg. 2006;41(6):1058-61.
99. Nayar PM, Thakral CL, Sajwani MJ. Congenital lobar emphysema and sequestration--treatment by embolization. Pediatr Surg Int. 2005;21(9):727-9.
100. Kravitz RM. Congenital malformations of the lung. Pediatr Clin North Am. 1994;41(3):453-72.
101. Rottier R, Tibboel D. Fetal lung and diaphragm development in congenital diaphragmatic hernia. Semin Perinatol. 2005;29(2):86-93.
102. Klaassens M, de Klein A, Tibboel D. The etiology of congenital diaphragmatic hernia: still largely unknown? Eur J Med Genet. 2009;52(5):281-6.
103. Beurskens N, Klaassens M, Rottier R, de Klein A, Tibboel D. Linking animal models to human congenital diaphragmatic hernia. Birth Defects Res A Clin Mol Teratol. 2007;79(8):565-72.
104. Veenma DC, de Klein A, Tibboel D. Developmental and genetic aspects of congenital diaphragmatic hernia. Pediatr Pulmonol. 2012;47(6):534-45.
105. Leeuwen L, Fitzgerald DA. Congenital diaphragmatic hernia. J Paediatr Child Health. 2014; 50(9):667-73.
106. Brady PD, Moerman P, De Catte L, Deprest J, Devriendt K, Vermeesch JR. Exome sequencing identifies a recessive PIGN splice site mutation as a cause of syndromic congenital diaphragmatic hernia. Eur J Med Genet. 2014;57(9):487-93.
107. Brady PD, Van Houdt J, Callewaert B, Deprest J, Devriendt K, Vermeesch JR. Exome sequencing identifies ZFPM2 as a cause of familial isolated congenital diaphragmatic hernia and possibly cardiovascular malformations. Eur J Med Genet. 2014;57(6):247-52.
108. Spitz L. Oesophageal atresia. Orphanet J Rare Dis. 2007;2:24.
109. de Jong EM, Felix JF, de Klein A, Tibboel D. Etiology of esophageal atresia and tracheoesophageal fistula: “mind the gap”. Curr Gastroenterol Rep. 2010;12(3):215-22.
110. Kalinichenko VV, Lim L, Stolz DB, Shin B, Rausa FM, Clark J, et al. Defects in pulmonary vasculature and perinatal lung hemorrhage in mice heterozygous null for the Forkhead Box f1 transcription factor. Dev Biol. 2001;235(2):489-506.
111. Bishop NB, Stankiewicz P, Steinhorn RH. Alveolar capillary dysplasia. Am J Respir Crit Care Med. 2011;184(2):172-9.

Chapter 2.

Sox2 regulates the emergence of lung basal cells by directly regulating the transcription of Trp63

Joshua K Ochieng, Kim Schilders, Heleen Kool, Anne Boerema-de Munck, Marjon Buscop-van Kempen, Cristina Gontan, Ron Smits, Frank G. Grosveld, Rene M.H. Wijnen, Dick Tibboel, Robbert J. Rottier

American Journal of Respiratory Cell and Molecular Biology 2014; 51(2)

Abstract

Lung development is determined by the coordinated expression of several key genes, and previously, we and others have shown the importance the SRY (sex determining region Y)-box 2 (Sox2) gene in lung development. Transgenic expression of Sox2 during lung development resulted in cystic airways and here we show that modulating the timing of ectopic Sox2 expression in the branching regions of the developing lung results in variable cystic lesions resembling the spectrum of the human congenital disorder Congenital Cystic Adenomatoid Malformation (CCAM). Sox2 dominantly differentiated naïve epithelial cells into the proximal lineage, irrespective of the presence of Fgf10. Sox2 directly induced the expression of Trp63, the master switch towards the basal cell lineage. In addition, Sox2 induced the expression of Gata6, a factor involved in the emergence of bronchioalveolar stem cells. In addition, we showed that SOX2 and TRP63 are co-expressed in the lungs of human CCAM type II patients. The combination of premature differentiation towards the proximal cell lineage and the induction of proliferation finally resulted in the cyst-like structures. Thus, we show that Sox2 is directly responsible for the emergence of two lung progenitor cells, basal cells by regulating the master gene Trp63, and bronchoalveolar stem cells by regulating Gata6.

Keywords

Mouse, lung, Trp63, Sox2, basal cells, Gata6, BASCs

Introduction

Development of the lung starts early after gastrulation when cells at the ventral site of the foregut form a primitive bud and invaginate the surrounding mesenchyme. Subsequently, this lung bud branches in a coordinated, repetitive process, called branching morphogenesis, to generate the primary bronchial tree (1-2). Failure to complete the lung morphogenesis program correctly may lead to congenital abnormalities, such as congenital diaphragmatic hernia and congenital cystic adenomatoid malformation of the lung (CCAM) (3). CCAMs are rare developmental lung defects characterized by cystic areas and adenomatous overgrowth of the terminal bronchioles (4). The pathology of the CCAMs displays a large variation and therefore patients are classified according to the different types of lesions (types 0-4). The incidence of CCAM is 1 in 35,000 live births and the pathogenesis of CCAM development is still unknown.

A putative role for the high mobility group (HMG) box transcription factor Sox2 in lung development was based on its expression pattern in the foregut, and recently, we and others showed the importance of Sox2 in lung development (5-7). Sox2 is cell-autonomously required in both embryonic and extra-embryonic cell types, and the lack of Sox2 results in peri-implantation lethality (8). Later in development, Sox2 is involved in several processes during neurogenesis and sensory organ formation, such as structures in the ear and eye (reviewed in (9)). Moreover, Sox2 is important to maintain pluripotency and self-renewal in embryonic stem (ES) cells as well as epithelial stem cells in multiple tissues (9). It is also one of the original factors required for reprogramming somatic cells into pluripotent stem cells (iPS) (10). In lung, Sox2 is expressed in epithelial cells of the foregut, which later develops into the pharynx, esophagus, trachea, bronchi, and bronchioles (5). However, Sox2 expression is excluded from the peripheral and alveolar regions of the lung. Hypomorphic mouse mutants with reduced Sox2 expression demonstrated that Sox2 is involved in the morphogenesis of the trachea and esophagus, as well as the differentiation of the esophageal epithelium (11). We showed that Sox2 is involved in branching morphogenesis and epithelial cell differentiation, since ectopic expression of Sox2 led to an increase in committed precursor-like cells, such as neuroendocrine and basal cells (5). Ectopic expression of Sox2 in Clara cells of adult mice resulted in the development of p63-positive carcinomas (12).

Basal cells are relatively undifferentiated cells present in the epithelium of the trachea and upper airways, and are the residing stem cell population of the upper airways that regenerates damaged epithelium (13-14). In mouse lungs, basal cells make up 30% of the pseudostratified mucociliary epithelium and they are characterized by the expression of the transcription factor Trp63 (p63) (14-15). Trp63 is a homologue of the tumor-suppressor p53 and functions as a master regulator of epidermal development. Trp63 is expressed in the basal or progenitor cell layer of stratified epithelia (e.g. squamous, urothelial, bronchial), in the basal cells of some glandular epithelia (e.g. prostate), as well as in myoepithelial cells of breast and salivary glands, trophoblasts and thymic epithelial cells (16). Mutations in Trp63 leads to dominantly inherited clinical conditions, like ectrodactyly (split hand/foot malformation), orofacial clefting and ectodermal dysplasia with defects in skin, hair, teeth, nails and exocrine glands. Mice deficient of Trp63 lack normal epidermis and die shortly after birth (15, 17-19). The Trp63 $^{-/-}$ mice completely lacked basal cells in the trachea and esophagus, and instead developed a highly ordered, columnar ciliated

epithelium. These observations indicated that Trp63 is for the commitment of early stem cells into basal cell progeny and the maintenance of basal cells (15).

Regulation of Trp63 is complex by the usage of different promoters, generating six isoforms, which are grouped into trans-activating (TAp63) and non-transactivating (ΔNp63) isoforms. Both the TAp63 and ΔNp63 transcripts are differentially spliced at the 3'-end generating proteins with unique C-termini, designated as α, β, and γ isoforms. The β and γ are shorter isoforms, while the longer Trp63α isoforms harbor a Sterile Alpha Motif (SAM) domain, which is thought to mediate protein-protein interactions. ΔNp63 is the predominant isoform in basal cells and can transcriptionally activate or repress target gene expression (20-23). Recently, we showed that ectopic Sox2 induces the expression of the ΔNp63 isoform in the lungs (5).

In order to study the role of Sox2 in the regulation of basal cells, we ectopically expressed Sox2 in mouse distal epithelial cells starting early in gestation, when the mouse lung starts to branch until the later phases of gestation. We observed a correlation between the time of transgene induction and the appearance and size of cystic lesions, which resembled the different forms of human CCAMs. Furthermore, we showed that Sox2 directly binds and transactivates the Trp63 promoter of the ΔN isoform, which indicates a direct involvement of Sox2 in the emergence of $Trp63^{+}$ basal cells. In addition, we showed that Sox2 directly influences the emergence of bronchoalveolar stem cells (BASCs) in the lung by regulating Gata6 expression. Lastly, we analysed the expression of SOX2 in lung samples of human type I and type II CCAM patients.

Materials and Methods

Detailed materials and methods section is available as supplemental data.

Tissue preparation and Immunohistochemistry

Human lung samples were retrieved from the archives of the Department of Pathology, Erasmus MC, Rotterdam, following approval by the Erasmus MC Medical Ethical Committee. Mouse lungs were processed according to routine protocols (5, 24).

Mesenchyme free cultures

Embryonic lung mesenchyme was isolated and cultures in MatrigelTM (BD Bioscience) with 250 ng/ml Fgf10 (R&D systems) and 0.6μM doxycycline.

Cell Transfection

HEK-293T cells were transiently transfected using Lipofectamine LTX (Invitrogen) with appropriate luciferase constructs and expression plasmids. Luciferase activity was measured using the Dual-Luciferase Reporter Assay system (Promega, Germany).

Chromatin Immunoprecipitation assays

ChIP assays were performed essentially as previously described, using 6x107 A549 cells cultured in 150 μM CoCl2 to induce hypoxia (24). PCR primers are listed in Table 1.

Results

Timed Sox2 expression in the lung leads to cyst-like malformations in distal lung

We first studied the morphological abnormalities caused by ectopic expression of Sox2 in the developing lung using the SPC-rtTA transgenic driver mouse line (iSox2$^{SPC\text{-}rtTA}$; (25)). The induction of Sox2 in the epithelial cells of the developing airway from the onset of lung development resulted in the appearance of large, cystic lesions, as we previously reported (fig. 1C) (5). Next, we analyzed whether modulation of the transgenic Sox2 expression had an effect on the size of the cystic abnormalities. Therefore, we varied the administration of doxycycline to express the transgenic Sox2 at later time points during gestation. Administration of doxycycline was started at the onset of branching morphogenesis (E10.5), at the pseudoglandular stage (E12.5) and at the canalicular stage (E15.5) to monitor the development of the lungs (fig. 1A). Lungs were isolated at gestational age 18.5, just prior to birth, and morphological analysis of the lungs showed that iSox2SPC-rtTA lungs had mild to severe cyst-like defects in the distal regions, which correlated with the duration of transgene induction (fig. 1D-1F). Lungs from wild type control mice, single transgenic animals, or non-induced iSox2$^{SPC\text{-}rtTA}$ animals appeared healthy and did not show apparent abnormalities (Fig. 1B).

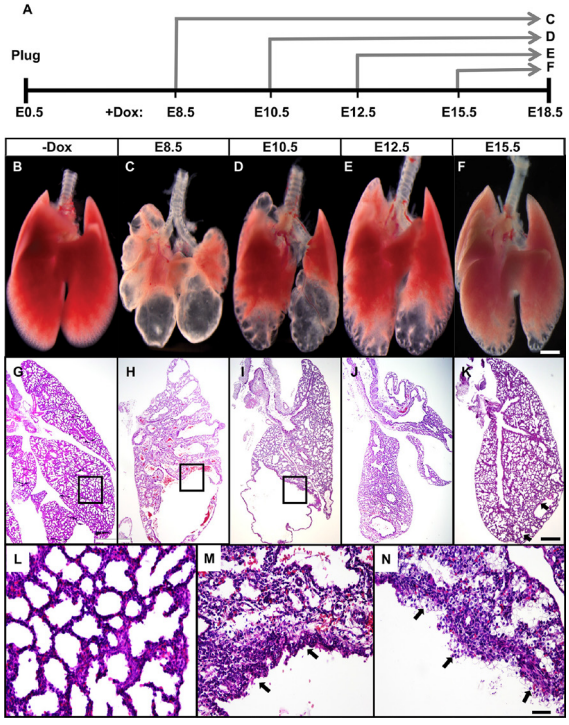

Figure 1. Ectopic Sox2 expression causes variable cyst sizes in the lung. Control and iSox2Spc-rtTA mice were treated with doxycycline for a specified period as indicated in the schematic overview (A). Lungs were isolated at E18.5 and analysis of the external appearances shows varied cystic abnormalities in lung structure, consisting of loss of peripheral airspaces and disruption of branching morphogenesis (B–F). Low (G-K) and high power images (L-N, enlarged boxes of G-I) of haematoxylin/eosin stained sections show the cystic malformations in the Sox2 transgenic lungs. Arrows indicate examples of disorganized epithelium. Scale bars: 2 mm (F, K) and 50 µm (N).

Histological analysis of the lungs showed that prolonged expression of Sox2 resulted in dilation of the developing airways with limited branched airways, suggesting that ectopic expression of Sox2 in the airway epithelial cells prevented branching morphogenesis (fig. 1G-1K). Microscopic examination of the iSox2$^{SPC\text{-}rtTA}$ lungs revealed a disorganized epithelium lining the cystic lesions (fig. 1 M, N; arrows), which was absent in control lungs (fig. 1L). Analysis with specific epithelial markers was done and showed a distribution as previously reported, with all differentiated cells being present, albeit their distribution was slightly changed depending on the penetration of the SPC-rtTA expression (data not shown; (5)). In order to analyze whether switching off iSox2 expression would restore normal lung branching and growth, the transgene was activated early in development at E6.5, after which the doxycycline was removed at different time points (E12.5, E14.5 or E16.5; suppl. fig. 1A). Analysis of the lungs at E18.5 showed that withdrawal of doxycycline led to the initiation, or reactivation, of the lung developmental program from the time the switching off of the transgene occurred (suppl. fig. 1B-E). The lungs showed cystic structures more internally in the lung and less to the periphery as compared to continuous iSox2 expression (compare suppl. fig. 1F-I with fig. 1H). Together, these data show that variation in cyst size is dependent on the timing and duration of transgenic Sox2 expression. Moreover, late induction of Sox2 resulted in normal development of the primary branches up to the point when expression of Sox2 was induced by doxycycline, suggesting that it has a dominant effect on the cells involved in branching.

Sox2 inhibits the response of cells to Fgf10

Since ectopic expression of Sox2 severely affected branching morphogenesis, we analysed whether expression of the iSox2 transgene affected the normal response of the epithelial tip cells to the branch-inducing growth factor Fgf10. Therefore, fetal lung explants were cultured in the presence of PBS or Fgf10 coated heparin beads. The airways of the control lungs that were in close proximity to the Fgf10 beads clearly grew towards these beads and started to engulf them within four days (fig 2A-C, arrows). In contrast, the airways of the doxycycline induced iSox2$^{SPC\text{-}rtTA}$ lung explants showed a severely reduced attraction towards the beads, indicating that expression of the Sox2 transgene inhibited tip cells from responding to Fgf10 (fig 2E-G). Subsequent immunostaining of the cultured explants revealed that the unresponsive regions expressed the transgenic Sox2 (fig. 2H). Moreover, the staining also showed the incomplete penetrance of the transgene, allowing epithelial cells that do not express the transgene to respond to Fgf10. The latter explained why the iSox2$^{SPC\text{-}rtTA}$ lungs would still show signs of branching. Next, we examined whether the lack of responsiveness of the epithelial tip cells was an autonomous effect of the airway epithelium expressing exogenous Sox2. Therefore, mesenchyme-free lung endoderm of E11.5 embryonic iSox2SPC-rtTA and control lungs were cultured in matrigel supplemented with Fgf10 in the presence or absence of doxycycline. Branching was readily detected in the control and non-induced iSox2SPC-rtTAlung endoderm cultures (fig. 2I/2L and 2J/2M). When doxycycline was added to the endoderm cultures from iSox2$^{SPC\text{-}rtTA}$ lungs, the branching process was severely hampered (Fig. 2K and 2N; quantification in fig. 2O), indicating that ectopic expression of Sox2 either prevented the response towards Fgf10, or induced the differentiation of cells which lead to the loss of FgfR2b expression. Additionally, we analyzed whether cells of the iSox2$^{SPC\text{-}rtTA}$ lungs were viable by performing a specific immunostaining on lung explants using the mitotic marker Phh3 (suppl. fig. 2). This showed that non-induced lung explants had only a few proliferative cells, whereas the

iSox2$^{SPC\text{-}rtTA}$ lungs had significantly more cycling cells. Taken together, these data showed that Sox2 expression in lung buds inhibits the response of the cells to Fgf10 without the ability to proliferate.

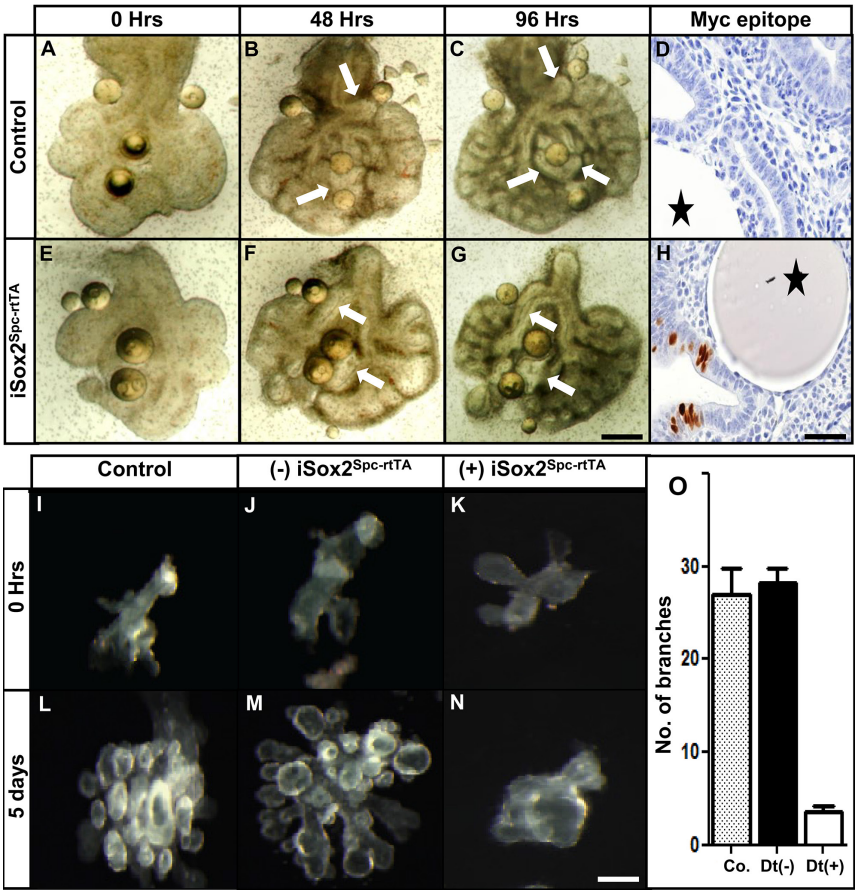

Figure 2. Transgenic Sox2 prevents Fgf10 induced branching. Lung explants of control (A-D) and iSox2$^{Spc\text{-}rtTA}$ (E-H) mice were grown for 96 h in medium containing doxycycline. Heparin beads coated with Fgf10 were placed with the explants. The airways of control lungs that are in close proximity of the beads grow towards the Fgf10 source (arrows in B, C), whereas the iSox2$^{SPC\text{-}rtTA}$ derived lungs show severe reduction of this effect (arrows in F, G). Sections were stained with the myc epitope to show expression of the transgene (D, H; stars indicate position of the beads). Scale bars: 500 µm (A-C; E-G) and 50 µm (D, H). Mesenchyme free lung endoderm from control and iSox2$^{SPC\text{-}rtTA}$ lungs was cultured in growth factor reduced matrigel supplemented with Fgf10, in the presence (I, K, L, N) or absence (J,M) of doxycycline. The control endoderm (I, L) and the iSox2SPC-rtTA derived endoderm grown in the absence (-) of doxycycline (J, M) clearly showed branching after five days of culture. iSox2$^{SPC\text{-}rtTA}$ derived endoderm grown in the presence of doxycycline showed no branching at all (K, N). Quantification of the number of branches revealed a six fold decrease in branching in Sox2-induced endoderm cultures (O). Scale bars: 100 µm.

Prolonged Sox2 expression affects basal cell differentiation in the respiratory epithelium

The emergence of basal cells during development showed a correlation with the duration of iSox2 expression (suppl. fig. 3). However, it is unclear if the emergence of basal cells depended on continuous expression of iSox2, or that precursor cells are primed to become basal cells, after which Sox2 is no longer required. We hypothesized that varying the timing and duration of the transgenic Sox2 expression would result in fluctuations in the number of basal cells. Therefore, the differentiation towards basal cells was examined after induction of Sox2 starting at embryonic, early and late pseudoglandular phases of gestation. The expression and distribution of iSox2 in correlation with the cystic lesions was first examined using an antibody against the myc-epitope present at the N-terminus of the iSox2 transgene. Strong nuclear staining was detected in the iSox2$^{SPC\text{-}rtTA}$ lungs when the transgene was induced from embryonic phase (fig. 3D, E) or pseudoglandular phase (fig. 3G, H), whereas no myc-epitope positive cells were observed in lungs of wild type or non-induced iSox2$^{SPC\text{-}rtTA}$ animals (fig. 3A, B). Varying the time of induction of Sox2 resulted in changes in the total number of differentiated basal cells. In control lungs, Trp63 and myc immune reactive cells were not observed in the distal epithelium (fig. 3A-C), although Trp63 positive cells were observed in the trachea (fig. 3K). However, in iSox2$^{SPC\text{-}rtTA}$ lungs, we detected cells expressing both the transgenic Sox2 and Trp63 using sequential sections of the distal epithelium of the lung, correlating with the time of doxycycline exposure (fig. 3D-I). Quantification of the number of Trp63 positive basal cells revealed a gradual decrease of basal cells correlating with the onset of induced expression of Sox2 in the iSox2$^{SPC\text{-}rtTA}$ lungs (fig. 3J). Only a few differentiated basal cells were identified when the transgene was induced late in gestation, whereas high numbers of basal cells emerged with an early induction of the transgene in the intra-lobular airways. Moreover, dual immunofluorescence staining revealed that Trp63 and Sox2 were expressed in the same cell, both in the trachea of control and iSox2$^{SPC\text{-}rtTA}$ mice , as well as in the aberrant Trp63 positive cells in the distal lungs of iSox2$^{SPC\text{-}rtTA}$ mice (fig. 3K, L). Together, these results demonstrate that a linear correlation between the expression of iSox2 and of the appearance of p63^{+} basal cells.

The basal cell specific Trp63 gene is a direct target of Sox2

Based on the correlation between the number of basal cells and the induced Sox2 expression, as well as the co-localization of Sox2 and Trp63 (fig. 3L), we analyzed whether Sox2 could directly regulate the expression of the Trp63 gene. Previously, we showed that the ΔNTrp63 isoform was predominantly induced in iSox2SPC-rtTA lungs (5), so we analyzed a 1500 bp region immediately upstream of the Trp63 ΔN isoform transcriptional start site (TSS) and identified five putative Sox2 binding motifs (fig. 4A). Based on the highest similarity scores for motifs I and II, a fragment covering 520 bp immediately upstream the TSS was subcloned upstream of a luciferase reporter construct. SMAD2 was used as positive control since it was previously shown to transactivate the Trp63 promoter (26). The full length Sox2 induced the Trp63 minimal promoter constructs containing the putative Sox2 consensus binding sites (fig. 4B). However, two mutant Sox2 constructs, lacking either the HMG DNA binding motif (ΔHMG) or the transactivating domain at the C-terminal part (ΔTAD), could not activate the Trp63 promoter constructs, suggesting that Sox2 transactivates the Trp63 promoter. Next, we performed a chromatin immunoprecipitation (ChIP) to analyze whether Sox2 would directly bind to the minimal promoter region of the Trp63 gene in vivo. Therefore, we used chromatin isolated from A549 human bronchiolar lung cells and showed that SOX2 bound to the region covering the putative conserved

SOX2 binding sites in the 500 bp Trp63 promoter region (fig. 4C). Collectively, our data indicate a direct regulatory role for Sox2 in the transcriptional activation of the Trp63 gene, leading to the differentiation of naive epithelial cells into committed basal cells.

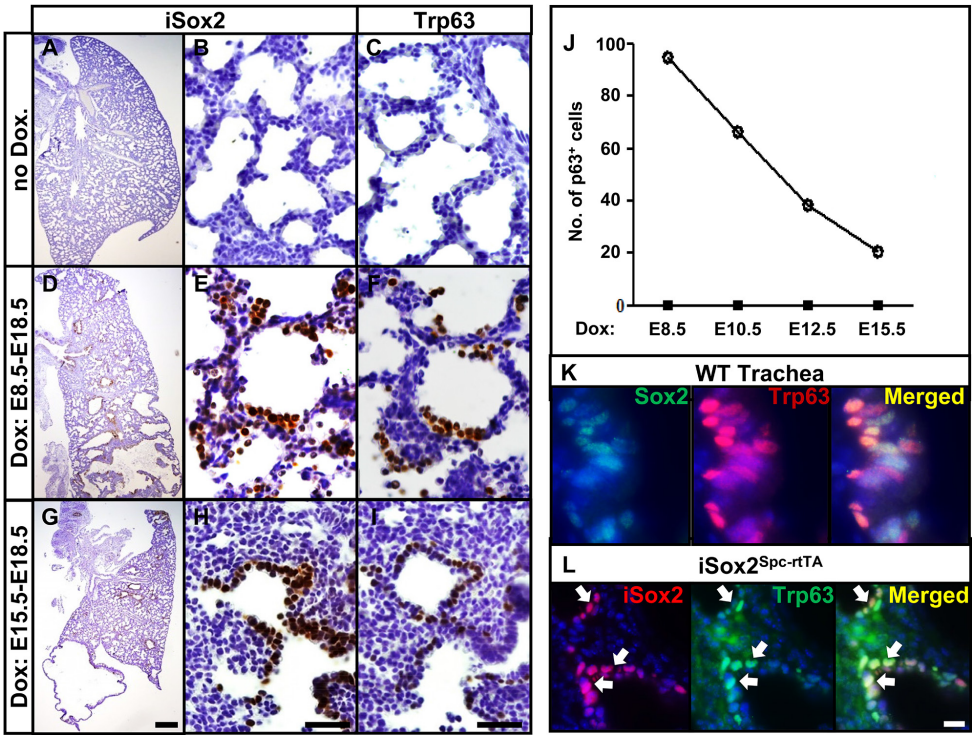

Figure 3. Progressive increase of basal cells in the alveolar epithelium with prolonged Sox2 induction. Control (A-C) and iSox2$^{SPC\text{-}rtTA}$ lungs exposed for 10 days (E8.5-E18.5; D-F) or 3 days (E15.5-E18.5; G-I) of doxycycline were isolated and analysed for the appearance of basal cells. The expression of the iSox2 transgene was evaluated using the myc-epitope specific antibody (A, D, G with corresponding details in B, E, H). Basal cells were detected in sequential sections with the Trp63 specific antibody in the distal, iSox2 positive regions of the iSox2SPC-rtTA lungs (C, F), but were completely absent in the controls (I). iSox2/Trp63 double positive cells were confirmed with immunofluorescence (L; iSox2 in red, Trp63 in green, double positive cells in yellow), and endogenous Trp63/Sox2 double positive cells were detected in the trachea of positive controls (K, Sox2 green, Trp63 red, Sox2 and Trp63 double positive cells in yellow). In iSox2$^{SPC\text{-}rtTA}$ lungs, the Trp63 expression decreased with the shorter time of doxycycline exposure. Quantification (J) of the number of differentiated basal cells (Y-axis) showed a linear correlation with iSox2 expression (start of expression indicated on X-axis). Open circles represent basal cell counts from the iSox2$^{SPC\text{-}rtTA}$ lungs, black boxes represent the control lungs. Three microscopic fields with a 40-times objective were analysed for intra-lobar Trp63 positive cells. The results are expressed as the average of the number of positive cells per field. Scale bars: 2mm (G), 50µm (H, I,) 25 µm (L).

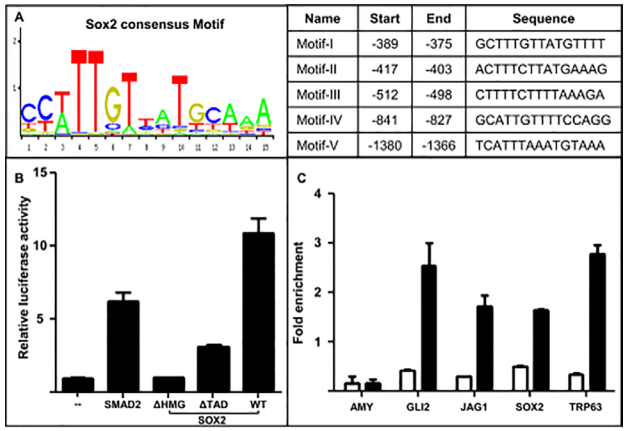

Name	Start	End	Sequence
Motif-I	-389	-375	GCTTTGTTATGTTTT
Motif-II	-417	-403	ACTTTCTTATGAAAG
Motif-III	-512	-498	CTTTTCTTTTAAAGA
Motif-IV	-841	-827	GCATTGTTTTCCAGG
Motif-V	-1380	-1366	TCATTTAAATGTAAA

Figure 4. Sox2 transactivates the Trp63 gene. (A) Schematic presentation of Sox2 consensus binding motif (left), and a table with the in silico analysis of Sox2 binding regions in a 1500 bp sequence immediately upstream the Trp63-ΔN promoter region. (B) Relative luciferase activity as a measurement of the transcriptional activity of the 500 bp Trp63-ΔN minimal promoter. The activity was significantly induced by the full length Sox2 (WT), but mutation of the HMG domain (ΔHMG) or the transactivation domain (ΔTAD) abolished the Sox2- mediated luciferase activity. SMAD2 served as positive control for the activation of the minimal promoter. (C) PCR analysis of A549 chromatin precipitated with IgG control immunoglobulins (white bars) or the Sox2 specific antibody (black bars). Negative control (AMY; Amylase), positive controls (GLI2 JAG1, SOX2), and the TRP63 specific primers flanking the TRP63-ΔN minimal promoter region were used in a standard PCR assay. Graphs depict representative results of 3 separate experiments performed in duplicate and expressed as mean standard deviation.

Aberrant Sox2 expression induces transcription factor Gata6

Recently, it was shown that numerous human squamous cell carcinomas showed increase expression of Trp63, which would promote proliferation and an increase in Gata6 expression (27). Based on the importance of Gata6 in the proximal-distal patterning of the lung (28) (29) and the capacity of Sox2 to differentiate naïve progenitors into Trp63 expressing basal cells (5), we investigated whether the induction of Trp63 by the transgenic Sox2 would also lead to an increased expression of Gata6. Dual immunofluorescence staining showed co-localization of Gata6 and iSox2 positive cells in induced iSox2$^{SPC\text{-}rtTA}$ lungs (fig. 5A). In contrast, very few Gata6 positive cells were detected in control lungs. In-silico matrix analysis of a minimal promoter region of the Gata6 gene surprisingly identified two putative Sox2 binding sites within 500 bp of a minimal Gata6 promoter. Subsequently, we showed that this fragment could be transcriptionally activated by the full length Sox2 in vitro, but not by the ΔHMG and ΔTAD mutant Sox2 (fig.5B). Moreover, SOX2 specifically bound this promoter region in vivo using a SOX2-specific ChIP on chromatin isolated from A549 cells (fig. 5C). Taken together, these data demonstrate that Sox2 directly regulated Gata6 expression in the lung.

Next, we showed that the Sox2 transgene induced proliferation by staining for phospho-Histone H3 (Phh3; fig. 5D), supporting the observed proliferation in the lung explants (fig. 2P-T), and that these Sox2/Phh3 double positive cells also expressed Gata6 (fig. 5E). Interestingly, the Gata6 positive cells also co-localized with the Trp63^{+} basal cells in the distal epithelium (fig 5F). Quantification of the different cell types, revealed that 17% of the Sox2^{+} cells were also Gata6^{+}, 21% was Sox2^{+}/Trp63^{+} and 15% was positive for all three

factors (fig.5G). Thus, our data indicated that Sox2 induced the activation of Trp63 and Gata6 leading to cellular changes, which eventually contributed to the morphological abnormalities in the Sox2$^{SPC\text{-}rtTA}$ lungs.

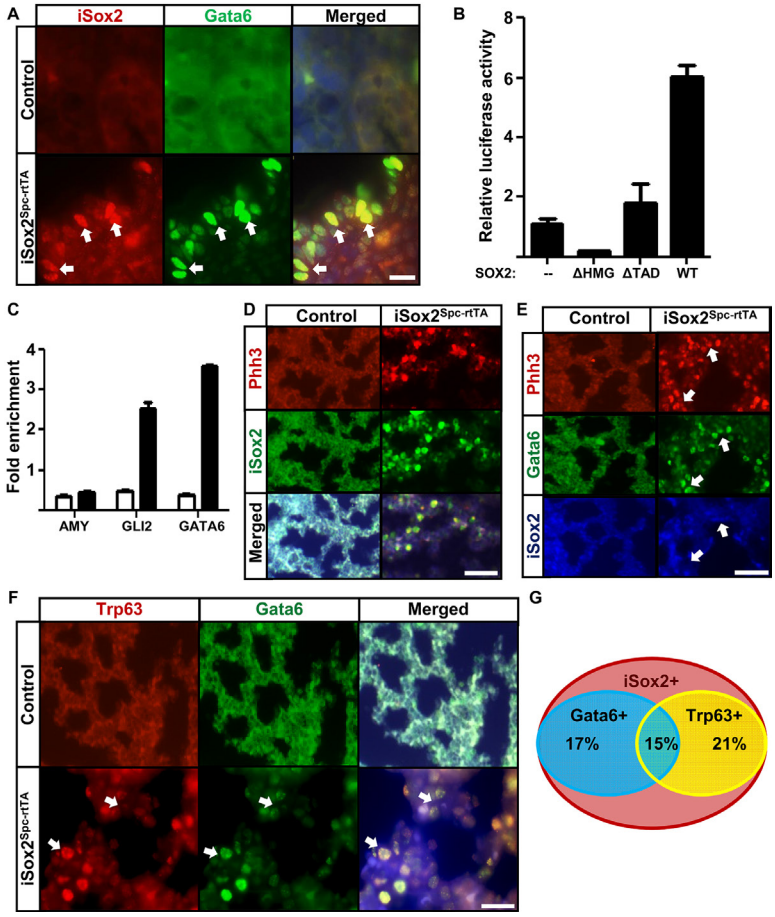

Figure 5. Sox2 induces proliferation and Gata6 expression. (A) Immunofluorescence detection of Myc-epitope (iSox2; red) and Gata6 (green) in E18.5 lung tissue from control (top) and iSox2SPC-rtTA (bottom) illustrating the co-expression of Gata6 and iSox2 (yellow, arrows). The full length Sox2 (WT) transactivates a 500 bp Gata6 promoter fragment (B), whereas the HMG domain (ΔHMG) or the transactivation domain (ΔTAD) mutated Sox2 did not. SOX2-specific ChIP analysis showed specific binding to this fragment in vivo (C; white bars represent the IgG immunoglobulin controls, black bars represent the SOX2 specific precipitation). Negative control (AMY, Amylase), positive control (GLI2) and GATA6 specific enrichment are indicated. Co-localization studies revealed that (D) Sox2 positive cells proliferate (Phh3 in red and myc-epitope in green), that (E) Sox2 (iSox2; blue) and Gata6 (green) double positive cells also proliferate (Phh3 in red), and that (F) Trp63 (red) and Gata6 (green) co-localize (yellow). Arrows in A, E and F indicate examples of positive cells. (G) Percentage of the total number of iSox2+ cells that are iSox2+/Gata6+ (17%), iSox2^{+}/Trp63^{+} (21%) or iSox2^{+}/Gata6^{+}/Trp63^{+} (15%). Scale bars: 100 µm (D, E) and,25 µm (A, F).

SOX2 expression in lungs of human CCAM patients

Since we observed a phenotype that resembled the human CCAM pathology, we analyzed the expression of SOX2 in lungs of human type I and type II CCAM patients. Surprisingly, no SOX2 positive cells were observed in the affected regions of the type I patients, but a prominent staining was present in the type II CCAM lungs (fig. 6A-F). In age-matched control lung samples no SOX2 positive cells were observed in the lung, although we did find positive cells in the upper bronchi. The SOX2 positive cells in the type II CCAM lungs co-expressed the TRP63 protein, which paralleled the findings in the $Sox2^{SPC\text{-}rtTA}$ mouse lungs.

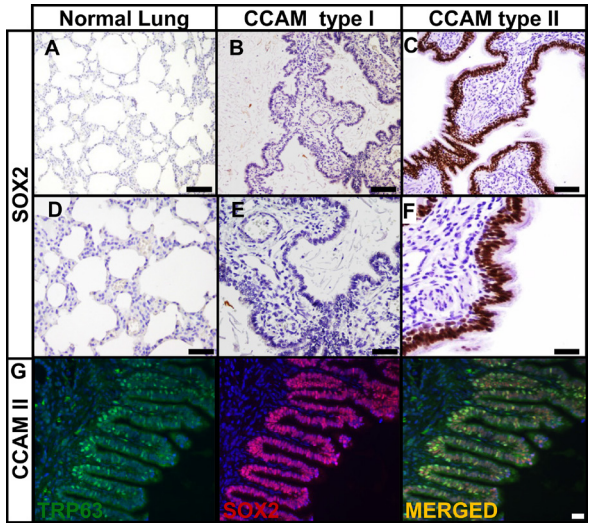

Figure 6. SOX2 expression in human lungs of type II CCAM patients

SOX2 expression is detected in lungs of human type II CCAM patients (C, F), but is absent in control (A, D) and type I CCAM samples (B, E). Moreover, the SOX2 positive cells (red) co-expressed the TRP63 (green) protein as detected by immunofluorescence (G). Scale bars: 200 µm (A-C) and 100 µm (D-G)

Discussion

The mammalian lung is a complex, highly branched organ consisting of airways and closely associated blood vessels required for life to exchange catabolic carbon dioxide and oxygen. The development from a primary bud protruding from the ventral foregut to the bronchial tree with a myriad of alveolar spaces can be described in five histologically defined stages: embryonal, pseudoglandular, canalicular, saccular and alveolar. However, at the cellular and molecular level it is more difficult to describe the development in separate stages, and the formation of the lung requires the intimate interaction between the endodermal epithelial cells and the surrounding mesenchyme. Several signaling cascades have been described that interact at different levels with each other to drive the expansion of the primitive branches. Over the years, many factors have been shown to be involved in the different processes, many of them are expressed in waves of cyclic expression patterns(1-2, 30). Sox2 is a key transcription factor involved in cell fate decision of neural and epithelial tissues (review by (9) and several studies by us and others have revealed specific roles of Sox2 in lung development by varying the level of expression (5-7). We have shown that ectopic expression of Sox2 induces the emergence of basal cells and neuroepithelial cells

(5). Here we show that Sox2 directly regulates the master gene Trp63, resulting in the differentiation of epithelial cells into basal cells. Moreover, we show that Sox2 directly regulates the expression of Gata6, which is possible involved in the emergence of the BASC cells.

Ectopic expression of iSox2 in the developing lung resulted in abnormal distal cysts resembling the human congenital disorder CCAM, which are congenital abnormalities of the respiratory tract characterized by multicystic lesions in pulmonary tissue with proliferation of bronchial structures (4). CCAMs can be detected by prenatal ultrasonography and the clinical manifestation ranges from total absence of abnormalities at birth till fetal polyhydramnios and hydrops fetalis. CCAMs are classified in five groups, depending on the size and histological appearance of the cyst. Type I CCAMs contain relatively large cysts, which can be solitary or multiple cysts; type II has multiple, small cysts, whereas type III is characterized by solid microcysts. Aside from these original three types of CCAMs, two additional types were added, type 0 with a bronchial-like histology, and type IV, with distal acinar lesions (4). The pathogenesis of CCAM is still elusive and most likely linked to developmental defects of the lung. So far, only a few studies have identified genes that may be associated with this abnormality, such as Fgf10, Hoxb5, CC10 and FABP-7 (reviewed in (31)). We analyzed the expression of SOX2 and TRP63 in the lungs of human CCAM type I and type II patients. Surprisingly, SOX2 was only detected in the affected areas of the type II CCAM samples and was completely absent in the type I CCAM samples. This indicates that the affected epithelium in the type I CCAMs is composed of totally different cell types than the type II CCAM epithelium. Moreover, it suggests that the developmental origin of the two types of CCAM is different, maybe related to the timing of the onset of the disease.

In order to further evaluate the putative involvement of Sox2 in CCAM pathogenesis, we modulated the timing of Sox2 transgene expression. This resulted in variable cysts in the iSox2$^{SPC\text{-}rtTA}$ mouse lungs, ranging from small to large, inversely correlating with the time of iSox2 expression. We speculated that the cysts were induced as a result of the premature differentiation of epithelial tip cells, leading to an arrest in branching of the epithelium. Therefore, we first wanted to know whether cells expressing the transgenic iSox2 were able to respond to the branch-inducing Fgf10 growth factor. Using lung explants and mesenchyme free endoderm cultures we showed that the cells expressing iSox2 do not respond to the branch inducing signaling molecule Fgf10. In situ hybridization and quantitative PCR analysis revealed no change in the expression of the FgfR2 isoforms IIIb and IIIc, indicating that Sox2 acts downstream of this signaling cascade ((5); data not shown). In addition, we previously showed that tip cells in the lungs of the iSox2$^{SPC\text{-}rtTA}$ mouse did not express nuclear phosphorylated ERK1/2 (phosphor-p42/44 MAP kinase), the activated downstream mediator of the Fgf10/FgfR signaling pathway. Instead, the activated mediator ot Bmp4 signaling, nuclear phosphorylated SMAD1/5/8, was increased, indicating that the cells were differentiating (5). This is in line with previous data from us and others showing that Fgf10/FgfR2 signaling acts upstream of Sox2 and is not influenced by manipulating the level of Sox2 expression (5, 7). Fgf10 signaling in tip cells activates β-catenin signaling, which in turn inhibits Sox2 expression and prevents Id2^{+} progenitor cells from differentiating into epithelial cells (11, 32-34). Indeed, the inability of the iSox2$^{SPC\text{-}rtTA}$ cells to respond to Fgf10 is caused by the dominant effect of Sox2 on cellular differentiation by directing cells towards a proximal cell fate, such as basal cells.

In addition, we also found that Sox2 induces proliferation in embryonic lungs and in fetal lung explants, extending previous results obtained in adult mice (6). Collectively, our data suggest that the cystic structures are caused by a combination of the fact that tip cells are induced by Sox2 to differentiate into cells with a proximal fate, thereby losing their ability to respond to Fgf10, and the fact that Sox2 induces proliferation. The proliferation caused the epithelial buds to grow without forming new branches, resulting in a ballooning of the existing bud.

Similar cyst-like abnormalities to those we observed in iSox2$^{SPC\text{-}rtTA}$ mice have been reported in several other studies. Ectopic expression of the Wnt downstream mediator β-catenin in the airway epithelium resulted in the loss of Sox2 and p63 expression in proximal derivatives, indicating that Wnt signaling inhibits the differentiation of Sox2 positive proximal cells (34). The mesenchymal-specific TgfβRII knockout showed increased levels of Ptc and Gli1, two downstream mediators of Shh signaling (35). Inhibition of the Wnt signaling pathway by either expressing the Dkk1 antagonist, or by tissue-specific deletion of β-catenin resulted in an expansion of proximal cell types at the expense of distal cells. Moreover, β-catenin and Lef/Tcf activated the promoter of Bmp4 (36). It was also shown that conditional deletion of the two Bmp receptors Bmpr1a and Bmpr1b early in lung development resulted in trachea agenesis, ectopic formation of lung buds and an expansion of Sox2 and p63 positive cells, indicating that Bmp signaling inhibits the differentiation of Sox2 positive cells, at least early in development (37). Later in development, Bmp signaling is required for the proliferation and survival of distal tip cells (38). It is clear that complex interactions of different signaling pathways, such as Wnt, Fgf and Bmp, are required for the correct development of the lung, and interfering with one of the players may affect the formation of the lung at different levels. Recently, it was shown that the molecular programs involved in airway branching to create the bronchial tree, and alveolar formation to increase the gas exchange area are mutual exclusive (39). Activating the branching program by expressing a hyperactive Kras, which is downstream of Fgf10/Fgfr signaling, in lung progenitors resulted in the abrogation of the alveolar program. In contrast, the conditional deletion of Sox9, a marker of distal, alveolar cells, resulted in reduced branching(39). These data perfectly fit with our data that premature differentiation of cells into the proximal airway fate prevent further branching.

We show that the induced cellular changes observed in the iSox2$^{SPC\text{-}rtTA}$ transgenic lungs are the result of the direct regulation of the basal cell specific Trp63 gene by Sox2. Previously, we showed by microarray analysis and RT-PCR that lungs from iSox2S$^{PC\text{-}rtTA}$ mice had increased levels of p63 and specifically the ΔN Trp63 isoform. Here, we show that Sox2 transactivates a minimal ΔN Trp63 promoter construct and also binds to the ΔN Trp63 promoter in vivo. These data now provide molecular evidence for previous findings by us and others that Sox2 would be upstream of Trp63 (5, 12, 34). Interestingly, Fgf10 prevented lung progenitor tip cells from differentiating into the proximal, Sox2^{+} lineage, but once epithelial cells were committed to the Sox2^{+} lineage, Fgf10 would positive regulate basal cell differentiation. However, the latter may also be regulated by other Fgfs, such as Fgf7 (40). Interestingly, it was reported that p63 directly transactivated the Fgfr2 gene, the major receptor for Fgf7 and Fgf10 (41). Since we did not find changes in the expression of Fgfr2, it may suggest that even the ectopically expressing Sox2 cells still express the Fgfr2, which would be required for correct differentiation into the basal cell lineage. Based on the putative relation between Trp63 and Gata6 (27), and the important role of Gata6 in

the regulation of yet another cell with progenitor properties, the bronchioalveolar stem cells (42), we analyzed the expression of Gata6 in our mouse model. Surprisingly, when we analyzed the transgenic lungs for the expression of Gata6, we found that Sox2 directly regulates transcription of Gata6, as shown by the co-localization of Sox2 and Gata6, luciferase activity assays and by ChIP technology. Gata transcription factors are zinc finger proteins which are an essential cis-acting element in the promoters and enhancers of a variety of genes. Gata6, a member of this family, is expressed during lung development and in proximal bronchiolar epithelium (28). Since the full knockout of Gata6 is lethal early during gestation (43), the effect of Gata6 on lung development is based on the manipulation of the expression levels (28, 42). These studies showed that Gata6 is required for lung branching and late epithelial cell differentiation (28). Moreover, conditional depletion of Gata6 showed its role in the emergence of lung $CC10^{+}/SPC^{+}$ progenitor cells (42). Therefore, the induced expression of Gata6 by Sox2 may contribute to the emergence of the observed phenotype. Moreover, the association of Gata6 with Wnt signaling (44), and the complex formation of Sox2 with the Wnt downstream mediator β-catenin (34) suggests a complex network of transcription factors and signaling molecules involving Sox2, Gata6 and Wnt. The present findings that Sox2 transactivates Gata6 support a potential regulatory role for Sox2 in Gata6 expression in late phases of lung development.

In conclusion, our results show for the first time that Sox2 directly binds and transactivates the ΔN Trp63 promoter, thereby initiating the emergence of the basal cell lineage in lung epithelium. Moreover, we show that Sox2 also activates the Gata6 promoter, which contributes to the development of bronchioalveolar stem cells. In normal lung development, Fgf10 is required to maintain the Id2+ population and the naïve epithelium in order to branch (40, 45). As cells become more distant from the Fgf10 source, they start to adopt the proximal cell fate and express Sox2, leading to the emergence of proximal cell types, such as basal cell, ciliated cells and Clara cells. Ectopic expression of Sox2 from an exogenous promoter (SPC) results cells that are not responsive anymore to Fgf10. Instead, the cells immediately become proximal cells, leading to a reduced branching. Moreover, the cells proliferate, thereby forming a cyst-like structure (fig. 7). Importantly, we correlated our findings of the $Sox2^{Spc\text{-}rtTA}$ mice with human CCAM patient material, which surprisingly showed that SOX2 and TRP63 are expressed in lungs from type II CCAM patients, but not in lungs from type I CCAM patients.

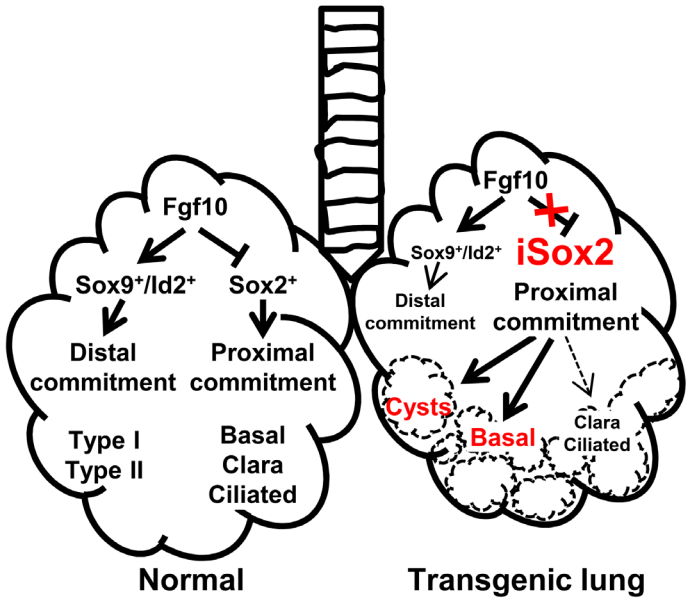

Figure 7. Schematic representation of our findings. Left part shows the normal developmental context of Sox2, whereas the right part shows the effect of the iSox2 expression. See text in the discussion for details.

Acknowledgements
This work was supported by the Sophia Foundation for Medical research, SSWO nr 585. We apologize for omitting references due to space restrains. We are indepted to professor Jeffrey Whitsett for providing the SPC-rtTA mice and professor Angie Rizzino for providing the Sox2 mutant plasmids.

References

1. Warburton D, El-Hashash A, Carraro G, Tiozzo C, Sala F, Rogers O, De Langhe S, Kemp PJ, Riccardi D, Torday J, Bellusci S, Shi W, Lubkin SR, Jesudason E. Lung organogenesis. Curr Top Dev Biol 2010;90:73-158.
2. Morrisey EE, Hogan BL. Preparing for the first breath: Genetic and cellular mechanisms in lung development. Dev Cell 2010;18(1):8-23.
3. Rottier R, Tibboel D. Fetal lung and diaphragm development in congenital diaphragmatic hernia. Semin Perinatol 2005;29(2):86-93.
4. Stocker JT, Madewell JE, Drake RM. Congenital cystic adenomatoid malformation of the lung. Classification and morphologic spectrum. Hum Pathol 1977;8(2):155-171.
5. Gontan C, de Munck A, Vermeij M, Grosveld F, Tibboel D, Rottier R. Sox2 is important for two crucial processes in lung development: Branching morphogenesis and epithelial cell differentiation. Dev Biol 2008;317(1):296-309.
6. Tompkins DH, Besnard V, Lange AW, Keiser AR, Wert SE, Bruno MD, Whitsett JA. Sox2 activates cell proliferation and differentiation in the respiratory epithelium. Am J Respir Cell Mol Biol 2011;45(1):101-110.
7. Que J, Luo X, Schwartz RJ, Hogan BL. Multiple roles for sox2 in the developing and adult mouse trachea. Development 2009;136(11):1899-1907.
8. Avilion AA, Nicolis SK, Pevny LH, Perez L, Vivian N, Lovell-Badge R. Multipotent cell lineages in early mouse development depend on sox2 function. Genes Dev 2003;17(1):126-140.
9. Sarkar A, Hochedlinger K. The sox family of transcription factors: Versatile regulators of stem and progenitor cell fate. Cell Stem Cell 2013;12(1):15-30.
10. Takahashi K, Yamanaka S. Induction of pluripotent stem cells from mouse embryonic and adult fibroblast cultures by defined factors. Cell 2006;126(4):663-676.
11. Que J, Okubo T, Goldenring JR, Nam KT, Kurotani R, Morrisey EE, Taranova O, Pevny LH, Hogan BL. Multiple dose-dependent roles for sox2 in the patterning and differentiation of anterior foregut endoderm. Development 2007;134(13):2521-2531.
12. Lu Y, Futtner C, Rock JR, Xu X, Whitworth W, Hogan BL, Onaitis MW. Evidence that sox2 overexpression is oncogenic in the lung. PLoS One 2010;5(6):e11022.
13. Evans MJ, Van Winkle LS, Fanucchi MV, Plopper CG. Cellular and molecular characteristics of basal cells in airway epithelium. Exp Lung Res 2001;27(5):401-415.
14. Rock JR, Onaitis MW, Rawlins EL, Lu Y, Clark CP, Xue Y, Randell SH, Hogan BL. Basal cells as stem cells of the mouse trachea and human airway epithelium. Proc Natl Acad Sci U S A 2009;106(31):12771-12775.
15. Daniely Y, Liao G, Dixon D, Linnoila RI, Lori A, Randell SH, Oren M, Jetten AM. Critical role of p63 in the development of a normal esophageal and tracheobronchial epithelium. Am J Physiol Cell Physiol 2004;287(1):C171-181.
16. Bilal H, Handra-Luca A, Bertrand JC, Fouret PJ. P63 is expressed in basal and myoepithelial cells of human normal and tumor salivary gland tissues. J Histochem Cytochem 2003;51(2):133-139.
17. Yang A, Schweitzer R, Sun D, Kaghad M, Walker N, Bronson RT, Tabin C, Sharpe A, Caput D, Crum C, McKeon F. P63 is essential for regenerative proliferation in limb, craniofacial and epithelial development. Nature 1999;398(6729):714-718.
18. Mills AA, Zheng B, Wang XJ, Vogel H, Roop DR, Bradley A. P63 is a p53 homologue required for limb and epidermal morphogenesis. Nature 1999;398(6729):708-713.
19. Romano RA, Smalley K, Magraw C, Serna VA, Kurita T, Raghavan S, Sinha S. Deltanp63 knockout mice reveal its indispensable role as a master regulator of epithelial development and differentiation. Development 2012;139(4):772-782.
20. Birkaya B, Ortt K, Sinha S. Novel in vivo targets of deltanp63 in keratinocytes identified by a modified chromatin immunoprecipitation approach. BMC Mol Biol 2007;8:43.
21. Helton ES, Zhu J, Chen X. The unique nh2-terminally deleted (deltan) residues, the pxxp motif, and the ppxy motif are required for the transcriptional activity of the deltan variant of p63. J Biol Chem 2006;281(5):2533-2542.
22. Ortt K, Raveh E, Gat U, Sinha S. A chromatin immunoprecipitation screen in mouse keratinocytes reveals runx1 as a direct transcriptional target of deltanp63. J Cell Biochem 2008;104(4):1204-1219.
23. Romano RA, Ortt K, Birkaya B, Smalley K, Sinha S. An active role of the deltan isoform of p63 in regulating basal keratin genes k5 and k14 and directing epidermal cell fate. PLoS One 2009;4(5):e5623.
24. Raghoebir L, Bakker ER, Mills JC, Swagemakers S, Buscop-van Kempen M, Boerema-de Munck A, Driegen S, Meijer D, Grosveld F, Tibboel D, Smits R, Rottier RJ. Sox2 redirects the developmental fate of the intestinal epithelium toward a premature gastric phenotype. J Mol Cell Biol 2012;4(6):377-385.
25. Perl AK, Tichelaar JW, Whitsett JA. Conditional gene expression in the respiratory epithelium of the mouse. Transgenic Res 2002;11(1):21-29.
26. Fukunishi N, Katoh I, Tomimori Y, Tsukinoki K, Hata R, Nakao A, Ikawa Y, Kurata S. Induction of deltanp63 by

the newly identified keratinocyte-specific transforming growth factor beta signaling pathway with smad2 and ikappab kinase alpha in squamous cell carcinoma. Neoplasia 2010;12(12):969-979.
27. Wang H, Liu Z, Li J, Zhao X, Wang Z, Xu H. Deltanp63alpha mediates proliferation and apoptosis in human gastric cancer cells by the regulation of gata-6. Neoplasma 2012;59(4):416-423.
28. Koutsourakis M, Keijzer R, Visser P, Post M, Tibboel D, Grosveld F. Branching and differentiation defects in pulmonary epithelium with elevated gata6 expression. Mech Dev 2001;105(1-2):105-114.
29. Yang H, Lu MM, Zhang L, Whitsett JA, Morrisey EE. Gata6 regulates differentiation of distal lung epithelium. Development 2002;129(9):2233-2246.
30. Metzger RJ, Klein OD, Martin GR, Krasnow MA. The branching programme of mouse lung development. Nature 2008;453(7196):745-750.
31. Correia-Pinto J, Gonzaga S, Huang Y, Rottier R. Congenital lung lesions--underlying molecular mechanisms. Semin Pediatr Surg 2010;19(3):171-179.
32. Ramasamy SK, Mailleux AA, Gupte VV, Mata F, Sala FG, Veltmaat JM, Del Moral PM, De Langhe S, Parsa S, Kelly LK, Kelly R, Shia W, Keshet E, Minoo P, Warburton D, Bellusci S. Fgf10 dosage is critical for the amplification of epithelial cell progenitors and for the formation of multiple mesenchymal lineages during lung development. Dev Biol 2007;307(2):237-247.
33. Nyeng P, Norgaard GA, Kobberup S, Jensen J. Fgf10 maintains distal lung bud epithelium and excessive signaling leads to progenitor state arrest, distalization, and goblet cell metaplasia. BMC Dev Biol 2008;8:2.
34. Hashimoto S, Chen H, Que J, Brockway BL, Drake JA, Snyder JC, Randell SH, Stripp BR. Beta-catenin-sox2 signaling regulates the fate of developing airway epithelium. J Cell Sci 2012;125(Pt 4):932-942.
35. Li M, Li C, Liu YH, Xing Y, Hu L, Borok Z, Kwong KY, Minoo P. Mesodermal deletion of transforming growth factor-beta receptor ii disrupts lung epithelial morphogenesis: Cross-talk between tgf-beta and sonic hedgehog pathways. J Biol Chem 2008;283(52):36257-36264.
36. Shu W, Guttentag S, Wang Z, Andl T, Ballard P, Lu MM, Piccolo S, Birchmeier W, Whitsett JA, Millar SE, Morrisey EE. Wnt/beta-catenin signaling acts upstream of n-myc, bmp4, and fgf signaling to regulate proximal-distal patterning in the lung. Dev Biol 2005;283(1):226-239.
37. Domyan ET, Ferretti E, Throckmorton K, Mishina Y, Nicolis SK, Sun X. Signaling through bmp receptors promotes respiratory identity in the foregut via repression of sox2. Development 2011;138(5):971-981.
38. Eblaghie MC, Reedy M, Oliver T, Mishina Y, Hogan BL. Evidence that autocrine signaling through bmpr1a regulates the proliferation, survival and morphogenetic behavior of distal lung epithelial cells. Dev Biol 2006;291(1):67-82.
39. Chang DR, Martinez Alanis D, Miller RK, Ji H, Akiyama H, McCrea PD, Chen J. Lung epithelial branching program antagonizes alveolar differentiation. Proc Natl Acad Sci U S A 2013.
40. Volckaert T, Campbell A, Dill E, Li C, Minoo P, De Langhe S. Localized fgf10 expression is not required for lung branching morphogenesis but prevents differentiation of epithelial progenitors. Development 2013;140(18):3731-3742.
41. Ramsey MR, Wilson C, Ory B, Rothenberg SM, Faquin W, Mills AA, Ellisen LW. Fgfr2 signaling underlies p63 oncogenic function in squamous cell carcinoma. J Clin Invest 2013;123(8):3525-3538.
42. Zhang Y, Goss AM, Cohen ED, Kadzik R, Lepore JJ, Muthukumaraswamy K, Yang J, DeMayo FJ, Whitsett JA, Parmacek MS, Morrisey EE. A gata6-wnt pathway required for epithelial stem cell development and airway regeneration. Nat Genet 2008;40(7):862-870.
43. Koutsourakis M, Langeveld A, Patient R, Beddington R, Grosveld F. The transcription factor gata6 is essential for early extraembryonic development. Development 1999;126(9):723-732.
44. Zhong Y, Wang Z, Fu B, Pan F, Yachida S, Dhara M, Albesiano E, Li L, Naito Y, Vilardell F, Cummings C, Martinelli P, Li A, Yonescu R, Ma Q, Griffin CA, Real FX, Iacobuzio-Donahue CA. Gata6 activates wnt signaling in pancreatic cancer by negatively regulating the wnt antagonist dickkopf-1. PLoS One 2011;6(7):e22129.
45. Rawlins EL, Clark CP, Xue Y, Hogan BL. The id2+ distal tip lung epithelium contains individual multipotent embryonic progenitor cells. Development 2009;136(22):3741-3745.

Supplemental materials and methods, Ochieng et al.

Mouse breeding and genotyping

Mice were kept standard conditions and experiments were performed according to guidelines of the local ethics committee. The iSox2 transgenic mouse line was crossed with the SPC-rtTA transgenic mice (generous gift of Jeffrey Whitsett, Cincinnati), subsequently referred to as iSox2SPC-rtTA (1, 2). Doxycycline was administered in drinking water (2 mg/ml doxycycline, 5% sucrose) and each experiment was executed on at least three independent litters containing iSox2SPC-rtTA, single transgenic and wild type pups.

Tissue preparation and Immunohistochemistry

Human lung samples were retrieved from the archives of the Department of Pathology, Erasmus MC, Rotterdam, following approval by the Erasmus MC Medical Ethical Committee. Mouse lungs were processed according to routine protocols (1, 3). Antibodies used: myc-epitope (1:800, Roche) Sox2 (1:500; Immune system), phospho-histone H3 (1:1000; Abcam), Trp63 (1:200; Santa Cruz), Gata6 (1:200; Santa Cruz). Secondary antibodies were either coupled with HRP, or fluorescently labelled (Alexa 350, 488 and 549).

Mesenchyme free lung epithelial tubes (MFLET)and lung explants

Embryos from iSox2SPC-rtTA mice were isolated at E11.5, incubated with 2U/ml Dispase (Roche) for 30 minutes on ice and the mesenchyme was subsequently removed using tungsten needles. MatrigelTM (BD Bioscience) was diluted 1:1 in culture medium (50% DMEM (Gibco), 50% Ham's F12 (CellGrow), with penicillin, streptomycin (Gibco). The isolated endoderm was embedded in matrigel with 250 ng/ml Fgf10 (R&D systems). After polymerization of the matrigel at 37oC, culture medium was added with or without 0.6µM doxycycline, and cultured at 37°C in 5% CO2/95% air for 5 days.

Air-liquid interphase lung explant cultures were established by isolating intact E11.5 mouse embryonic lungs, which were placed on 8.0µm Whatman Nucleopore membranes (Whatman) floating on 1:1 DMEM:F12 culture medium (Invitrogen). Heparin beads were soaked in Fgf10 (500 ng/µl) or PBS and carefully added to the explants.

Cloning, Cell Culture and Transfection

The minimal promoters of the Trp63 ΔN gene and the Gata6 gene were PCR-amplified from mouse genomic DNA (primers listed in Table 1), and cloned into the pGL4 luciferase vector (Promega, Germany). HEK-293T cells were transiently transfected using Lipofectamine LTX (Invitrogen) with the Renilla luciferase plasmid (transfection control), one of the firefly luciferase reporter plasmids (pGL4, pGL4-Trp63-500bp or pGL4-Gata6-500bp), and 2.5 µg of expression plasmid (pcDNA3-control, , Sox2-WT, Sox2-ΔHMG or Sox2-ΔTAD; generous gifts of Angie Rizzino)(4). Luciferase activity was measured using the Dual-Luciferase Reporter Assay system (Promega, Germany).

Chromatin Immunoprecipitation assays

ChIP assays were performed essentially as previously described, using 6x107 A549 cells cultured in 150 µM CoCl2 to induce hypoxia (3, 5). Crosslinking chromatin was incubated with protein A/G plus beads and normal mouse IgG (1.5 µg) or 5 µg ChIP grade SOX2 (Millipore). were reverse crosslinked by incubation in 0.3 M NaCl and RNase A at 65°C overnight. DNA was isolated by phenol/chloroform extraction, ethanol precipitation and resuspended in 50 µl H20. DNA from the DNA-protein complexes was analysed by QPCR.

The fold enrichment of SOX2-precipitated DNA relative to IgG control samples was based on the ΔC(t) method and normalized to input samples. PCR primers are listed in table 1.

References

1. Gontan C, de Munck A, Vermeij M, Grosveld F, Tibboel D, Rottier R. Sox2 is important for two crucial processes in lung development: Branching morphogenesis and epithelial cell differentiation. Dev Biol 2008;317(1):296-309.
2. Perl AK, Tichelaar JW, Whitsett JA. Conditional gene expression in the respiratory epithelium of the mouse. Transgenic Res 2002;11(1):21-29.
3. Raghoebir L, Bakker ER, Mills JC, Swagemakers S, Buscop-van Kempen M, Boerema-de Munck A, Driegen S, Meijer D, Grosveld F, Tibboel D, Smits R, Rottier RJ. Sox2 redirects the developmental fate of the intestinal epithelium toward a premature gastric phenotype. J Mol Cell Biol 2012;4(6):377-385.
4. Cox JL, Mallanna SK, Luo X, Rizzino A. Sox2 uses multiple domains to associate with proteins present in sox2-protein complexes. PLoS One 2010;5(11):e15486.
5. Huang Y, Kapere Ochieng J, Kempen MB, Munck AB, Swagemakers S, van Ijcken W, Grosveld F, Tibboel D, Rottier RJ. Hypoxia inducible factor 3alpha plays a critical role in alveolarization and distal epithelial cell differentiation during mouse lung development. PLoS One 2013;8(2):e57695.

Table 1. Primers used for ChIP and PCR-cloning

Primers used for quantitative-PCR		
	Forward	**Reverse**
hSOX2	5' CATGCACCGCTACGACG 3'	5' CGGACTTGACCACCGAAC 3'
h JAG1	5' GCA GAG CGG TAA GCA CTT AAT 3'	5' GTT TGG ATG GCG GTT TAT TT 3'
hGLI2	5' TAG AAT TGC TCC TGC ACT TC 3'	5' ATG TCG GAT GAC CCT TTC TC 3'
hAMYLASE	5' GGG AAAA GGC AGC ATA TTG 3'	5' CAC GCT AAA TTG CCT GTG AA 3'
TRP63	5' ATG GGA AAG GCT TTG CCA CC 3'	5' CAG TCT CTT CTT GCT AGG TA 3'
GATA6	5' ATCTTGGTTAAAGCGGCGATGG 3'	5'CAGCGGTGAATCAAGCGGTA 3'
PCR and Cloning Oligos		
0,5 kb Trp63 Promoter	5' CAGCTCGAGATGGCAAGA-CAAGTTACTTC 3'	5' CAGAGATCTCTAGACAACA-GAATGGTCAA 3'
0,5 kb Gata6 Promoter	5' CAGAGATCTCAATGACCTTTCCGG-CAACC 3'	5' CAGCTCGAGCCAAC-GATACGGGTCACCTT 3'

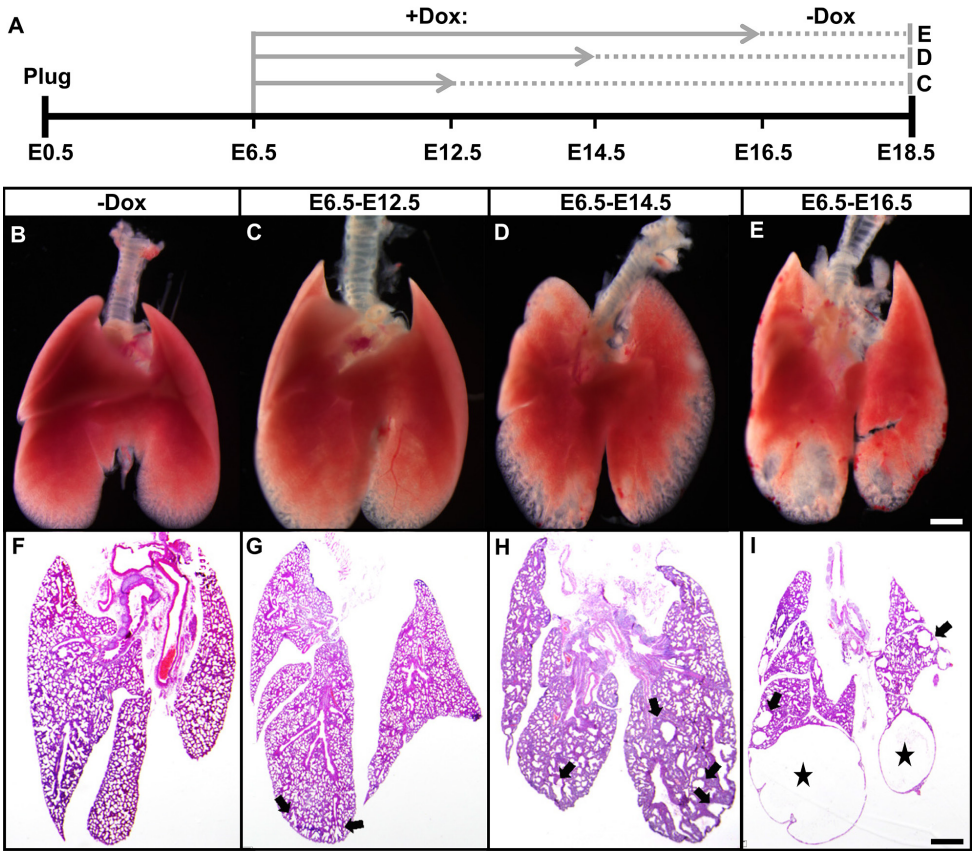

Supplemental figure 1. Reactivation of branching morphogenesis upon silencing of ectopic Sox2 expression. Control and iSox2$^{Spc\text{-}rtTA}$ mice were treated with doxycycline for a specified period (solid line), after which the mice were switched towards drinking water without doxycycline (dotted line) as indicated in the schematic overview (A). Lungs were isolated at E18.5 and analysis of the external appearances shows that the lung development was initiated or reactivated upon reversal to non-doxycycline water (B-E). Low power images (F-I) of haematoxylin/eosin stained sections show the cystic malformations in the Sox2 transgenic lungs. Scale bars: 2 mm (E, I).

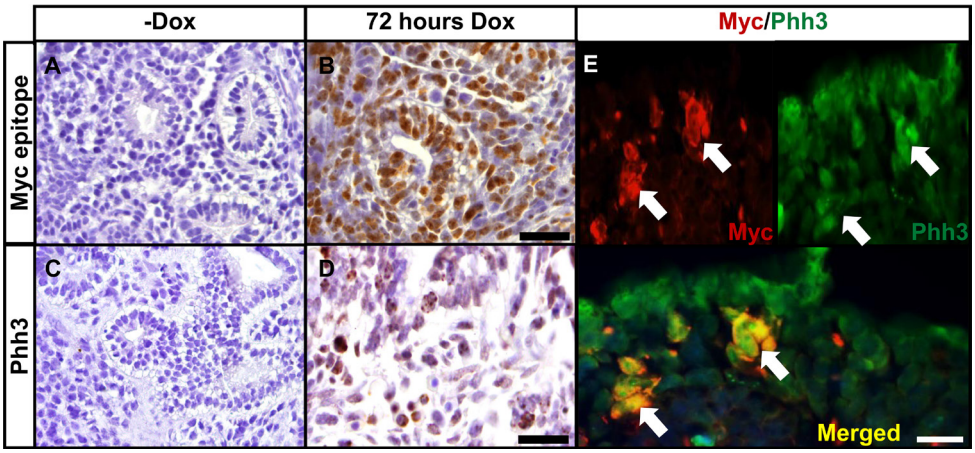

Supplemental figure 2. Induction of ectopic Sox2 induces proliferation in lung explants. Lung explants of iSox2$^{Spc\text{-}rtTA}$ untreated (A, C) or treated with doxycycline for 72 hours (B, D) stained with antibodies against the myc-epitope (A, B) or Phh3 (C, D) shows specific proliferation in the iSox2Spc-rtTA explants. Co-localization (yellow) of the iSox2 (Myc, red) and Phh3 (green) was only observed in the doxycycline treated explants (E). Scale bars: 50 µm (P, Q, R, S) and 25 µm (T).

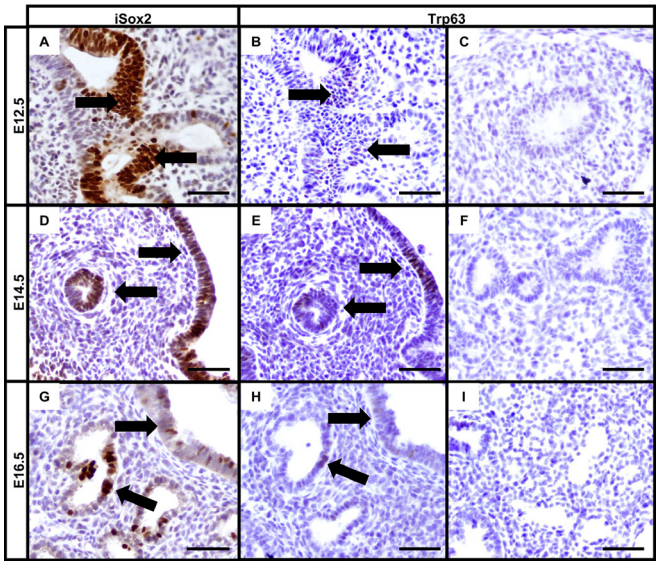

Supplemental figure 3. Induction of Trp63 upon iSox2 expression. Control (C, F, G) and iSox2$^{Spc\text{-}rtTA}$ mice (A-B, D-E, G-H) were treated with doxycycline from E6.5 until the lungs were isolated at E12.5 (A-C), E14.5 (D-F) or E16.5 (G-I). Sections were stained with the myc epitope to detect the transgenic protein (iSox2; A, D, G), which was absent in the control samples (not shown). Trp63 staining revealed a gradual increase of Trp63+ cells in the lungs of the iSox2$^{Spc\text{-}rtTA}$ mice (B, E, H), which correlated with the site of iSox2 expression (arrows show examples). No Trp63 positive cells were detected in the control samples (C, F, I). Size bars:50 µm

Chapter 3.

Differentiated type II pneumocytes can be reprogrammed by ectopic Sox2 expression

Joshua Kapere Ochieng, Kim Schilders, Heleen Kool, Marjon Buscop-van Kempen, Anne Boerema-De Munck, Frank Grosveld, Rene Wijnen, Dick Tibboel, Robbert J Rottier

PLoS ONE 2014; 9(9)

Abstract

The adult lung contains several distinct stem cells, although their properties and full potential are still being sorted out. We previously showed that ectopic Sox2 expression in the developing lung manipulated the fate of differentiating cells. Here, we addressed the question whether fully differentiated cells could be redirected towards another cell type. Therefore, we used transgenic mice to express an inducible Sox2 construct in type II pneumocytes, which are situated in the distal, respiratory areas of the lung. Within three days after the induction of the transgene, the type II cells start to proliferate and form clusters of cuboidal cells. Prolonged Sox2 expression resulted in the reversal of the type II cell towards a more embryonic, precursor-like cell, being positive for the stem cell markers Sca1 and Ssea1. Moreover, the cells started to co-express Spc and Cc10, characteristics of bronchioalveolar stem cells. We demonstrated that Sox2 directly regulates the expression of Sca1. Subsequently, these cells expressed Trp63, a marker for basal cells of the trachea. So, we show that the expression of one transcription factor in fully differentiated, distal lung cells changes their fate towards proximal cells through intermediate cell types. This may have implications for regenerative medicine, and repair of diseased and damaged lungs.

Introduction

The mammalian lung is a complex organ with a large and highly vascularized epithelial surface area. The airway epithelium is lined with a diversity of cell types that vary in abundance along the proximal-distal axis. The conducting airways have a pseudostratified epithelium to facilitate mucociliary transport, which gradually transforms into a simple columnar and cuboidal epithelium. Finally, the respiratory part of the lungs consists of squamous epithelium for efficient gas exchange. Cellular homeostasis is important for the maintenance of the lung, and in mature lungs, cell turnover and proliferation is low (1). However, after bronchiolar injury, either infections or mechanical insults such as artificial ventilation to the lung, the respiratory epithelium extensively proliferate to regenerate and repair the injured lung, indicating the presence of lung progenitor cells (2, 3).

In general, lung stem/progenitor cells should have the capacity to self-renew and differentiate into specialized cell lineages. In mouse, endogenous adult progenitor/stem cells function to repopulate the damaged lung epithelium (4-6). Several distinct populations of stem/progenitor cells have been described to be present in the conducting and respiratory epithelium (2, 6-10). Lineage tracing studies in mice have shown that the proximal airway basal cells act as stem cells, giving rise to Clara and ciliated cells during lung injury (11, 12). On the other hand, recent data suggest that Clara cells may differentiate into Trp63 positive basal cells in damaged lung parenchyma and into alveolar type II cells upon bleomycin treatment or influenza infection (2, 13). Other putative proximal stem cells include a subpopulation of toxin-resistant Clara cells that function as bronchiolar stem cells located within two discrete cell niches: the neuroepithelial body (NEB) and the bronchoalveolar duct junction (BADJ) (11, 14, 15). Moreover, several studies have shown the differentiation of type II cells into type I cells (2, 16). Thus, intrinsic cell populations exist in the lung that may be triggered to differentiate into distinct cell types.

Sox2 is among other transcription factors essential for lung development and maturation (17-19). Sox2 is a member of the highly conserved HMG box family of transcription factors and required early in embryonic development to maintain pluripotency and self-renewal in embryonic stem (ES) cells. In mice, Sox2 is required for normal morphogenesis and homeostasis of diverse tissues, including neural stem cells; retinal stem cells taste buds; hair sensory follicles in the ear; and epithelia of trachea, lung, and esophagus (17, 20-22). Sox2 is one of the original factors together with Oct4, Klf4, and c-Myc required for the reprogramming of somatic cells (23). In the embryonic lung, Sox2 is expressed in the developing respiratory epithelium, whereas in adult lungs, expression of Sox2 is restricted in epithelial cells, in the adult trachea, airway/bronchiolar epithelium and the conducting airways (17, 24, 25). Sox2 is completely absent from the respiratory airways, where another member of the Sry-box family, Sox9, is expressed. Thus, Sox2 and Sox9 show a reciprocal expression pattern in the lung.

Many reports have described variations of the original cocktail of factors to generate multipotent iPS cells in vitro (reviewed in 26, 27). Lineage conversion or trans differentiation have recently been reported in vitro and in vivo (review 28-31). Mouse and human fibroblasts and other types of cells have been trans-differentiated directly into post-mitotic neurons with combinations of transcription factors (32-37). It was recently reported that the combination of three or more factors can reprogram mouse fibroblasts into induced

neural stem cells (iNSCs) with self-renewing ability (38-41).

Recently, we showed that ectopic expression of Sox2 during lung development induced the differentiation of embryonic epithelial cells into basal and neuroendocrine cells (18). Since subsets of epithelial cells in the developing lung may still be multipotent, we wondered whether ectopic expression of Sox2 could change the faith of fully differentiated alveolar type II cells in vivo. Therefore, we ectopically expressed Sox2 in alveolar type II cells using a tet-inducible, bi-transgenic approach. We show that conditional expression of Sox2 in the alveolar epithelium results in emphysematous lungs concomitant with the emergence of aberrant structures containing cuboidal cells in the periphery of the lungs. Moreover, Sox2 was found to induce progenitor-like cells which become proliferative and differentiate into cuboidal and basal-like cells, implying that fully differentiated type II cells can be reprogrammed with a single transcription factor to develop into cells expressing proximal markers.

Materials and methods

Mouse breeding and genotyping

Mice were kept under pathogen-free conditions and all experiments described in this study were performed according to the guidelines and with the written approval of the local ethics committee, "Dier Ethische Commissie" (Animal Ethics Commission), permit number EMC 2206. Generation of the Sox2 transgenic mouse line has been described before (18). Lung-specific expression of the myc-Sox2 transgene was obtained by breeding the myc-Sox2 line with the SPC-rtTA transgenic mice (generous gift of Jeffrey Whitsett, Cincinnati), subsequently referred to as iSox2$^{SPC\text{-}rtTA}$. Doxycycline was administered in the drinking water (2 mg/ml doxycycline, 5% sucrose), and lungs were harvested after 1, 3, 6, 9, or 28 days. Transgenic mice were genotyped by PCR of tail-tip DNA using transgene specific primers as previously described. Each experiment was executed on at least three independent lungs of iSox2$^{SPC\text{-}rtTA}$, single transgenic and wild type pups.

Immunohistochemistry and Immunofluorescence

Lungs of adult mice were inflated with 4% paraformaldehyde/phosphate-buffered saline (PBS), subsequently fixed by immersion overnight at 4°C, and processed according to standard protocols for paraffin embedding. Immunohistochemistry (IHC) was performed as previously described using primary antibodies for goat-anti Sox2 (1:500 immune system), mouse anti myc (1:1000, Roche) rabbit anti-phospho-histone H3 (1:1000; Millipore), rabbit anti-CCSP (1:1000, 7-Hills), Mouse anti Ssea (1:200, Millipore), rabbit anti-cyclin D1 (1:500; Abcam), rat anti-Sca-1 (1:500; Abcam), rabbit anti-proSP-C (1:1000; Seven Hills), Mouse anti-Trp63 (1:200; Santa cruz), and Goat anti-CCSP (1:1,000; Seven Hills) (42). Briefly, sections (5 µm) were deparaffinised, rehydrated and microwave treated for antigen retrieval in 10 mM citric acid buffer, pH 6.0. Slides were incubated with primary antibodies diluted in PBS/0,5% Triton/0.5% BSA overnight at 4°C, followed by incubation with the appropriate secondary antibody (1:100; Vector Labs) and amplification with ABC reagent (Vectastain Elite ABC kit; Vector Labs). Antigen localization was detected with nickel-diaminobenzidine. Sections were counterstained with haematoxylin and coverslipped using Permount (Fisher Scientific). Quantification of IHC staining was performed by counting positive cells in five separate microscopic fields with a 40× objective of three independent experiments, after which a bar graph was prepared using PRISM graphpad.

Data are represented as the average of the number of positive cells per field, including the standard error of the mean (SEM).
Immunofluorescence was performed as described above, but substituting the secondary antibodies with fluorophore labelled antibodies (Alexa Fluor-350, Alexa Fluor-488, and Alexa Fluor-594; Molecular Probes). Sections were mounted with Vectashield anti-fade reagent containing DAPI (Vector Labs). Brightfield and fluorescent images were obtained using a Zeiss Axioplan2 microscope equipped with AxioVision Software or a Leica SP5 confocal microscope.

Isolation and culturing of alveolar type II cells (AVTII)
Alveolar epithelial cells were isolated from the lungs of $Sox2^{SPC\text{-}rtTA}$ mice by Dispase (BD, Pharmingen) digestion as described previously with few modifications (43). Lungs were exsanguinated by perfusing through the right ventricle with 4 ml PBS after opening the peritoneum, clipping the vena cava inferior and removing the ribcage. 1 ml Dispase (BD, Pharmingen) was instilled over a tracheal cannula into the lung, immediately a sterilized suture (Braun) was used to tighten a node around the cannulised trachea. Lungs were isolated, incubated for 45 minutes in 1 ml Dispase at room temperature and transferred to a culture dish containing 5 ml DMEM/F12 medium (Gibco) supplemented with 0.04 mg/ml DNase I (AppliChem), 3.6 mg/ml D-(+)-Glucose (AppliChem) and 1% Penicillin/Streptomycin (P/S). The small airways were gently removed and the obtained cell suspension was serially filtered through 100, 70 and 40 µm nylon meshes and centrifuged at 200 g for 10 minutes at 15°C. The supernatant was discarded and the cell pellet was resuspended in 500 µl DMEM/F12 (Gibco) medium supplemented with 3.6 mg/ml D-(+)-Glucose (AppliChem), 1% P/S and 2% FCS. AVTII cells were cultured in DMEM/F10 containing 10% FCS and 1% P/S in tissue culture cover slip immersed in 12 well plates (Corning, NY) previously coated with collagen (Inamed); cultures were maintained in a 5% CO_2/air incubator.

Plasmids, Cell culture and Luciferase Reporter Assays
A 500 bp minimal promoter fragment immediately upstream of the Sca1 transcriptional start site was PCR amplified from genomic DNA using the primers Forward 5'-TAAACGCGCACACGTTTCTC-3' and Reverse 5'-GGCCAGCATCTGACCTCTTT-3', and cloned into the pGL4 luciferase. Human embryonic kidney HEK 293T cells maintained under standard culture conditions were plated on 6-well plates (3.5×10^5 cells per well). 24 hours after plating, the HEK-293Tcells were transiently transfected using Lipofectamine LTX (Invitrogen) with 2.5 µg of the following Firefly luciferase reporter plasmids (pGL4-Sca-1 1µg of Renilla luciferase plasmid (transfection control), and 2.5µg of empty vector (pcDNA3) or plasmids expressing full length Sox2 (WT-Sox2), or one of the mutant Sox2 (ΔTAD and ΔHMG) (44). After 24 hr, cells were harvested and luciferase activity was measured using the Dual-Luciferase Reporter Assay system (Promega). The lysate was assayed for luciferase and Renilla activity using the GloMax 96 Microplate Luminometer with Dual Injectors (Promega, Madison, WI), according to the Dual-Luciferase Reporter Assay system kit protocol (Promega). The luciferase activity was calculated relative to the TK Renila. All reporter assays were performed in triplicate, and the bars in the figures denote the standard error of the mean (SEM).

Chromatin Immunoprecipitation
Human lung adenocarcinoma epithelial A549 cells were cultured in hypoxic conditions and

the ChIP assays were performed essentially as described previously using $6x10^7$ cells (45-47). The immunoprecipitated DNA was analysed with specific primers in a Q-PCR assay to assess the enrichment of the promoter regions of the Amylase (Amy), Sca1 and Gli2 genes. The amount of immunoprecipitated DNA with SOX2 and control IgG was calculated based on threshold cycle [C(t)] using the ΔC(t) method and normalized to input samples. Results are expressed as fold enrichment of SOX2 immunoprecipitated samples relative to IgG controls, and represent the average of three replicates of two independent experiments including the SEM. PCR primers are listed in Table 1.

Results

Expression of Sox2 in alveolar type II cells results in morphological changes

Ectopic expression of iSox2 in relative uncommitted, naïve epithelial cells during development resulted in their differentiation into proximal epithelial cells, primarily basal cells (18, 46). We wondered whether induced expression of iSox2 in fully differentiated cells would affect the cells in an autonomous manner. Therefore, we expressed the iSox2 transgene in adult lungs using the SPC-rtTA transgene, which was reported to be expressed in a subset of type II cells in adult lungs (48). The immediate effect of the expression of the transgene was evaluated after one, three, six, and nine days of doxycycline induction, as well as prolonged expression for four weeks. The mice did not show typical lung-related phenotypic abnormalities, such as breathing problems, and were indistinguishable from control mice. However, histological analysis of HE stained sections revealed significant structural abnormalities after treatment with doxycycline for four weeks in the lungs of the $Sox2^{SPC\text{-}rtTA}$ mice, which resembled an emphysematous-like appearance (fig. 1B, stars). The air spaces in the lungs of $iSox2^{SPC\text{-}rtTA}$ mice were significantly enlarged and accompanied by the destruction of the normal alveolar architecture compared to control mice (fig. 1A-C). The disrupted areas were interspersed within relative normal alveolar regions, indicating that the phenotype was not uniform throughout the lung of $iSox2^{SPC\text{-}rtTA}$ mice. The normal appearance of lung architecture in some regions was an indication of incomplete penetrance of the transgene (fig. 1B arrow).

There was no evidence of inflammatory cells in the alveolar parenchyma and airway spaces, nor were any fibrotic changes observed. Careful analysis of the lungs exposed to doxycycline showed the emergence of clusters of cuboidal cells already after three days of doxycycline treatment (Figure 1C, arrows). Next, we analyzed the extend of the transgene expression after the specified time points by immunohistochemistry with an antibody against the myc epitope (Myc), which is present at the N-terminus of the iSox2 transgenic protein. In contrast to lungs of wild type control or non-induced transgenic mice (Figure 1D), clear positive cells were already detected after one day of doxycycline exposure in subsets of type II cells in the lungs of the $iSox2^{SPC\text{-}rtTA}$ mice (fig. 1E), which progressively increased with prolonged exposure to doxycycline for 3, 6, 9 and 28 days (fig. 1F-I). Moreover, the iSox2 expressing cells were positive for the type II cell marker Prospc, indicating that indeed the transgene was expressed in type II cells (fig. 1J-L, arrows indicate positive clusters; fig. S1). Although the appearance of positive cells after one day did not change the overall structure of the lung, the gradual increase of Sox2 positive cells caused cellular changes, from typical type II cells to cuboidal shaped cells. The appearance of these clusters of cuboidal cells suggested that the transgenic iSox2 induced cellular changes in the type II cells. Therefore, we analyzed the expression of the type II cell differentiation marker

lysophosphatidylcholine acyltransferase 1, Lpcat1, which is involved in the production of the main phospholipid of surfactant, dipalmitoylphosphatidylcholine. Lungs of iSox2$^{SPC\text{-}rtTA}$ were analyzed after the induction of the transgene with dual immunofluorescence staining (fig. 2). Colocalization of Lpcat and iSox2 was observed after one (fig. 2A) and six (fig. 2B) days of doxycycline, but vanished after longer exposure with doxycycline (fig. 2C), indicating that these cells lost the differentiated type II cell characteristics. Thus, expression of iSox2 in peripheral respiratory epithelial cells expanded with the duration of doxycycline administration and induced the appearance of clusters of cuboidal shaped cells, leading to disorganized alveolar septa and loss of the normal lung architecture.

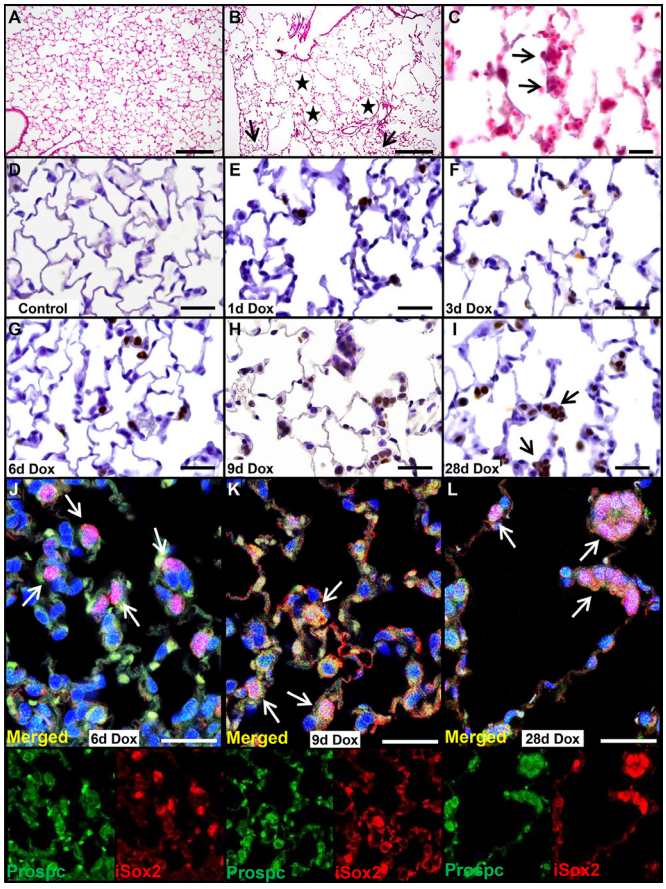

Figure 1. Ectopic Sox2 expression induces abnormal cell clusters. Representative HE staining of a control lung (A) demonstrating the normal lung architecture and of iSox2$^{SPC\text{-}rtTA}$ lungs after 4 weeks doxycycline treatment (B) showing numerous, enlarged emphysematous structures (asterisks) with cuboidal cell clusters (C). Representative IHC staining for the myc-epitope in wild type control (D) and iSox2$^{SPC\text{-}rtTA}$ lungs (E-I) after 1, 3, 6, 9 and 28 days of doxycycline treatment. Transgenic iSox2 positive myc staining is already evident after 1day of dox administration (E), which gradually increased in time (F-I). The positive cells are clearly forming cuboidal clusters (arrows in I). Dual immunofluorescence staining shows the colocalization of the transgenic Sox2 (iSox2, red) with the type II cell marker Prospc (green) after 6 days (J), 9 days (K) and 28 days (L) of doxycycline treatment. Scale bars 200µm (A, B), 100µm (C), 50µm (D-I) and 25µm (J-L).

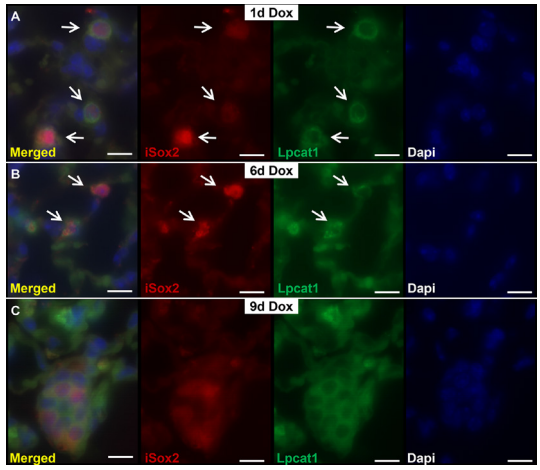

Figure 2. Sox2 induces a gradual loss of differentiated type II cells. Dual immunofluorescence staining of lungs treated with doxycycline for 1 (A), 6 (B) and 9 (C) days shows a gradual loss of colocalization of the type II cell differentiation marker Lpcat1 (green) and the transgenic Sox2 (iSox2, red), indicating that Sox2 induces cellular changes in the type II cells. Scale bar: 25µm.

Sox2 induces proliferation in alveolar type II cells in vivo

Although cell turnover and proliferation is low during homeostasis in mature lungs, we and others previously showed that Sox2 induced proliferation in lung epithelium (18, 19, 46). Since Sox2 induced the appearance of an increasing number of cell clusters within the alveolar epithelium, we analyzed whether Sox2 induced proliferation in fully differentiated alveolar type II cells using an antibody against the mitotic cell marker phospho-histone H3 (Phh3). Contrasting the non-proliferative, homeostatic lungs derived from control lungs, Phh3 positive cells were observed in the cuboidal clusters of the lungs of iSox2$^{SPC\text{-}rtTA}$ exposed to doxycycline (fig. 3A versus 3B-D). The number of proliferative cells gradually increased with the duration of transgene expression in iSox2$^{SPC\text{-}rtTA}$, starting to become apparent after six days of induction (fig. 3E). Dual immunofluorescence staining revealed co-localization of Phh3 and iSox2 in the induced clusters of alveolar cells, confirming that proliferation occurred within the transgene-expressing cells (fig. 3F; fig. S2). So, iSox2 induced type II cells to proliferate and induced cellular changes, ultimately leading to abnormal lung architecture.

iSox2 induces expression of Clara-like and basal-like cells in AVTII cells

Since iSox2 induced the emergence of proximal cell types when expressed during lung development (18, 46), we analyzed if the expression of iSox2 in terminal differentiated type II cells also induced genes specific for proximal airway cells differentiation. Therefore, the expression of Cc10 and Trp63, two markers of the proximal Clara cells and basal cells, respectively, was analyzed. Although Cc10 positive cells were present in the proximal epithelium of the control lungs, the alveolar regions were completely devoid of them fig. 4A, C, E). In contrast, Cc10 positive cells were readily detected in the alveolar regions in the lungs of the iSox2$^{SPC\text{-}rtTA}$ mice, even after one day of doxycycline induction, and increased with prolonged exposure (fig. 4B, D, F). Interestingly, these CC10 positive cells also expressed the type II cell marker Spc, indicating that the iSox2 transgene induced the emergence of a transient, bronchoalveolar stem cell (BASC)-like population (CC10^{+}/Spc^{+};

arrows in fig. 4G-I; arrowheads indicate CC10 negative cells). The BASC population has been described to serve as a progenitor like population which is induced upon damage to re-populate the airway epithelium (49, 50).

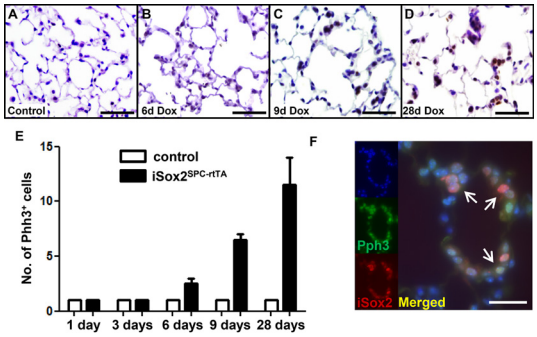

Figure 3. Sox2 induces proliferation in terminally differentiated alveolar type II pneumocytes. Lungs of control (A) and iSox2$^{SPC\text{-}rtTA}$ mice treated with doxycycline for 6 (B), 9 (C) or 28 (D) days were analyzed with an antibody against the mitotic cell marker Phh3. Representative images show proliferation in individual type II cells after 6 days of iSox2 induction (B), which gradually develop into proliferative clusters of cells (C, D). (E) Quantification of Phh3 staining indicates the correlation between the increase of Phh3 positive cells and time of doxycycline expression. (F) Colocalization of iSox2 and Phh3 is shown by dual immunofluorescence labeling after 28 days of doxycycline exposure (areas arrows indicate double positive cells). Scale bars: 200µm (A), 100µm (B, C, D) and 25µm (F).

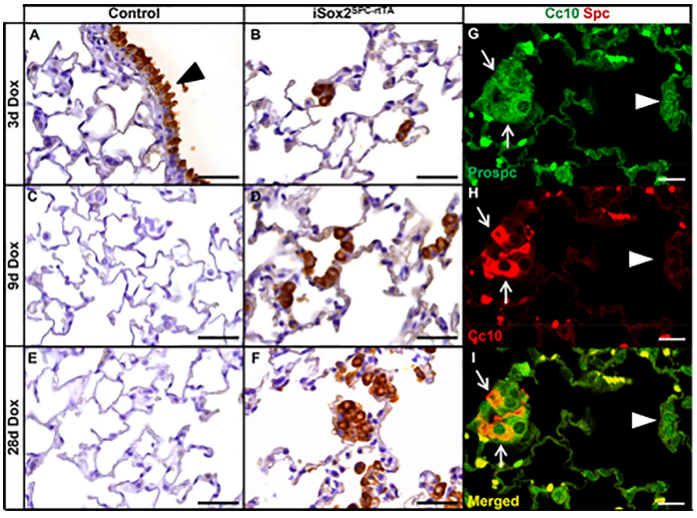

Figure 4. Sox2 induces Clara-like cells and BASC cells. Lungs of control (A, C, E) and iSox2$^{SPC\text{-}rtTA}$ (B, D, F) lungs treated with doxycycline for 3 (A, B), 9 (C, D) and 28 (E, F) days were stained with the Clara cell marker Cc10. Endogenous expression of Cc10 is demonstrated in the conducting airways (A, arrowhead), which also shows the absence of Cc10 positive cells in the distal airways (A, C, E) of control lungs. The progressive increase in number of Clara-like cells (Cc10+) in the iSox2$^{SPC\text{-}rtTA}$ lungs with prolonged induction of iSox2 is clearly noticeable (B, D, F). Colocalization of Cc10 (red) and Prospc (green) is demonstrated with dual immunofluorescence staining (G-I), indicating the emergence of BASC cells (arrows). Arrowheads show Prospc positive cells that lack CC10 (and iSox2) expression. Scale bars: 50 µm (B, D, F), 25µm (G-I).

Ectopic Sox2 expression induces progenitors-like cells

Since we observed the emergence of proximal markers in the distal type II cells and the appearance of Spc$^+$/CC10$^+$ double positive BASC-like cells, we wondered whether the differentiation of proximal Clara and basal cells occurred through intermediate, progenitor-like cells. Therefore, we analyzed the lungs of control and iSox2$^{SPC\text{-}rtTA}$ mice, isolated at different time points after doxycycline treatment, for the expression of Sca1 and Ssea1, two markers normally expressed in progenitor cells (51, 52). Sca1and Ssea1 were readily detected in the alveolar epithelium in iSox2$^{SPC\text{-}rtTA}$ after 3 days of doxycycline exposure to these mice (fig. 5B, F). This pattern of expression progressively increased after 9 days of transgene induction (fig. 5C, G), and after four weeks of doxycycline induction virtually all clusters of cells expressed Sca1 and Ssea1 (fig. 5D, H). Sca1 and myc-epitope double immunofluorescence staining on lungs of iSox2$^{SPC\text{-}rtTA}$ animals exposed for four weeks to doxycycline clearly showed co-localization of Sca1 with the transgenic protein (fig. 5I-K). Moreover, the previously identified Spc$^+$/CC10$^+$ cells also appeared to express Sca1. In addition, Sca1 also co-expressed with the basal cell marker Trp63 after four weeks of iSox2 induction, sugges ting that the Sca-1$^+$ cells gradually differentiate into more committed cells (fig. 6A-D; fig. S3). Moreover, the Trp63 positive cells represent the ectopic appearance of basal-like cells in the distal epithelium of the iSox2$^{SPC\text{-}rtTA}$ lungs. Thus, Sca1 was specifically induced in the subset of AVTII cells that expressed transgenic iSox2, which indicates that iSox2 is able to induce progenitor-like cells in terminally differentiated type II cells.

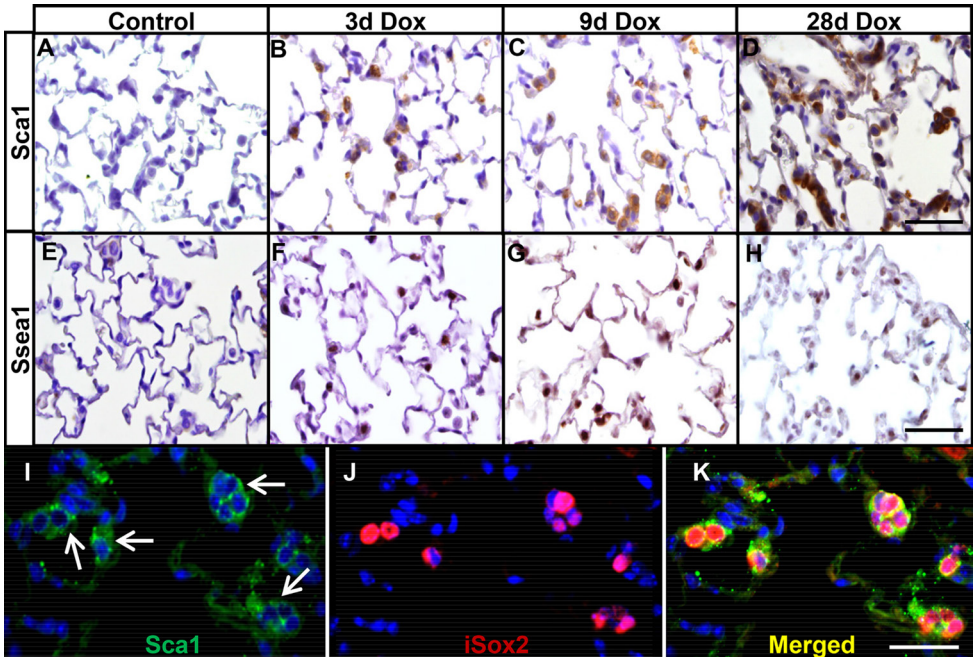

Figure 5. iSox2 induces the appearance of stem cell markers. Immunohistochemistry for Sca1 (A-D) and Ssea1 (E-H) was performed on lungs of controls (A, E), and of iSox2$^{SPC\text{-}rtTA}$ mice after 3 (B, F), 9 (C, G) and 28 (D, H) days of doxycycline exposure. Sca1 and Ssea1 expressing cells are completely absent in control lungs (A, E), but readily detectable after 3 days of exposure and progressively increased with duration of transgene activation. Sca1 is clearly associated with iSox2$^+$ cells, as shown by dual immunofluorescence staining (I-K). Scale bar 100µm (D, H), 50µm (K).

Sox2 activates promoter-Luciferase construct for Sca-1

Next, we wondered whether Sca1 expression is directly regulated by Sox2. Therefore, the Sca1 gene was analyzed for putative Sox2 binding sites and within a region of 500 bp immediately upstream of the transcriptional start site, a well-conserved Sox2 binding motif was found. The functionality of this potential Sox2 site was tested in vitro using a luciferase reporter assay. The full length Sox2 protein (WT) induced the transcriptional activity of the Sca1-luciferase construct sevenfold as compared to baseline expression, whereas mutant Sox2 proteins lacking either the transactivation domain (ΔTAD) or the HMG domain (ΔHMG) did not transactivate the minimal Sca1 promoter (fig. 6E). Next, the in vivo binding of SOX2 to this putative Sox2 binding site was analyzed by chromatin immunoprecipitation (ChIP), which revealed that SOX2 directly bound to this Sox2 motif of the SCA1 gene in the human bronchiolar cell line A549 (fig. 6F). These results demonstrated the direct binding and activation of the Sca1 promoter by Sox2, and thus highlights a novel transcriptional target gene of Sox2.

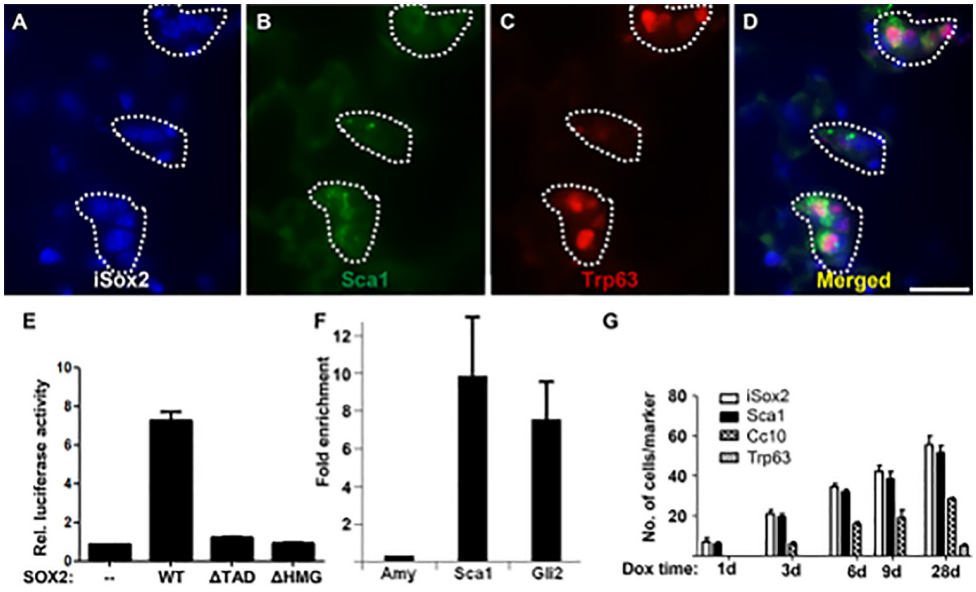

Figure 6. Sox2 induces Sca1 positive cells by directly transactivating the Sca-1 gene. Triple immunofluorescence staining with Myc (iSox2, blue), Sca1 (green) and Trp63 (red) on lungs of iSox2$^{SPC\text{-}rtTA}$ animals treated for 28 days with doxycycline demonstrate the emergence of Sca1/Trp63 positive cells (dotted areas; A-D). (E) Luciferase assay shows in vitro transactivation of the Sca1 minimal promoter by the full length Sox2 (WT), but not by deletion constructs lacking the transactivation domain (ΔTAD) or the HMG domain (ΔHMG). The graph represents the average of three independent experiments, and the bars denote the standard error of the mean (SEM). (F) SOX2 specific ChIP analysis showing specific enrichment of the Sca1 promoter region used in the luciferase assay. The SEM is indicated of two independent experiments. (G) Quantification of the expression of the different lung markers in vivo after the indicated time of doxycycline exposure. The graph shows the average of the number of positive cells of five microscopic fields with a 40 x objective of three independent experiments, including the corresponding SEM. Scale bar: 25μm (D).

Transgenic Sox2 induces proximal markers in primary AVTII cells

Quantification of the appearance of the different markers and cell types in relation to the timing of doxycycline exposure, suggested that Sox2 first initiates the appearance of markers associated with progenitor-like cells (fig. 6G; $Sca1^{+}$). In time, differentiation markers emerge, as evidenced by the number of $Cc10^{+}$ and $Trp63^{+}$ cells. To determine the observed plasticity of AVTII cells in vitro, we isolated type II cells from 4 weeks old non-doxycycline exposed $iSox2^{SPC\text{-}rtTA}$ mice and cultured these primary cells with or without doxycycline (fig. S4). After three, six and nine days the cultures were analyzed for the expression of the myc epitope (iSox2), Cc10, Sca1 and Trp63. The non-doxycycline treated cells expressed Spc, indicative for AVTII cells, but obviously lacked expression of Cc10, Sca1 and Trp63 (fig. 7D). However, in cells treated with doxycycline for 3 days (fig. 7A), 6 days (fig. 7B) and 9 days (fig. 7C), AVTII cells expressed Sca1, and Cc10, while Trp63 positive cells were observed only in the cultures exposed to doxycycline for nine days, which correlated with the in vivo observations (fig. 6D). Taken together, these data demonstrate that AVTII cells also exhibit phenotypic plasticity in vitro.

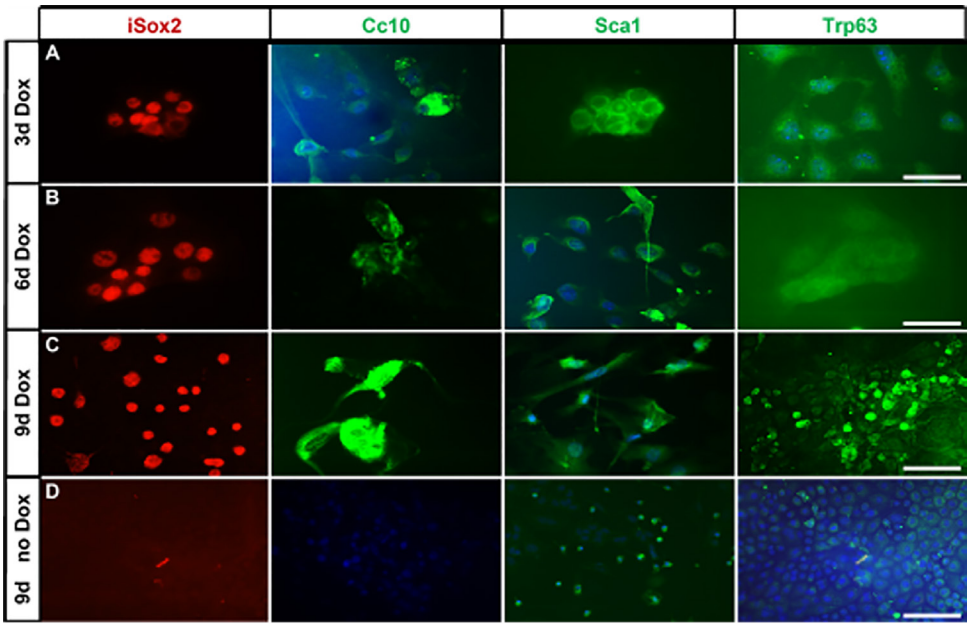

Figure 7. Primary alveolar type II cells can be reprogrammed in vitro. Representative immunofluorescence images showing expression of iSox2 (Red), Cc10 (Green), Sca1(Green) and Trp63 (Green) after culturing the primary type II cells with doxycycline for 3 days (A), 6 days (B) and 9 days (C). AVTII cells cultured for 9 days without doxycycline served as negative controls (D). The results demonstrate that in vitro cultures of AVTII cells have comparable phenotypic plasticity as AVTII cells in vivo. Scale bar 50µm (A-C), 100µm (D).

Discussion

The idea that the future potential of differentiated cells is limited has been gradually adapted, starting with the seminal work of nuclear replacement in frogs and culminated in the complete reversal of differentiated fibroblast into multipotent cells by only four factors (23, 53). These experiments have led to an expansion of experimental approaches to manipulate and modify cells to give them multipotent potential (54). Several adaptations to this original combination of four factors have been shown to result in pluripotent cells, depending on the starting source of cells used as target (55-58). Recently, in vivo reprogramming has been show, for instance of resident brain astrocytes in both young adults and mice with Sox2 only (31).

Our previous study established that ectopic expression of Sox2 during lung development caused cystic lesions and aberrant differentiation of the epithelial cells (18). Recently, we showed that Sox2 directly induced Trp63 and Gata6 expression, which caused naïve epithelial cells to be become unresponsive to the branch inducing signal Fgf10 (46). This led to a skewing of the developmental potential of the uncommitted cells towards a proximal cell fate, primarily basal cells. In the current study we investigated whether Sox2 would be sufficient to redirect the fate of terminally differentiated alveolar type II cells.

After bleomycin induced injury, type II cells start to proliferate and repopulate the alveolar epithelium by self-renewal and functioning as progenitor cells for type I cells (59). We showed that induction of Sox2 expression in alveolar type II cells resulted in the immediate emergence of proliferative cells. Sox2, together with the Wnt downstream mediator β-catenin, was shown to directly regulate the promoter of Ccnd1 in breast cancer cells, and we show that the iSox2 positive cells were expressing Pph3 and cyclinD1 (60). Sox17 was also suggested to regulate the Ccnd1 promoter directly, although no ChIP analysis was done (61). Tompkins et al. added that upon Sox2 expression several other genes involved in cell cycle initiation and progression were upregulated (19). Within the first week of doxycycline induction, the iSox2 expressing cells started to express the Sca1 and Ssea1 stem cell markers (51, 52). Moreover, we showed a direct binding and transactivation of the Sca1 promoter by Sox2, thereby initiating a progenitor-like program. This suggests that iSox2^{+}/Sca1^{+}/Ssea1^{+} cells represent an initial sign of dedifferentiating type II cells, indicating that Sox2 may initiate alveolar epithelial cell plasticity by first regulating the emergence of proliferative intermediate cells, perhaps progenitor-like cells. Thus, our data suggest a mechanism where Sox2 first induces proliferative Ssea1^{+}/Sca1^{+} progenitor cells, which increase over time and subsequently promote differentiation of these cells into proximal epithelial cells. Detailed analysis of the progenitor-like, iSox2/Sca1^{+}/Ssea1^{+} cells showed a gradual differentiation towards proximal epithelial cell fate, since these cells started to express Cc10 and Trp63 after longer exposure to doxycycline, both in vivo and in vitro. A number of these cells co-expressed Spc and Cc10, a population also referred to as the bronchoalveolar stem cells (BASC), which are normally located at the bronchio-alveolar junctions (49). These authors also showed that the BASC cells expressed Sca1, which became proliferative after naphthalene injury. The cells with characteristics of BASC cells in the iSox2 expressing lungs also expressed Sca1 (Spc^{+}/Cc10^{+}/Sca1^{+}), contrasting earlier findings obtained with ectopic Sox17 expression that did not find these triple positive cells (61). The Sca1 marker has been used to purify BASC through fluorescence activated cell sorting (FACS) using CD45^{-}CD31^{-}Sca1^{+}, but other studies described this population

to be more heterogeneous (49, 62, 63). BASC cells self-renew and have the potential to differentiate into proximal and distal epithelial cells (34). Lineage tracing experiments using a CCSP-CreEr followed by hyperoxia injury suggested that BASC cells did not give rise to alveolar cells (50), but after bleomycin injury they did (59). This would suggest that BASC cells respond differently to various triggers.

Recently, lineage tracing studies using bleomycin induced lung damage in Scgb1a1-CreER mice showed that basal cells ($Trp63^+$) in the damaged parenchyma were directly derived from Clara cells ($Scgb1a1^+$) (64). Moreover, upon SO_2-induced damage or viral infection, Clara cells also dedifferentiated into basal cells (65). Exposure to naphtalene or hyperoxia revealed that Clara cells may contribute to maintenance and repair of the conducting airways without dedifferentiating into basal cells (50). Our current findings demonstrate that Clara and basal cells may originate from $iSox2^+/Sca1^+$ progenitor cells. However, it remains to be determined whether these cells are derived from $Sca1^+$ progenitor cells by genetic lineage tracing experiments.

The continuous proliferation of iSox2 positive cells led to the emergence of clusters of cells in the alveolar walls with a cuboidal to columnar appearance, which became apparent after 9 days. Concomitant with the development of these clusters was the disruption of the alveolar structure, as evidenced by the emphysema-like phenotype observed after four weeks of iSox2 expression. The combination of proliferation and the induction of progenitor-like characteristics resulted in the loss of structural integrity. The conversion of cell fate combined with the increased proliferation induced by iSox2 may have changed the secretion and composition of the extra cellular matrix, which may have weakened the alveolar structure. This in turn may enhance the activity of local proteases to digest the tissue matrix and induce septal rupture, leading to emphysematous-like lungs.

Long term and high ectopic expression of Sox2 in Cc10 positive cells was shown to result in adenocarcinomas in fifty percent of the mice (66), but we and others did not find evidence that Sox2 induced lung cancer in our mouse models (19). The difference in the various transgenic approaches may contribute to this discrepancy. However, SOX2 has been associated with human squamous cell lung tumors (76).

The only solution for patients with end-stage, severe chronic lung disease, like COPD and idiopathic pulmonary fibrosis, is lung transplantation. However, the shortage of suitable donors may result in a significant mortality of patients. Therefore, a potential future treatment for these severe lung diseases is a (temporary) transplantation with engineered lungs or stem/progenitor cells (67-69). However, the approaches for generating these cells have been limited to the use of combination of factors in vitro (23, 34, 70, 71). In addition, a variety of in vitro protocols exist for differentiating a range of pulmonary epithelial cell types, including alveolar type II cells (67-69, 72-74). Recently, the direct conversion of cellular fate has been reported in vivo in a study demonstrating that neurons can be generated from endogenous mouse astrocytes that are reprogrammed by viral delivery in situ (75). In addition, it has been shown that SOX2 is also capable of converting resident astrocytes into proliferative neuroblasts (31). We showed that Sox2 alone is sufficient to induce alveolar plasticity in resident lung alveolar type II cells into progenitors in adult mice. Our study demonstrates a feasible strategy for using Sox2 to reprogram alveolar type

II cells in vivo and in vitro. In the future, studies to identify the signaling pathways that regulate the differentiation of progenitors and the induction of proliferation in alveolar type II cells will be critical to facilitate the understanding of alveolar plasticity for future regenerative me- dicine. Lineage reprogramming would be applicable in translational medicine if this event can be triggered by a factor, whether transcription factor or small molecule, which acts transiently and exerts a complete effect.

In conclusion, we ectopically expressed one of the Yamanaka reprogramming factors, Sox2, in type II cells cells using our previously described system (18, 46). We show that these dedifferentiate into progenitor-like cells and subsequently commit to the proximal pulmonary epithelial cell lineages, like basal cells, extending previous findings with Sox2 and Sox17 (19, 61). Moreover, we show that aside from directly activating the promoter of the key gene in basal cell development, Trp63, Sox2 also binds and activates the progenitor cell marker Sca1, providing molecular evidence for a direct role of Sox2 in the dedifferentiation process (46).

Acknowledgements
We like to thank professor Jeffrey Whitsett for providing the SPC-rtTA mice and professor Angie Rizzino for providing the Sox2 mutant plasmids. We thank Dr Gert-Jan Kremers for technical assistance with the fluorescent microscopy and Dr Ron Smits for assistance with the luciferase assays.

Table 1: Primers used for ChIP-qPCR

Gene	Forward	Revers
SOX2	5' CATGCACCGCTACGACG 3'	5' CGGACTTGACCACCGAAC 3'
GLI2	5' TAGAATTGCTCCTGCACTTC 3'	5' ATGTCGGATGACCCTTTCTC 3'
AMY	5' GGGAAAAGGCAGCATATTG 3'	5' CACGCTAAATTGCCTGTGAA 3'
SCA1	5' ATGCCTTTATAGCCCCTCT 3'	5' GTCATGAGCAGCAATCCACA 3'

References

1. Kauffman SL (1980) Cell proliferation in the mammalian lung. Int Rev Exp Pathol 22: 131-191.
2. Rock JR, Hogan BL (2011) Epithelial progenitor cells in lung development, maintenance, repair, and disease. Annu Rev Cell Dev Biol 27: 493-512.
3. Wansleeben C, Barkauskas CE, Rock JR, Hogan BL (2013) Stem cells of the adult lung: their development and role in homeostasis, regeneration, and disease. Wiley Interdiscip Rev Dev Biol 2: 131-148.
4. Driscoll B, Kikuchi A, Lau AN, Lee J, Reddy R, et al. (2012) Isolation and characterization of distal lung progenitor cells. Methods Mol Biol 879: 109-122.
5. Reynolds SD, Brechbuhl HM, Smith MK, Smith RW, Ghosh M (2012) Lung epithelial healing: a modified seed and soil concept. Proc Am Thorac Soc 9: 27-37.
6. Rackley CR, Stripp BR (2012) Building and maintaining the epithelium of the lung. J Clin Invest 122: 2724-2730.
7. Weiss DJ, Bertoncello I, Borok Z, Kim C, Panoskaltsis-Mortari A, et al. (2011) Stem cells and cell therapies in lung biology and lung diseases. Proc Am Thorac Soc 8: 223-272.
8. McQualter JL, Bertoncello I (2012) Concise review: Deconstructing the lung to reveal its regenerative potential. Stem Cells 30: 811-816.
9. Weiss DJ (2013) Current status of stem cells and regenerative medicine in lung biology and diseases. Stem Cells.
10. Chen H, Matsumoto K, Brockway BL, Rackley CR, Liang J, et al. (2012) Airway epithelial progenitors are region specific and show differential responses to bleomycin-induced lung injury. Stem Cells 30: 1948-1960.
11. Ghosh M, Brechbuhl HM, Smith RW, Li B, Hicks DA, et al. (2011) Context-dependent differentiation of multipotential keratin 14-expressing tracheal basal cells. Am J Respir Cell Mol Biol 45: 403-410.
12. Rock JR, Randell SH, Hogan BL (2010) Airway basal stem cells: a perspective on their roles in epithelial homeostasis and remodeling. Dis Model Mech 3: 545-556.
13. Zheng D, Limmon GV, Yin L, Leung NH, Yu H, et al. (2013) A cellular pathway involved in Clara cell to alveolar type II cell differentiation after severe lung injury. PLoS One 8: e71028.
14. Hong KU, Reynolds SD, Giangreco A, Hurley CM, Stripp BR (2001) Clara cell secretory protein-expressing cells of the airway neuroepithelial body microenvironment include a label-retaining subset and are critical for epithelial renewal after progenitor cell depletion. Am J Respir Cell Mol Biol 24: 671-681.
15. Giangreco A, Arwert EN, Rosewell IR, Snyder J, Watt FM, et al. (2009) Stem cells are dispensable for lung homeostasis but restore airways after injury. Proc Natl Acad Sci U S A 106: 9286-9291.
16. Chapman HA, Li X, Alexander JP, Brumwell A, Lorizio W, et al. (2011) Integrin alpha6beta4 identifies an adult distal lung epithelial population with regenerative potential in mice. J Clin Invest 121: 2855-2862.
17. Que J, Luo X, Schwartz RJ, Hogan BL (2009) Multiple roles for Sox2 in the developing and adult mouse trachea. Development 136: 1899-1907.
18. Gontan C, de Munck A, Vermeij M, Grosveld F, Tibboel D, et al. (2008) Sox2 is important for two crucial processes in lung development: branching morphogenesis and epithelial cell differentiation. Dev Biol 317: 296-309.
19. Tompkins DH, Besnard V, Lange AW, Keiser AR, Wert SE, et al. (2011) Sox2 activates cell proliferation and differentiation in the respiratory epithelium. Am J Respir Cell Mol Biol 45: 101-110.
20. Graham V, Khudyakov J, Ellis P, Pevny L (2003) SOX2 functions to maintain neural progenitor identity. Neuron 39: 749-765.
21. Kiernan AE, Pelling AL, Leung KK, Tang AS, Bell DM, et al. (2005) Sox2 is required for sensory organ development in the mammalian inner ear. Nature 434: 1031-1035.
22. Okubo T, Pevny LH, Hogan BL (2006) Sox2 is required for development of taste bud sensory cells. Genes Dev 20: 2654-2659.
23. Takahashi K, Yamanaka S (2006) Induction of pluripotent stem cells from mouse embryonic and adult fibroblast cultures by defined factors. Cell 126: 663-676.
24. Tompkins DH, Besnard V, Lange AW, Wert SE, Keiser AR, et al. (2009) Sox2 is required for maintenance and differentiation of bronchiolar Clara, ciliated, and goblet cells. PLoS One 4: e8248.
25. Que J, Okubo T, Goldenring JR, Nam KT, Kurotani R, et al. (2007) Multiple dose-dependent roles for Sox2 in the patterning and differentiation of anterior foregut endoderm. Development 134: 2521-2531.
26. Ladewig J, Koch P, Brustle O (2013) Leveling Waddington: the emergence of direct programming and the loss of cell fate hierarchies. Nat Rev Mol Cell Biol 14: 225-236.
27. Graf T, Enver T (2009) Forcing cells to change lineages. Nature 462: 587-594.
28. Sancho-Martinez I, Baek SH, Izpisua Belmonte JC (2012) Lineage conversion methodologies meet the reprogramming toolbox. Nat Cell Biol 14: 892-899.
29. Abad M, Mosteiro L, Pantoja C, Canamero M, Rayon T, et al. (2013) Reprogramming in vivo produces teratomas and iPS cells with totipotency features. Nature 502: 340-345.
30. Zhou Q, Brown J, Kanarek A, Rajagopal J, Melton DA (2008) In vivo reprogramming of adult pancreatic exocrine

cells to beta-cells. Nature 455: 627-632.
31. Niu W, Zang T, Zou Y, Fang S, Smith DK, et al. (2013) In vivo reprogramming of astrocytes to neuroblasts in the adult brain. Nat Cell Biol 15: 1164-1175.
32. Ambasudhan R, Talantova M, Coleman R, Yuan X, Zhu S, et al. (2011) Direct reprogramming of adult human fibroblasts to functional neurons under defined conditions. Cell Stem Cell 9: 113-118.
33. Caiazzo M, Dell'Anno MT, Dvoretskova E, Lazarevic D, Taverna S, et al. (2011) Direct generation of functional dopaminergic neurons from mouse and human fibroblasts. Nature 476: 224-227.
34. Kim J, Efe JA, Zhu S, Talantova M, Yuan X, et al. (2011) Direct reprogramming of mouse fibroblasts to neural progenitors. Proc Natl Acad Sci U S A 108: 7838-7843.
35. Marro S, Pang ZP, Yang N, Tsai MC, Qu K, et al. (2011) Direct lineage conversion of terminally differentiated hepatocytes to functional neurons. Cell Stem Cell 9: 374-382.
36. Pang ZP, Yang N, Vierbuchen T, Ostermeier A, Fuentes DR, et al. (2011) Induction of human neuronal cells by defined transcription factors. Nature 476: 220-223.
37. Vierbuchen T, Ostermeier A, Pang ZP, Kokubu Y, Sudhof TC, et al. (2010) Direct conversion of fibroblasts to functional neurons by defined factors. Nature 463: 1035-1041.
38. Xue Y, Ouyang K, Huang J, Zhou Y, Ouyang H, et al. (2013) Direct conversion of fibroblasts to neurons by reprogramming PTB-regulated microRNA circuits. Cell 152: 82-96.
39. Lujan E, Chanda S, Ahlenius H, Sudhof TC, Wernig M (2012) Direct conversion of mouse fibroblasts to self-renewing, tripotent neural precursor cells. Proc Natl Acad Sci U S A 109: 2527-2532.
40. Sheng C, Zheng Q, Wu J, Xu Z, Wang L, et al. (2012) Direct reprogramming of Sertoli cells into multipotent neural stem cells by defined factors. Cell Res 22: 208-218.
41. Ji S, Zhang L, Hui L (2013) Cell fate conversion: direct induction of hepatocyte-like cells from fibroblasts. J Cell Biochem 114: 256-265.
42. Huang Y, Kempen MB, Munck AB, Swagemakers S, Driegen S, et al. (2012) Hypoxia-inducible factor 2alpha plays a critical role in the formation of alveoli and surfactant. Am J Respir Cell Mol Biol 46: 224-232.
43. Corti M, Brody AR, Harrison JH (1996) Isolation and primary culture of murine alveolar type II cells. Am J Respir Cell Mol Biol 14: 309-315.
44. Cox JL, Mallanna SK, Luo X, Rizzino A (2010) Sox2 uses multiple domains to associate with proteins present in Sox2-protein complexes. PLoS One 5: e15486.
45. Raghoebir L, Bakker ER, Mills JC, Swagemakers S, Kempen MB, et al. (2012) SOX2 redirects the developmental fate of the intestinal epithelium toward a premature gastric phenotype. J Mol Cell Biol 4: 377-385.
46. Ochieng JK, Schilders K, Kool H, Boerema-de Munck A, Buscop-van Kempen M, et al. (2014) Sox2 Regulates the Emergence of Lung Basal Cells by Directly Activating the Transcription of Trp63. Am J Respir Cell Mol Biol.
47. Huang Y, Kapere Ochieng J, Kempen MB, Munck AB, Swagemakers S, et al. (2013) Hypoxia inducible factor 3alpha plays a critical role in alveolarization and distal epithelial cell differentiation during mouse lung development. PLoS One 8: e57695.
48. Perl AK, Tichelaar JW, Whitsett JA (2002) Conditional gene expression in the respiratory epithelium of the mouse. Transgenic Res 11: 21-29.
49. Kim CF, Jackson EL, Woolfenden AE, Lawrence S, Babar I, et al. (2005) Identification of bronchioalveolar stem cells in normal lung and lung cancer. Cell 121: 823-835.
50. Rawlins EL, Okubo T, Xue Y, Brass DM, Auten RL, et al. (2009) The role of Scgb1a1+ Clara cells in the long-term maintenance and repair of lung airway, but not alveolar, epithelium. Cell Stem Cell 4: 525-534.
51. Holmes C, Stanford WL (2007) Concise review: stem cell antigen-1: expression, function, and enigma. Stem Cells 25: 1339-1347.
52. Solter D, Knowles BB (1978) Monoclonal antibody defining a stage-specific mouse embryonic antigen (SSEA-1). Proc Natl Acad Sci U S A 75: 5565-5569.
53. Gurdon JB (1962) The developmental capacity of nuclei taken from intestinal epithelium cells of feeding tadpoles. J Embryol Exp Morphol 10: 622-640.
54. Lensch MW, Mummery CL (2013) From Stealing Fire to Cellular Reprogramming: A Scientific History Leading to the 2012 Nobel Prize. Stem Cell Reports 1: 5-17.
55. Wu T, Wang H, He J, Kang L, Jiang Y, et al. (2011) Reprogramming of trophoblast stem cells into pluripotent stem cells by Oct4. Stem Cells 29: 755-763.
56. Liu Y, Cheng H, Gao S, Lu X, He F, et al. (2013) Reprogramming of MLL-AF9 leukemia cells into pluripotent stem cells. Leukemia.
57. Najm FJ, Lager AM, Zaremba A, Wyatt K, Caprariello AV, et al. (2013) Transcription factor-mediated reprogramming of fibroblasts to expandable, myelinogenic oligodendrocyte progenitor cells. Nat Biotechnol 31: 426-433.
58. Nemajerova A, Kim SY, Petrenko O, Moll UM (2012) Two-factor reprogramming of somatic cells to pluripotent

stem cells reveals partial functional redundancy of Sox2 and Klf4. Cell Death Differ 19: 1268-1276.
59. Rock JR, Barkauskas CE, Cronce MJ, Xue Y, Harris JR, et al. (2011) Multiple stromal populations contribute to pulmonary fibrosis without evidence for epithelial to mesenchymal transition. Proc Natl Acad Sci U S A 108: E1475-1483.
60. Chen Y, Shi L, Zhang L, Li R, Liang J, et al. (2008) The molecular mechanism governing the oncogenic potential of SOX2 in breast cancer. J Biol Chem 283: 17969-17978.
61. Lange AW, Keiser AR, Wells JM, Zorn AM, Whitsett JA (2009) Sox17 promotes cell cycle progression and inhibits TGF-beta/Smad3 signaling to initiate progenitor cell behavior in the respiratory epithelium. PLoS One 4: e5711.
62. Kim D, Kim CH, Moon JI, Chung YG, Chang MY, et al. (2009) Generation of human induced pluripotent stem cells by direct delivery of reprogramming proteins. Cell Stem Cell 4: 472-476.
63. McQualter JL, Yuen K, Williams B, Bertoncello I (2010) Evidence of an epithelial stem/progenitor cell hierarchy in the adult mouse lung. Proc Natl Acad Sci U S A 107: 1414-1419.
64. Zheng D, Yin L, Chen J (2013) Evidence for Scgb1a1 Cells in the Generation of p63 Cells in the Damaged Lung Parenchyma. Am J Respir Cell Mol Biol.
65. Tata PR, Mou H, Pardo-Saganta A, Zhao R, Prabhu M, et al. (2013) Dedifferentiation of committed epithelial cells into stem cells in vivo. Nature 503: 218-223.
66. Lu Y, Futtner C, Rock JR, Xu X, Whitworth W, et al. (2010) Evidence that SOX2 overexpression is oncogenic in the lung. PLoS One 5: e11022.
67. Mou H, Zhao R, Sherwood R, Ahfeldt T, Lapey A, et al. (2012) Generation of multipotent lung and airway progenitors from mouse ESCs and patient-specific cystic fibrosis iPSCs. Cell Stem Cell 10: 385-397.
68. Green MD, Chen A, Nostro MC, d'Souza SL, Schaniel C, et al. (2011) Generation of anterior foregut endoderm from human embryonic and induced pluripotent stem cells. Nat Biotechnol 29: 267-272.
69. Van Haute L, De Block G, Liebaers I, Sermon K, De Rycke M (2009) Generation of lung epithelial-like tissue from human embryonic stem cells. Respir Res 10: 105.
70. Han DW, Tapia N, Hermann A, Hemmer K, Hoing S, et al. (2012) Direct reprogramming of fibroblasts into neural stem cells by defined factors. Cell Stem Cell 10: 465-472.
71. Ring KL, Tong LM, Balestra ME, Javier R, Andrews-Zwilling Y, et al. (2012) Direct reprogramming of mouse and human fibroblasts into multipotent neural stem cells with a single factor. Cell Stem Cell 11: 100-109.
72. Longmire TA, Ikonomou L, Hawkins F, Christodoulou C, Cao Y, et al. (2012) Efficient derivation of purified lung and thyroid progenitors from embryonic stem cells. Cell Stem Cell 10: 398-411.
73. Wang D, Haviland DL, Burns AR, Zsigmond E, Wetsel RA (2007) A pure population of lung alveolar epithelial type II cells derived from human embryonic stem cells. Proc Natl Acad Sci U S A 104: 4449-4454.
74. Rippon HJ, Polak JM, Qin M, Bishop AE (2006) Derivation of distal lung epithelial progenitors from murine embryonic stem cells using a novel three-step differentiation protocol. Stem Cells 24: 1389-1398.
75. Torper O, Pfisterer U, Wolf DA, Pereira M, Lau S, et al. (2013) Generation of induced neurons via direct conversion in vivo. Proc Natl Acad Sci U S A 110: 7038-7043.
76. Hussenet T, du Manoir S (2010) SOX2 in squamous cell carcinoma Amplifying a pleiotropic oncogene along carcinogenesis. Cell cycle 9: 1480-1486

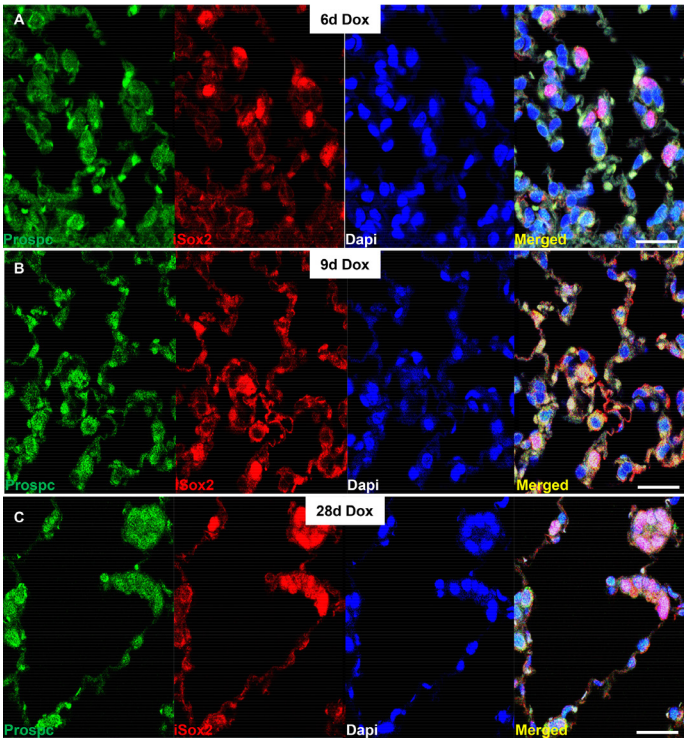

Figure S1. Dual immunofluorescence staining shows the colocalization of the transgenic Sox2 (iSox2, red) with the type II cell marker Prospc (green) after 6 days (A), 9 days (B) and 28 days (C) of doxycycline treatment. Scale bars 25µm.

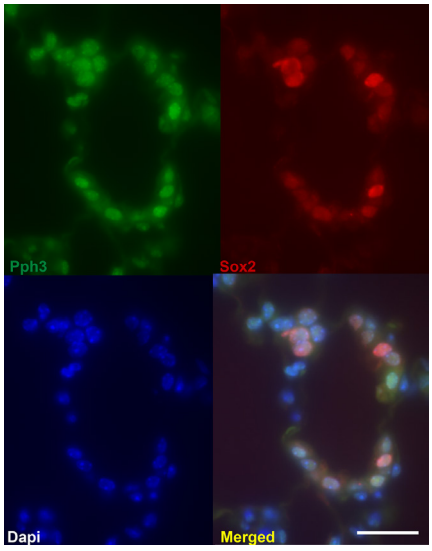

Figure S2. Colocalization of iSox2 and Phh3 is shown by dual immunofluorescence labeling after 28 days of doxycycline exposure. Scale bars 25µm.

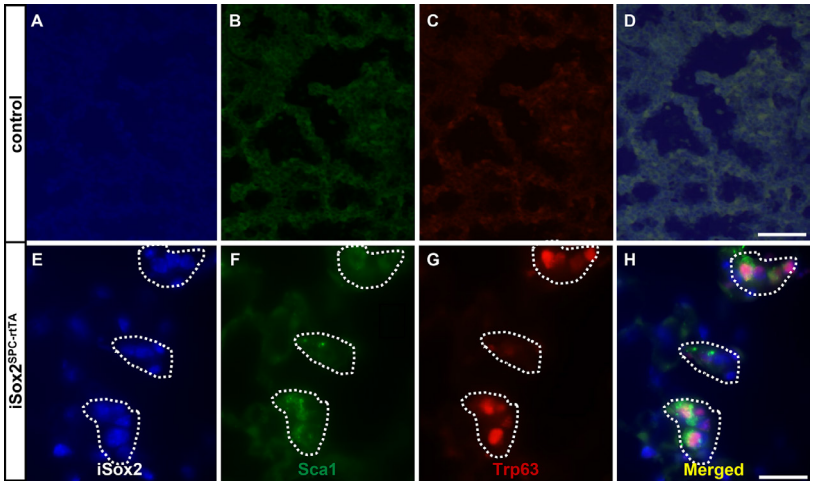

Figure S3. Triple immunofluorescence staining with Myc (iSox2, blue), Sca1 (green) and Trp63 (red) on lungs of control (A-D) and iSox2$^{SPC\text{-}rtTA}$ (E-H) animals treated for 28 days with doxycycline demonstrate the emergence of Sca1/Trp63 positive cells (dotted areas; E-H).

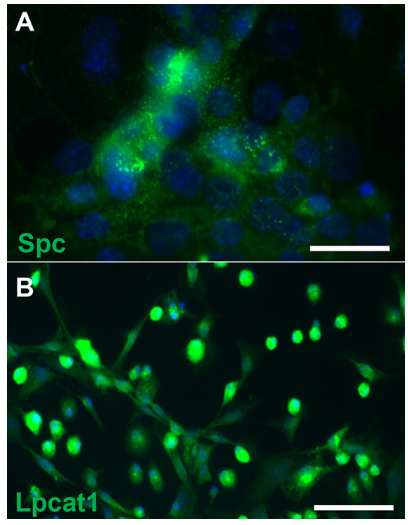

Figure S4. Immunofluorescence staining with Prospc (A) or Lpcat1 (B) of isolated type II cells after one day in culture, showing a high percentage of positive cells after the isolation.

Chapter 4.

An *in vivo* biotin-tagged affinity purification to identify interaction partners of Sox2 protein in the developing mouse lung

Kim Schilders, Evelien Eenjes, Anne Boerema – de Munck, Marjon Buscop – van Kempen, Jeroen Demmers, Petros Kolovos, René Wijnen, Dick Tibboel, Robbert Rottier

Abstract

Sox2 is a Sry-box containing family member of related transcription factors sharing homology in their DNA binding domain. Sox2 is important during different stages of development, and previously we showed that Sox2 plays an important role in branching morphogenesis and epithelial cell differentiation in lung development. The transcriptional activity of Sox2 depends on its interaction with other proteins, leading to 'complex-specific' DNA binding and transcriptional regulation.

In this study, we generated a mouse model containing a biotinylatable-tag targeted at the translational start site of the endogenous Sox2 gene (bioSox2). This tag was biotinylated by the bacterial birA protein and the resulting bioSox2 protein was used to identify associating partners of Sox2 at different phases of lung development in vivo (the Sox2 interactome) and to identify in vivo chromatin binding sites of Sox2 in the lung. Homozygous bioSox2 mice are viable and fertile irrespective of the biotinylation of the bio tag, indicating that the bioSox2 gene is normally expressed and the protein is functional in all tissues. This suggests that partners of Sox2 are most likely able to associate with the bioSox2 protein.

BioSox2 complexes were isolated with high affinity using streptavidin beads and analyzed by MALDI-ToF mass spectrometry analysis. Several of the identified binding partners, including Akap8, Ank3, Dkc1, Cavin (Ptrf) and Safb, were already shown to have a respiratory phenotype. Chromatin immunoprecipitations were performed to determine targets of Sox2 and several of the identified target genes could be linked to lung and respiratory tube development.

Introduction

Sox2 is a Sry-box containing family member of related transcription factors sharing homology in their DNA binding domain. Sox2 is highly conserved across species and is involved in several developmental processes (1). Sox2 expression is temporally and spatially regulated during development and starts to be expressed at the morula-stage of development (2, 3). Expression becomes restricted to the inner cell mass of the blastocyst and continues in the epiblast, which will give rise to the embryo and germ cells (3). Early during development, expression of Sox2 is restricted to the anterior ectoderm, from which the neuroectoderm and anterior surface ectoderm will arise (4, 5). At later gestational ages, Sox2 is expressed in several tissues derived from the primitive foregut endoderm and post-natal it is present in the epithelium of foregut derived organs including the trachea and proximal lung epithelium (3, 6-11).

We and others have shown that Sox2 plays an important role in lung epithelial cell differentiation and branching morphogenesis (11-13). In iSox2$^{SPC\text{-}rtTA}$ mice lung, where Sox2 expression is induced in the epithelial cells of the developing airways, cystic lesions were observed (11). The size of these cyst-like structures correlated with the timing and duration of ectopic Sox2 expression (14). The epithelium of these dilated airway structures had increasing numbers of basal cells and neuroendocrine cells (11). In control lung Sox2 expression in the epithelial tip cells is inhibited by Fgf10 induced β-catenin signaling, which prevents these cells to differentiate in proximal epithelial cells (15, 16). Ectopic expression of Sox2 in these distal epithelial cells aberrantly induced these cells to differentiate into proximal cells, leading to the emergence of basal and neuroendocrine cells. Sox2 directly activated the ΔN Trp63 promoter, indicating that Sox2 is directly responsible for the emergence of basal cells (14).

The transcriptional activity of Sox2 depends on its interaction with other proteins, leading to 'complex-specific' DNA binding and transcriptional regulation (17). Several studies have identified Sox2 associating partners *in vitro* using different kinds of cells (18) (19) (20) (21) (7, 22-25). One of the partners identified in neural stem cells is Chd7. Sox2 and Chd7 cooperate to regulate genes involved in human syndromes that are genetically unrelated but do show a similarity in symptoms (21). By performing large scale immunoprecipitations in stable FLAG/Sox2 transgene embryonic stem (ES) cells, several partners were identified including ES cell self-renewal factors and several lineage-specific transcription factors. Also, Xpo4 was identified as a Sox2 partner, functioning as a nuclear import receptor for Sox2 (26).

Processes in which Sox2 is involved in lung development could be the influenced by specific interaction partners and therefore *in vivo* binding partners of Sox2 were identified in this study, using a mouse model containing a biotinylated Sox2 (bioSox2). The biotinylated Sox2 was efficiently isolated, including associating protein complexes due to the very high affinity of the biotin-streptavidin interaction, which is several magnitudes higher than antibody-antigen interactions (27).

BioSox2 containing complexes were efficiently isolated from mouse embryonic day 18 lungs and brains using streptavidin and subsequently analyzed by mass spectrometry. We identified a number of putative binding partners involved in lung development, including

Akap8, Ank3, Dkc1, Cavin (Ptrf) and Safb. In vivo binding sites for Sox2 were determined by chromatin immunoprecipitations and we found several target genes involved in lung development and respiratory tube development including GLI2 and β-catenin.

Materials and methods

Generation of bioSox2/birA mice

To generate an N-terminal biotin-tagged Sox2 allele (bioSox2), Sox2 genomic DNA was isolated from library with 129 genomic DNA and a NheI – Asp718 fragment containing the Sox2 exon was used to generate the recombination construct used for targeting IB10 ES cells. Genomic DNA of individual clones was digested with EcoRI and screened with specific probes. The neomycin resistance gene was removed from positive clones by transiently expressing Cre in ES cells, and individual clones were genotyped and karyotyped before injection in blastocysts. Chimaeric mice were crossed and maintained on C57/bl6 background. BioSox2 mice were crossed with birA mice to biotinylate the biotag. Mice were kept under standard conditions and experiments were performed following guidelines of the ethics committee of the Erasmus Medical Center.

Large scale tissue immunoprecipitations

Lungs and brains were isolated from bioSox2/birA and birA mice E18. Tissue were minced into small pieces and a single cell solution was prepared using a cell strainer. Immunoprecipitations were essentially done as previously published (21, 26). Cells were lysed in cell lysis buffer (10 mM Hepes 7.6, 1.5 mM MgCl2, 10 mM KCl; add 0.5 mM DTT + protease inhibitors prior to use), followed by lysis of the nuclei in nuclei lysis buffer (20 mM Hepes pH 7.6, 20 % glycerol, 420 mM NaCl, 1.5 mM MgCl2, 0.2 mM EDTA, add 0.5 mM DTT +1 x CEF prior to use). Nuclear extracts were diluted 1:1 in low-salt buffer (20 mM Hepes pH7.6, 20% glycerol, 1.5 mM $MgCl_2$, 0.2 mM EDTA) and incubated with 40 µl Dynabeads®M-280 Streptavidin (Cat. No. 112.06 D, Invitrogen) for at least 1 hour rotating at 4°C in non-stick tubes. After washing with wash buffer (20 mM Hepes pH7.6, 20% glycerol, 100 mM KCl, 1.5 mM $MgCl_2$, 0.2 mM EDTA, 0.02% NP-40; add 1 x CEF prior to use), the beads were resuspended in 40 µl sample buffer (60mM Tris-HCl pH 6.8, 2% SDS, 0.02% bromophenol blue, 10% glycerol, 1% β-mercaptoethanol, 5 mM DTT) and heated for 10 min at 95°C. Samples were loaded on pre-cast gel and send to the department of Biochemistry for Matrix Assisted Laser Desorption/Ionization – Time of Flight Mass Spectrometry (MALDI-TOF MS) analysis.

Cell culture

HEK cells and A549 cells were cultured in DMEM (Lonza, Verviers, Belgium) with 5% fetal calf serum and 1% penicillin-streptomycin under standard culture conditions. NCCIT cells were cultured in DMEM (Lonza, Verviers, Belgium) with 10% fetal calf serum and 1% penicillin-streptomycin under standard culture conditions. H441 cells were cultured with RPMI with 10% fetal calf serum and 1% penicillin-streptomycin under standard culture conditions.

BioSox2 immunoprecipitation in transfected HEK cells

HEK cells were transfected with a bioSox2 and birA expression constructs using Lipofectamine-2000 (Invitrogen) according to the manufacturer's manual. Cells were

harvested 24 hours after transfection and nuclear extracts were prepared by lysing the cells with cell lysis buffer, followed by nuclei lysis buffer. Nuclear extracts were diluted 1:1 in low-salt buffer and incubated with Dynabeads®M-280 Streptavidin for at least 1 hour rotating at 4°C in non-stick tubes. After washing with wash buffer, the beads were resuspended in 40 µl sample buffer and heated for 10 min at 95°C. Mock-transfected HEK cells were used as a control.

Sox2 immunoprecipitation in NCCIT, A549 and H441 cells

NCCIT, A549 and H441 cells were grown to ~85% confluency and collected. Nuclear extracts were prepared by lysing the cells with cell lysis buffer, followed by nuclei lysis buffer. Nuclear extracts were diluted 1:1 in low-salt buffer and incubated with antibodies against Sox2 (sc-17320) and goat IgG (Santa Cruz) O/N rotating at 4°C in non-stick tubes. Samples were incubated with Protein A/G agarose beads for 1 hour rotating at 4°C and then washed with wash buffer. After washing, the beads were resuspended in 40 µl sample buffer and heated for 10 min at 95°C.

Generation of a stable 2xFLAGbioSox2 A549 cell line and large scale FLAG immunoprecipitation

A549 cells were transfected with linearized 2xFLAGbioSox2 using the Amaxa Nucleofector kit (Lonza) according to the manufacturer's manual, followed by neomycin selection (26). Positive clones were expanded, grown to ~85% confluency and collected. As a control wild-type A549 cell were collected similar. Nuclear extracts were prepared by lysing the cells with cell lysis buffer, followed by nuclei lysis buffer. Nuclear extracts were diluted 1:1 in low-salt buffer and incubated with antibody against FLAG (F1804) O/N rotating at 4°C in non-stick tubes. Samples were incubated with Protein G agarose beads for 1 hour rotating at 4°C and then washed with wash buffer. After washing, the beads were resuspended in 40 µl sample buffer and heated for 10 min at 95°C. Samples were loaded on pre-cast gel and send to the department of Biochemistry for MALDI-TOF MS analysis.

Co-transfections and co-immunoprecipitations

HEK cells were transfected with either a myc-tagged TCF3 expression construct, together with 2xFLAGbio-Sox2 , or with a FLAG-tagged WDR5 construct, together with myc-Sox2 (28, 29). X-tremeGENE HP DNA Transfection Reagent (Roche, Basel, Switzerland) was used for the transfection according to the manufacturer's manual. Cells were harvested 24 hours after transfection. Total cell extracts were prepared in 300 µl carin buffer (20mM Tris pH8, 137mM NaCl, 10mM EDTA, 1% NP40, 10% glycerol) with Complete protease inhibitor (Roche, Basel, Switzerland). 50 µl was incubated for 2 hours at 4°C in 250 µl carin buffer with antibodies against myc (1668149, Roche) and FLAG (F1804), followed by 1 hour incubation with protein G beads (Sigma-Aldrich, St. Louis, MO). After washing with carin buffer, the beads were resuspended in 20 µl sample buffer and heated for 10 min at 95°C.

Western blotting

Samples were separated on SDS-PAGE gel and transferred to a PVDF membrane by wet blotting for 2 hours at 100 V and 400 mA, or semi-dry blotting for 1 hour at 100 mA/membrane. Membranes were blocked in TBS with 0.5% Tween-20 and 5% BSA. Membranes were labeled with antibodies against myc (ab9106) and FLAG (F7425) for 2 hours, followed

by an 1 hour incubation with secondary HRP-labeled antibody. Membranes were developed with ECL incubation (Thermo Fisher Scientific INC., Waltham, MA) on the Alliance (Uvitec, Cambridge, UK).

Chromatin immunoprecipitation

Approximately $120x10^6$ NCCIT cells were double cross-linked with 2mM disuccinimidyl glutate (Thermo Fisher Scientific) and 1% formaldehyde, or single cross-linked with 1% formaldehyde (30). Cells were lysed in ChIP cell lysis buffer (10 mM Tris pH 8.0, 10 mM NaCl, 0.2 % NP-40, 1x CEF (prior to use)), followed by lysis of the nuclei in ChIP nuclei lysis buffer (50 mM Tris pH 8.0, 10 mM EDTA, 1% SDS, 1x CEF (prior to use). Samples were sheared with a multiprobe bioruptor (double cross-linked: 75 min, 30 sec. high, 30 sec. off; single cross-linked: 30 min, 30 sec. high, 30 sec. off). Samples were diluted 10 x with ChIP dilution buffer (16.7 mM Tris-HCl pH 8.1, 167 mM NaCl, 1.2 mM EDTA, 1.1% TritonX-100, 0.01% SDS), precleared and incubated O/N with antibodies against CHD4 (ab72418), CUX1 (sc-6327), DACH1 (proteintech), SOX2 (#2748 cell signaling) and goat IgG (Santa Cruz) and rabbit IgG (Santa Cruz) as negative control. Samples were incubated with Protein A/G agarose beads 1 hour rotating at 4°C and then washed with Low Salt Immune Complex Buffer (20 mM Tris-HCl pH8.0, 150 mM NaCl, 2 mM EDTA, 0.1% TritonX-100, 0.1% SDS), High Salt Immune Complex Buffer (20 mM Tris-HCl pH8.0, 500 mM NaCl, 2 mM EDTA, 0.1% TritonX-100, 0.1% SDS), LiCl Immune Complex Buffer (10 mM Tris-HCl pH8.0, 1 mM EDTA, 0.25 M LiCl, 1% NP-40, 1% deoxycholate) and TE (10 mM Tris-HCl pH8.0, 1 mM EDTA pH 8.0). Bound chromatin was eluted with freshly prepared elution buffer (1% SDS, 0.1 M $NaHCO_3$), de-cross-linked and purified DNA was send to the department of Biomics for analysis.

Results

Generation of bioSox2 mice

Most studies identifying Sox2 associating proteins were identified using different cell lines (18-21). *In vitro* cell culture models do not have the same cellular microenvironment as cells *in vivo*. This might result in aberrant expression patterns and therefore a difference in partners *in vitro* and *in vivo*. Since the expression of Sox2 is temporally and spatially regulated, it is expected that there is a dynamic change in interaction partners during the different stages of gestation. To gain more knowledge about the Sox2-partner complexes that are involved during different stages of lung development, associating factors were identified *in vivo* by purifying Sox2 containing complexes from lung tissue.

To increase the specificity of purifying Sox2 containing complexes, we focused on a previously described biotinylatable tag which can be purified with a much higher affinity using streptavidin compared to using Sox2 specific antibodies. Therefore, we targeted an oligonucleotide encoding for the small artificial peptide tag of seventeen amino acids (biotag) to the N-terminus of the endogenous Sox2 locus using homologous recombination in ES cells (bioSox2, fig. 1A). This tag can be biotinylated at a specific lysine residue by the bacterial birA ligase, as previously shown (27). The bioSox2 mice were subsequently crossed with a mouse line ubiquitously expressing a HA-tagged birA from the ROSA26 locus to generate bioSox2/birA mice (31). First, the functionality of the biotinylated Sox2 protein was tested in vitro by co-expressing the N-terminal bio-tagged Sox2 with a bacterial birA biotin ligase expressing construct in HEK cells. Previously it was shown that a N-terminal

FLAG-tagged Sox2 protein was fully functional (21, 26). The bio-tag was efficiently biotinylated by birA, as shown by western blot and by streptavidin specific precipitation of the biotinylated Sox2 from nuclear extracts (fig. 1B). Moreover, we also showed that the biotinylated Sox2 was able to bind to the Sox2 consensus binding site in vitro by an electrophoretic mobility shift assay (data not shown).

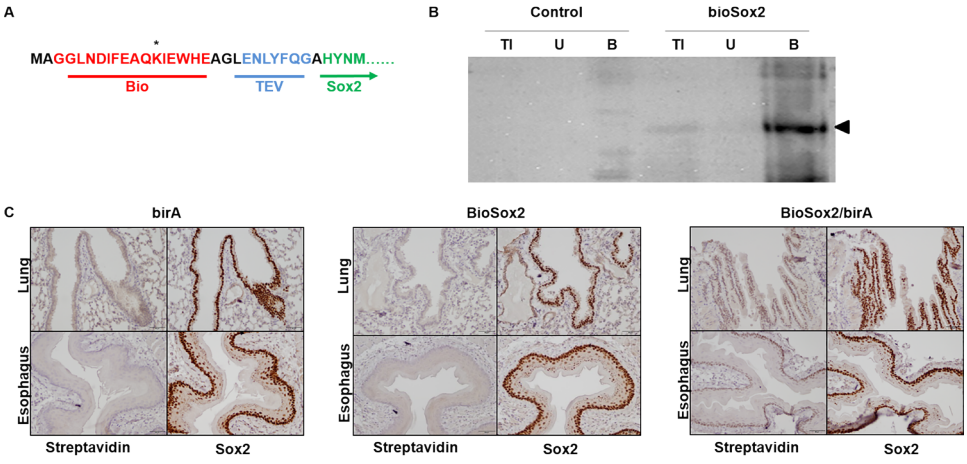

Figure 1. A) BioSox2. Red = biotin tag, blue = TEV protease cleavage site, green = Sox2. **B) Purification of transfected bioSox2 in HEK cells.** BioSox2 was specifically purified from nuclear extraxts of bioSox2 transfected HEK-cells. Blot is labeled with streptavidine coupled HRP. TI = total input, U = unbound fraction, B = purified fraction. **C) The bioSox2 gene is normally expressed and results in a functional protein in mice.** Immunohistochemistry showed that expression of bioSox2 is similar to the endogenous Sox2 expression in lung and esophagus.

Homozygous bioSox2 mice with or without the biotin ligated to the N-terminal tag were born at Mendelian ratios, were viable and fertile. The expression of the tagged bioSox2 in brain, esophagus and trachea of mice was comparable to normal, untagged Sox2, and the bioSox2 was efficiently biotinylated in vivo by the birA protein. Immunohistochemistry showed that expression pattern of the bioSox2 in the brain, esophagus and lung is similar to the endogenous Sox2 expression (fig 1C). Collectively, this indicated that the gene is normally expressed and the tagged protein is fully functional in all tissues. It also implies that all the partners of Sox2 are still able to associate with bioSox2 and fulfill their biological roles, since the absence of correct complex formation will lead to lethal phenotypes.

BioSox2 affinity-purification

To identify specific partners of Sox2 in the trachea and lung during differentiation of the airway epithelium, fetal lungs just prior to birth were investigated. At this phase of development, the epithelium of the trachea and upper airways consists of Sox2 positive cells, so total lungs were isolated at day 18.5 of gestation of bioSox2/birA and birA pups. Brain tissue was isolated as positive control for the procedure. After preparation of a single cell suspension using a cell strainer, nuclear extracts were prepared and bioSox2 complexes were purified with streptavidin-coupled magnetic beads.

After the purification step the precipitated protein complexes need to be released from the magnetic streptavidin beads for subsequent analysis. The bioSox2 protein contained a

Tobacco Etch Virus (TEV) endoprotease recognition site in between the biotin tag and the Sox2 protein. This TEV site is recognized and subsequently cleaved with high specificity by the TEV protease. BioSox2 and associating factors were purified from nuclear extracts of bioSox2/birA transfected HEK cells using magnetic streptavidin beads and precipitated proteins were released either by incubation with the TEV protease or by heating the beads for ten minutes. Western blot analysis showed that the TEV protease recognized and processed the bioSox2 protein, but the cleaved Sox2 did not elute from the beads (fig. 2A). Therefore, we decided to purify the bioSox2 complexes with magnetic beads and subsequently heat the beads to elute the precipitated proteins.

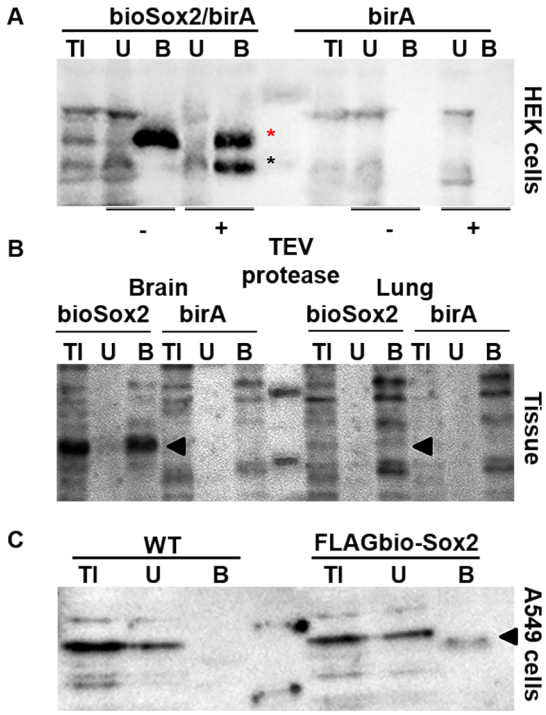

Fig 2. A) TEV protease to cleave bioSox2 in transfected HEK cells. After bioSox2 purification in transfected HEK cells, dynabeads were incubated with TEV protease for different time spans, but bioSox2 was not detected in the eluated fraction. Boiling of the dynabeads revealed that Sox2 was not eluted of the beads by using TEV protease, but TEV protease was able to cut the TEV protease recognition site, showing a bioSox2 (red asterix) and Sox2 (black asterix) band, compared to only a bioSox2 band in sample not incubated with TEV protease. Tl = total input, U = unbound fraction, B = purified fraction, - = no TEV protease added, + = TEV protease added. **B) In vivo purification of bioSox2 in brain and lung tissue.** BioSox2 purification from nuclear extracts of brain and lung tissue E18. Red circles indicate bioSox2. Blot is labeled with streptavidine coupled HRP. Tl = total input, U = unbound fraction, B = purified fraction. Arrows indicate bioSox2. **C) FLAG-Sox2 immunoprecipitation in 2xFLAG-bioSox2 A549 cells.** FLAG-Sox2 was precipitated in 2xFLAG-bioSox2 A549 cells using α-FLAG (F1804). Blot is labeled with α-FLAG (F7425). Tl = total input, U = unbound fraction, B = precipitated fraction.

The bioSox2 purification was performed in triplicate, with a protein input of 400 µg protein in the first pull-down, 2.9 mg protein in the second pull-down and 1 mg protein in the third pull-down. The trachea and lungs were only separated for the first purification, but remained united for the other two purifications. The efficiency of the precipitation was first evaluated, which indicated that the bioSox2 was purified from the bioSox2/birA mouse samples compared to the control birA only samples. (fig. 2B). It also showed that the bioSox2 protein was less prominently present in the lung samples, which indicated that the analysis of the birA samples is essential to subtract the non-specific bands. The total precipitated proteins were separated on a polyacrylamide gel, which was stained with Coomassie Brilliant Blue and analyzed by MALDI-TOF MS. Candidate binding partners identified by mass spectrometry are given in table 1 (lung) and table 2 (brain). 875 unique proteins were identified with a mascot score enriched at least two times compared to the control, from which 124 proteins were enriched in at least two of the lung IPs. In the brain IPs 343 unique proteins were found, from which 29 proteins were enriched in at least two IPs. 153 of these proteins are overlapping. Several of these potential partners were previously linked the respiratory phenotypes in mice, including Akap8, Ank3, Dkc1, Cavin (Ptrf) and Safb.

To complement our in vivo large scale IPs, we also generated a stable transformed A549 cell line using the previously used 2xFLAGbio-Sox2 construct (26) (21). This stable cell line was used to perform an immunoprecipitation with FLAG-coupled beads followed by mass spectrometry directed identification of the eluted proteins (Fig. 2C). The significant enriched set of proteins was compared to the set of proteins identified with those identified with the lung tissue IPs and there was an overlap of 28 proteins (Table 1).

Wdr5 and Tcf3 are binding partners of Sox2

Putative binding partners were initially selected on the basis of their Mascot scores and the number of peptides retrieved in the mass spectrometry analysis. This set of proteins was subsequently analyzed for known cellular functions and possible roles in lung development, which resulted in a short list of putative Sox2 interacting proteins. As a positive control in our validation assays, we used the WD repeat domain 5 (Wdr5) and Transcription factor 3 (Tcf3) proteins, since Wdr5 was previously described as a potential Sox2 binding partner in ES cells and we previously identified Tcf3 as a putative Sox2 binding protein in neural stem cells (21, 32).

Next, HEK cells were transiently transfected with expression constructs of a FLAG-tagged Sox2 and a myc-tagged Tcf3, or a myc-tagged Sox2 with a FLAG/HA tagged Wdr5 to analyze their physical interaction. Extracts of transfected cells were incubated with the appropriate antibodies to immunoprecipitate the tagged Sox2 or Tcf3/Wdr5 and co-precipitated proteins were analyzed.

We first analyzed whether we could detect the interaction between Sox2 and one of its known partners, Wdr5. Immunoprecipitation of FLAG-Wdr5 with a FLAG antibody efficiently co-precipitated the myc-Sox2 protein as indicated by the myc positive signal (fig. 3A). In the reverse experiment, immunoprecipitation of myc-Sox2 with a myc antibody showed co-precipitation the FLAG-Wdr5 protein with the FLAG antibody (fig. 3B). Next, we analyzed whether the putative partner, Tcf3, could also be co-precipitated with Sox2.

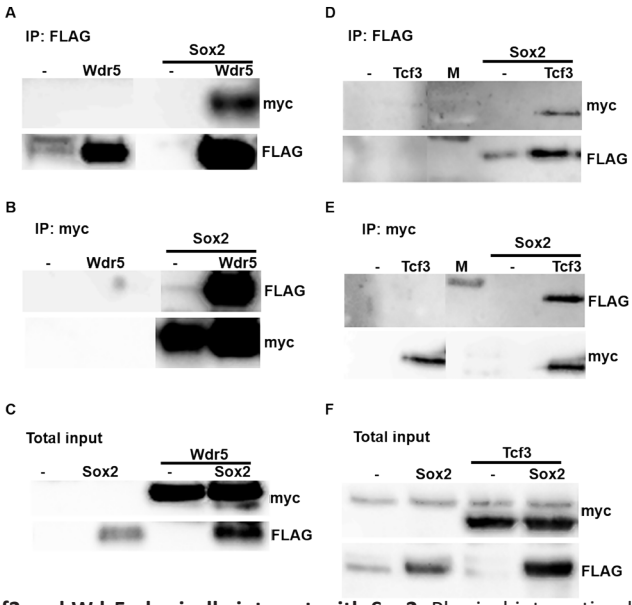

Figure 3. Both Tcf3 and Wdr5 physically interact with Sox2. Physical interaction between Tcf3 and Wdr5 with Sox2 was confirmed in co-immunoprecipitations. A) By precipitating FLAG-Sox2 using FLAG antibody (F1804), we confirmed that myc-Tcf3 was also precipitated. B) By precipitating myc-TCF3 using myc antibody (1668149, Roche), FLAG-Sox2 was co-precipitated. C) Total input shows the expression of myc-TCF3 and FLAG-Sox2. D) By precipitating FLAG-WDR5 using FLAG antibody (F1804), we confirmed that myc-Sox2 was also precipitated. E) By precipitating myc-Sox2 using myc antibody (1668149, Roche), FLAG-Wdr5 was co-precipitated. F) Total input shows the expression of FLAG-WDR5 and myc-Sox2. Blots were labeled with antibodies against FLAG (F7425) and myc (ab9106).

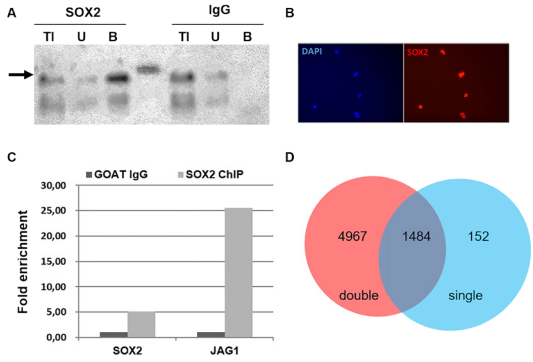

Figure 4. A) Endogenous SOX2 immunoprecipitation in NCCIT cells. Endogenous SOX2 was precipitated in NCCIT cells using α-Sox2(Y-17; sc-17320). Arrow indicates SOX2. TI = total input, U = unbound fraction, B = precipitated fraction. **B) Sox2 expression in NCCIT cells.** NCCIT cells express Sox2. Nuclei are stained with Dapi. **C) Target gene enrichment single cross-linked SOX2 ChIP in NCCIT cells.** An enrichment was observed in SOX2 and JAG1, which are both SOX2 target genes, in the ChIP using a specific SOX2 antibody, compared to the IgG ChIP. **D) Venn diagram showing the overlap of target genes between the single and double cross-linked Sox2 ChIP.** 1636 target genes were identified in the single cross-linked ChIP, compared to 6451 target genes in the double cross-linked ChIP. Between the two ChIPS there is an overlap of 1484 common targets.

Indeed, the FLAG-Sox2 efficiently associated with myc-Tcf3 as shown by the FLAG and myc specific precipitations (fig. 3D, E). Thus, our data showed that aside from Wdr5, we identified Tcf3 as a specific partner of Sox2 in vitro.

Identification of in vivo Sox2 DNA binding sites

To identify common binding sites of Sox2, chromatin immunoprecipitation (ChIP) were performed using the human pluripotent embryonal teratocarcinoma NCCIT cell line, which express SOX2 (fig. 4A, B). Chromatin from NCCIT cells was single cross-linked to evaluate direct protein-DNA interactions, as well as double cross-linked to identify protein-protein-DNA interactions. The latter allows us to identify target genes of the Sox2-partner complex if only one of them is directly bound to DNA.

The quality of the SOX2 ChIP was validated by analyzing known SOX2 targets. Indeed, we found enrichment of SOX2 and JAG1, which are both known to be SOX2 target genes (fig. 4C). ChIP-Seq data were analyzed for individual binding sites and the binding site motifs. Between the single and double cross-linked Sox2 ChIP there was an overlap of 1484 target genes (fig. 4D). Gene ontology showed that 6 of the identified target genes in the single cross-linked SOX2 ChIP were involved in lung development and respiratory tube development: GLI2, SMAD2, TBX4, β-catenin, HHIP and PDPN. These same 6 genes were identified in the double cross-linked ChIP, as well as GLI3, HOPX, BMPR1A, CTGF, CYP1A2, EPAS1, PSEN and TNS3, which are also involved in lung development and respiratory tube development (table 3).

Discussion

Several studies have identified Sox2 interaction partners *in vitro* using different cell lines (18-21). To gain more knowledge about the role of Sox2-partner complexes during lung development, we identified candidate binding partners *in vivo* using a biotinylated-Sox2 mouse model. With this model we were able to efficiently purify the tagged Sox2 protein using streptavidin in a single-step approach. We first optimized the extraction of proteins from embryonic lung and brain tissue. The method has to be stringent enough to obtain a single cell suspension, but protein-protein interaction should be maintained. The most efficient way to reach this is the use of a cell strainer for preparing single-cell suspension followed by nuclear protein extraction. The addition of the biotinylatable tag including the TEV protease recognition site at the N-terminus of the Sox2 protein did not hamper its function as shown by the viability of the mice. This is in concert with previous reports where a N-terminal tagged Sox2 functioned normally (18, 26).

The mass spectrometry of the three large scale immunoprecipitation, resulted in low scores of the bait-Sox2. This is partially due to the unfavorable distribution of the tryptic cleavage sites in the Sox2 protein and the presence of acidic amino acids within some of its peptides. Also there is a low number of $Sox2^+$ cells in the lung (~10%) compared to the brain where the bait-Sox2 score is much higher, showing that the assay itself works very efficiently.

Tcf3 and Wdr5 were used to validate physical interaction with Sox2. Tcf3 was previously identified as a potential Sox2 partner in a large scale purification assay in neural stem cells (21). Here, we validated the interaction between Sox2 and Tcf3. Wdr5 is involved in

seve- ral processes including cell cycle progression and gene regulation. It interacts with Hdac3 under hypoxic conditions and then induces mesenchymal gene expression (33). As such, it plays a crucial role in hypoxia-induced epithelial-mesenchymal transition, which is important in processes as organ development and fibrosis. Wdr5 is also a direct target of Sry, as well as an interaction partner, and the Wdr5-Sry complex activates Sox9 and represses β-catenin expression in sex determination (34). In embryonic stem cells, Wdr5 is identified as a regulator of embryonic stem cell renewal. In these cells, Wdr5 is a direct binding partner of Oct4 and it has been shown that they have an overlap in gene regulatory functions. Immunoprecipitations done in the same study, also suggested interaction between Sox2 and Wdr5 (32). Co-immunoprecipitations that we performed validated this interaction. Wdr5 was also enriched in our first large scale bioSox2 immunoprecipitation in both the lung and trachea, suggesting that the Wdr5-Sox2 protein complex can be involved in lung development.

To validate our results and to translate our findings to the human lung, we used the human lung cell lines, A549 and H441. Although some studies show that these cell lines express Sox2, we were not able to detect this expression efficiently using both IPs and immunofluorescence (35). Immunofluorescent showed that Sox2 expression in A549 cells is very heterogeneous and that not all cells expressed Sox2. Therefore, we developed a stable 2xFLAGbio-Sox2 transgene cell line. We performed a large scale IP with these cells and analyzed them with the same method as the tissue IPs. Comparing the outcome of this IP with the tissue IP, we found several overlapping putative binding partners. Differences between both data sets are probably caused by the difference in human versus mouse and the fact that A549 cells are a carcinomic cell line, making its expression pattern different compared to healthy lung cells *in vivo*. Using human primary bronchial epithelial cells may be more comparable to the SOX2 interactome *in vivo* compared to tumor cell lines.

Several of the potential partners identified in the lung tissue IP can be linked to a respiratory phenotype in mice (table 4). Akap 8 (AKAP95), a member of the A-kinase anchor protein family, is a scaffold protein. Akap8 is together with fidgetin critical for palatogenesis in mice. Mice with only Akap8 mutations do not show any abnormalities, but mice with both Akap8 and fidgetin defiency show symptoms of respiratory distress and die due to cleft palate (36). Ankyrin 3 (Ank3/Ankyrin G) is a protein that is linked to integral membrane proteins. In bronchial epithelial cells, Ankyrin G is necessary for the biogenesis and preservation of the lateral membrane (37, 38). Ank3 mutant mice show abnormal bronchus epithelium morphology (39). Dyskerin (DKC1) is linked to dyskeratosis congenital, which is characterized by premature aging and a higher tumor susceptibility. Patients suffering from this disease also display interstitial lung fibrosis (40-42). Hypomorphic Dkc1 mutant mice show lung abnormalities, including abnormal morphology of the pulmonary parenchyma, alveolus and alveolus wall, lung inflammation and pulmonary interstitial fibrosis (42). Cavin1 (Ptrf) is a protein that is involved in the regulation of rRNA transcription. Deletion of Cavin1 results in loss of caveolae in the lung, increased density of lung tissue and elevated pulmonary arterial pressure(43). Deletion of Cavin2 results in loss of endothelial caveolae in lung tissue (44). Ptrf abnormal lung morphology and abnormal vasculature morphology. Scaffold attachment factor B (Safb) is involved in development, growth and reproduction. abnormal lung alveolus development and $Safb1^{-/-}$ mice show defects in lung maturation resulting in abnormal development of the alveoli (45).

To identify DNA targets, we performed chromatin IPs with antibodies against Sox2 and its potential binding partners using NCCIT cells. These cells show high expression of SOX2 and we also detected expression of potential candidate partners of interest. Although the NCCIT cell line is an embryonic carcinoma cell line, it is very useful to validate the obtained list of putative SOX2 partners. In both the single cross-linked and the double cross-linked ChIP several target genes involved in lung development and respiratory tube development were identified. Gli2 and Gli3 are involved in the formation of trachea lung and esophagus. Mice that lack function of Gli2 show lung hypoplasia and defects of the esophagus and trachea while mice that lack both Gli2 and Gli3 do not form trachea, lung and esophagus (46). GLI3 is also linked to Pallister-Hall syndrome in which the airways can be affected, and to Greig Cephalopolysyndactyly syndrome in which the head, face and limbs are affected.

β-catenin was also identified as a Sox2 target gene in the single cross-linked Sox2 ChIP. β-catenin is a component of the canonical Wnt signaling pathway. During early lung development, Wnt ligands Wnt2 and Wnt2b are highly expressed in the ventral side of the foregut where they specify lung progenitors in the foregut endoderm by signaling through the β-catenin pathway (47, 48). During later phases of lung development, β-catenin is involved in proper proximal-distal patterning of the lung (49). When β-catenin is deleted from the endoderm, there is no formation of trachea and lung (47). Also, conditional deletion of β-catenin in the airway epithelium, causes loss of alveolar structures (50). Activation of β-catenin results in expansion of Nkx2.1, which is the earliest respiratory marker, and loss of Sox2 (47). It also results in enlargement of the air spaces, goblet cell hyperplasia and formation of alveolar type II cells in the upper airways structures (50). β-catenin is required for the formation of distal airways cells. When it is deleted from the epithelial cells of the developing lung prior to E14.5, there are mainly proximal epithelial cells present in the lung. This suggests that β-catenin is preventing differentiation into proximal cells structures (50). Since Sox2 is involved in the differentiation of the proximal epithelial cells and we identified β-catenin as a Sox2 target gene, β-catenin could be down-regulated by Sox2 in the proximal epithelial cells, thereby preventing these cells from differentiation into distal epithelial cells. Previous studies also showed that Sox2 and β-catenin are interaction partners (51). In breast cancer cells, β-catenin can also regulate the transcriptional activity of Sox2 (51).

Another target gene identified in the double cross-linked SOX2 ChIP was Grhl2, suggesting that Sox2 can indirectly regulate Grhl2 gene expression through interaction with a partner. This transcription factor is involved in regulation of epithelial cells, barrier formation and wound healing (52). It is associated with several human congenital anomalies, including deafness (autosomal dominant 28) and ectodermal dysplasia/short stature syndrome. Grhl2 mutant mice show defects in the closure of several embryonic tissues including the cranial neural tube and cleft face. These embryos also show lung defects, which is manifested by smaller airways (53). During development, Grhl2 is highly expressed in the developing lung at E12.5. At E16.5, the trachea, bronchi and bronchioles all show expression levels of Grhl2. At E16.5 this expression is reduced and Grhl2 is only detected in the parenchyma (54). In the human airway epithelium, GRHL2 is expressed in $Trp63^{+}/KRT5^{+}$ basal cells and here it functions as a regulator of cell morphogenesis, adhesion and motility (55). In airway progenitor cells, Grhl2 is a direct regular of Notch signaling and loss of Grhl2 results in inhibition of both Notch and ciliogenesis gene expression and differentiation of

ciliated cells (56). Grhl2 also directly regulates ΔN Trp63, which is also the predominant isoform in basal cells (60). Previously we have shown that ectopic Sox2 expression induces this Trp63 isoform in the lung and that Sox2 directly binds and transactivates the ΔN Trp63 promoter (11, 14).

In this study, we generated a mouse model containing a biotinylatable-tag targeted at the translational start site of the endogenous Sox2 gene (bioSox2). BioSox2 containing complexes were isolated from mouse embryonic day 18.5 lungs and brains analyzed by mass spectrometry. We identified a number of putative binding partners involved in lung development and by performing chromatin immunoprecipitations we found several Sox2 target genes involved in lung development and respiratory tube development.

Acknowledgements

We would like to thank Dr. David Skalnik for the Wdr5 construct, Dr. Brad Merrill for the Tcf3 construct and Prof. Dies Meijer and Dr. Martine Jaegle for the birA mice. Furthermore, we would like to thank Dr. Raymond Poot for his help by initiating the experiments and Dr. Cristina Gontan for starting the work with the bioSox2 mice.

References

1. Pevny L, Placzek M. SOX genes and neural progenitor identity. Curr Opin Neurobiol. 2005;15(1):7-13.
2. Liu K, Lin B, Zhao M, Yang X, Chen M, Gao A, et al. The multiple roles for Sox2 in stem cell maintenance and tumorigenesis. Cell Signal. 2013;25(5):1264-71.
3. Avilion AA, Nicolis SK, Pevny LH, Perez L, Vivian N, Lovell-Badge R. Multipotent cell lineages in early mouse development depend on SOX2 function. Genes Dev. 2003;17(1):126-40.
4. Wood HB, Episkopou V. Comparative expression of the mouse Sox1, Sox2 and Sox3 genes from pre-gastrulation to early somite stages. Mech Dev. 1999;86(1-2):197-201.
5. Papanayotou C, Mey A, Birot AM, Saka Y, Boast S, Smith JC, et al. A mechanism regulating the onset of Sox2 expression in the embryonic neural plate. Plos Biol. 2008;6(1):e2.
6. Ishii Y, Rex M, Scotting PJ, Yasugi S. Region-specific expression of chicken Sox2 in the developing gut and lung epithelium: regulation by epithelial-mesenchymal interactions. Dev Dyn. 1998;213(4):464-75.
7. Donner AL, Episkopou V, Maas RL. Sox2 and Pou2f1 interact to control lens and olfactory placode development. Dev Biol. 2007;303(2):784-99.
8. Schlosser G, Ahrens K. Molecular anatomy of placode development in Xenopus laevis. Dev Biol. 2004;271(2):439-66.
9. Uchikawa M, Ishida Y, Takemoto T, Kamachi Y, Kondoh H. Functional analysis of chicken Sox2 enhancers highlights an array of diverse regulatory elements that are conserved in mammals. Dev Cell. 2003;4(4):509-19.
10. Taranova OV, Magness ST, Fagan BM, Wu Y, Surzenko N, Hutton SR, et al. SOX2 is a dose-dependent regulator of retinal neural progenitor competence. Genes Dev. 2006;20(9):1187-202.
11. Gontan C, de Munck A, Vermeij M, Grosveld F, Tibboel D, Rottier R. Sox2 is important for two crucial processes in lung development: branching morphogenesis and epithelial cell differentiation. Dev Biol. 2008;317(1):296-309.
12. Tompkins DH, Besnard V, Lange AW, Keiser AR, Wert SE, Bruno MD, et al. Sox2 Activates Cell Proliferation and Differentiation in the Respiratory Epithelium. Am J Resp Cell Mol. 2011;45(1):101-10.
13. Que J, Luo X, Schwartz RJ, Hogan BL. Multiple roles for Sox2 in the developing and adult mouse trachea. Development. 2009;136(11):1899-907.
14. Ochieng JK, Schilders K, Kool H, Boerema-de Munck A, Buscop-van Kempen M, Gontan C, et al. Sox2 Regulates the Emergence of Lung Basal Cells by Directly Activating the Transcription of Trp63. Am J Respir Cell Mol Biol. 2014.
15. Volckaert T, Campbell A, Dill E, Li C, Minoo P, De Langhe S. Localized Fgf10 expression is not required for lung branching morphogenesis but prevents differentiation of epithelial progenitors. Development. 2013;140(18):3731-42.
16. Domyan ET, Ferretti E, Throckmorton K, Mishina Y, Nicolis SK, Sun X. Signaling through BMP receptors promotes respiratory identity in the foregut via repression of Sox2. Development. 2011;138(5):971-81.
17. Kamachi Y, Kondoh H. Sox proteins: regulators of cell fate specification and differentiation. Development. 2013;140(20):4129-44.
18. Cox JL, Mallanna SK, Luo X, Rizzino A. Sox2 Uses Multiple Domains to Associate with Proteins Present in Sox2-Protein Complexes. Plos One. 2010;5(11).
19. Cox JL, Wilder PJ, Gilmore JM, Wuebben EL, Washburn MP, Rizzino A. The SOX2-Interactome in Brain Cancer Cells Identifies the Requirement of MSI2 and USP9X for the Growth of Brain Tumor Cells. Plos One. 2013;8(5).
20. Fang XF, Yoon JG, Li LS, Tsai YSS, Zheng S, Hood L, et al. Landscape of the SOX2 protein-protein interactome. Proteomics. 2011;11(5):921-34.
21. Engelen E, Akinci U, Bryne JC, Hou J, Gontan C, Moen M, et al. Sox2 cooperates with Chd7 to regulate genes that are mutated in human syndromes. Nat Genet. 2011;43(6):607-U153.
22. Kondoh H, Kamachi Y. SOX-partner code for cell specification: Regulatory target selection and underlying molecular mechanisms. Int J Biochem Cell B. 2010;42(3):391-9.
23. Ahmed M, Xu JS, Xu PX. EYA1 and SIX1 drive the neuronal developmental program in cooperation with the SWI/SNF chromatin-remodeling complex and SOX2 in the mammalian inner ear. Development. 2012;139(11):1965-77.
24. Boyer LA, Lee TI, Cole MF, Johnstone SE, Levine SS, Zucker JP, et al. Core transcriptional regulatory circuitry in human embryonic stem cells. Cell. 2005;122(6):947-56.
25. Kamachi Y, Uchikawa M, Tanouchi A, Sekido R, Kondoh H. Pax6 and SOX2 form a co-DNA-binding partner complex that regulates initiation of lens development. Genes Dev. 2001;15(10):1272-86.
26. Gontan C, Guttler T, Engelen E, Demmers J, Fornerod M, Grosveld FG, et al. Exportin 4 mediates a novel nuclear import pathway for Sox family transcription factors. J Cell Biol. 2009;185(1):27-34.
27. de Boer E, Rodriguez P, Bonte E, Krijgsveld J, Katsantoni E, Heck A, et al. Efficient biotinylation and single-step purification of tagged transcription factors in mammalian cells and transgenic mice. Proc Natl Acad Sci U S A. 2003;100(13):7480-5.
28. Lee JH, Skalnik DG. CpG-binding protein (CXXC finger protein 1) is a component of the mammalian Set1

histone H3-Lys4 methyltransferase complex, the analogue of the yeast Set1/COMPASS complex. J Biol Chem. 2005;280(50):41725-31.
29. Pereira L, Yi F, Merrill BJ. Repression of Nanog gene transcription by Tcf3 limits embryonic stem cell self-renewal. Mol Cell Biol. 2006;26(20):7479-91.
30. Nowak DE, Tian B, Brasier AR. Two-step cross-linking method for identification of NF-kappaB gene network by chromatin immunoprecipitation. Biotechniques. 2005;39(5):715-25.
31. Driegen S, Ferreira R, van Zon A, Strouboulis J, Jaegle M, Grosveld F, et al. A generic tool for biotinylation of tagged proteins in transgenic mice. Transgenic Research. 2005;14(4):477-82.
32. Ang YS, Tsai SY, Lee DF, Monk J, Su J, Ratnakumar K, et al. Wdr5 mediates self-renewal and reprogramming via the embryonic stem cell core transcriptional network. Cell. 2011;145(2):183-97.
33. Wu MZ, Tsai YP, Yang MH, Huang CH, Chang SY, Chang CC, et al. Interplay between HDAC3 and WDR5 Is Essential for Hypoxia-Induced Epithelial-Mesenchymal Transition. Mol Cell. 2011;43(5):811-22.
34. Xu Z, Gao XX, He YH, Ju JY, Zhang MM, Liu RH, et al. Synergistic Effect of SRY and Its Direct Target, WDR5, on Sox9 Expression. Plos One. 2012;7(4).
35. Chou YT, Lee CC, Hsiao SH, Lin SE, Lin SC, Chung CH, et al. The emerging role of SOX2 in cell proliferation and survival and its crosstalk with oncogenic signaling in lung cancer. Stem Cells. 2013;31(12):2607-19.
36. Yang Y, Mahaffey CL, Berube N, Frankel WN. Interaction between fidgetin and protein kinase A-anchoring protein AKAP95 is critical for palatogenesis in the mouse. J Biol Chem. 2006;281(31):22352-9.
37. Kizhatil K, Bennett V. Lateral membrane biogenesis in human bronchial epithelial cells requires 190-kDa ankyrin-G. J Biol Chem. 2004;279(16):16706-14.
38. Kizhatil K, Davis JQ, Davis L, Hoffman J, Hogan BL, Bennett V. Ankyrin-G is a molecular partner of E-cadherin in epithelial cells and early embryos. J Biol Chem. 2007;282(36):26552-61.
39. Jenkins PM, Vasavda C, Hostettler J, Davis JQ, Abdi K, Bennett V. E-cadherin polarity is determined by a multifunction motif mediating lateral membrane retention through ankyrin-G and apical-lateral transcytosis through clathrin. J Biol Chem. 2013;288(20):14018-31.
40. Kirwan M, Dokal I. Dyskeratosis congenita, stem cells and telomeres. Biochim Biophys Acta. 2009;1792(4):371-9.
41. Kropski JA, Mitchell DB, Markin C, Polosukhin VV, Choi L, Johnson JE, et al. A novel dyskerin (DKC1) mutation is associated with familial interstitial pneumonia. Chest. 2014;146(1):e1-7.
42. Ruggero D, Grisendi S, Piazza F, Rego E, Mari F, Rao PH, et al. Dyskeratosis congenita and cancer in mice deficient in ribosomal RNA modification. Science. 2003;299(5604):259-62.
43. Sward K, Sadegh MK, Mori M, Erjefalt JS, Rippe C. Elevated pulmonary arterial pressure and altered expression of Ddah1 and Arg1 in mice lacking cavin-1/PTRF. Physiol Rep. 2013;1(1):e00008.
44. Hansen CG, Shvets E, Howard G, Riento K, Nichols BJ. Deletion of cavin genes reveals tissue-specific mechanisms for morphogenesis of endothelial caveolae. Nat Commun. 2013;4:1831.
45. Ivanova M, Dobrzycka KM, Jiang S, Michaelis K, Meyer R, Kang K, et al. Scaffold attachment factor B1 functions in development, growth, and reproduction. Mol Cell Biol. 2005;25(8):2995-3006.
46. Motoyama J, Liu J, Mo R, Ding Q, Post M, Hui CC. Essential function of Gli2 and Gli3 in the formation of lung, trachea and oesophagus. Nat Genet. 1998;20(1):54-7.
47. Harris-Johnson KS, Domyan ET, Vezina CM, Sun X. beta-Catenin promotes respiratory progenitor identity in mouse foregut. Proc Natl Acad Sci U S A. 2009;106(38):16287-92.
48. Goss AM, Tian Y, Tsukiyama T, Cohen ED, Zhou D, Lu MM, et al. Wnt2/2b and beta-catenin signaling are necessary and sufficient to specify lung progenitors in the foregut. Dev Cell. 2009;17(2):290-8.
49. Shu W, Guttentag S, Wang Z, Andl T, Ballard P, Lu MM, et al. Wnt/beta-catenin signaling acts upstream of N-myc, BMP4, and FGF signaling to regulate proximal-distal patterning in the lung. Dev Biol. 2005;283(1):226-39.
50. Mucenski ML, Wert SE, Nation JM, Loudy DE, Huelsken J, Birchmeier W, et al. beta-Catenin is required for specification of proximal/distal cell fate during lung morphogenesis. J Biol Chem. 2003;278(41):40231-8.
51. Ye XX, Wu F, Wu CS, Wang P, Jung KR, Gopal K, et al. beta-Catenin, a Sox2 binding partner, regulates the DNA binding and transcriptional activity of Sox2 in breast cancer cells. Cell Signal. 2014;26(3):492-501.
52. Walentin K, Hinze C, Werth M, Haase N, Varma S, Morell R, et al. A Grhl2-dependent gene network controls trophoblast branching morphogenesis. Development. 2015;142(6):1125-36.
53. Pyrgaki C, Liu A, Niswander L. Grainyhead-like 2 regulates neural tube closure and adhesion molecule expression during neural fold fusion. Dev Biol. 2011;353(1):38-49.
54. Auden A, Caddy J, Wilanowski T, Ting SB, Cunningham JM, Jane SM. Spatial and temporal expression of the Grainyhead-like transcription factor family during murine development. Gene Expr Patterns. 2006;6(8):964-70.
55. Gao X, Vockley CM, Pauli F, Newberry KM, Xue Y, Randell SH, et al. Evidence for multiple roles for grainyheadlike 2 in the establishment and maintenance of human mucociliary airway epithelium. P Natl Acad Sci USA. 2013;110(23):9356-61.

56. Gao X, Bali AS, Randell SH, Hogan BL. GRHL2 coordinates regeneration of a polarized mucociliary epithelium from basal stem cells. J Cell Biol. 2015;211(3):669-82.
57. Mehrazarin S, Chen W, Oh JE, Liu ZX, Kang KL, Yi JK, et al. The p63 Gene Is Regulated by Grainyhead-like 2 (GRHL2) through Reciprocal Feedback and Determines the Epithelial Phenotype in Human Keratinocytes. Journal of Biological Chemistry. 2015;290(32):19999-20008.

Table 1. Identified binding partners of Sox2 in lung tissue using mass spectrometry analysis.
Large scale tissue IP using nuclear extracts prepared from lung tissue E18.5.

	First large scale lung purification		Second large scale lung purification		Third large scale lung purification	
Symbol	**Mascot[a]**	**Peptides[b]**	**Mascot[a]**	**Peptides[b]**	**Mascot[a]**	**Peptides[b]**
Abcf2	201 (N.A.)	5 (0)				
Ablim1	220 (N.A.)	4 (0)			390 (N.A.)	10 (0)
Ablim3					151 (N.A.)	2 (0)
Ace					169 (N.A.)	4 (0)
Acin1	762 (N.A.)	16 (0)				
Acsl5			112 (44)	3 (1)		
Acta1	1094 (488)	18 (9)				
Acta2[A]	1096 (N.A.)	18 (0)				
Actl6a	268 (N.A.)	6 (0)				
Actn1	821 (N.A.)	13 (0)				
Actn2	1367 (N.A.)	22 (0)			2144 (872)	35 (16)
Actn4	511 (N.A.)	8 (0)				
Actr3					278 (87)	6 (1)
Actr5	276 (102)	5 (2)				
Add1					91 (N.A.)	2 (0)
Afap1l1					289 (N.A.)	7 (0)
Ager			348 (164)	8 (4)		
Ahnak	110 (N.A.)	5 (0)			1935 (624)	50 (15)
Ahnak2					133 (N.A.)	3 (0)
Aif1l					156 (N.A.)	3 (0)
Akap13[A]	146 (N.A.)	2 (0)				
Akap2			1062 (N.A.)	20 (0)		
Akap5					110 (47)	2 (1)
Akap8	176 (N.A.)	2 (0)				
Alb					125 (N.A.)	3 (0)
Alcam					223 (N.A.)	5 (0)
Alyref	265 (N.A.)	5 (0)				
Alyref2			168 (N.A.)	3 (0)		
Ank3	773 (N.A.)	15 (0)				
Ankrd1	127 (N.A.)	3 (0)				
Anxa1[A]			194 (N.A.)	4 (0)		
Anxa11[A]	608 (128)	10 (3)	224 (N.A.)	4 (0)		
Anxa2	469 (N.A.)	8 (0)				
Anxa3			113 (N.A.)	2 (0)		
Anxa6	493 (N.A.)	8 (0)			333 (92)	8 (2)
Anxa7	135 (40)	2 (1)				
Ap2a2	148 (N.A.)	3 (0)				
Ap2b1					431 (N.A.)	10 (0)
Ap2m1					99 (N.A.)	2 (0)

	First large scale lung purification		Second large scale lung purification		Third large scale lung purification	
Symbol	**Mascot[a]**	**Peptides[b]**	**Mascot[a]**	**Peptides[b]**	**Mascot[a]**	**Peptides[b]**
Apmap			103 (48)	2 (1)		
Aqp1					131 (N.A.)	2 (0)
Aqr	293 (N.A.)	6 (0)			452 (124)	12 (4)
Arcn1	98 (N.A.)	2 (0)				
Arf1	290 (N.A.)	5 (0)			214 (N.A.)	3 (0)
Arf2	290 (N.A.)	5 (0)				
Arf3	290 (N.A.)	5 (0)			214 (N.A.)	3 (0)
Arf4	236 (N.A.)	4 (0)				
Arf5	238 (N.A.)	5 (0)				
Arhgef15			219 (N.A.)	5 (0)		
Arl8a	232 (N.A.)	4 (0)			106 (N.A.)	2 (0)
Arpc1b			181 (N.A.)	2 (0)	122 (N.A.)	2 (0)
Arpc2	82 (N.A.)	2 (0)			380 (N.A.)	7 (0)
Arpc5l					141 (N.A.)	2 (0)
Ascc3	120 (N.A.)	3 (0)	183 (73)	4 (1)		
Asf1a	133 (59)	2 (1)				
Atp1a1					929 (46)	17 (1)
Atp2a2					288 (N.A.)	7 (0)
Atp2b1					230 (N.A.)	4 (0)
Atp2b4			108 (N.A.)	3 (0)		
Atp5a1	973 (N.A.)	14 (0)				
Atp5b	855 (N.A.)	13 (0)				
Atp6v0d1					84 (N.A.)	2 (0)
Atrx	137 (N.A.)	3 (0)				
Baz1b					620 (284)	13 (6)
Bcam					136 (N.A.)	2 (0)
Bcap31					147 (47)	3 (1)
Bcas2	231 (N.A.)	5 (0)				
Bclaf1	335 (N.A.)	8 (0)			935 (465)	21 (11)
Bnip1			82 (N.A.)	2 (0)		
Brd7	115 (N.A.)	2 (0)				
Brd8	98 (N.A.)	1 (0)				
Bub3	393 (157)	6 (3)				
Bud13					155 (N.A.)	4 (0)
Bud31			210 (103)	4 (3)		
Cactin			82 (N.A.)	1 (0)	300 (120)	7 (3)
Cald1					593 (283)	11 (5)
Canx					237 (N.A.)	6 (0)
Caprin1	141 (N.A.)	3 (0)				
Capza1	387 (N.A.)	7 (0)	366 (N.A.)	7 (0)		
Capzb			683 (N.A.)	11 (0)		
Casq1	128 (N.A.)	2 (0)				

	First large scale lung purification		Second large scale lung purification		Third large scale lung purification	
Symbol	**Mascot[a]**	**Peptides[b]**	**Mascot[a]**	**Peptides[b]**	**Mascot[a]**	**Peptides[b]**
Casq2	286 (N.A.)	5 (0)				
Casz1			198 (N.A.)	4 (0)		
Cav2			253 (87)	5 (2)		
Cbr2			285 (113)	7 (2)		
Cbx3	326 (136)	6 (2)				
Ccar1	154 (N.A.)	4 (0)			190 (N.A.)	5 (0)
Cct2	289 (N.A.)	6 (0)				
Cct3	558 (N.A.)	11 (0)				
Cct4	223 (N.A.)	4 (0)				
Cct5	226 (N.A.)	3 (0)			133 (48)	3 (1)
Cct7	134 (N.A.)	3 (0)				
Cct8	879 (N.A.)	13 (0)				
Cdc16	92 (N.A.)	2 (0)				
Cdc40	88 (N.A.)	2 (0)	288 (89)	7 (2)	436 (142)	10 (4)
Cdc5l	685 (N.A.)	14 (0)				
Cdk11b[A]			185 (N.A.)	4 (0)	430 (143)	8 (3)
Cdk12			167 (64)	4 (2)		
Cdk13			267 (64)	6 (2)	594 (N.A.)	14 (0)
Cdyl	100 (N.A.)	2 (0)				
Cebpz					85 (N.A.)	2 (0)
Celf1	146 (N.A.)	3 (0)			96 (N.A.)	2 (0)
Celf2					114 (51)	3 (1)
Cenpv			122 (58)	2 (1)	283 (67)	6 (1)
Ces1d			121 (N.A.)	2 (0)		
Cggbp1	250 (N.A.)	5 (0)				
Cgn					437 (N.A.)	9 (0)
Cgnl1					412 (47)	9 (1)
Chd2			290 (N.A.)	7 (0)	203 (99)	5 (2)
Chd3	222 (N.A.)	5 (0)				
Chd4	319 (N.A.)	7 (0)				
Chd8			132 (N.A.)	4 (0)		
Cherp	143 (N.A.)	4 (0)				
Chtop	284 (N.A.)	5 (0)				
Ckap4					595 (N.A.)	11 (0)
Clasp1	86 (40)	2 (1)				
Cldn3					116 (N.A.)	3 (0)
Clec3a	102 (N.A.)	2 (0)				
Clk3					102 (N.A.)	2 (0)
Cltc	323 (N.A.)	7 (0)				
Cmss1			143 (N.A.)	3 (0)		
Col12a1	81 (N.A.)	2 (0)				
Col14a1	386 (N.A.)	8 (0)				

	First large scale lung purification		Second large scale lung purification		Third large scale lung purification	
Symbol	**Mascot[a]**	**Peptides[b]**	**Mascot[a]**	**Peptides[b]**	**Mascot[a]**	**Peptides[b]**
Col2a1	99 (N.A.)	2 (0)				
Colec12					94 (N.A.)	2 (0)
Copb2	108 (N.A.)	3 (0)				
Cope					103 (N.A.)	3 (0)
Coro2b	83 (N.A.)	1 (0)	146 (52)	3 (2)		
Cpm					171 (N.A.)	4 (0)
Cpsf1	395 (N.A.)	7 (0)			1044 (416)	20 (9)
Cpsf2	122 (N.A.)	3 (0)				
Cpsf3	250 (N.A.)	6 (0)	757 (261)	16 (6)		
Cpsf3l	155 (68)	2 (1)				
Cpsf7	120 (N.A.)	2 (0)				
Crnkl1	230 (N.A.)	4 (0)			784 (279)	16 (6)
Csnk1a1	107 (N.A.)	2 (0)				
Cstf2	93 (N.A.)	2 (0)				
Cstf3	201 (N.A.)	4 (0)	641 (288)	12 (5)		
Ctnna2					80 (N.A.)	2 (0)
Ctnnbl1	146 (N.A.)	3 (0)	357 (95)	8 (2)		
Ctnnd1	538 (N.A.)	11 (0)				
Cttn					408 (116)	10 (3)
Cul7					875 (369)	18 (8)
Cux1[A]	476 (N.A.)	8 (0)				
Cwc25					92 (N.A.)	2 (0)
Cyb5a					147 (43)	3 (1)
Cyp2f2			633 (227)	13 (5)	221 (77)	6 (2)
Dapk1					116 (N.A.)	3 (0)
Dazap1	300 (N.A.)	4 (0)				
Dbn1					300 (N.A.)	5 (0)
Ddost			184 (78)	5 (2)		
Ddx1	98 (N.A.)	3 (0)				
Ddx17	845 (53)	15 (1)				
Ddx18			150 (N.A.)	4 (0)	235 (91)	5 (2)
Ddx23	341 (N.A.)	8 (0)				
Ddx26b					99 (N.A.)	3 (0)
Ddx39a	376 (N.A.)	7 (0)				
Ddx39b	700 (N.A.)	12 (0)				
Ddx3x	783 (N.A.)	15 (0)				
Ddx3y	783 (N.A.)	15 (0)	1362 (N.A.)	24 (0)		
Ddx42			123 (N.A.)	2 (0)	316 (81)	7 (2)
Ddx46	107 (N.A.)	2 (0)				
Ddx47	327 (130)	6 (2)				
Ddx5	823 (53)	16 (1)				
Ddx50	494 (85)	10 (2)				

	First large scale lung purification		Second large scale lung purification		Third large scale lung purification	
Symbol	**Mascot[a]**	**Peptides[b]**	**Mascot[a]**	**Peptides[b]**	**Mascot[a]**	**Peptides[b]**
Ddx51	116 (55)	3 (1)				
Decr1	113 (N.A.)	2 (0)				
Dek	101 (N.A.)	1 (0)	608 (243)	14 (5)		
Dennd2a	103 (N.A.)	3 (0)				
Des	589 (N.A.)	9 (0)			876 (280)	17 (6)
Dhrs4	192 (N.A.)	2 (0)	425 (188)	8 (4)	330 (118)	6 (3)
Dhx15	717 (N.A.)	16 (0)				
Dhx16	86 (N.A.)	2 (0)				
Dhx30					445 (N.A.)	10 (0)
Dhx35			132 (N.A.)	4 (0)		
Dhx37					105 (N.A.)	3 (0)
Dhx8[A]					139 (N.A.)	3 (0)
Dhx9	1028 (N.A.)	20 (0)			2086 (888)	36 (16)
Dkc1	135 (N.A.)	2 (0)				
Drg1	360 (45)	6 (1)				
Dst					130 (60)	4 (2)
Dync1h1					806 (201)	21 (5)
Dync2h1	123 (N.A.)	3 (0)				
Ebna1bp2			244 (105)	6 (3)		
Eef1a1	495 (69)	8 (1)				
Eef1g	146 (N.A.)	2 (0)				
Eftud2	1342 (N.A.)	22 (0)			1800 (856)	32 (16)
Ehmt1	113 (N.A.)	3 (0)				
Eif2a[A]	97 (N.A.)	2 (0)				
Eif2s1	301 (N.A.)	6 (0)				
Eif3k	99 (N.A.)	2 (0)				
Eif3l	95 (N.A.)	2 (0)				
Eif4a1	253 (N.A.)	5 (0)				
Eif4a3	739 (N.A.)	14 (0)				
Elavl1	450 (N.A.)	7 (0)				
Eln	93 (N.A.)	2 (0)				
Enpep					376 (44)	8 (1)
Eprs	85 (N.A.)	1 (0)				
Ercc3	141 (N.A.)	3 (0)				
Erh	89 (N.A.)	1 (0)				
Erlin1			126 (N.A.)	2 (0)		
Ewsr1	111 (N.A.)	1 (0)				
Ezr					293 (N.A.)	6 (0)
Fam101b[A]			112 (43)	3 (1)		
FAM120[A]	381 (N.A.)	6 (0)				
Fam208a			307 (N.A.)	7 (0)	509 (152)	12 (5)
Fat2					87 (N.A.)	3 (0)

	First large scale lung purification		Second large scale lung purification		Third large scale lung purification	
Symbol	**Mascot[a]**	**Peptides[b]**	**Mascot[a]**	**Peptides[b]**	**Mascot[a]**	**Peptides[b]**
Fbl	183 (N.A.)	5 (0)				
Fen1	107 (N.A.)	1 (0)				
Fip1l1	171 (N.A.)	3 (0)				
Fiz1	122 (N.A.)	2 (0)				
Fkbp9	82 (N.A.)	2 (0)				
Flii					1259 (479)	25 (7)
Flna	1052 (N.A.)	23 (0)			1348 (460)	25 (9)
Flnb					870 (N.A.)	16 (0)
Flnc	118 (N.A.)	2 (0)				
Fmo2			537 (259)	10 (4)		
Fmod	183 (N.A.)	3 (0)				
Fn1			943 (430)	19 (9)		
Foxp1	146 (N.A.)	3 (0)				
FoxP2	62 (N.A.)	2 (0)				
Foxp4	86 (N.A.)	2 (0)				
Frg1	89 (N.A.)	2 (0)				
Fubp1	177 (N.A.)	4 (0)				
Fubp3	342 (N.A.)	9 (0)				
Fus	125 (N.A.)	3 (0)				
Fxr1	134 (N.A.)	3 (0)			368 (184)	9 (4)
Fyttd1[A]	281 (N.A.)	5 (0)	321 (137)	5 (3)		
G3bp1	203 (N.A.)	4 (0)				
G3bp2	93 (N.A.)	3 (0)				
Gapdh	147 (N.A.)	3 (0)				
Gar1			258 (70)	5 (2)		
Gata6			87 (N.A.)	2 (0)		
Gatad2a	149 (N.A.)	3 (0)				
Gatad2b	334 (N.A.)	6 (0)				
Gcom1	212 (N.A.)	3 (0)	727 (298)	13 (5)		
Glud1	406 (N.A.)	7 (0)				
Glyr1	161 (N.A.)	2 (0)				
Gm10036	146 (N.A.)	2 (0)				
Gm10093	324 (N.A.)	5 (0)				
Gm10094	194 (N.A.)	3 (0)				
Gm10110	84 (N.A.)	2 (0)				
Gm10260	187 (N.A.)	4 (0)				
Gm10288	146 (N.A.)	2 (0)				
Gm10335	165 (N.A.)	3 (0)				
Gm16477	122 (N.A.)	2 (0)				
Gm17087				144 (N.A.)	2 (0)	
Gm20425				116 (N.A.)	3 (0)	
Gm20521			86 (N.A.)	2 (0)		

	First large scale lung purification		Second large scale lung purification		Third large scale lung purification	
Symbol	**Mascot[a]**	**Peptides[b]**	**Mascot[a]**	**Peptides[b]**	**Mascot[a]**	**Peptides[b]**
Gm21992	101 (N.A.)	3 (0)				
Gm4782				258 (98)	7 (3)	
Gm4968				416 (N.A.)	7 (0)	
Gm5093	146 (N.A.)	2 (0)				
Gm5428	259 (N.A.)	4 (0)				
Gm5449	181 (N.A.)	3 (0)				
Gm5619	122 (N.A.)	2 (0)				
Gm5828	98 (N.A.)	2 (0)				
Gm6472	150 (N.A.)	3 (0)		232 (N.A.)	4 (0)	
Gm6793	511 (113)	7 (3)				
Gm7293	147 (N.A.)	3 (0)				
Gm7729	567 (N.A.)	7 (0)				
Gm8991	511 (113)	7 (3)				
Gm9242	511 (113)	7 (3)				
Gm9493	150 (N.A.)	3 (0)				
Gm9755	183 (62)	4 (2)				
Gm9825	224 (N.A.)	3 (0)				
Gna11			114 (N.A.)	3 (0)		
Gnai3					120 (N.A.)	3 (0)
Gnb1	138 (N.A.)	3 (0)				
Gnb2	138 (N.A.)	3 (0)			201 (40)	5 (1)
Gnb2l1	740 (122)	11 (3)				
Gsn			222 (N.A.)	4 (0)		
Gtf2h4	122 (43)	2 (1)				
Gtf3c1			432 (198)	10 (4)		
Gtl3	123 (N.A.)	2 (0)				
Gtpbp2			168 (73)	4 (2)		
H1f0					331 (56)	5 (1)
Hadha	171 (N.A.)	3 (0)	584 (212)	11 (3)		
Hadhb			223 (N.A.)	5 (0)		
Hba	107 (N.A.)	2 (0)				
Hbb-b1	476 (N.A.)	7 (0)	731 (N.A.)	11 (0)		
Hbb-b2	287 (N.A.)	5 (0)	527 (N.A.)	10 (0)		
Hdac1	248 (N.A.)	4 (0)				
Hdac2	286 (N.A.)	5 (0)				
Hdgfrp2	101 (43)	2 (1)	199 (92)	5 (2)	100 (N.A.)	2 (0)
Hdlbp	611 (N.A.)	14 (0)				
Hip1					218 (N.A.)	4 (0)
Hist1h1t					242 (N.A.)	3 (0)
Hist1h2bb	95 (N.A.)	1 (0)				
Hist1h2bc	99 (N.A.)	1 (0)				
Hist1h2bf	95 (N.A.)	1 (0)				

	First large scale lung purification		Second large scale lung purification		Third large scale lung purification	
Symbol	**Mascot[a]**	**Peptides[b]**	**Mascot[a]**	**Peptides[b]**	**Mascot[a]**	**Peptides[b]**
Hist1h2bh	99 (N.A.)	1 (0)				
Hist1h2bk	95 (N.A.)	1 (0)				
Hist1h2bm	99 (N.A.)	1 (0)				
Hist1h2bp	95 (N.A.)	1 (0)				
Hist1h2bq	95 (N.A.)	1 (0)				
Hist2h2bb	99 (N.A.)	1 (0)				
Hist2h2be	99 (N.A.)	1 (0)				
Hist3h2ba	95 (N.A.)	1 (0)				
Hist3h2bb	95 (N.A.)	1 (0)				
Hmbox1			300 (104)	5 (2)		
Hmga1	153 (N.A.)	2 (0)				
Hmga2	144 (49)	2 (1)				
Hmgb2			136 (N.A.)	4 (0)	87 (N.A.)	3 (0)
Hnrnpa0	302 (N.A.)	4 (0)				
Hnrnpa1	385 (114)	5 (2)				
Hnrnpa2b1	512 (126)	7 (3)				
Hnrnpa3	539 (113)	8 (3)				
Hnrnpab	260 (N.A.)	4 (0)				
Hnrnpc	573 (N.A.)	10 (0)				
Hnrnpd	267 (45)	4 (1)				
Hnrnpdl	104 (N.A.)	2 (0)				
Hnrnpdl1	102 (N.A.)	2 (0)				
Hnrnpf	515 (N.A.)	8 (0)				
Hnrnph1	721 (N.A.)	11 (0)				
Hnrnph2	654 (N.A.)	11 (0)				
Hnrnph3	190 (N.A.)	4 (0)				
Hnrnpk	812 (N.A.)	11 (0)				
Hnrnpl	793 (N.A.)	13 (0)	954 (N.A.)	14 (0)		
Hnrnpm	1252 (N.A.)	16 (0)				
Hnrnpr	257 (N.A.)	5 (0)				
Hnrnpu	992 (90)	16 (2)				
Hnrnpul1	293 (N.A.)	6 (0)				
Hnrnpul2	239 (N.A.)	5 (0)				
Hp1bp3	197 (N.A.)	5 (0)				
Hsd17b11			119 (N.A.)	3 (0)		
Hsp90aa1	369 (N.A.)	6 (0)				
Hsp90ab1	660 (N.A.)	11 (0)				
Hsp90b1	615 (N.A.)	12 (0)				
Hspa12b	128 (N.A.)	2 (0)				
Hspa5	641 (N.A.)	12 (0)				
Hspa8	1067 (N.A.)	17 (0)				
Hspa9	130 (N.A.)	3 (0)				

	First large scale lung purification		Second large scale lung purification		Third large scale lung purification	
Symbol	**Mascot[a]**	**Peptides[b]**	**Mascot[a]**	**Peptides[b]**	**Mascot[a]**	**Peptides[b]**
Hspd1	103 (N.A.)	2 (0)				
Hspg2[A]			250 (N.A.)	6 (0)		
Igf2bp2	451 (N.A.)	10 (0)				
Ik	289 (N.A.)	7 (0)			402 (186)	10 (4)
Il33			84 (N.A.)	2 (0)		
Ilf2	177 (N.A.)	3 (0)				
Ilf3	134 (N.A.)	4 (0)				
Ina					91 (N.A.)	2 (0)
Ino80c	85 (N.A.)	1 (0)				
Isy1	151 (N.A.)	2 (0)				
Itga1					172 (N.A.)	4 (0)
Itgb1					336 (68)	6 (2)
Kank3	299 (N.A.)	6 (0)				
Kansl3	175 (N.A.)	3 (0)				
Kat8	179 (73)	4 (2)				
Kdelr1	124 (N.A.)	2 (0)				
Kdm1a	187 (N.A.)	3 (0)				
Khsrp	125 (N.A.)	3 (0)				
Kiaa0020			165 (N.A.)	4 (0)		
Kiaa1429			105 (N.A.)	2 (0)	409 (122)	9 (2)
Kmt2a					98 (N.A.)	2 (0)
Kmt2b			163 (63)	4 (2)		
Kpna1	80 (N.A.)	1 (0)				
Kpna6	80 (N.A.)	1 (0)				
Kpnb1	156 (N.A.)	4 (0)				
krt1	214 (N.A.)	3 (0)				
krt18	564 (N.A.)	9 (0)				
krt19	1239 (N.A.)	20 (0)				
krt20	124 (N.A.)	3 (0)				
krt7	433 (N.A.)	9 (0)				
krt8	650 (N.A.)	13 (0)				
Kxd1	86 (N.A.)	2 (0)				
Lad1					105 (N.A.)	3 (0)
Lama3[A]					95 (N.A.)	2 (0)
Lamb3					182 (N.A.)	4 (0)
Lck			80 (N.A.)	2 (0)		
Ldb3	434 (N.A.)	9 (0)				
Lepre1[A]	93 (N.A.)	2 (0)				
Lima1					266 (N.A.)	7 (0)
Limch1	451 (N.A.)	7 (0)				
Lman2					111 (N.A.)	2 (0)
Lmna	781 (N.A.)	12 (0)				

	First large scale lung purification		Second large scale lung purification		Third large scale lung purification	
Symbol	**Mascot[a]**	**Peptides[b]**	**Mascot[a]**	**Peptides[b]**	**Mascot[a]**	**Peptides[b]**
Lmnb1	272 (N.A.)	6 (0)				
Lmo7			2132 (N.A.)	38 (0)		
Lpcat1			112 (N.A.)	2 (0)	123 (N.A.)	2 (0)
Lrp1					179 (N.A.)	4 (0)
Lrrc59					112 (N.A.)	2 (0)
Lrrfip1			116 (N.A.)	2 (0)		
Lrrfip2					985 (228)	16 (3)
Lsp1					134 (N.A.)	2 (0)
Luc7l2	178 (N.A.)	3 (0)				
Luc7l3	154 (N.A.)	2 (0)				
Lum	113 (N.A.)	2 (0)				
Luzp1					301 (N.A.)	7 (0)
Lyn					134 (64)	3 (2)
Mad1l1	80 (N.A.)	2 (0)				
Magoh	264 (N.A.)	5 (0)				
Magohb	264 (N.A.)	5 (0)			210 (N.A.)	3 (0)
Map3k6			84 (N.A.)	3 (0)		
Matn1	194 (N.A.)	3 (0)				
Matr3	897 (N.A.)	17 (0)			2072 (956)	36 (16)
Mbnl1			94 (N.A.)	3 (0)		
Mcam					234 (N.A.)	5 (0)
Mccc1	323 (N.A.)	6 (0)				
Mccc2	187 (N.A.)	4 (0)				
Mecp2			224 (N.A.)	5 (0)		
Men1	176 (N.A.)	3 (0)	387 (157)	7 (4)		
Mettl7a1			148 (N.A.)	3 (0)		
Mfap1	228 (N.A.)	5 (0)			307 (138)	6 (3)
Mgst3			128 (59)	2 (1)		
Mlec					102 (N.A.)	2 (0)
Morf4l1	127 (N.A.)	2 (0)				
Mov10					530 (62)	12 (2)
Mprip			655 (205)	11 (3)		
Msi1	136 (N.A.)	2 (0)				
Msi2	147 (N.A.)	3 (0)				
Msn					442 (126)	9 (3)
Mta1	206 (N.A.)	4 (0)	134 (N.A.)	3 (0)		
Mta2	111 (N.A.)	3 (0)				
Murc	124 (N.A.)	2 (0)				
Mybpc1	1952 (N.A.)	35 (0)				
Mybpc3	507 (N.A.)	9 (0)				
Mybphl			374 (N.A.)	8 (0)		
Myef2	195 (N.A.)	4 (0)			589 (237)	11 (5)

	First large scale lung purification		Second large scale lung purification		Third large scale lung purification	
Symbol	**Mascot[a]**	**Peptides[b]**	**Mascot[a]**	**Peptides[b]**	**Mascot[a]**	**Peptides[b]**
Myh1[A]					3853 (N.A.)	54 (0)
Myh11					4218 (1429)	66 (23)
Myh14					6782 (2852)	94 (49)
Myh2	1463 (N.A.)	28 (0)				
Myh3	1366 (N.A.)	25 (0)				
Myh4			3636 (N.A.)	56 (0)	3725 (N.A.)	53 (0)
Myh6	2047 (360)	32 (8)				
Myh8	2212 (324)	38 (8)				
Myl1	259 (N.A.)	6 (0)				
Myl4	305 (N.A.)	6 (0)				
Myl7	131 (N.A.)	3 (0)				
Mylpf	101 (N.A.)	2 (0)				
Myo18a	1095 (N.A.)	19 (0)	1137 (202)	22 (4)	2429 (647)	42 (13)
Myo1b					2479 (802)	44 (15)
Myo1c					3054 (1338)	45 (26)
Myo1d					2082 (644)	38 (14)
Myo1e					1269 (392)	24 (8)
Myo1f			349 (N.A.)	6 (0)	553 (N.A.)	11 (0)
Myo1g					369 (N.A.)	8 (0)
Myo5b[A]					320 (99)	6 (2)
Myo5c					1620 (181)	32 (5)
Myo6					1539 (518)	27 (10)
Myom1	632 (N.A.)	12 (0)	101 (N.A.)	2 (0)		
Myom2	815 (N.A.)	14 (0)				
Myom3	86 (N.A.)	1 (0)				
Myot	210 (N.A.)	5 (0)				
Myzap	212 (N.A.)	3 (0)	727 (298)	13 (5)		
Nat10			139 (68)	3 (2)	159 (N.A.)	4 (0)
Ncbp1	158 (N.A.)	4 (0)				
Ncbp2			144 (48)	4 (1)		
Ncoa5	133 (N.A.)	3 (0)	265 (57)	6 (2)	436 (65)	10 (1)
Neb	101 (N.A.)	2 (0)				
Nes	117 (N.A.)	3 (0)				
Nexn					460 (220)	9 (5)
Nfia	173 (N.A.)	3 (0)				
Nfic	210 (N.A.)	4 (0)				
Nfix	110 (N.A.)	2 (0)				
Ngp			103 (N.A.)	3 (0)		
Nhp2	155 (N.A.)	2 (0)				
Nhp2l1	85 (N.A.)	2 (0)				
Nkx2-4					91 (N.A.)	1 (0)
Nkx2-5					91 (N.A.)	1 (0)

	First large scale lung purification		Second large scale lung purification		Third large scale lung purification	
Symbol	**Mascot[a]**	**Peptides[b]**	**Mascot[a]**	**Peptides[b]**	**Mascot[a]**	**Peptides[b]**
Nono	118 (N.A.)	3 (0)				
Nop2					290 (102)	4 (2)
Nop56	124 (N.A.)	3 (0)				
Nop58	107 (N.A.)	2 (0)				
Nostrin[A]					280 (N.A.)	7 (0)
Npm1	226 (N.A.)	4 (0)				
Nr2c2	126 (N.A.)	4 (0)				
Nr2f1	182 (N.A.)	5 (0)				
Nr2f2	212 (N.A.)	6 (0)			328 (N.A.)	6 (0)
Nsf	356 (N.A.)	7 (0)				
Nudt16l1	158 (N.A.)	4 (0)				
Nudt21	141 (N.A.)	3 (0)				
Numa1	806 (N.A.)	12 (0)				
Nup107	97 (N.A.)	2 (0)				
Nup133	96 (N.A.)	2 (0)				
Nup214					85 (N.A.)	2 (0)
Nup62					165 (N.A.)	4 (0)
Nup98	85 (N.A.)	2 (0)				
Nvl					208 (N.A.)	5 (0)
Nxf1					502 (213)	10 (4)
Obscn	123 (N.A.)	2 (0)				
Ogt					88 (N.A.)	2 (0)
Orc3	83 (N.A.)	2 (0)				
Pabpc1	84 (N.A.)	2 (0)				
Pabpc4	84 (N.A.)	2 (0)				
Pabpn1			86 (N.A.)	2 (0)		
Paf1	138 (N.A.)	3 (0)				
Parp1	174 (N.A.)	5 (0)				
Paxbp1			364 (N.A.)	6 (0)	405 (112)	8 (2)
Pbrm1[A]	377 (N.A.)	9 (0)				
Pbx1	258 (100)	5 (2)				
Pbx3	111 (N.A.)	2 (0)				
Pc	213 (N.A.)	5 (0)				
Pcbp1	443 (N.A.)	7 (0)				
Pcbp2	385 (N.A.)	6 (0)				
Pcbp3			228 (N.A.)	4 (0)		
Pcca	301 (N.A.)	5 (0)				
Pcolce	301 (N.A.)	5 (0)				
Pcx	213 (N.A.)	5 (0)				
Pdcd11					132 (N.A.)	3 (0)
Pdcd6	168 (61)	4 (1)				
Pdia6	271 (N.A.)	4 (0)	265 (N.A.)	5 (0)	376 (N.A.)	6 (0)

	First large scale lung purification		Second large scale lung purification		Third large scale lung purification	
Symbol	**Mascot[a]**	**Peptides[b]**	**Mascot[a]**	**Peptides[b]**	**Mascot[a]**	**Peptides[b]**
Pdlim5	92 (N.A.)	2 (0)				
Pdlim7	88 (N.A.)	2 (0)				
Pecam1			391 (193)	8 (4)		
Pelp1	89 (N.A.)	3 (0)				
Pes1					87 (N.A.)	2 (0)
Pfkl	98 (N.A.)	2 (0)				
Phf10	111 (N.A.)	2 (0)				
Phf2			165 (N.A.)	4 (0)		
Phf3			121 (N.A.)	3 (0)		
Picalm	220 (89)	4 (2)				
Pkp3			120 (42)	3 (1)		
Plec	1925 (N.A.)	41 (0)			10063 (4425)	178 (90)
Plrg1	357 (N.A.)	8 (0)	682 (287)	14 (6)	439 (N.A.)	10 (0)
Pml	194 (N.A.)	4 (0)				
Pnn	281 (N.A.)	5 (0)				
Poldip3	190 (N.A.)	4 (0)				
Polr2a[A]					138 (40)	3 (1)
Polr2c	106 (N.A.)	3 (0)				
Polr2e	113 (N.A.)	3 (0)				
Polr2h	129 (N.A.)	2 (0)				
Pon3			135 (N.A.)	4 (0)		
Por					82 (N.A.)	2 (0)
Postn	675 (N.A.)	11 (0)				
Ppfibp1					306 (89)	8 (2)
Pphln1			221 (48)	5 (1)		
Ppie	126 (N.A.)	4 (0)	107 (N.A.)	3 (0)		
Ppig					149 (N.A.)	3 (0)
Ppil1	192 (N.A.)	3 (0)				
Ppil4	86 (N.A.)	2 (0)				
Ppp1cb	184 (N.A.)	3 (0)				
Ppp1r10					262 (124)	5 (3)
Ppp1r12a					1425 (N.A.)	25 (0)
Ppp1r12b					297 (N.A.)	4 (0)
Ppp1r18					315 (N.A.)	7 (0)
Ppp1r9a[A]					87 (N.A.)	2 (0)
Ppp1r9b					535 (N.A.)	10 (0)
Prkra					153 (N.A.)	4 (0)
Prpf19	535 (N.A.)	10 (0)			579 (250)	11 (4)
Prpf3	183 (N.A.)	4 (0)				
Prpf31	373 (N.A.)	5 (0)				
Prpf38a			170 (49)	4 (1)		
Prpf38b			228 (N.A.)	6 (0)		

	First large scale lung purification		Second large scale lung purification		Third large scale lung purification	
Symbol	**Mascot[a]**	**Peptides[b]**	**Mascot[a]**	**Peptides[b]**	**Mascot[a]**	**Peptides[b]**
Prpf4	223 (N.A.)	5 (0)				
Prpf40a	267 (N.A.)	6 (0)				
Prpf4b			462 (91)	8 (2)	704 (207)	12 (5)
Prpf6	763 (N.A.)	13 (0)				
Prpf8	1974 (N.A.)	39 (0)				
Prrc2c			84 (N.A.)	3 (0)		
Prss1	168 (N.A.)	2 (0)				
Psmc2	85 (N.A.)	1 (0)				
Ptbp1	1210 (N.A.)	17 (0)				
Ptbp3	142 (N.A.)	3 (0)	417 (N.A.)	10 (0)		
Ptk7					148 (N.A.)	3 (0)
Ptrf	603 (N.A.)	7 (0)				
Puf60	633 (N.A.)	11 (0)				
Pum2	176 (N.A.)	4 (0)	456 (149)	9 (3)		
Purb	111 (N.A.)	2 (0)				
Rab11a	240 (N.A.)	4 (0)				
Rab11b	240 (N.A.)	4 (0)				
Rab12					107 (N.A.)	2 (0)
Rab1b	94 (N.A.)	2 (0)				
Rab4b			138 (N.A.)	2 (0)		
Rai14					2028 (367)	34 (7)
Raly	470 (N.A.)	8 (0)				
Rangap1	89 (N.A.)	2 (0)				
Rap1a			324 (N.A.)	6 (0)		
Rap2a			175 (68)	4 (2)	134 (N.A.)	3 (0)
Rasip1					624 (269)	9 (6)
Rasl2-9					85 (N.A.)	2 (0)
Rbbp4	239 (N.A.)	5 (0)				
Rbbp5	81 (N.A.)	2 (0)				
Rbbp6			96 (N.A.)	3 (0)		
Rbbp7	232 (N.A.)	5 (0)				
Rbm10	279 (N.A.)	6 (0)				
Rbm12b1			187 (N.A.)	4 (0)	86 (N.A.)	3 (0)
Rbm12b2			187 (N.A.)	4 (0)		
Rbm14	104 (N.A.)	2 (0)				
Rbm15	181 (N.A.)	4 (0)	887 (404)	18 (9)		
Rbm17	205 (N.A.)	3 (0)			327 (146)	6 (4)
Rbm22	112 (N.A.)	3 (0)			90 (N.A.)	2 (0)
Rbm25	451 (N.A.)	11 (0)				
Rbm26	103 (N.A.)	2 (0)			98 (N.A.)	2 (0)
Rbm28					187 (N.A.)	5 (0)
Rbm39	330 (N.A.)	5 (0)				

	First large scale lung purification		Second large scale lung purification		Third large scale lung purification	
Symbol	**Mascot[a]**	**Peptides[b]**	**Mascot[a]**	**Peptides[b]**	**Mascot[a]**	**Peptides[b]**
Rbm4	101 (N.A.)	3 (0)				
Rbm47			501 (243)	9 (4)		
Rbm5	222 (N.A.)	5 (0)	331 (50)	6 (1)		
Rbm8a	141 (N.A.)	3 (0)				
Rbms1			324 (102)	7 (2)		
Rbms3			193 (90)	4 (2)	159 (N.A.)	3 (0)
Rbmx	620 (N.A.)	10 (0)				
Rbmxl1[A]	668 (N.A.)	10 (0)				
Rc3h1			82 (N.A.)	1 (0)		
Rc3h2			82 (N.A.)	1 (0)		
Rdx					343 (126)	6 (3)
Rfc1	143 (66)	4 (1)				
Rfc2	211 (N.A.)	4 (0)				
Rfc3	174 (N.A.)	3 (0)				
Rfc4	122 (N.A.)	4 (0)				
Rfc5	84 (N.A.)	2 (0)				
Rfx2	85 (N.A.)	2 (0)				
RhocA					88 (N.A.)	3 (0)
Rnps1	224 (N.A.)	3 (0)				
Rpf2			224 (68)	4 (2)	107 (N.A.)	2 (0)
Rpl10	123 (N.A.)	2 (0)				
Rpl11	146 (N.A.)	2 (0)				
Rpl12	363 (N.A.)	5 (0)				
Rpl13	135 (N.A.)	2 (0)				
Rpl13a	111 (N.A.)	2 (0)				
Rpl13a-ps1	111 (N.A.)	2 (0)				
Rpl17	240 (N.A.)	4 (0)				
Rpl18	108 (N.A.)	2 (0)				
Rpl19	161 (N.A.)	2 (0)				
Rpl22	212 (N.A.)	3 (0)				
Rpl23	112 (N.A.)	2 (0)				
Rpl23a	165 (N.A.)	3 (0)				
Rpl23a-ps3	165 (N.A.)	3 (0)				
Rpl26	347 (N.A.)	7 (0)				
Rpl27	107 (N.A.)	2 (0)				
Rpl30	171 (N.A.)	3 (0)				
Rpl31	116 (N.A.)	2 (0)				
Rpl35	219 (76)	4 (1)				
Rpl37a			117 (58)	2 (1)		
Rpl38	180 (56)	4 (1)				
Rpl4	178 (N.A.)	4 (0)				
Rpl5	396 (N.A.)	7 (0)				

	First large scale lung purification		Second large scale lung purification		Third large scale lung purification	
Symbol	**Mascot[a]**	**Peptides[b]**	**Mascot[a]**	**Peptides[b]**	**Mascot[a]**	**Peptides[b]**
Rpl6	259 (N.A.)	4 (0)				
Rpl7	164 (N.A.)	4 (0)				
Rpl7a	122 (N.A.)	2 (0)				
Rpl7a-ps10	122 (N.A.)	2 (0)				
Rpl7a-ps3	122 (N.A.)	2 (0)				
Rpl7a-ps5	122 (N.A.)	2 (0)				
Rpl7l1			90 (N.A.)	2 (0)		
Rpl9	285 (N.A.)	5 (0)				
Rpl9-ps6	285 (N.A.)	5 (0)				
Rplp0	390 (N.A.)	8 (0)				
Rpn1					415 (110)	9 (3)
Rpn2					281 (N.A.)	6 (0)
Rprd1a			212 (N.A.)	4 (0)		
Rprd1b	230 (85)	5 (2)				
Rps10	211 (N.A.)	4 (0)				
Rps12	167 (62)	3 (1)				
Rps13	181 (N.A.)	3 (0)				
Rps14	246 (N.A.)	4 (0)				
Rps15	190 (N.A.)	3 (0)				
Rps15a	182 (N.A.)	4 (0)				
Rps16	98 (N.A.)	3 (0)				
Rps17	216 (N.A.)	4 (0)				
Rps18	187 (N.A.)	4 (0)				
Rps19	164 (N.A.)	3 (0)				
Rps2	335 (N.A.)	6 (0)				
Rps24	100 (N.A.)	2 (0)				
Rps25	113 (N.A.)	2 (0)				
Rps27l			105 (N.A.)	2 (0)		
Rps3	528 (N.A.)	9 (0)				
Rps3a3	284 (N.A.)	5 (0)				
Rps4x	404 (N.A.)	7 (0)				
Rps6	86 (N.A.)	1 (0)				
Rps7	150 (N.A.)	3 (0)				
Rps8	204 (N.A.)	3 (0)				
Rps9	167 (N.A.)	5 (0)				
Rpsa	790 (339)	12 (5)				
Rpsa-ps10	790 (339)	12 (5)				
Rras					123 (49)	2 (1)
Rrbp1	132 (N.A.)	3 (0)				
Rreb1			201 (N.A.)	5 (0)		
Rrp8					82 (N.A.)	1 (0)
Rsl1d1					280 (61)	5 (1)

	First large scale lung purification		Second large scale lung purification		Third large scale lung purification	
Symbol	**Mascot[a]**	**Peptides[b]**	**Mascot[a]**	**Peptides[b]**	**Mascot[a]**	**Peptides[b]**
Rtcb	190 (N.A.)	3 (0)			228 (65)	4 (2)
Ruvbl1	411 (N.A.)	8 (0)				
Ruvbl2	826 (N.A.)	13 (0)				
Safb	318 (N.A.)	7 (0)	1238 (229)	23 (5)	973 (351)	16 (8)
Safb2	349 (N.A.)	8 (0)	1198 (69)	20 (1)	775 (269)	12 (6)
Samd1	97 (N.A.)	2 (0)	181 (N.A.)	4 (0)		
Sap18	194 (N.A.)	3 (0)				
Sart1	600 (N.A.)	12 (0)				
Scn7a			130 (N.A.)	3 (0)		
Sdpr	108 (N.A.)	2 (0)			187 (76)	5 (2)
Sec61a1			92 (N.A.)	2 (0)		
Serbp1	319 (83)	7 (2)				
Serpinh1	869 (N.A.)	13 (0)				
Setd2			89 (N.A.)	2 (0)		
Sf1	291 (N.A.)	5 (0)			250 (88)	7 (3)
Sf3a1	577 (N.A.)	12 (0)				
Sf3a2					189 (N.A.)	4 (0)
Sf3a3	443 (N.A.)	9 (0)				
Sf3b1	1211 (N.A.)	21 (0)				
Sf3b14	83 (N.A.)	2 (0)				
Sf3b2	923 (N.A.)	17 (0)				
Sf3b3	1716 (N.A.)	27 (0)			1861 (868)	29 (14)
Sf3b4	177 (N.A.)	2 (0)	435 (180)	6 (2)		
Sfpq	417 (N.A.)	9 (0)				
Sfswap	95 (N.A.)	2 (0)	116 (42)	3 (1)	508 (185)	10 (4)
Sftpa1					199 (56)	3 (1)
Shank3			460 (211)	11 (5)		
Sipa1					90 (N.A.)	2 (0)
Six5	161 (N.A.)	2 (0)				
Skiv2l2					292 (81)	6 (2)
Slc25a4	85 (N.A.)	2 (0)				
Slc27a6					170 (N.A.)	4 (0)
Sltm			733 (223)	13 (4)		
Smarca4	401 (N.A.)	9 (0)				
Smarca5	177 (N.A.)	4 (0)				
Smarcb1	144 (N.A.)	3 (0)				
Smarcc2	344 (N.A.)	6 (0)				
Smarcd1	106 (N.A.)	2 (0)				
Smarcd2	375 (N.A.)	7 (0)				
Smarcd3	299 (N.A.)	5 (0)				
Smarce1[A]	192 (N.A.)	3 (0)				
Smc1a	211 (N.A.)	4 (0)				

	First large scale lung purification		Second large scale lung purification		Third large scale lung purification	
Symbol	**Mascot[a]**	**Peptides[b]**	**Mascot[a]**	**Peptides[b]**	**Mascot[a]**	**Peptides[b]**
Smndc1			168 (43)	3 (1)		
Smu1	430 (N.A.)	7 (0)			472 (217)	9 (3)
Smyd1	93 (N.A.)	2 (0)				
Snap23			85 (N.A.)	2 (0)	89 (N.A.)	2 (0)
Snd1	396 (N.A.)	9 (0)				
Snip1	82 (N.A.)	1 (0)				
Snrnp200	2214 (N.A.)	37 (0)				
Snrnp40	512 (N.A.)	9 (0)				
Snrnp70	179 (N.A.)	3 (0)				
Snrpa	128 (N.A.)	3 (0)				
Snrpa1	330 (N.A.)	6 (0)				
Snrpb	104 (N.A.)	1 (0)				
Snrpd1	176 (N.A.)	3 (0)				
Snrpd2	207 (N.A.)	4 (0)				
Snrpd3	149 (N.A.)	3 (0)				
Snrpf	96 (N.A.)	1 (0)	90 (N.A.)	1 (0)		
Snrpn	104 (N.A.)	1 (0)				
Snw1	462 (N.A.)	10 (0)	660 (277)	11 (5)		
Sorbs3					92 (N.A.)	2 (0)
Sort1					236 (87)	3 (1)
Sp3A			85 (N.A.)	1 (0)		
Specc1l			168 (N.A.)	3 (0)	1746 (83)	29 (2)
Spen	81 (N.A.)	1 (0)				
Sptan1	391 (N.A.)	10 (0)				
Sptb			282 (N.A.)	6 (0)	277 (N.A.)	6 (0)
Sptbn1	935 (N.A.)	19 (0)				
Sptbn4	131 (N.A.)	3 (0)				
Srbd1			433 (97)	10 (2)		
Srl	138 (N.A.)	2 (0)				
Srp54	510 (232)	10 (4)				
Srp54c	98 (N.A.)	2 (0)				
Srp68	514 (124)	10 (2)				
Srp72	214 (N.A.)	4 (0)				
Srprb					90 (N.A.)	2 (0)
Srrm1	436 (160)	9 (3)				
Srrm2	727 (N.A.)	16 (0)				
Srrt	143 (N.A.)	3 (0)				
Srsf1	448 (N.A.)	8 (0)				
Srsf10	257 (N.A.)	4 (0)				
Srsf3	265 (N.A.)	4 (0)				
Srsf4	97 (N.A.)	2 (0)				
Srsf6	90 (N.A.)	2 (0)				

	First large scale lung purification		Second large scale lung purification		Third large scale lung purification	
Symbol	**Mascot[a]**	**Peptides[b]**	**Mascot[a]**	**Peptides[b]**	**Mascot[a]**	**Peptides[b]**
Srsf7	246 (N.A.)	5 (0)				
Srsf9	153 (N.A.)	3 (0)				
Ssr4					134 (N.A.)	2 (0)
Ssrp1	135 (N.A.)	3 (0)				
Stag1	104 (N.A.)	2 (0)			83 (N.A.)	2 (0)
Stau1	170 (N.A.)	4 (0)				
Stt3a					90 (N.A.)	3 (0)
Sub1			212 (91)	5 (2)		
Supt16	150 (N.A.)	4 (0)				
Supt16h	150 (N.A.)	4 (0)				
Supt6h			216 (59)	5 (2)	308 (61)	7 (1)
Surf4			143 (49)	2 (1)		
Svil			127 (N.A.)	2 (0)	1047 (N.A.)	18 (0)
Syf2			193 (67)	4 (1)		
Sympk	283 (N.A.)	6 (0)				
Syncrip	156 (N.A.)	3 (0)	656 (N.A.)	13 (0)	708 (N.A.)	13 (0)
Synpo2					94 (N.A.)	2 (0)
Synpo2l	107 (N.A.)	2 (0)				
Taok3			535 (223)	10 (4)		
Tardbp	475 (N.A.)	7 (0)				
Tbx2					250 (107)	5 (2)
Tcp1	235 (N.A.)	5 (0)				
Tecr					88 (N.A.)	2 (0)
Terf2	111 (N.A.)	2 (0)				
Tex10	109 (N.A.)	2 (0)				
Tfcp2	108 (N.A.)	2 (0)				
Tfcp2l1			90 (N.A.)	2 (0)		
Tfip11			647 (310)	14 (9)	480 (212)	11 (6)
Thoc1	116 (N.A.)	3 (0)				
Thoc3			98 (48)	2 (1)		
Thoc5	88 (N.A.)	2 (0)	618 (119)	12 (3)		
Thoc6	96 (N.A.)	2 (0)	288 (130)	7 (3)		
Thrap3	556 (N.A.)	12 (0)				
Tia1	286 (N.A.)	5 (0)				
Tial1	177 (N.A.)	3 (0)				
Tjp1					1162 (483)	21 (10)
Tjp2					812 (98)	17 (2)
Tmed4[A]			119 (N.A.)	2 (0)		
Tmod1			245 (118)	5 (3)	257 (94)	5 (2)
Tnni3			153 (51)	3 (1)		
Tnnt2	199 (82)	5 (2)				
Tns1[A]					538 (233)	14 (5)

	First large scale lung purification		Second large scale lung purification		Third large scale lung purification	
Symbol	**Mascot[a]**	**Peptides[b]**	**Mascot[a]**	**Peptides[b]**	**Mascot[a]**	**Peptides[b]**
Top1	189 (N.A.)	5 (0)				
Top2a	449 (N.A.)	6 (0)				
Top2b	1450 (N.A.)	23 (0)				
Tox4[A]	98 (N.A.)	2 (0)				
Tpm1	870 (N.A.)	14 (0)	773 (N.A.)	14 (0)	1036 (N.A.)	18 (0)
Tra2a	155 (N.A.)	3 (0)				
Tra2b	347 (N.A.)	5 (0)				
Trap1	94 (N.A.)	2 (0)				
Trim10			104 (N.A.)	3 (0)	138 (N.A.)	3 (0)
Trim25			391 (132)	8 (4)		
Trim28	741 (N.A.)	12 (0)				
Trim3	478 (231)	9 (6)				
Trim55	179 (N.A.)	4 (0)				
Trim56	126 (N.A.)	2 (0)				
Trim72	87 (N.A.)	2 (0)				
Triobp					170 (N.A.)	5 (0)
Trip11	86 (N.A.)	3 (0)				
Trrap[A]	102 (N.A.)	2 (0)				
Try4	121 (60)	2 (1)				
Try5	121 (60)	2 (1)				
Tspan8			81 (N.A.)	2 (0)		
Ttn	2503 (N.A.)	61 (0)				
Tuba1a	457 (N.A.)	8 (0)				
Tuba1b	377 (N.A.)	7 (0)	768 (N.A.)	13 (0)		
Tuba1c	377 (N.A.)	7 (0)			639 (N.A.)	11 (0)
Tuba4a					458 (N.A.)	10 (0)
Tubb2a	755 (N.A.)	12 (0)				
Tubb2b	755 (N.A.)	12 (0)	908 (N.A.)	16 (0)		
Tubb3	559 (N.A.)	9 (0)				
Tubb4b	794 (N.A.)	13 (0)				
Tubb5	886 (N.A.)	14 (0)				
Tubg2					87 (N.A.)	2 (0)
Tufm	183 (62)	4 (2)				
Txnl4a	116 (N.A.)	2 (0)				
U2af1	361 (N.A.)	6 (0)				
U2af2	375 (N.A.)	6 (0)				
U2surp	175 (N.A.)	5 (0)				
Ubp1	91 (N.A.)	2 (0)				
Upf1	81 (N.A.)	2 (0)				
Urb1					124 (42)	2 (1)
Urb2			102 (N.A.)	2 (0)		
Uso1	121 (N.A.)	3 (0)				

	First large scale lung purification		Second large scale lung purification		Third large scale lung purification	
Symbol	**Mascot[a]**	**Peptides[b]**	**Mascot[a]**	**Peptides[b]**	**Mascot[a]**	**Peptides[b]**
Utrn	96 (N.A.)	3 (0)				
Vapa					103 (51)	3 (1)
Vat1			106 (N.A.)	2 (0)		
Vcl	163 (N.A.)	4 (0)				
Vcp					511 (42)	10 (1)
Vezf1	104 (N.A.)	2 (0)	273 (99)	6 (2)		
Vim	1286 (N.A.)	21 (0)				
Wbp11[A]	138 (N.A.)	3 (0)	517 (166)	10 (3)	342 (N.A.)	8 (0)
Wdr18	255 (N.A.)	4 (0)				
Wdr5	91 (N.A.)	3 (0)				
Wdr82	141 (N.A.)	3 (0)				
Wibg	88 (N.A.)	2 (0)				
Wiz	316 (68)	6 (2)				
Wtap			132 (N.A.)	3 (0)	240 (65)	4 (1)
Xab2	275 (N.A.)	6 (0)			578 (200)	11 (5)
Ybx1	162 (N.A.)	3 (0)				
Yeats4	140 (45)	3 (1)				
Ythdc1			320 (N.A.)	8 (0)	233 (N.A.)	5 (0)
Ythdf2	80 (N.A.)	2 (0)			161 (66)	4 (1)
Ywhaq	87 (N.A.)	1 (0)				
Zbtb7a	90 (N.A.)	2 (0)				
Zc3h11a	118 (N.A.)	2 (0)			141 (N.A.)	3 (0)
Zc3h13			94 (N.A.)	2 (0)		
Zc3h14	182 (N.A.)	3 (0)				
Zc3h18	134 (N.A.)	3 (0)				
Zfml					527 (98)	13 (3)
Zfp185					83 (N.A.)	2 (0)
Zfp36l1			80 (N.A.)	2 (0)		
Zfr	196 (N.A.)	4 (0)				
Zkscan3					337 (N.A.)	7 (0)
Zmat2			106 (N.A.)	3 (0)		
Zmpste24			96 (N.A.)	2 (0)		
Zmynd8	195 (N.A.)	4 (0)	368 (79)	6 (1)	150 (N.A.)	3 (0)
Znf148	97 (N.A.)	3 (0)				
Znf326	591 (N.A.)	11 (0)				
Znf512					919 (217)	17 (6)
Znf638					527 (98)	13 (3)
Znf687	115 (54)	2 (1)			166 (71)	4 (2)

[a] Mascot score of the identified binding partner, mascot score of the control is between brackets.
[b] Number of unique proteins for the identified binding partner, number of unique proteins of the control is between brackets.
[A]Partners also identified in A54 cells.

Table 2. Identified binding partners of Sox2 in brain tissue using mass spectrometry analysis.
Large scale tissue IP using nuclear extracts prepared from brain tissue E18.5. Only partners enriched in at least two of the IPs are shown.

	First large scale brain purification		Second large scale brain purification		Third large scale brain purification	
Symbol	**Mascot[a]**	**Peptides[b]**	**Mascot[a]**	**Peptides[b]**	**Mascot[a]**	**Peptides[b]**
Adar			130 (43)	2 (1)	109 (N.A.)	2 (0)
Arl8a	301 (114)	4 (2)			191 (N.A.)	3 (0)
Bud13	108 (N.A.)	1 (0)			139 (N.A.)	3 (0)
Cbx8	156 (43)	4 (1)			115 (N.A.)	3 (0)
Cdc40	98 (49)	2 (1)			217 (N.A.)	5 (0)
Ctif	87 (N.A.)	2 (0)	98 (N.A.)	2 (0)		
Cxxc4			200 (71)	4 (2)	120 (60)	3 (2)
Epc2	115 (N.A.)	3 (0)	371 (87)	10 (2)		
Ercc4	410 (80)	7 (1)			128 (N.A.)	2 (0)
Kmt2a			316 (N.A.)	5 (0)	105 (N.A.)	3 (0)
Leo1			347 (128)	7 (3)	172 (86)	5 (2)
Mark4			161 (N.A.)	3 (0)	181 (N.A.)	5 (0)
Myh10			2232 (N.A.)	40 (0)	1336 (N.A.)	27 (0)
Ncoa5	110 (N.A.)	2 (0)			219 (84)	6 (2)
Nsd1	138 (N.A.)	3 (0)	316 (152)	7 (4)	170 (59)	3 (1)
Phf3			1420 (635)	30 (15)	295 (53)	7 (2)
Polr2b	389 (103)	6 (3)			252 (74)	7 (2)
Ppfia2	107 (N.A.)	2 (0)	160 (71)	3 (1)		
Ppie	208 (70)	5 (2)	200 (78)	5 (2)		
Ppig			200 (85)	4 (2)	180 (N.A.)	4 (0)
Satb1	181 (N.A.)	4 (0)	297 (N.A.)	6 (0)		
Son			527 (256)	12 (6)	157 (73)	4 (1)
Sox2	111 (N.A.)	3 (0)	428 (135)	7 (4)	199 (N.A.)	4 (0)
Spen			1273 (N.A.)	26 (0)	122 (N.A.)	2 (0)
Sugp2	149 (71)	2 (2)	371 (137)	8 (3)	241 (N.A.)	5 (0)
Taf11	90 (N.A.)	1 (0)	120 (59)	2 (1)		
Tcf7l2	131 (N.A.)	2 (0)			213 (N.A.)	4 (0)
Vezf1	160 (N.A.)	3 (0)			131 (49)	4 (1)
Zeb1	83 (N.A.)	2 (0)	124 (N.A.)	3 (0)		

[a] Mascot score of the identified binding partner, mascot score of the control is between brackets.
[b] Number of unique proteins for the identified binding partner number of unique proteins of the control is between brackets.

Table 3. Sox2 target genes involved in lung development and respiratory tube development.

Single cross-linked	Double cross-linked
GLI2	GLI2
SMAD2	SMAD2
TBX4	TBX4
β-catenin	β-catenin
HHIP	HHIP
PDPN	PDPN
	GLI3
	HOPX
	BMPR1A
	CTGF
	CYP1A2
	EPAS1
	PSEN2
	TNS3

Table 4. Sox2 partners with a respiratory phenotype in lung tissue.

	BioSox purification tissue #1		BioSox purification tissue #2		BioSox purification tissue #3	
Symbol	**Mascot[a]**	**Peptides[b]**	**Mascot[a]**	**Peptides[b]**	**Mascot[a]**	**Peptides[b]**
Akap8	176 (N.A.)	2 (0)	530 (438)	10 (8)	432 (317)	9 (6)
Ank3	773 (N.A.)	15 (0)	1200 (N.A.)	20 (0)	432 (317)	9 (6)
Dkc1	135 (N.A.)	2 (0)	926 (746)	16 (13)	510 (393)	9 (7)
Ptrf	603 (N.A.)	7 (0)	1040 (923)	15 (14)	699 (548)	9 (8)
Safb1	318 (N.A.)	7 (0)	1238 (229)	23 (5)	973 (351)	16 (8)

[a] Mascot score of the identified binding partner, mascot score of the control is between brackets.
[b] Number of unique proteins for the identified binding partner, mascot score of the control is between brackets.
[#] Only enriched in the trachea tissue sample

Chapter 5.

Chd4, FoxP2/4 and Cux1 are Sox2 interaction partners during lung development

Kim Schilders, Bianca Oresta, Judith Birkhoff, Anne Boerema – de Munck, Marjon Buscop – van Kempen, Petros Kolovos, René Wijnen, Dick Tibboel, Robbert Rottier

Abstract

The Sry related HMG box protein Sox2 is important during lung development for proper differentiation of the lung epithelium and for branching morphogenesis. The transcriptional activity of Sox2 depends on interaction with other proteins and to gain more insight in the Sox2-partner complexes during lung development, we purified bioSox2-partner complex from E18 bioSox2/birA mouse lungs to identify *in vivo* binding partners of Sox2. Among the potential partners that were identified, were Chromodomain Helicase DNA binding protein 4 (Chd4), the Forkhead box family members FoxP1, FoxP2 and FoxP4, and Cut-Like Homeobox1 (Cux1). Here, we analyzed the expression patterns of Chd4, FoxP2/4 and Cux1 in lung during development and showed co-localization with Sox2. Co-immunoprecipitations showed interaction between Sox2 and Chd4, FoxP2/4 and Cux1. Furthermore, we analyzed the effects of the Sox2-Chd4 complex on different target genes. ChIP data indicated that that SOX2 and CHD4 could be involved in co-regulation of genes involved in the respiratory system.

Introduction

The lung is a complex organ, consisting of multiple different cell types. In mice, lung development starts at embryonic day (E) 9.5 as a primitive bud that originates from the ventral side of the foregut, followed by the formation of the bronchial tree through repetitive and stereotyped branching (1). The conducting airway epithelium starts to differentiate around E14, while the alveolar epithelium starts to differentiate at E16.5 (2-7). Many genes and signaling pathways are involved in these processes and one of these genes is the Sry related HMG box protein Sox2. Endogenous Sox2 is exclusively expressed in the non-branching developing airway epithelium and remains expressed in the epithelial cells of the conducting airways postnatally. It has been shown that Sox2 plays an important role in lung epithelial differentiation and branching morphogenesis (8-10). In the epithelial tip cells, β-catenin signaling is activated by Fgf10 signaling, thereby inhibiting Sox2 expression, which prevents these $Id2^+$ cells to differentiate into proximal epithelial cells (11, 12). By becoming more distant from the Fgf10 source, cells start to express Sox2, resulting in proximal airway differentiation, leading to the emergence of basal cells, ciliated cells and Club cells (12, 13). It was also shown that Sox2 is responsible for initiating the emergence of basal cells, by directly activating the ΔN Trp63 promoter (13). Ectopic Sox2 expression in virtually all epithelial cells during development resulted in a decreased number of airways, enlarged airspaces and abnormal alveolar formation. Aside from these structural abnormalities, cellular changes of the epithelium were notable with an increase in basal cells and neuroendocrine cells (8). Interestingly, the size of these cyst-like structures depended on timing and duration of ectopic Sox2 expression (13).

The transcriptional activity of Sox2 depends on its interaction with other proteins, leading to 'complex-specific' DNA binding and subsequent transcriptional regulation. Some of the earliest identified partners are -Oct3/4, which plays a role in stem cell regulation, and Pax6, which has a role in lens development (14-16). Recently, we described two novel partners, Xpo4, which is involved in nucleo-cytoplasmic trafficking, and Chd7, which may explain the overlap between the two human complex syndromes AEG and CHARGE (17). However, for lung development it is still unknown if specific partners are involved in the differentiation of proximal epithelium.

To identify *in vivo* binding partners of Sox2 during different phases of lung development, a mouse model containing a biotinylatable-tag targeted to the endogenous Sox2 locus (bioSox2) was developed. An additional mouse strain ubiquitously expressing the bacterial biotin birA ligase was used to biotinylate the bioSox2 in vivo(18). The biotin-tagged Sox2 can be purified with streptavidin, which has a much higher affinity for biotin than regular antibodies have for antigens (19). Also, the biotinylation of Sox2 does not affect interaction with proteins and DNA-binding properties and this works very efficiently in mice making this an efficient method to purify bioSox-complexes from lung extracts.

In this study we identified Chd4, FoxP2, FoxP4 and Cux1 as a Sox2 interaction partner during lung development. We analyzed the expression patterns of these partners in the lung during gestation and confirmed co-localization with Sox2. Co-immunoprecipitations confirmed interaction between Sox2 and Chd4, FoxP2, FoxP4 and Cux1. Furthermore, the effects of the Sox2-Chd4 complex and Sox2-Cux1 complex on different target genes were analyzed.

Materials and methods

Generation of bioSox2/birA mice

To generate an N-terminal biotin-tagged Sox2 allele (bioSox2), Sox2 genomic DNA was isolated from library with 129 genomic DNA and a NheI – Asp718 fragment containing the Sox2 exon was used to generate the recombination construct used for targeting IB10 ES cells. Genomic DNA of individual clones was digested with EcoRI and screened with specific probes. The neomycin resistance gene was removed from positive clones by transiently expressing Cre in ES cells, and individual clones were genotyped and karyotyped before injection in blastocysts. Chimaeric mice were crossed and maintained on C57/bl6 background. BioSox2 mice were crossed with birA mice to biotinylate the biotag. Mice were kept under standard conditions and experiments were performed following guidelines of the ethics committee of the Erasmus Medical Center.

Large scale tissue immunoprecipitations

Lungs and brains were isolated from bioSox2/birA and birA mice E18. Tissue were minced into small pieces and a single cell solution was prepared using a cell strainer. Immunoprecipitations were essentially done as previously published (17, 20). Cells were lysed in cell lysis buffer (10 mM Hepes 7.6, 1.5 mM MgCl2, 10 mM KCl; add 0.5 mM DTT + protease inhibitors prior to use), followed by lysis of the nuclei in nuclei lysis buffer (20 mM Hepes pH 7.6, 20 % glycerol, 420 mM NaCl, 1.5 mM MgCl2, 0.2 mM EDTA, add 0.5 mM DTT +1 x CEF prior to use). Nuclear extracts were diluted 1:1 in low-salt buffer (20 mM Hepes pH7.6, 20% glycerol, 1.5 mM $MgCl_2$, 0.2 mM EDTA) and incubated with 40 µl Dynabeads®M-280 Streptavidin (Cat. No. 112.06 D, Invitrogen) for at least 1 hour rotating at 4°C in non-stick tubes. After washing with wash buffer (20 mM Hepes pH7.6, 20% glycerol, 100 mM KCl, 1.5 mM $MgCl_2$, 0.2 mM EDTA, 0.02% NP-40; add 1 x CEF prior to use), the beads were resuspended in 40 µl sample buffer (60mM Tris-HCl pH 6.8, 2% SDS, 0.02% bromophenol blue, 10% glycerol, 1% β-mercaptoethanol, 5 mM DTT) and heated for 10 min at 95°C. Samples were loaded on pre-cast gel and send to the department of Biochemistry for Matrix Assisted Laser Desorption/Ionization – Time of Flight Mass Spectrometry (MALDI-TOF MS) analysis.

Immunohistochemistry

Lungs from wild type mouse embryos from E11 till E18 were dissected and fixed in 4% PFA overnight at 4°C before processing for paraffin embedding. Sections of 5 µm were dewaxed and rehydrated, followed by antigen retrieval with microwave treatment in Tris-EDTA buffer pH9.0. Samples were blocked in PBS with 5 % Triton X-100 and 1 % BSA for 1 hour at room temperature and then incubated with antibody against Chd4 (Abcam; ab72418), FoxP2 (Abcam; ab16046), FoxP4 (Santa Cruz; sc-292474) or Cux1 (Abcam, Ab54583) diluted in blocking buffer at 4°C overnight. After washing in PBS with 0.1% Triton X-100, slides were incubated in blocking buffer with biotin conjugated secondary antibody for 30 min. at room temperature. Then samples were incubated with VECTASTAIN® ABC Reagent (Vector) for 30 min., followed by incubation with diaminobenzidine (Fluka). Slides were counterstained with hematoxyline and mounted with pertex. Sections were analyzed using Olympus BX41 microscope.

Immunofluorescent stainings

Lungs from wild type mouse embryos from E11 till E18 were dissected and fixed in 4%

PFA overnight at 4°C before processing for paraffin embedding. Sections of 5 µm were dewaxed and rehydrated, followed by antigen retrieval with microwave treatment in Tris-EDTA buffer pH9.0. Samples were blocked in PBS with 5 % Triton X-100 and 1 % BSA for 1 hour at room temperature and then incubated with antibodies against Chd4 (ab72418) and Sox2 (GTI5098), FoxP2 (ab16046) and Sox2, and Cux1 (Abcam, Ab54583) and Sox2 diluted in blocking buffer at 4°C overnight. After washing in PBS with 0.1% Triton X-100, slides were incubated in blocking buffer with fluorophore conjugated secondary antibody (Alexa Fluor-488, Alexa Fluor-594; Molecular Probes, Eugene, Or) for 90 min at room temperature. Slides were mounted in Vectashield Mounting Medium with Dapi (Vector laboratories, Burlingame, CA). Digital images were captured using a ZEISS imager Z1 AX10 microscope.

Cell culture

HEK cells cells and A549 were cultured in DMEM (Lonza, Verviers, Belgium) with 5% fetal calf serum and 1% penicillin-streptomycin under standard culture conditions. NCCIT cells were cultured in DMEM (Lonza, Verviers, Belgium) with 10% fetal calf serum and 1% penicillin-streptomycin under standard culture conditions.

Co-transfections and co-immunoprecipitations

HEK cells were single or double transfected with different combinations of pcDNA3 based plasmids expressing FLAG-tagged Chd4, FLAG-HA-tagged WDR5, myc-Sox2, myc-tagged FoxP2, myc-tagged FoxP4, myc-tagged TCF3 and FLAG-Sox2. Similar co-transfections and co-immunoprecipitations were performed using pcDNA3-myc-HA-tagged Cux1 and different Sox2 constructs that were described previously (21-26). X-tremeGENE HP DNA Transfection Reagent (Roche, Basel, Switzerland) was used for the transfection according to the manufacturer's manual. Cells were harvested 24 hours after transfection. Total cell extracts were prepared in 300 µl carin buffer (20mM Tris pH8, 137mM NaCl, 10mM EDTA, 1% NP40, 10% glycerol) with Complete protease inhibitor (Roche, Basel, Switzerland). 50 µl was incubated for 2 hours at 4°C in 250 µl carin buffer with antibodies against myc (Roche; 1668149) and FLAG (Sigma-Aldrich; F1804), followed by 1 hour incubation with protein G beads (Sigma-Aldrich, St. Louis, MO). After washing with carin buffer, the beads were resuspended in 20 µl sample buffer and heated for 10 min at 95°C.

Western blotting

Samples were separated on a SDS-PAGE gel and transferred to a PVDF membrane by wet blotting for 2 hours at 100 V and 400 mA. Membranes were blocked in TBS with 0.5% Tween-20 and 5% BSA. Membranes were labeled with antibodies against myc (Abcam; ab9106) and FLAG (Sigma-Aldrich; F7425) for 2 hours, followed by an 1 hour incubation with secondary HRP-labeled antibody. Membranes were developed with ECL incubation (Thermo Fisher Scientific INC., Waltham, MA) on the Alliance (Uvitec, Cambridge, UK).

Cell cycle experiment

A549 cells were synchronized by starvation. After 24 hours, starvation medium was replaced by normal growth medium. Cells were pelleted every 3 hours for a period of 24 hours. Extracts were prepared and analyzed by Western blot.

Cathepsin L experiment
A549 cells were synchronized by starvation. After 24 hours, starvation medium was replaced by normal growth medium, and 1 hour later 30 µM Cathepsin L inhibitor (Santa Cruz) was added. Cells were pelleted at 1, 3, 5, 21, 25 and 29 hours after addition of Cathepsin L. Also a reference plate was pelleted at each time-point. Extracts were prepared and analyzed by Western blot.

GST-fusion tags
Generation of GST fusion-tags and bacterial lysates is previously described (27) (20). HEK cells were grown ~85% confluent and nuclear extracts were prepared. 10 µg of the bacterial lysate was incubated with 25 µl glutathione sepharose UB beads (GE Healthcare)/1% fish skin gelatin for 2 hours rotating at 4°C. Beads are washed 4 x with bacteria lysis buffer (20 mM Hepes-NaOH pH7.6, 150 mM KCl, 10% glycerol, 0.5 mM EDTA, 10% triton; add 0.5 mM DTT + 1 x CEF prior to use), 2 x with wash buffer (20 mM Hepes pH7.6, 20% glycerol, 100 mM KCl, 1.5 mM $MgCl_2$, 0.2 mM EDTA, 0.02% NP-40; add 1 x CEF prior to use) and are then incubated for 2 hours with nuclear cell extracts rotating at 4°C. After washing 4 x with wash buffer, 40 µl 2 x sample buffer is added and beads are heated for 10 min. at 95°C. Western blotting was used to detect Sox2 binding partners. Extracts were incubated for 2 hours with at 4°C. After washing 4 x with wash buffer, 40 µl 2 x sample buffer is added and beads are heated for 10 min. at 95°C. Western blotting was used to detect Chd4.

Chromatin immunoprecipitation
~$120x10^6$ NCCIT cells were double cross-linked with 2mM disuccinimidyl glutate (Thermo Fisher Scientific) and 1% formaldehyde, or single cross-linked with 1% formaldehyde (28). Cells were lysed in ChIP cell lysis buffer (10 mM Tris pH 8.0, 10 mM NaCl, 0.2 % NP-40, 1x CEF (prior to use)), followed by lysis of the nuclei in ChIP nuclei lysis buffer (50 mM Tris pH 8.0, 10 mM EDTA, 1% SDS, 1x CEF (prior to use). Samples were sheared with a multiprobe bioruptor (double cross-linked: 75 min, 30 sec. high, 30 sec. off; single cross-linked: 30 min, 30 sec. high, 30 sec. off). Samples were diluted 10 x with ChIP dilution buffer (16.7 mM Tris-HCl pH 8.1, 167 mM NaCl, 1.2 mM EDTA, 1.1% TritonX-100, 0.01% SDS), precleared and incubated O/N with antibodies against CUX1 (Santa cruz; sc-6327), SOX2 (#2748 cell signaling) and CHD4(Abcam, ab72418) and goat IgG (Santa Cruz) and rabbit IgG (Santa Cruz) as negative control. Samples were incubated with Protein A/G agarose beads 1 hour rotating at 4°C and then washed with Low Salt Immune Complex Buffer (20 mM Tris-HCl pH8.0, 150 mM NaCl, 2 mM EDTA, 0.1% TritonX-100, 0.1% SDS), High Salt Immune Complex Buffer (20 mM Tris-HCl pH8.0, 500 mM NaCl, 2 mM EDTA, 0.1% TritonX-100, 0.1% SDS), LiCl Immune Complex Buffer (10 mM Tris-HCl pH8.0, 1 mM EDTA, 0.25 M LiCl, 1% NP-40, 1% deoxycholate) and TE (10 mM Tris-HCl pH8.0, 1 mM EDTA pH 8.0). Bound chromatin was eluted with freshly prepared elution buffer (1% SDS, 0.1 M $NaHCO_3$), de-cross-linked and purified DNA was send to the department of Biomics for analysis.

Results

Endogenous expression of Chd4, FoxP2/4 and Cux1 in the lung
To identify Sox2-partner complexes during lung development, biotin-tagged Sox2-complexes were precipitated from E18 mouse lung and based on mascot score and peptide enrichment potential Sox2 partners were selected including Chd4, FoxP2, FoxP4 and Cux1 (table 1; chapter 4 of this thesis). First, the endogenous expression of these putative bin-

ding partners during lung development in mice is studied using immunohistochemistry. CHD4 was not detected in the embryonic lung until E16, but significant expression was present in the epithelial cells of the proximal airways from the canalicular stage onwards (fig. 1A-D, supplementary fig. 1). In the adult lung, Chd4 was still expressed in the epithelial cells of the large airways albeit at lower level. FoxP2 expression was restricted to the distal lung epithelium during the late pseudoglandular, canalicular and saccular phases of lung development (fig. 1E-H, supplementary fig. 2). FoxP4 expression was detected at first at E14 in the epithelium of the developing airways and the surrounding mesenchyme. During the canalicular phase, FoxP4 expression became more restricted to the proximal and distal airway epithelium. A similar expression pattern was observed in the saccular phase and postnatally (fig. 1I-L, supplementary fig. 3). Cux1 was expressed at the mesenchyme at the earliest stages of lung development until E16 while at the canalicular and saccular phases of the lung significant expression was detected in the epithelial cells of the airways (fig. 1M-P, supplementary fig. 4). In the adult mouse lung Cux1 remained exclusively expressed in the epithelial cells of the major airways.

Table 1. Identification of Chd4, FoxP1/2/4 and Cux1 as Sox2 candidate binding partners in lung tissue using mass spectrometry analysis.

	BioSox purification lung tissue		BioSox2 purification trachea tissue	
Symbol	Mascot[a]	Peptides[b]	Mascot[a]	Peptides[b]
Chd4	1343 (939)	26 (21)	319 (N.A.)	7 (0)
Cux1	476 (N.A.)	8 (0)	N.A.	N.A.
FoxP1	146 (N.A.)	3 (0)	N.A.	N.A.
FoxP2	61 (N.A.)	2 (0)	N.A.	N.A.
FoxP4	86 (N.A.)	2 (0)	N.A.	N.A.

[a] Mascot score of the identified binding partner, mascot score of the control is between brackets.
[b] Number of unique proteins for the identified binding partner, mascot score of the control is between brackets.

Chd4, FoxP2 and Cux1 co-localize with Sox2 in the developing lung

Previously, our group studied Sox2 expression during the different phases of lung development in mouse, and Sox2 was detected in the epithelial cells of the foregut at E9.5, from E10.5 till E14.5 it was exclusively expressed in the epithelial cells of the non-branching developing airways and it remained expressed in these cells of the conducting airways (8). As the airway epithelium consists of several cell types, we performed immunofluorescence on embryonic lung tissue at different gestational ages to determine whether the candidate proteins are expressed in the same cell as Sox2. For Chd4, no specific expression was detected until E16. At E18, co-localization of Sox2 and Chd4 was observed in the epithelial cells lining the proximal airways (fig. 2A). Thus, at the final stages of embryonic lung development, the spatial and temporal expression patterns of Sox2 and Chd4 overlap. FoxP2 and Sox2 were co-expressed in cells localized at the branching site between the proximal and distal region during the embryonic and early pseudoglandular phases of lung development (fig. 2B). During later stages of lung development, FoxP2 is restricted to the distal epithelial cells, while Sox2 is restricted to the proximal epithelial cells. Cux1 is expressed in the mesenchyme surrounding $Sox2^{+}$ epithelial cells of the non-branching airways from E11 till E15. However, the expression of Cux1 and Sox2 overlap in epithelial

cells of the major conducting airways starting at E16, which indicated co-expression of Sox2 and Cux1 in these epithelial cells during the canalicular (E16.5-E17.5) and saccular (E17.5-PN5) phases of lung development (fig. 2C).

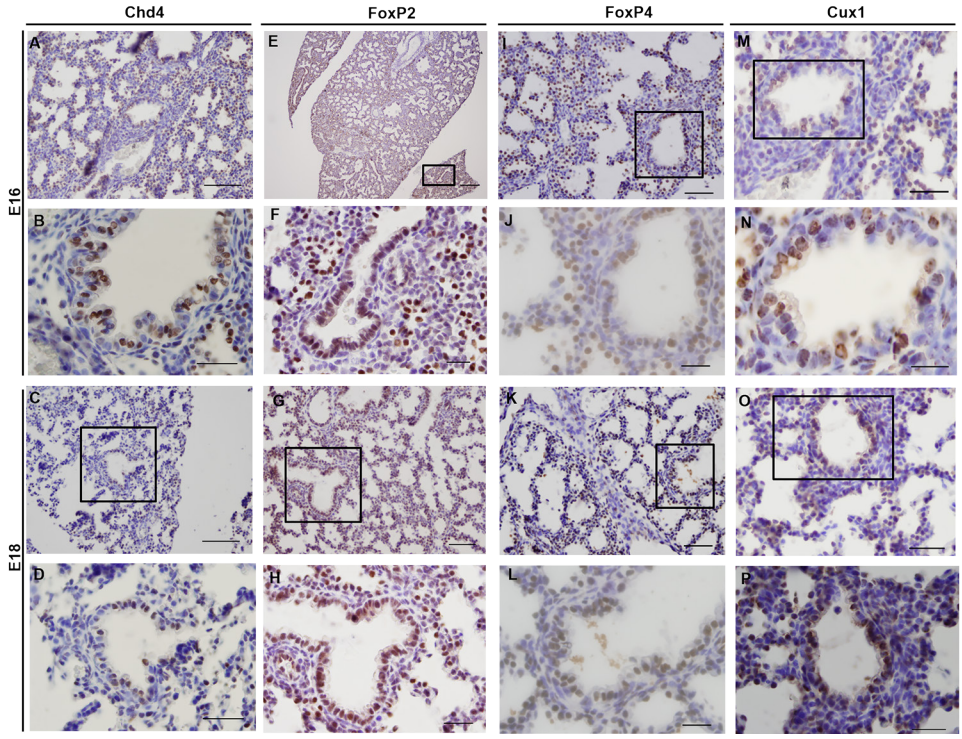

Figure 1. Endogenous Chd4, FoxP2/4 and Cux1 expression at E16 and E18 in mice. (A-D) Chd4 is primarily expressed in the conducting airways of the lung at E16 (A, B) and E18 (C, D). (E-H) At E16 (E, F) and E18 (G, H) FoxP2 is exclusively expressed in the distal airway epithelium. (I-L) At E16 (I, J), FoxP4 expression becomes restricted to the epithelial cells and this pattern remains at E18 (K, L). (M-P) At E16 and E18, Cux1 is expressed in epithelial cells of the conducting airways and surrounding alveolar regions. Sections are frontal and scale bars are 20 µm (E), 10 µm (A, C, G, I, K, M, O) and 5 µm (B, D, F, H, J, L, N, P). Black boxes indicate magnified areas.

Chd4, FoxP2/4 and Cux1 physically interact with Sox2

Since the spatial and temporal expression of Sox2 and its putative partners overlap, the potentially interaction between the proteins was validated. Therefore transient transfections were performed using a myc tagged Sox2 (myc-Sox2) and FLAG tagged Chd4 (FLAG-Chd4, and myc tagged FoxP2 (myc-FoxP2) and FoxP4 (myc-FoxP4) together with FLAG tagged Sox2 (FLAG-Sox2). Immunoprecipitation of FLAG-Chd4 with FLAG antibody co-precipitated the myc-Sox2 protein (fig. 3A). Vice versa, immunoprecipitation of myc-Sox2 with myc antibody co-precipitated the FLAG-Chd4 protein (fig. 3B), indicating that Sox2 and Chd4 can physically interact. Immunoprecipitation of FLAG-Sox2 with FLAG antibody co-precipitated both myc-FoxP2 and myc-FoxP4 (fig. 3D, G). Vice versa, immunoprecipitation of myc-FoxP2 and myc-FoxP4 with myc antibody, co-precipitated FLAG-Sox2 (fig. 3E, H). This indicates that both FoxP2 and FoxP4 can physically interact with Sox2.

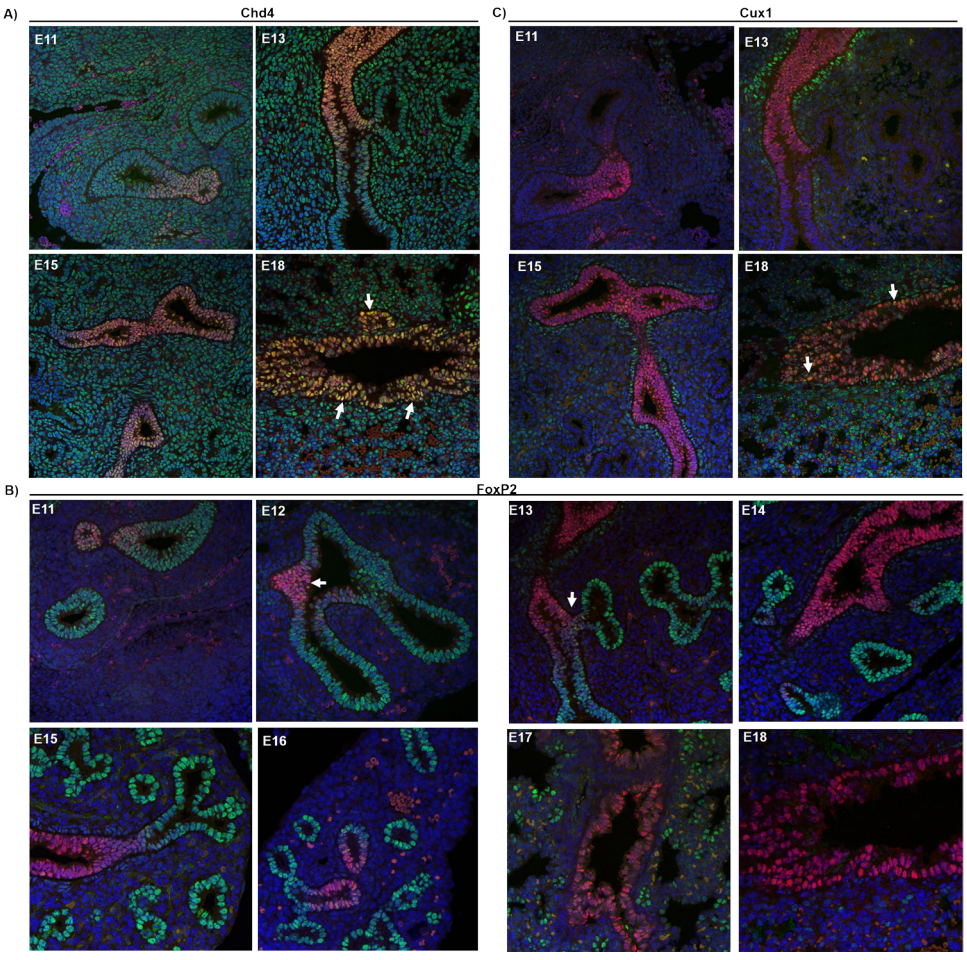

Figure 2. Co-localization of Sox2 and Chd4, FoxP2 and Cux1. A) Co-localization of Sox2 and Chd4 in the proximal airways at E18. CHD4 and SOX2 are co-localized in the nuclei of the epithelial cells that line the proximal airways at E18. Green = Chd4, red = Sox2, blue = dapi. B) Co-localization of Sox2 and FoxP2 at E11 - E13 in the developing mouse lung. During E11 – E13, some epithelial cells localized in the branching site between the proximal and distal region show co-localization of Sox2 and FoxP2. Red = Sox2, green = FoxP2, blue = dapi. White arrows indicate co-localization. C) Sox2 and Cux1 co-localize in the lung epithelium at E16 and E18. Cux1 and Sox2 co-localize in the nuclei of epithelial cells that line the proximal airways during E18. The arrows indicate the epithelial cells that express both Sox2 (green) and Cux1 (red).

Several isoforms of Cux1 are expressed in a cell cycle dependent manner and Cathepsin L is the key protease responsible for the proteolytic cleavage of Cux1. In order to better understand the interactions between Sox2 and Cux1, we analyzed the occurrence of different isoforms during the cell cycle in the lung adenocarcinoma cell line A549, which has an approximate cell cycle of 24 hours. As shown before, A549 cells also displayed a cell cycle dependent expression (fig. 4A).Expression of the p110 isoform was first reduced and became stronger during later phases of the cell cycle. Expression of the p75 and p55 isoforms were also variable during the cell cycle. In order to control the appearance of

the isoforms, we analyzed whether Cathepsin L inhibition would hamper the processing of Cux1 and thus facilitate the identification of the Sox2 interacting Cux1 isoform. The addition of Cathepsin L significantly reduced the expression of the p55 isoform, which indicated that the pro- cessing of the p200 full length Cux1 was completely abolished (fig. 4B).

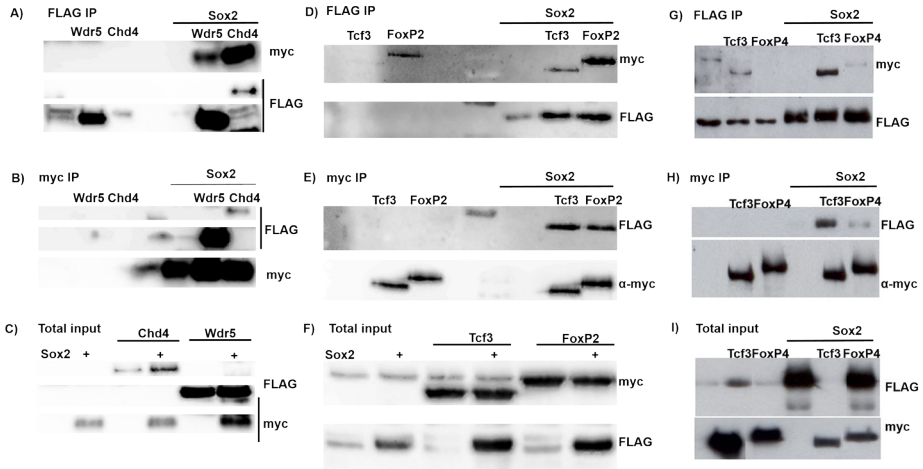

Figure 3. Chd4, FoxP2 and FoxP4 can physically interact with Sox2. Physical interaction between Chd4, FoxP2 and FoxP4 with Sox2 was confirmed in co-immunoprecipitations. A) By precipitating FLAG-Chd4 using FLAG antibody, we confirmed that myc-Sox2 was also precipitated. B) By precipitating myc-Sox2 using myc antibody, FLAG-Chd4 was co-precipitated. C) Total input shows the expression of the FLAG-Chd4 and myc-Sox2. Wdr5 was used as positive control for the immunoprecipitation. D, G) By precipitating FLAG-Sox2 using FLAG antibody pull downs we confirmed that myc-FoxP2 and myc-FoxP4 were also precipitated. E, H) By precipitating myc-FoxP2 and myc-FoxP4 using myc antibody, FLAG-Sox2 was co-precipitated. F,I) Total input shows the expression of myc-FoxP2, myc-FoxP4 and FLAG-Sox2. Tcf3 was used as positive control for the immunoprecipitation. Blots were labeled with antibodies against FLAG and myc.

Next, transient transfections using the FLAG-Sox2 and a myc/HA double tagged Cux1 (myc-Cux1-HA) were performed to validate the putative interaction between Sox2 and Cux1 (fig. 4C). Since the myc-tag is located at the N-terminus of the full length Cux1, a myc antibody was used to detect the different isoforms containing the N-terminus, such as the full-length Cux1 protein (p200) and the p55 isoform (fig. 4D). The HA-tag is located at the C-terminus, so an HA antibody was used to detect the different C-terminus containing isoforms. This showed the processing of the p200 isoform into the presumptive p150, p110, p90, p80 and p75 isoforms (fig. 4E). In addition, 2 Cux1 specific antibodies raised against different domains of the endogenous protein were used, which both detected only the full-length p200 Cux1 protein (fig. 4F-G).

Immunoprecipitations were performed using the antibodies against the endogenous Cux1 protein. One of these antibodies was raised against a peptide at the C-terminus of the Cux1 protein, while the other antibody was raised against aa521-621, which is located between cut repeat 1 and 2. In both immunoprecipitations, the Sox2 protein was efficiently co-precipitated (fig. 4H), indicating that Cux1 and Sox2 physically interact.

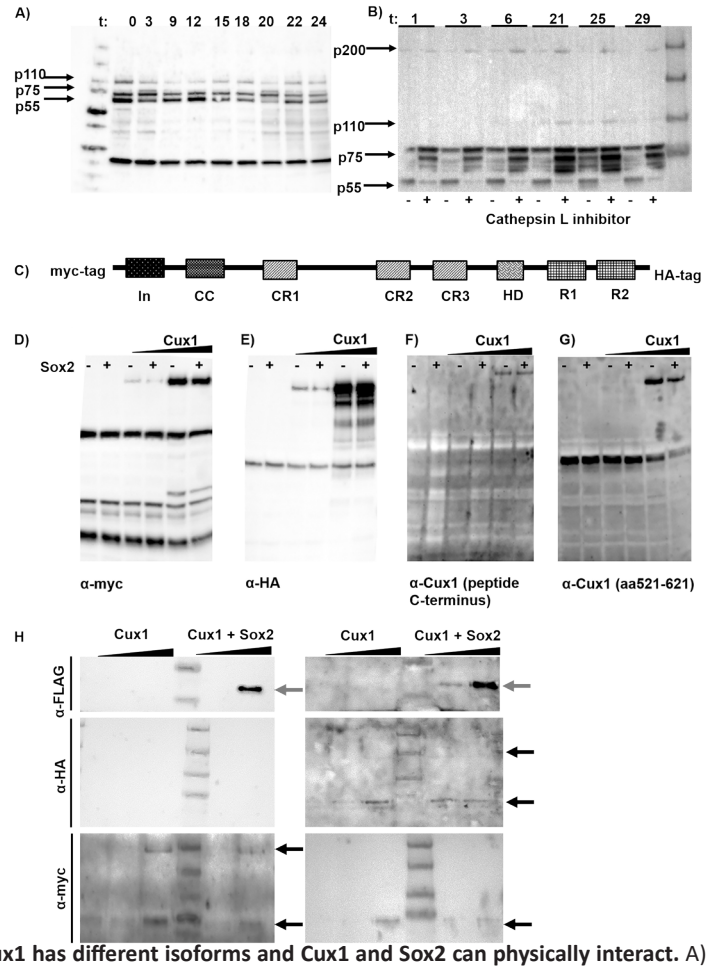

Figure 4. Cux1 has different isoforms and Cux1 and Sox2 can physically interact. A) Different Cux1 isoforms during cell cycle. A549 cells were cultured under starvation for 24 hours, switched back to normal growth medium and harvested every 3 hours over a time span of 24 hours. Cell extracts were prepared and by analyzing these samples by western blot, differences in expression pattern of Cux1 over time were detected. Blot was labeled with α-Cux1 (ab54583). t indicates time points at which samples were taken. B) Influence of Cathepsin L on different Cux1 isoforms. A549 cells were synchronized by starvation for 24 hours, and then put back on normal growth medium. Cathepsin L inhibitor 1 hour later. Cells were harvested at different time points, extracts were prepared and analyzed by western blot. In the samples where Cathepsin L inhibitor is added, more of the p200 isoform is detected, while we see less expression of the P55 isoform. Blot was labeled with α-Cux1 (ab54583). C) For co-transfections and co-immunoprecipitations we used a Cux1 construct with a myc-tag at the N-terminus and a HA-tag at the C-terminus (myc-Cux1-HA). Figure is adapted from Moon et al. 2001 (25). D) Total input myc-Cux1-HA analyzed with antibody against myc. E) Total input myc-Cux1-HA analyzed with antibody against HA. F) Total input myc-Cux1-HA analyzed with antibody against Cux1 raised against a peptide mapping at the C-terminus. G) Total input myc-Cux1-HA analyzed with antibody against Cux1 raised against aa521-621. H) By precipitating myc-Cux1-HA with both Cux1 antibodies, FLAG-Sox2 was detected in the precipitated fraction, indicating interaction between Sox2 and Cux1. Gray arrows indicate the precipitated FLAG-Sox2, black arrows indicate the precipitated myc-Cux1-HA.

To determine which Sox2 domains are important in this interaction, the association of Cux1 to several mutant Sox2 proteins lacking functional domains was analyzed. Therefore, myc-Cux1-HA was co-expressed with Sox2 mutant proteins, either lacking the HMG domain (Sox2-ΔHMG) or lacking the C-terminal transactivation domain (FLAG-Sox2(1-123), or only expressing the Sox2-HMG domain (FLAG-Sox2-HMG) (fig. 5A) (26). Immunoprecipitation of the myc-Cux1-HA protein with the HA antibody only co-purified the FLAG-Sox2(1-123) (fig. 5B-C), which indicated that the Cux1-Sox2 interaction requires the N-terminal and DNA-binding HMG domain of Sox2.

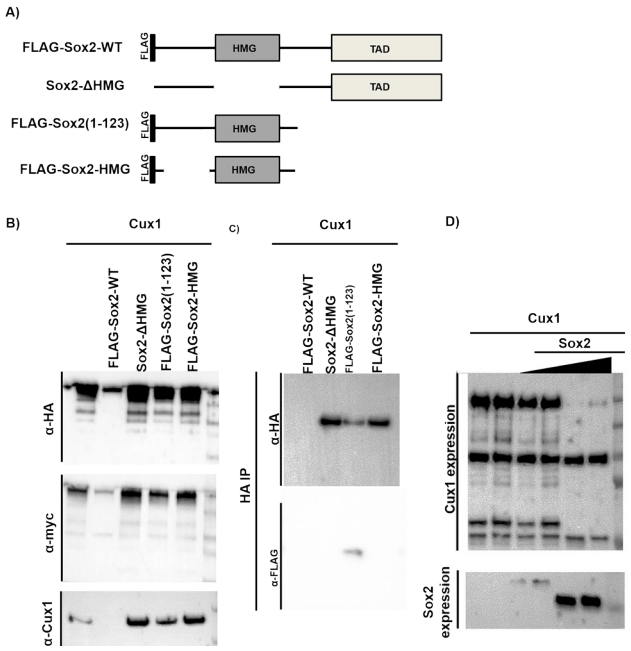

Figure 5. The N-terminal domain and DNA-binding domain of Sox2 are necessary for interaction with Cux1. A) Flag-Sox2-WT, Sox2-DHMG, FLAG-Sox2(1-123) and FLAG-Sox2-HMG constructs (26). HMG = High Mobility Group, TAD = transactivation domain. B) Total input Cux1. C) HA immunoprecipitations shows that Cux1 and Sox2 can only interact when the Sox2 N-terminal and DNA-binding domain are intact. D) Sox2 overexpression prevents formation Cux1 isoforms. A higher expression of Sox2 results in prevention of formation of Cux1 isoforms. For Sox2, 2 different Sox2 constructs are used, a 2xFLAG-Sox2 (low expression) and a FLAG-Sox2 (high expression).

By analyzing the Cux1 expression in HEK cells transfected with myc-Cux1-HA only, or together with these Sox2 constructs, we noticed that Cux1 isoforms were not detected when the full length Sox2 was co-expressed (fig. 5B). Further analysis showed that high levels of Sox2 apparently prevented the proteolytic processing of full length Cux1, suggesting that Sox2 can inhibit the processing of Cux1 (fig. 5D).

GST-Sox2 fusion proteins interact with Cux1, but not with Chd4

In order to investigate the nature of the interactions between Sox2 and Cux1 or Chd4, we used bacterial produced GST-Sox2 fusion proteins. Aside from the wild type Sox2, three mutant Sox2 constructs were included with mutations in critical basic amino-acid residues

of the nuclear localization signals (fig. 6A) (27). These mutant GST-Sox2 fusion proteins allowed us to analyze whether the conserved residues in the NLS sequence were required for the interaction with Chd4 or Cux1, as previously was shown for the interaction between Sox2 and Xpo4 (20). Nuclear extracts of HEK cells were incubated with the GST-Sox2 fusion proteins. Only with the wild-type Sox2 with an intact HMG domain, the P75 Cux1 was precipitated (fig. 6B). Interaction between Chd4 and Sox2 could not be validated using the GST-Sox2 fusion proteins (fig. 6C). These results indicate that the p75 isoform of Cux1 interacts with Sox2 and that this interaction depends on an intact HMG domain, whereas no direct binding was detected between Sox2 and Chd4 using this method.

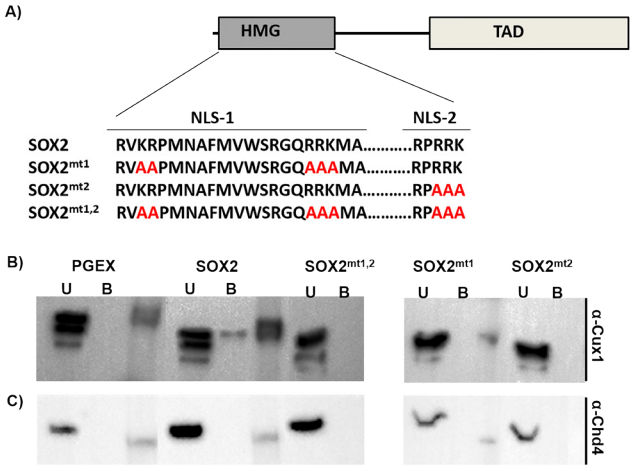

Figure 6. Incubation with GST-fusion tags showed direct interaction between Sox2 and Cux1 but not between Sox2 and Chd4. A) GST-fusion tags with different SOX2 a wild-type SOX2, a SOX2 with a mutation at the beginning of the HMG-box, a SOX2 with a mutation at the end of the HMG-box and a SOX2 with both mutation. Figure is adapted from Yasuhara et al. 2007 and Cox et al. 2010 (26, 27). B) Cux1 binds with Sox2 through conserved residues of its HMG domain. p75 Cux1 only interacts with the wild-type Sox2. U = unbound fraction, B = precipitated fraction. C) No Chd4 is only detected in the eluate, not in the precipitated fractions.

Common CHD4, CUX1 and SOX2 target in NCCIT

To get more insight in the functionality of the CHD4-SOX2 and CUX1-SOX2 complex during lung development, a chromatin immunoprecipitation (ChIP) was performed with NCCIT cells, followed by total sequencing of the bound DNA fragments. For this purpose, NCCIT cells were used, because these cells both express CUX1, CHD4 and SOX2 (fig. 7A-B). Chromatin was either single or double cross-linked. To validate the efficiency of the ChIP, qPCRs were performed to measure the enrichment of known target genes in antibody-specific ChIPs compared to IgG controls. For the single cross-linked SOX2 and CHD4 ChIPs, enrichment in SOX2 and JAG1 was detected, indicating that the ChIP was done efficiently (fig. 7C, D). The generated sequencing data were analyzed to identify individual binding sites of the individual transcription factors, to locate co-occupied binding sites between SOX2 and the candidate partners and to reveal the binding site motifs that were enriched. In the single cross-linked CHD4 and SOX2 ChIPS there was an overlap of 73 target regions, while in the double cross-linked ChIPs an overlap of 145 target regions between SOX2 and CHD4 was found (fig. 7E). Some of the target genes identified in the single cross-

linked CHD4 ChIP, could be linked to a respiratory phenotype including Basagin (BSG) and PhosphoDiesterase 4D Interacting Protein (PDE4DIP). PDE4DIP was also identified as a target gene in the single cross-linked SOX2 ChIP. Also in the double cross-linked CHD4 ChIP some interesting target genes involved in the respiratory system were found including Inhibitor of DNA binding 1 (ID1). ID1 was also identified as a direct SOX2 target gene. The overlap in binding may indicate that SOX2 and CHD4 can co-regulate genes involved in the respiratory system. In the single cross-linked CUX1 and SOX2 ChIPS there was an overlap of 7 target regions, while in the double cross-linked ChIPs an overlap of 72 target regions between SOX2 and CUX1was found (fig. 7E). None of these targets could be linked to a respiratory phenotype.

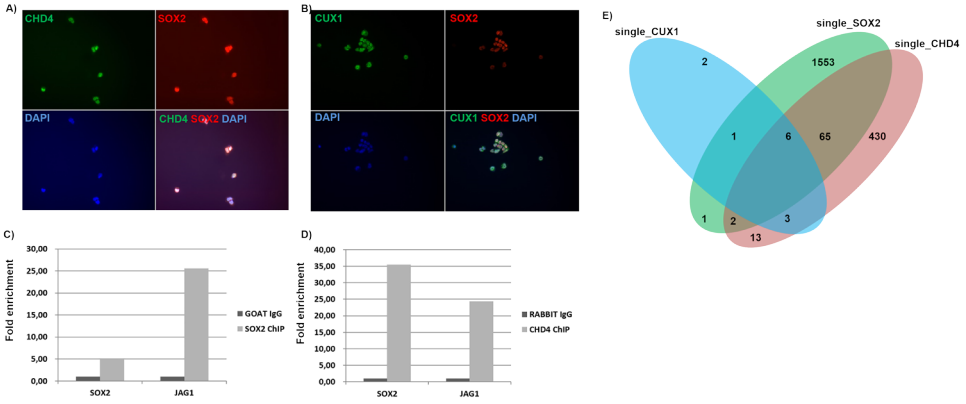

Figure 7. A,B) SOX2, CHD4 and CUX1 expression in NCCIT cells. A) NCCIT cells express both CHD4 (green) and SOX2 (red). Nuclei are stained with dapi (blue). Arrows indicate co-localization. B) Both CUX1 (green) and SOX2 (red) are expressed in NCCIT cells. Arrow indicated that SOX2 and CUX1 are co-localizing. **C,D) Target gene enrichment single cross-linked SOX2 and CHD4 ChIP in NCCIT cells.** An enrichment was observed in SOX2 and JAG1, which are both SOX2 and CHD4 target genes, in the ChIP using a specific SOX2 antibody (C) and a specific CHD4 antibody (D), compared to the IgG ChIP. **E) Venn diagram showing overlapping target genes between SOX2, CHD4 and CUX1 ChIP.**

Discussion

Previously, we and others have shown the importance of Sox2 in branching morphogenesis and lung epithelium differentiation (8-10). Transcriptional activity of Sox2 depends on its interaction partners and by performing large scale biotin-tagged Sox2 affinity purifications using E18 lung we identified several partners *in vivo*. From the list of putative associating factors, we characterized a number of them in more detail, like the Chromodomain Helicase DNA-binding protein 4 (Chd4). In another study, we already identified Chd4 as a possible Sox2 interaction partner, but had not validated this interaction or examined the functionality of this protein complex (Gontan, unpublished data)(17).

Chd4 is one of the catalytic subunits of the nucleosome remodeling and deacetylase (NuRD) complex, which makes DNA accessible to proteins and protein complexes to mediate several processes including transcription and repair (29) (30). Other components of this complex are HDAC1/2, which are histone deacetylases, the non-enzymatic proteins MBD2/3, the retinoblastoma-binding proteins MTA1/2/3 and GATAD2A/B (30). Several

other studies also showed potential interaction between Sox2 and MTA1/2/3, MBD2, GATAD2A/B and HDAC1/2 in different cell lines, including embryonic stem cells, neural stem cells and embryonal carcinoma cells (17, 26, 31). Because the NuRD complex is associated with several diseases, including cancer, its components are interesting potential therapeutic targets (30, 32). The NuRD complex is an interactor of Oct4 and involved in induction of pluripotency in neural stem cells (33-36). The NuRD complex is also involved in epithelial injury response in the lung by interacting with the FoxP1/2/4 family, suggesting that this complex is involved in lung injury repair and regeneration (37). This mechanism acts as a response to hyperoxic injury. Premature babies that need oxygen supply after birth are mechanically ventilated and thereby exposed to high concentrations of oxygen, causing lung injury (38). Based on the findings of Chokas and colleagues, the NuRD complex and its core component Chd4 could be involved in the repair of this injured lungs, making it worthwhile to further investigate the role of Chd4 as a potential partner of Sox2 during lung development.

Co-immunoprecipitations validated that Chd4 and Sox2 can physically interact, although this could not be confirmed by the GST fusion tag pull downs. This could be due to the physiological conditions under which the experiments were performed. Cells were cultured under normoxic circumstances, while the lung develops in a quite hypoxic environment. It has been shown that there is an upregulation of Chd4 under hypoxic circumstances, and it could be possible that Sox2 is capable of binding Chd4 when there is a higher extent of expression. This could be validated by culturing cells under hypoxic circumstances and then investigate whether there is direct interaction.

It could also be possible that interaction between Chd4 and Sox2 might be mediated by other components of the NuRD complex. Another member of the histone deacetylase family, HDAC3, has also been identified as a Sox2 partner (17, 31). Previous research showed that activity of HDAC is decreased in lungs of COPD patients, and that expression of HDAC2 is significantly decreased (39). Furthermore, Hdac1/2 are involved in the development and regeneration of $Sox2^+$ lung endoderm progenitors. Deletion of Hdac1/2 in the epithelial cells of the lung during early development results in loss of branching morphogenesis, resulting in enlarged airspaces. Sox2 expression was also decreased in these lungs, indicating that Hdac1/2 are required for development of $Sox2^+$ progenitors in the proximal airways (40). HDAC1/2 are already validated as interaction partners by Cox and co-workers (26). This suggests that Sox2 interacts with Chd4 via a direct interaction of Sox2 with HDAC1/2 as part of the NuRD complex.

Besides studying the interaction between Sox2 and Chd4, we have also studied the functionality of this complex. ChIP data revealed that Sox2 and Chd4 have several previously identified common target genes. In the single crosslinked ChIPs, there was an enrichment in JAG1 in both the CHD4 and SOX2 ChIP. This suggest that Sox2 and Chd4 could co-regulate the expression of JAG1, although it is unknown if Sox2 and Chd4 bind in the same region. JAG1 is involved in Alagille syndrome, in which the liver and heart are affected. Patients can also have distinctive facial features and unusual shaped bones. In the single crosslinked Chd4 ChIP we also detected an enrichment of Sox2. In Chd4 knock-out mice, where Chd4 is conditionally knock-out in Schwann cells, several genes including Sox2 are upregulated indicating that Sox2 is a target gene of Chd4 (41). Since this is not confirmed

by ChIP, it is unknown if this is a direct effect. So besides a role of the Chd4-Sox2 complex (either direct or indirect), this regulatory mechanisms could also be involved in cell lineage specification during lung development. Another common target gene of Sox2 and Chd4 is Id2, which is the marker for the distal lung epithelium. Sox2 and Chd4 could be involved in the downregulation of Id2, thereby preventing cells from a distal cell fate. If Sox2 is indeed repressing the expression of Id2, this is also in line with the fact that Id2 is not expressed in the proximal epithelial cells of the lung and only in the distal cells where Sox2 is not expressed. In endothelial cells where Chd4 is deleted, there is an upregulation of Id2 (42). During chondrogenic differentiation Chd4 can inhibit downregulation of Sox9, which is also a distal epithelial progenitor cell marker (43). It would be interesting to determine the effect of a Chd4 knock-down on Sox2, Sox9 and Id2 in the developing lung. This could give more insight of a potential role for Chd4 in the distal-proximal cell lineage specification in the lung.

Some of the target genes identified in the single cross-linked CHD4 ChIP, could be linked to a respiratory phenotype including Basigin (BSG) and PhosphoDiesterase 4D Interacting Protein (PDE4DIP). Bsg is a member of the Ig superfamily and is involved interactions between neuronal and glial cells in the development of the retina. It is also necessary for peri-implantation and $Bsg^{-/-}$ mice mainly die during this stage. Mice that did survive show difficulties in breathing, showed signs of interstitial pneumonia and their lungs have a thickening of the alveolar septum (44). Bsg is also linked to pulmonary hypertension and thought to play a role in alveolar injury, since Bsg expression is increased in the distal lung epithelium after bleomycin-induced injury (45, 46). PDE4DIP was identified as a target gene in both the single cross-linked SOX2 ChIP and single cross-linked CHD4 ChIP, indicating that an interaction between SOX2 and CHD4 could be involved in the regulation of this gene. PDE4DIP is linked to Usher syndrome, which is affecting hearing and vision of patients, and eosinophilia, in which the lungs can be affected.

Three other candidate Sox2 partners that were also identified with our bioSox2 purification were FoxP1, FoxP2 and FoxP4. FoxP1, FoxP2 and FoxP4 are involved in various biological processes, including lung development. FoxP1 and FoxP2 are both involved in development of the esophagus and lungs and loss of FoxP2 results in defects of lung alveolarization as shown in $FoxP2^{-/-}$ mice (47). $FoxP1^{-/-}$ and $FoxP4^{-/-}$ mice die at E13.5 but do not show any lung abnormalities till that stage. $FoxP2^{-/-}$;$FoxP1^{+/-}$ mice die at birth due to respiratory failure. The lungs of these mice are reduced in size and have dilated airways (47). Both FoxP1 and FoxP2 are able to repress the CC10 promoter and human surfactant protein C promoter, indicating an important role as lung epithelial transcription regulators (22). FoxP1/4 is involved of cell fate choice restriction during lung development. FoxP1/4 inhibits differentiation of secretory cells, followed by induction of the goblet cell lineage program. This is necessary for the development of a functional airway epithelium and for regeneration of the airway epithelium in adult lung (48). Although Sox2 is restricted to the proximal airways and FoxP2 to the distal airways during later stages of development, co-localization was observed during the embryonic and early pseudoglandular phase. These cells were localized in the branching site between the proximal and distal region, suggesting that the FoxP2-Sox2 complex could be involved in early branching in lung development. In this region, the broncho-alveolar duct junction, bronchoalveolar stem cells are located, suggesting a role for the Sox2-FoxP2 partner complex in these cells (49).

In this study, interaction of Sox2 with both FoxP2 and FoxP4 was validated. During (lung) development there is an overlap of the expression of the different FoxP factors and specific dimer combinations of FoxP1, FoxP2 and FoxP4 regulate various subsets of target genes, including genes of the Notch and Wnt signaling pathway. This could lead to tissue specific development (50). Interplay between FoxP1 and FoxP2 is necessary for proper lung airway morphogenesis and development of the esophagus (47). FoxP1 together with FoxP4 is involved in epithelial cell fate during both development and repair. A conditional knock-down of both factors result in a loss of secretory cells, indicating that FoxP1/4 is involved in secretory cell fate (48). Since these cells are derived from $Sox2^{+}$ progenitor cells, interplay between Sox2 and FoxP1/4 could be involved in this process.

One of the target genes identified in the SOX2 ChIP is T1-α, which is involved in the formation of the alveoli. T1-α null mutant mice show aberrant distal lung morphology and a different distal cell marker expression pattern. These mice die shortly after birth due to respiratory failure (51). T1-α is also a direct *in vivo* target of FoxP1 and FoxP2 and interaction between Sox2 and FoxP1/2 could be involved in regulation of this gene, although it is unknown if Sox2 and FoxP2 bind in the same region (47). If Sox2 expression is involved in repression of T1-α, this could contribute to the plasticity of these cells and their ability to get a proximal cell fate.

Besides interacting with Sox2, FoxP1/2/4 can also interact with the NuRD-complex via Gatad2b. This complex has been associated with injury protection of the alveolar epithelium and it would be interesting to determine the expression pattern of other component of the NuRD complex in the proximal airways as well (37). If there are certain subsets of cells in the upper airway epithelium that both express Sox2 and components of the NuRD complex, it would to interesting to investigate whether an interaction of Sox2 and the NuRD complex is involved in injury protection in the upper airways using the same mechanism as FoxP1/2/4-NuRD interaction in protection of the alveolar epithelium (37). Hdac1/2 are expressed at E12.5 in the endoderm and mesenchyme. Later in development, Hdac2 expression becomes restricted to the epithelial cells of the proximal airways at E17.5 (40).

Another candidate binding partner identified is Cut-Like Homeobox1 (Cux1). This transcription factor is previously also identified as a Sox2 partner in neural stem cells (17). Cux1 is expressed in many cell types and organs, including the lung, and is involved in diverse processes, such as cell migration, cell adhesion and motility and it is involved in brain and liver development and cancer. Cux1 contains five evolutionary conserved regions: a coiled-coil domain, a CUT homeodomain and three CUT repeats (52, 53). These CUT-repeats exhibit different sequence-specific DNA-binding (54). There is also an inhibitory domain present at the amino-terminus and two active repression domain at the carboxy-terminus. Besides the full size P200 Cux1 protein, there are six other isoforms. The P75 and P55 isoforms are a product of a different mRNA transcript, while the P150, P110, P90, P80 are the result of proteolytic cleavage. The DNA binding properties of these different isoforms depend on the DNA binding domains present in the isoform (52, 53).

Several Cux1 mutant mice have been generated. $Cux1^{tm1Ejn}$ mice that carry a deletion that includes cut repeat 1 have wavy hair, curly whispers and lactation defects (55). When these

mice were cross-breeded with Cys1^{cpk} mice, who develop cystic kidneys, the cysts were larger than in Cys1^{cpk} mice, suggesting that Cux1 accelerates the growth of these cysts (56). In Cux/CDP$^{DHD/DHD}$ the C-terminus, including the homeodomain and repression domain is deleted. These mice are smaller and have an aberrant skin compared to wild-type mice from the same litter. They also show abnormalities in fur, whiskers, bones and hair follicles and they have defects in development of lymphoid and myeloid as well as hematopoietic defects (57). Another strain in which the C-terminus is deleted, CDP/Cux $^{\Delta C-/-}$ showed the same morphological abnormalities, deregulated hair cycle and a reduction in male fertility, which indicated that Cux1 is involved in dermal functions and the reproductive system(58). t is shown by a fourth mouse model by Ellis et al. that Cux1 is involved in lung development. Cutl1$^{z/z}$ mice, which express an inactive Cux1 protein, showed retardation of the lung epithelium, resulting in a thick, non-functional epithelium and mutant mice die shortly after birth of respiratory distress. They suggested that Cux1 is important for the differentiation of the cuboidal epithelial precursor cells into functional alveolar type I and II cells (59). We did see a similar enlargement of the airways in our iSox2$^{SPC\text{-}rtTA}$ mice, in which Sox2 is ectopically expressed in the epithelial cells of the developing airways.

We first showed that co-localization of Cux1 and Sox2 was detected in the epithelial cells of the proximal airways by IF. However, there were also single positive cells, expressing either Sox2 or Cux1. In *Drosophila* the Cux1 homologue Cut is expressed in the multipotent progenitor cells of the abdominal airway during early development, while in later stages it is only expressed in a subset of cell where it is possibly involved in cell proliferation (60). This could be similar in lung development in mice, explaining why not all cells in the proximal epithelium express Cux1.

Sox2 and Cux1 can physically interact and this interaction is dependent on the N-terminal and DNA-binding domain of Sox2 (26). For Sall4 it was shown that it can interact with both the full-length Sox2 as well as the FLAG-Sox2(1-123) construct, although in lower extends (26). This indicates the importance of the C-terminal in that particular interaction (26). It was also shown that multiple Sox2 domains are involved in the interaction between HDAC1 and Sox2, while for the interaction with HDAC2 only the HMG domain is involved (26). The importance of the conserved residues in the HMG box of Sox2, has also been shown for interaction between Sox2 and Xpo4 (20).

Interestingly, the level of Sox2 expression seemed to influence the processing of Cux1 isoforms. In embryonic stem cells, where Sox2 is highly expressed, it represses proliferative genes, thereby preventing cell cycle progression (61). In the developing and adult central nerve system, it is shown that Sox2 regulates stem and progenitor cell proliferation in a dose-dependent manner and thereby able to keep neural cells in an undifferentiated stage. These cells do not express Cux1, while as these cells start to differentiate they lose Sox2 expression and start to express Cux1 (61). Low levels of Sox2 allowed the Cux1 protein to be post-translationally processed, whereas high levels prevented this process. This could mean that Cux1 is only expressed in small amounts in Sox2^{+} progenitor cells and that this expression becomes higher in more differentiated cells which could be the reason why Sox2 and Cux1 are not co-localizing in all the proximal epithelial cells**.** It was shown that Wnt signaling inhibits differentiation of Sox2^{+} proximal cells and induces Cux1. Our data offer a possible molecular explanation for this observation, as cells that start to express

Sox2 may lose Cux1.

Since we also wanted to show the functionality of the SOX2-CUX1 complex, we performed a chromatin immunoprecipitation (ChIP) in NCCIT cells to identify common target genes of SOX2 and CUX1, with both single and double cross-linked chromatin. In the single cross-linked ChIPS an overlap of 7 target regions was found, while in the double cross-linked ChIPs an overlap of 72 target regions was found between SOX2 and CUX1, but most of these target regions were pseudogene or non-coding regions. This could be caused by inefficiency of the used antibody. None of the identified target genes could be linked to a respiratory phenotype which is probably due to the use of NCCIT cells for the ChIP, which is an embryonic carcinoma cell line instead of a lung cell line.

It is shown previously that Sox2 and Cux1 have several common target genes, including Chn1 (involved in Duane Retraction Syndrome), Homer2 (linked to Congenital diaphragmatic hernia, Hif1an and Kccn2 (both involved in hypoxia), Wdr37, FoxP4 and Arl6 (involved in Bardet-Biedl syndrome) (62, 63). Cux1 is also involved in the transcriptional regulation of several Wnt genes and overexpression of several Wnt genes in mutant Cux1 mouse mammary tumors indicated that some of the genes participate with CUX1 in the transcriptional activation of Wnt genes (64). These targets were not identified in the ChIP in the NCCIT cells. This could either be due to the type of cells that were used or due inefficiency of the antibody used for the ChIP.

In conclusion, we identified Chd4, FoxP2/4 and Cux1 as a Sox2 interaction partner during lung development. We validated that Sox2 and these partners can physically interact. ChIP data indicated that that SOX2 and CHD4 could be involved in co-regulation of genes involved in the respiratory system.

Acknowledgements
We would like to thank Dr. Yoshihiro Yoneda for the GST-Sox2 constructs, Dr. Svaren for providing the Chd4 plasmid, Dr. Morrisey for providing the FoxP2 and FoxP4 constructs, professor Angie Rizzino for providing the Sox2 mutant plasmids, Dr. Alain Nepveu for providing the Cux1 plasmid and Dr. Brad Merrill for the Tcf3 construct.

References

1. Metzger RJ, Klein OD, Martin GR, Krasnow MA. The branching programme of mouse lung development. Nature. 2008;453(7196):745-50.
2. Hashimoto S, Chen H, Que J, Brockway BL, Drake JA, Snyder JC, et al. beta-Catenin-SOX2 signaling regulates the fate of developing airway epithelium. J Cell Sci. 2012;125(Pt 4):932-42.
3. Chang I, Bramall AN, Baynash AG, Rattner A, Rakheja D, Post M, et al. Endothelin-2 deficiency causes growth retardation, hypothermia, and emphysema in mice. Journal of Clinical Investigation. 2013;123(6):2643-53.
4. Rockich BE, Hrycaj SM, Shih HP, Nagy MS, Ferguson MA, Kopp JL, et al. Sox9 plays multiple roles in the lung epithelium during branching morphogenesis. Proc Natl Acad Sci U S A. 2013;110(47):E4456-64.
5. Alanis DM, Chang DR, Akiyama H, Krasnow MA, Chen JC. Two nested developmental waves demarcate a compartment boundary in the mouse lung. Nat Commun. 2014;5.
6. Desai TJ, Brownfield DG, Krasnow MA. Alveolar progenitor and stem cells in lung development, renewal and cancer. Nature. 2014;507(7491):190-+.
7. Treutlein B, Brownfield DG, Wu AR, Neff NF, Mantalas GL, Espinoza FH, et al. Reconstructing lineage hierarchies of the distal lung epithelium using single-cell RNA-seq. Nature. 2014;509(7500):371-5.
8. Gontan C, de Munck A, Vermeij M, Grosveld F, Tibboel D, Rottier R. Sox2 is important for two crucial processes in lung development: branching morphogenesis and epithelial cell differentiation. Dev Biol. 2008;317(1):296-309.
9. Tompkins DH, Besnard V, Lange AW, Keiser AR, Wert SE, Bruno MD, et al. Sox2 Activates Cell Proliferation and Differentiation in the Respiratory Epithelium. Am J Resp Cell Mol. 2011;45(1):101-10.
10. Que J, Luo X, Schwartz RJ, Hogan BL. Multiple roles for Sox2 in the developing and adult mouse trachea. Development. 2009;136(11):1899-907.
11. Rawlins EL, Clark CP, Xue Y, Hogan BLM. The Id2(+) distal tip lung epithelium contains individual multipotent embryonic progenitor cells. Development. 2009;136(22):3741-5.
12. Volckaert T, Campbell A, Dill E, Li C, Minoo P, De Langhe S. Localized Fgf10 expression is not required for lung branching morphogenesis but prevents differentiation of epithelial progenitors. Development. 2013;140(18):3731-42.
13. Ochieng JK, Schilders K, Kool H, Boerema-de Munck A, Buscop-van Kempen M, Gontan C, et al. Sox2 Regulates the Emergence of Lung Basal Cells by Directly Activating the Transcription of Trp63. Am J Respir Cell Mol Biol. 2014.
14. Kamachi Y, Cheah KS, Kondoh H. Mechanism of regulatory target selection by the SOX high-mobility-group domain proteins as revealed by comparison of SOX1/2/3 and SOX9. Mol Cell Biol. 1999;19(1):107-20.
15. Kamachi Y, Kondoh H. Sox proteins: regulators of cell fate specification and differentiation. Development. 2013;140(20):4129-44.
16. Kamachi Y, Uchikawa M, Tanouchi A, Sekido R, Kondoh H. Pax6 and SOX2 form a co-DNA-binding partner complex that regulates initiation of lens development. Genes Dev. 2001;15(10):1272-86.
17. Engelen E, Akinci U, Bryne JC, Hou J, Gontan C, Moen M, et al. Sox2 cooperates with Chd7 to regulate genes that are mutated in human syndromes. Nat Genet. 2011;43(6):607-U153.
18. Driegen S, Ferreira R, van Zon A, Strouboulis J, Jaegle M, Grosveld F, et al. A generic tool for biotinylation of tagged proteins in transgenic mice. Transgenic Research. 2005;14(4):477-82.
19. de Boer E, Rodriguez P, Bonte E, Krijgsveld J, Katsantoni E, Heck A, et al. Efficient biotinylation and single-step purification of tagged transcription factors in mammalian cells and transgenic mice. Proc Natl Acad Sci U S A. 2003;100(13):7480-5.
20. Gontan C, Guttler T, Engelen E, Demmers J, Fornerod M, Grosveld FG, et al. Exportin 4 mediates a novel nuclear import pathway for Sox family transcription factors. J Cell Biol. 2009;185(1):27-34.
21. Srinivasan R, Mager GM, Ward RM, Mayer J, Svaren J. NAB2 represses transcription by interacting with the CHD4 subunit of the nucleosome remodeling and deacetylase (NuRD) complex. J Biol Chem. 2006;281(22):15129-37.
22. Shu WG, Yang HH, Zhang LL, Lu MM, Morrisey EE. Characterization of a new subfamily of winged-helix/forkhead (Fox) genes that are expressed in the lung and act as transcriptional repressors. Journal of Biological Chemistry. 2001;276(29):27488-97.
23. Li SR, Weidenfeld J, Morrisey EE. Transcriptional and DNA binding activity of the Foxp1/2/4 family is modulated by heterotypic and homotypic protein interactions. Molecular and Cellular Biology. 2004;24(2):809-22.
24. Pereira L, Yi F, Merrill BJ. Repression of Nanog gene transcription by Tcf3 limits embryonic stem cell self-renewal. Mol Cell Biol. 2006;26(20):7479-91.
25. Moon NS, Premdas P, Truscott M, Leduy L, Berube G, Nepveu A. S phase-specific proteolytic cleavage is required to activate stable DNA binding by the CDP/Cut homeodomain protein. Molecular and Cellular Biology. 2001;21(18):6332-45.
26. Cox JL, Mallanna SK, Luo X, Rizzino A. Sox2 Uses Multiple Domains to Associate with Proteins Present in Sox2-

Protein Complexes. Plos One. 2010;5(11).
27. Yasuhara N, Shibazaki N, Tanaka S, Nagai M, Kamikawa Y, Oe S, et al. Triggering neural differentiation of ES cells by subtype switching of importin-alpha. Nat Cell Biol. 2007;9(1):72-9.
28. Nowak DE, Tian B, Brasier AR. Two-step cross-linking method for identification of NF-kappaB gene network by chromatin immunoprecipitation. Biotechniques. 2005;39(5):715-25.
29. Ahringer J. NuRD and SIN3 histone deacetylase complexes in development. Trends Genet. 2000;16(8):351-6.
30. Allen HF, Wade PA, Kutateladze TG. The NuRD architecture. Cell Mol Life Sci. 2013;70(19):3513-24.
31. Cox JL, Wilder PJ, Gilmore JM, Wuebben EL, Washburn MP, Rizzino A. The SOX2-Interactome in Brain Cancer Cells Identifies the Requirement of MSI2 and USP9X for the Growth of Brain Tumor Cells. Plos One. 2013;8(5).
32. Sperlazza J, Rahmani M, Beckta J, Aust M, Hawkins E, Wang SZ, et al. Depletion of the chromatin remodeler CHD4 sensitizes AML blasts to genotoxic agents and reduces tumor formation. Blood. 2015;126(12):1462-72.
33. Ding J, Xu H, Faiola F, Ma'ayan A, Wang J. Oct4 links multiple epigenetic pathways to the pluripotency network. Cell Res. 2012;22(1):155-67.
34. Liang J, Wan M, Zhang Y, Gu P, Xin H, Jung SY, et al. Nanog and Oct4 associate with unique transcriptional repression complexes in embryonic stem cells. Nat Cell Biol. 2008;10(6):731-9.
35. Pardo M, Lang B, Yu L, Prosser H, Bradley A, Babu MM, et al. An expanded Oct4 interaction network: implications for stem cell biology, development, and disease. Cell Stem Cell. 2010;6(4):382-95.
36. van den Berg DL, Snoek T, Mullin NP, Yates A, Bezstarosti K, Demmers J, et al. An Oct4-centered protein interaction network in embryonic stem cells. Cell Stem Cell. 2010;6(4):369-81.
37. Chokas AL, Trivedi CM, Lu MM, Tucker PW, Li SR, Epstein JA, et al. Foxp1/2/4-NuRD Interactions Regulate Gene Expression and Epithelial Injury Response in the Lung via Regulation of Interleukin-6. Journal of Biological Chemistry. 2010;285(17):13304-13.
38. Baraldi E, Filippone M. Current concepts: Chronic lung disease after premature birth. New Engl J Med. 2007;357(19):1946-55.
39. Ito K, Ito M, Elliott WM, Cosio B, Caramori G, Kon OM, et al. Decreased histone deacetylase activity in chronic obstructive pulmonary disease. N Engl J Med. 2005;352(19):1967-76.
40. Wang Y, Tian Y, Morley MP, Lu MM, DeMayo FJ, Olson EN, et al. Development and Regeneration of Sox2+ Endoderm Progenitors Are Regulated by a HDAC1/2-Bmp4/Rb1 Regulatory Pathway. Developmental Cell. 2013;24(4):345-58.
41 Hung H, Kohnken R, Svaren J. The Nucleosome Remodeling and Deacetylase Chromatin Remodeling (NuRD) Complex Is Required for Peripheral Nerve Myelination. J Neurosci. 2012;32(5):1517-27.
42. Curtis CD, Griffin CT. The Chromatin-Remodeling Enzymes BRG1 and CHD4 Antagonistically Regulate Vascular Wnt Signaling. Molecular and Cellular Biology. 2012;32(7):1312-20.
43. Sun FY, Yang QY, Weng WH, Zhang Y, Yu YC, Hong A, et al. Chd4 and associated proteins function as corepressors of Sox9 expression during BMP-2-induced chondrogenesis. J Bone Miner Res. 2013;28(9):1950-61.
44. Igakura T, Kadomatsu K, Kaname T, Muramatsu H, Fan QW, Miyauchi T, et al. A null mutation in basigin, an immunoglobulin superfamily member, indicates its important roles in peri-implantation development and spermatogenesis. Dev Biol. 1998;194(2):152-65.
45. Satoh K, Satoh T, Kikuchi N, Omura J, Kurosawa R, Suzuki K, et al. Basigin mediates pulmonary hypertension by promoting inflammation and vascular smooth muscle cell proliferation. Circ Res. 2014;115(8):738-50.
46. Betsuyaku T, Kadomatsu K, Griffin GL, Muramatsu T, Senior RM. Increased basigin in bleomycin-induced lung injury. Am J Respir Cell Mol Biol. 2003;28(5):600-6.
47. Shu WG, Lu MM, Zhang YZ, Tucker PW, Zhou DY, Morrisey EE. Foxp2 and Foxp1 cooperatively regulate lung and esophagus development. Development. 2007;134(10):1991-2000.
48. Li SR, Wang Y, Zhang YZ, Lu MM, DeMayo FJ, Dekker JD, et al. Foxp1/4 control epithelial cell fate during lung development and regeneration through regulation of anterior gradient 2. Development. 2012;139(14):2500-9.
49. Kim CF, Jackson EL, Woolfenden AE, Lawrence S, Babar I, Vogel S, et al. Identification of bronchioalveolar stem cells in normal lung and lung cancer. Cell. 2005;121(6):823-35.
50. Sin C, Li HY, Crawford DA. Transcriptional Regulation by FOXP1, FOXP2, and FOXP4 Dimerization. J Mol Neurosci. 2015;55(2):437-48.
51. Ramirez MI, Millien G, Hinds A, Cao Y, Seldin DC, Williams MC. T1alpha, a lung type I cell differentiation gene, is required for normal lung cell proliferation and alveolus formation at birth. Dev Biol. 2003;256(1):61-72.
52. Sansregret L, Nepveu A. The multiple roles of CUX1: Insights from mouse models and cell-based assays. Gene. 2008;412(1-2):84-94.
53. Ramdzan ZM, Nepveu A. CUX1, a haploinsufficient tumour suppressor gene overexpressed in advanced cancers. Nat Rev Cancer. 2014;14(10):673-82.
54. Aufiero B, Neufeld EJ, Orkin SH. Sequence-Specific DNA-Binding of Individual Cut Repeats of the Human Ccaat Displacement/Cut Homeodomain Protein. P Natl Acad Sci USA. 1994;91(16):7757-61.

55. Tufarelli C, Fujiwara Y, Zappulla DC, Neufeld EJ. Hair defects and pup loss in mice with targeted deletion of the first cut repeat domain of the Cux/CDP homeoprotein gene. Dev Biol. 1998;200(1):69-81.
56. Alcalay NI, Sharma M, Vassmer D, Chapman B, Paul B, Zhou J, et al. Acceleration of polycystic kidney disease progression in cpk mice carrying a deletion in the homeodomain protein Cux1. Am J Physiol Renal Physiol. 2008;295(6):F1725-34.
57. Sinclair AM, Lee JA, Goldstein A, Xing D, Liu S, Ju R, et al. Lymphoid apoptosis and myeloid hyperplasia in CCAAT displacement protein mutant mice. Blood. 2001;98(13):3658-67.
58. Luong MX, van der Meijden CM, Xing D, Hesselton R, Monuki ES, Jones SN, et al. Genetic ablation of the CDP/Cux protein C terminus results in hair cycle defects and reduced male fertility. Mol Cell Biol. 2002;22(5):1424-37.
59. Ellis T, Gambardella L, Horcher M, Tschanz S, Capol J, Bertram P, et al. The transcriptional repressor CDP (Cutl1) is essential for epithelial cell differentiation of the lung and the hair follicle. Gene Dev. 2001;15(17):2307-19.
60. Pitsouli C, Perrimon N. The homeobox transcription factor cut coordinates patterning and growth during Drosophila airway remodeling. Sci Signal. 2013;6(263):ra12.
61. Hagey DW, Muhr J. Sox2 Acts in a Dose-Dependent Fashion to Regulate Proliferation of Cortical Progenitors. Cell Rep. 2014;9(5):1908-20.
62. Wat MJ, Enciso VB, Wiszniewski W, Resnick T, Bader P, Roeder ER, et al. Recurrent microdeletions of 15q25.2 are associated with increased risk of congenital diaphragmatic hernia, cognitive deficits and possibly Diamond-Blackfan anaemia. J Med Genet. 2010;47(11):777-81.
63. Yu L, Wynn J, Ma LJ, Guha S, Mychaliska GB, Crombleholme TM, et al. De novo copy number variants are associated with congenital diaphragmatic hernia. J Med Genet. 2012;49(10):650-9.
64. Cadieux C, Kedinger V, Yao L, Vadnais C, Drossos M, Paquet M, et al. Mouse Mammary Tumor Virus p75 and p110 CUX1 Transgenic Mice Develop Mammary Tumors of Various Histologic Types. Cancer Res. 2009;69(18):7188-97.

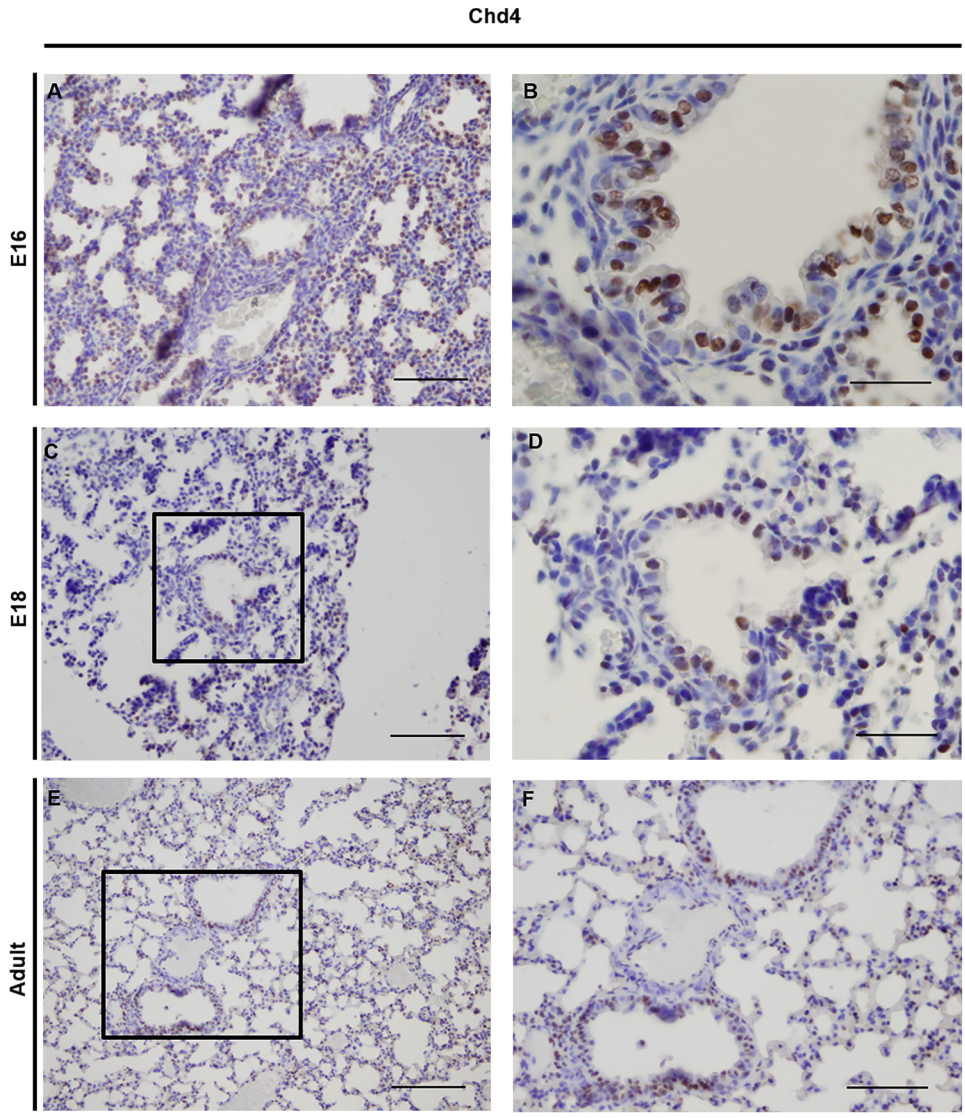

Supplementary figure 1. Endogenous Chd4 expression during lung development in mice. Chd4 is primarily expressed in the conducting airways of the lung at E16 (A, B) and E18 (C, D) and remains expressed in the epithelium of the major airways of the adult lung (E, F). Sections are frontal and scale bars are 10 µm (A, C, E) and 5 µm (B, D, F). Black boxes indicate magnified areas.

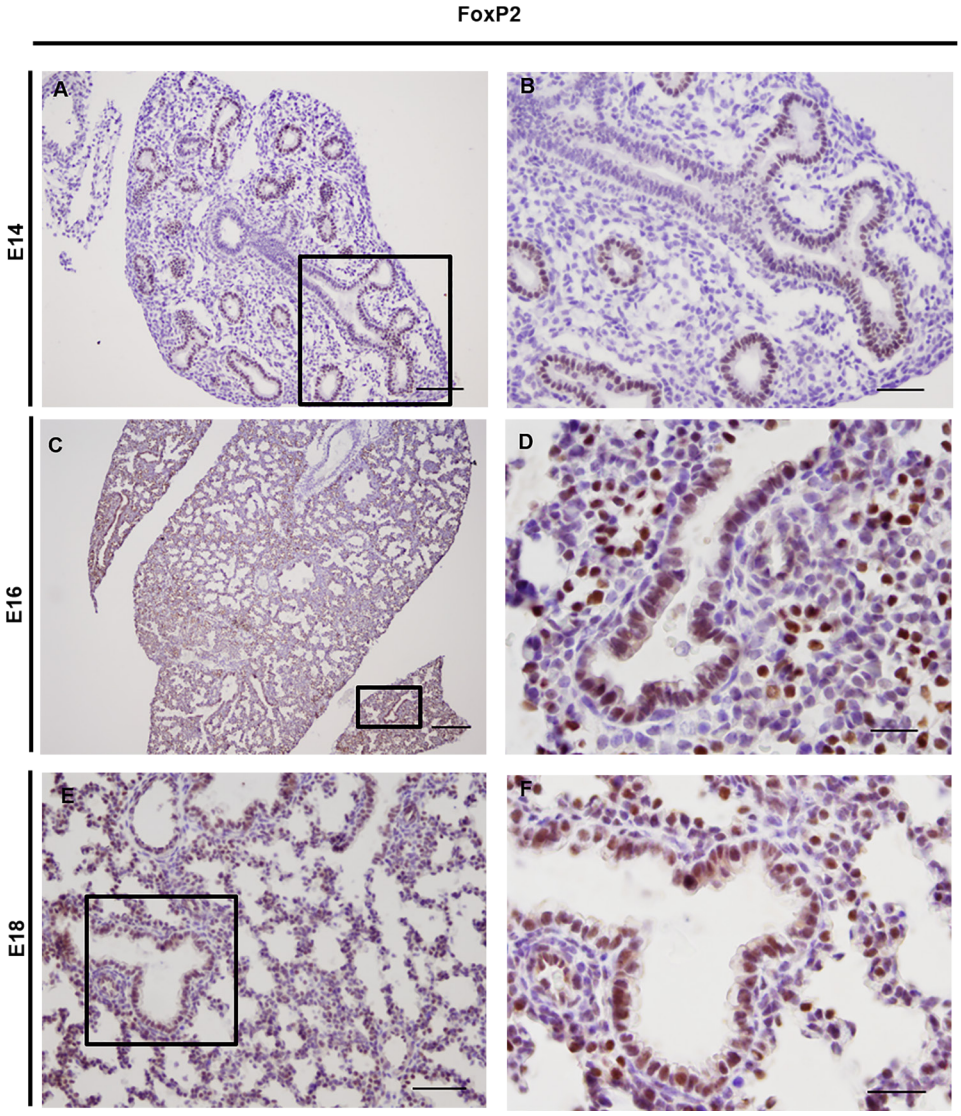

Supplementary figure 2. Endogenous FoxP2 expression during lung development in mice. At E14 (A, D), FoxP2 is expressed in the epithelial cells of the distal developing airways. At E16 (B, E) and E18 (C, F) FoxP2 is exclusively expressed in the distal airway epithelium. Sections are frontal and scale bars are 20 µm (A, C), 10 µm (B) and 5 µm (D, E, F). Black boxes indicate magnified areas.

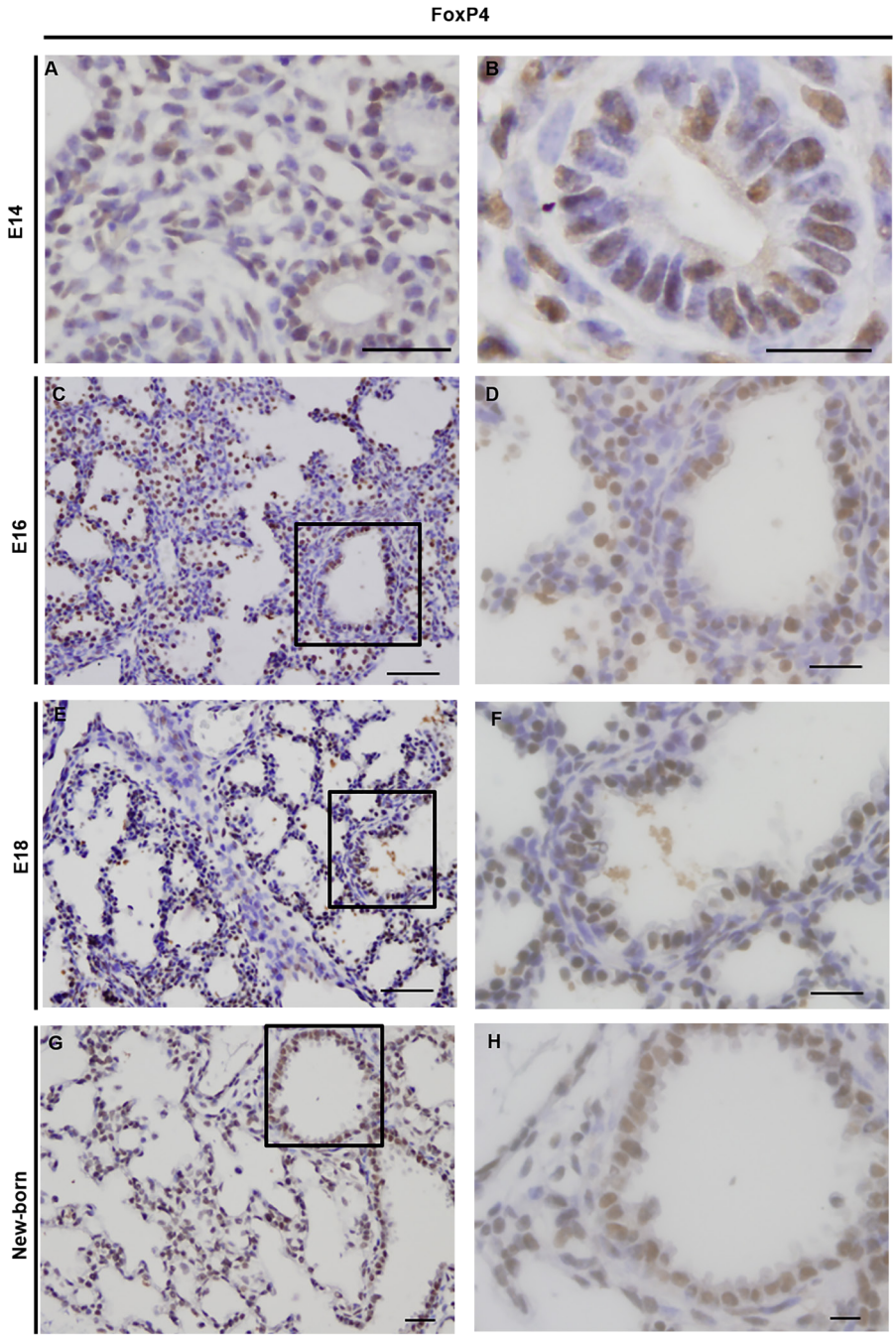

Supplementary figure 3. Endogenous FoxP4 expression during lung development in mice. At E14 (A, B), FoxP4 was expressed in the epithelial cells of both the proximal and distal airways, as well as in the surrounding mesenchyme. At E16 (C,D), this expression becomes more restricted to the epithelial cells and this pattern remains at E18 (E, F) and in new-borns (G, H). Sections are frontal and scale bars are 10 µm (A, C, E, G) and 5 µm (B, D, F, H). Black boxes indicate magnified areas.

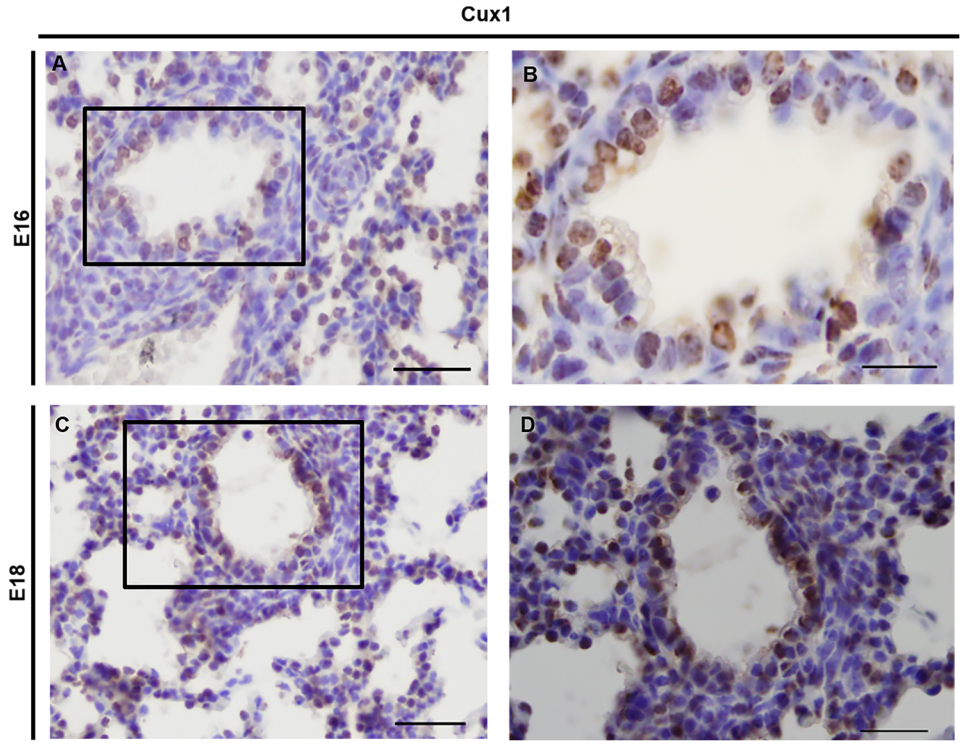

Supplementary figure 4. Endogenous Cux1 expression during lung development in mice. At E16 and E18, Cux1 is expressed in epithelial cells of the conducting airways and surrounding alveolar regions. Sections are frontal and scale bars are 10 µm (A, C) and 5 µm (B, D). Black boxes indicate magnified areas.

Chapter 6.

Regeneration of the lung: Lung stem cells and the development of lung mimicking devices

Kim A.A. Schilders, Evelien Eenjes, Sander van Riet, André A. Poot, Dimitrios Stamatialis, Roman Truckenmüller, Pieter S. Hiemstra and Robbert J. Rottier

Respiratory Research (2016) 17:44

Abstract

Inspired by the increasing burden of lung associated diseases in society and an growing demand to accommodate patients, great efforts by the scientific community produce an increasing stream of data that are focused on delineating the basic principles of lung development and growth, as well as understanding the biomechanical properties to build artificial lung devices. In addition, the continuing efforts to better define the disease origin, progression and pathology by basic scientists and clinicians contributes to insights in the basic principles of lung biology. However, the use of different model systems, experimental approaches and readout systems may generate somewhat conflicting or contradictory results. In an effort to summarize the latest developments in the lung epithelial stem cell biology, we provide an overview of the current status of the field. We first describe the different stem cells, or progenitor cells, residing in the homeostatic lung. Next, we focus on the plasticity of the different cell types upon several injury-induced activation or repair models, and highlight the regenerative capacity of lung cells. Lastly, we summarize the generation of lung mimics, such as air-liquid interface cultures, organoids and lung on a chip, that are required to test emerging hypotheses. Moreover, the increasing collaboration between distinct specializations will contribute to the eventual development of an artificial lung device capable of assisting reduced lung function and capacity in human patients.

Keywords: Lung, Stem cells, Regeneration, Tissue engineering, Lung mimics

Background

Although the lung has a low rate of cellular turnover during homeostasis, it has a remarkable ability to regenerate cells after injury [1]. Disruption of this regeneration potential is the cause of several lung diseases. Therefore, understanding the underlying mechanisms of the regenerative capacity of the lung offers potential in identifying novel therapeutic targets. Much can be learned from studies on lung development as processes involved in the differentiation of cell lineages during development are recapitulated during repair [2]. Recent advances in the identification of new cell markers, the analysis of cell fate by in vivo lineage tracing experiments, the use of embryonic and induced pluripotent stem cells, and improvements in organoid cultures have increased the knowledge about the presence of potential stem cells in the lung [3–6]. The goal of this review is to survey the latest developments in endogenous lung regeneration and bioengineering of lung models for therapeutic applications in the future. We will first provide an overview of the latest insights in lung progenitor cells and their potential to differentiate into lung epithelial cells, which is of interest for the in vivo regeneration of lung tissue. Next, we will discuss the plasticity of the different epithelial cells in the lung and their potential to contribute to epithelial regeneration. Finally, we will highlight the possible clinical applications of this knowledge, focusing on different populations of stem cells, lung mimics and tissue engineering.

Potential epithelial stem cells of the lung

Different subsets of epithelial cells and potential stem cell niches have been identified in the lung. The airways of the human lung are lined by a pseudostratified epithelium made up of basal cells, secretory cells (Scgb1a1$^+$ club cells and goblet cells), ciliated cells and neuroendocrine cells (fig. 1a). The trachea of the mouse, a frequently used model in research, has a similar architecture as the human airways. In human airways, basal cells decrease in frequency from the large to the distal airways [7]. The airways of the mouse and the respiratory smallest bronchioles of the human lung are covered by a cuboidal epithelium. This epithelium lacks basal cells and contains ciliated cells, secretory cells and neuroendocrine cells that are usually clustered in neuroendocrine bodies (NEBs) (Fig. 2a) [8]. The alveoli of both human and mouse are composed of two functional distinct cell types, flat and extended alveolar type I (ATI) cells to allow gas exchange and cuboidal alveolar type II (AT-II) cells for surfactant protein production and secretion (fig. 2a) [2, 9]. New emerging technologies, such as single cell RNA-sequencing and proteomic analysis, revealed molecular signatures that hint at different subpopulations of type I and type II cells. It remains to be seen whether such signatures reflect functionally different cell types, or that it represents similar cells at physiologically or metabolically different phases. However interesting, this is not the focus of this review, and therefore we only refer to the current literature [10–12].

Basal-like stem cells: the stem cells of the epithelium

Basal cells are being characterized by the expression of Trp63, Ngfr, podoplanin (Pdpn, also known as T1α), GSIβ4 lectin and cytokeratin5 (Krt5). They have the capacity to self-renew and to form secretory and ciliated cells (fig. 1b) [13–15]. Notch signaling plays a major role in determining the differentiation of basal cells to either the secretory lineage or the ciliated lineage [15–17]. A small subset of the basal cells (<20 %) expresses Krt14 under

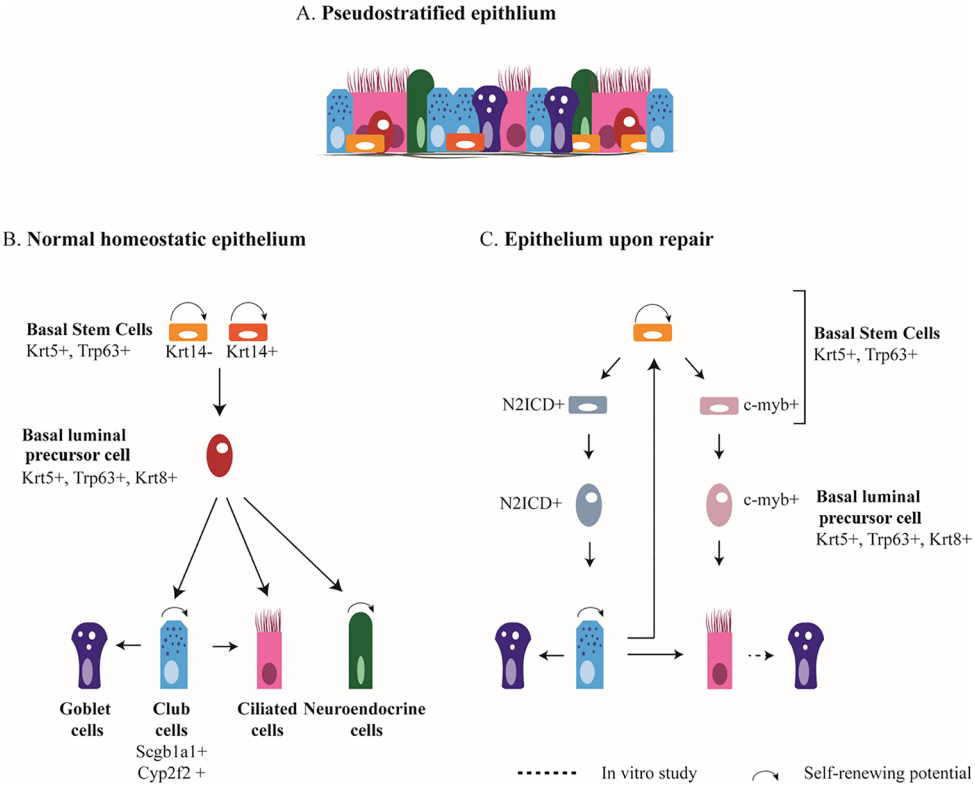

Figure 1. Regeneration of pseudostratified airway epithelium of the lung. A) The airways are lined by a pseudostratified epithelium consisting of secretory cells (goblet and club cells), ciliated cells, neuroendocrine cells and basal cells. Goblet cells are abundant in the human epithelium, but are rare in mice. B) The relationship between the different epithelial cells during normal homeostasis. The basal cells are progenitor cells of the pseudostratified epithelium which are heterogeneous for the expression of Krt14. The basal cell becomes a Krt8 positive luminal precursor cell before further differentiation. A basal cell differentiate into secretory cells and neuroendocrine cells under homeostatic conditions. Neuroendocrine cells are also capable to self-renew [168]. Scgb1a1^{+} secretory cells are a self-renewing population and can give rise to ciliated cells. In homeostatic epithelium, there is a very low turnover of cells. It is likely that the dividing secretory cell population is sufficient to regenerate ciliated cells in homeostatic condition. However, their generation from basal cells is not excluded. Upon allergen exposure, secretory cells are the main source of goblet cells [169], but it is unknown whether basal cells can directly differentiate into goblet cells. C) Upon depletion of luminal cells by SO_2 exposure, basal cells proliferate and subdivide into two populations, N2ICD and c-myb positive, respectively, differentiating into secretory and ciliated cells. After the loss of basal cells, secretory cells (de)differentiate into functional progenitor basal stem cells. In a normal pseudostratified epithelium, only a few scattered goblet cells are present. Increases in goblet cells are observed upon immune stimuli and in diseases like COPD. Lineage tracing studies show that goblet cells can arise from Scgb1a1^{+} secretory cells and recently a trans-differentiation of foxj1^{+} ciliated cells to goblet cells was observed upon smoke exposure in culture.

homeostatic conditions. These cells are thought to be a self-renewing population involved in maintenance of the Krt5$^+$ basal cell population. This proportion is highly increased and becomes multipotent after naphthalene induced depletion of secretory cells [18, 19]. Lineage tracing studies show that Krt14$^+$ cells can directly regenerate secretory and ciliated cells [18, 20]. Recently, two distinct populations of basal cells were identified in the adult lung using long-term lineage tracing experiments and single-cell gene expression profiling: basal stem cells (BSCs) and basal luminal precursor cells (BLPCs). Both cell types are Krt5$^+$ and Trp63$^+$ with rare detection of Krt14, indicating that Krt14 is not a robust marker for stem cell identity [21]. However, the rapid up-regulation of Krt14 post-injury suggests that Krt14 may be an important marker to identify activated stem cells in the regenerating epithelium. Within homeostatic conditions, BSCs divide via asymmetric division to produce one new BSC and one BLPC, which can further differentiate into a neuro-endocrine and secretory cell (fig. 1b). The BLPCs have a low or negligible rate of self-amplification, lack any overt signs of differentiation, and are distinct from BSCs by their expression of Krt8 [21]. This model is consistent with a previous observation in human basal cells addressing the potential of individual basal cells to self-renew and differentiate [22]. Additionally, the emergence of a Krt5$^+$/Krt8$^+$ parabasal cell population, which have comparable characteristics as the previously described BLPCs, was shown to be controlled by active Notch3 signaling [16]. Notch3$^{-/-}$ mice showed an increase in basal cells and parabasal cells, but not in multiciliated and secretory cells, suggesting that Notch3 is involved in restricting the expansion of the basal and parabasal population [16]. Interestingly, binding of the transcription factor Grainyhead-like 2 (Grhl2) to the promotor region of Notch3 was observed, suggesting a role for Grhl2 in the transcription of Notch3 [23]. BSC-specific ablation of Grhl2 showed only a decrease in the number of ciliated cells, but no other changes in the morphology of the epithelium [24]. Whether Grhl2 is important in the Notch3 dependent regulation of the BSC and parabasal cell population still has to be explored. Krt8$^+$/Krt5$^+$ double positive cells were previously identified in mice as a marker for progenitor cells upon regeneration following injury induced by reactive oxygen species and sulfur dioxide (SO2) [15, 25]. Interestingly, using the SO2 injury model, it was observed that Trp63$^+$ basal cell populations segregate in subpopulations prior to the formation of the Krt8$^+$ progenitor cell. These dividing Trp63$^+$ basal stem cell populations are either N2ICD$^+$ (the active Notch2 intracellular domain) cells that differentiate into mature secretory cells, or c-myb$^+$ cells that differentiate into ciliated cells (Fig. 1c) [26]. This specific segregation of progenitor cells was not found in homeostatic epithelium, which indicates that post-injury mechanisms may lead to different subsets of progenitor cells compared to the homeostatic epithelium [26]. A new study shows Trp73 as a regulator of ciliated cell differentiation, which expression was observed in terminally differentiated ciliated cells as well as in Trp63$^+$ basal cells. This indicates a direct transition from basal cell to ciliated cell as well as a segregation of epithelial cell fate at the basal cell level [27]. The role for Trp73 in response to damage and the trigger that is responsible for a Trp73$^+$ basal cell to initiate ciliated cell differentiation is not yet studied. This would be essential in understanding the role of Trp73 in the Trp63$^+$ basal cell population.

Clusters of Trp63$^+$/Krt5$^+$ cells, called distal alveolar stem cells (DASCs), are present in the distal airways after H1N1 influenza virus infection and have the capacity to replace injured alveolar cells (Fig. 2b) [28, 29]. Despite sharing similarity in markers, the tracheal basal stem cells (TBSCs) and DASCs show different fates in culture and in vivo transplantation.

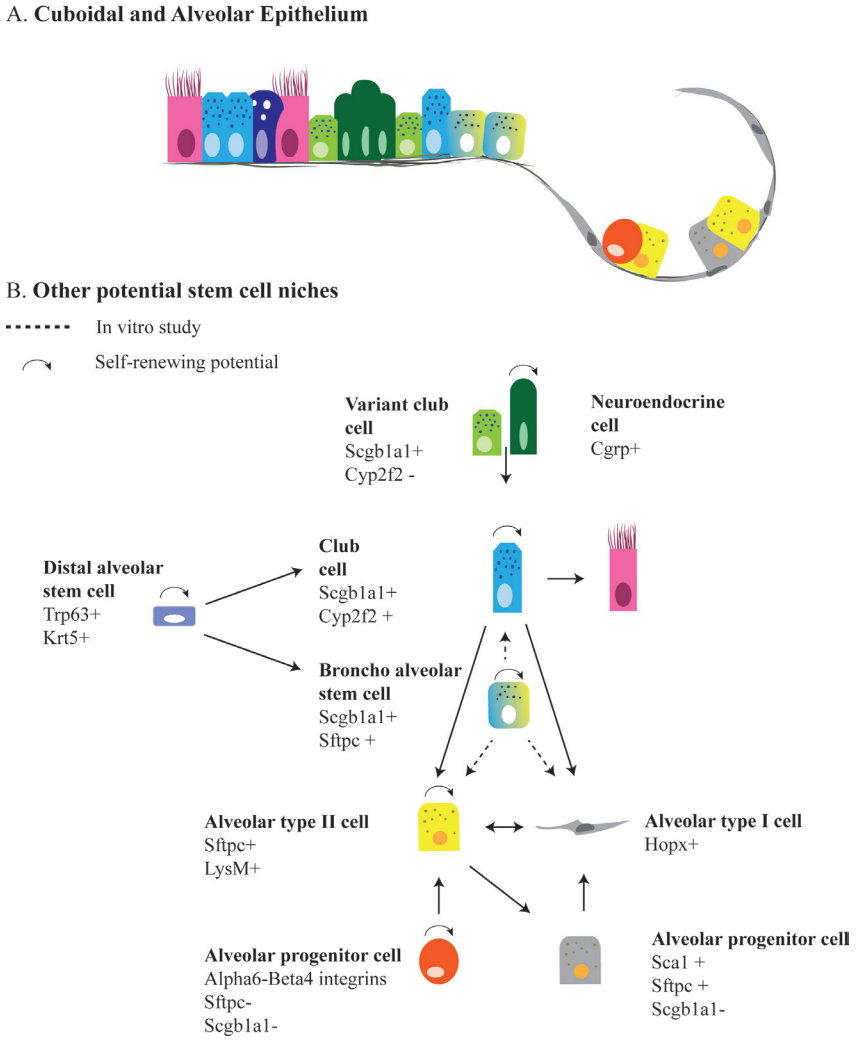

Figure 2. Regeneration of distal and alveolar airway epithelium after injury. A) The small airways lack basal cells and consist of cuboidal epithelium, containing secretory and ciliated cells, as well as clusters of neuroendocrine cells. The cuboidal epithelium passes into a broncho-alveolar duct junction which is the niche of broncho-alveolar stem cells. The alveolar epithelium consists of alveolar type I, type II cells and alveolar progenitor cells. B) Variant club cells ($Cyp2f2^-$) are a variant of secretory cells that survive naphtalene injury and give rise to $cyp2f2^+$ club cells. Lineage tracing of $Cgrp^+$ cells showed that after depletion of club cells by naphtalene injury neuroendocrine cells contribute to the regeneration of these cells. At the broncho-alveolar duct junction, broncho-alveolar stem cells were isolated and shown to differentiate into bronchiolar and alveolar lineages in culture (dashed lines). $Scgb1a1^+$ cells have the potential to form alveolar type I and type II cells after bleomycin injury, but not after hyperoxia-induced injury (dashed line). AT-II cells can self-renew and differentiate to AT-I cells. After pneumonectomy, a contribution of AT-I cells to regenerate AT-II cells was observed. An alveolar progenitor cell expressing α6-β4 integrins can regenerate AT-II cells after injury. Yet another cell type was identified expressing $Sca1^+$ arising from AT-II cells and regenerating AT-I cells. Distal alveolar stem cells appear after severe injury and give rise to secretory and alveolar cells.

The TBSCs give rise to more proximal epithelium both in culture and in vivo, while the DASCs can form alveolar spheres in vitro and give rise to alveolar cells and secretory cells in vivo [29]. Krt5 lineage tracing studies concluded that these cells were not present before infection and were generated as a response to injury [29]. In addition to this finding, Vaughan and colleagues proposed a lineage negative epithelial precursor (LNEP) cell expressing $Trp63^+$ and $Krt5^+$ that helps to regenerate the alveoli after bleomycin injury. Transcriptional profiling of these cells indicate a very heterogeneous population suggesting that different cell types are present in the $Trp63^+/Krt5^+$ population [30]. Moreover, active Notch signaling was required to activate $Trp63^+/Krt5^+$ expression in LNEPs and active Notch prevents the further differentiation into AT-II cells [31]. This suggests that the hyperactive Notch signaling observed in lung diseases possibly contributes to failure of regeneration. In conclusion, basal cells can function as tissue-specific stem cells of the airway epithelium, but the heterogeneity in the population of basal cells is not yet completely understood. Since the identification of different subsets of basal cells is studied using lineage-tracing studies in mice, validation of these subsets of basal cells in human lung is of importance. Differences in progenitor populations are found in homeostatic epithelium compared to damaged epithelium. This suggests that in response to injury, molecular mechanisms are triggered that lead to the appearance of different subsets of epithelial progenitor cells, perhaps derived from one general homeostatic basal cell. Currently, signaling pathways are being identified that influence the expansion of basal cells and differentiation into specific cell types, but the precise underlying molecular mechanisms still need to be identified (table 1). Furthermore, it is increasingly recognized that basal cells not only contribute to tissue repair, but are also a target for respiratory pathogens and contribute to host defense against infection [32]. Further studies, including those aimed at identifying subsets of basal cells that display these properties, are needed to better understand the link between this immune basal cell response and repair of the epithelium.

Table 1 Overview Basal-like Stem Cell Populations

Cell type	Subtypes	Differentiation potential	Signaling Cues
(Tracheal) Basal Stem Cells	Trp63, Krt5, $Krt14^{+/-}$	Self-Renewal	Notch [25], Hippo signaling [44]
	Trp63, Krt5, Krt8	Basal Luminal Precursor Cell	Notch 3 signaling [16], Grhl2[24]
		Neuroendocrine	Notch1[164, 165] and Hes1[166]
	Trp63, Krt5, N2ICD	Club	$Notch^{high}$ signaling [15], Notch1 [167], Notch2 [164]
	Trp63, Krt5, c-Myb / Trp73	Ciliated	$Notch^{low}$ signaling [15], Notch 1 and 2 [164]
Distal Alveolar Stem Cells *	Trp63, Krt5	Self-Renewal	Increased Notch activity, Notch1 [31]
		AT-II Club	Inhibition of Notch [31]

*Only observed after H1N1 influenza virus infection or bleomycin induced injury, AT-II=Alveolar Type II Cells

Other epithelial progenitor cells

Basal cells are not the only identified multipotent cells in the lung (Table 2). Variant club cells, a subset of secretory cells that are positive for secretoglobin family 1a member 1 (Scgb1a1) and negative for Cyp2f2, have been shown to self-renew and to differentiate into Cyp2f2$^+$ secretory cells after naphthalene injury [3, 33, 34]. Interestingly, another subset of Scgb1a1$^+$ cells co-expressing the AT-II marker surfactant protein C (Sftpc) was shown to differentiate into bronchiolar and alveolar lineages in vitro. These cells were called broncho alveolar stem cells (BASCs) and are located at the broncho-alveolar duct junction (BADJ) (fig. 2b) [35]. However, conflicting results are reported based on lineage tracing of Scgb1a1$^+$ cells after lung injury. Scgb1a1$^+$ cells differentiate into alveolar epithelial cells after influenza and bleomycin-induced injury, but not after hyperoxia-induced alveolar injury [34, 36]. This contradiction could result from different subsets of cells being labeled by the Scgb1a1-driven Cre driver, or from the activation of different pathways by hyperoxia and bleomycin. Cell-specific lineage tracing tools are required to give more clarity about the potential of BASCs and the variant club cells.

Table 2 Other Potential Epithelial Stem Cells

Cell type	Marker genes	Differentiation potential	Hallmarks
Variant Club Cells	Scgb1a1$^+$, Cyp2f2$^-$	Club, Ciliated Ciliated	Located near NEBs Survive Naphthalene injury
Broncho-Alveolar Stem Cells	Scgb1a1$^+$, Sftpc$^+$	AT-II, Ciliated	Wnt signaling induces proliferation BASC [168] Located at BADJ
Itgα6$^+$, Itgβ4$^+$Alveolar progenitor	Scgb1a1$^-$, Sftpc$^-$, Itgα6$^+$, Itgβ4$^+$	AT-II, Club	Located at BADJ and alveolar wall
AT-II	Sftpc+, LysM	Sca1$^+$, Sftpc$^+$ AT-I progenitor cell AT-I	EGF induced proliferation [37] Wnt dependent conversion to AT-I [41]

NEBs=Neuroendocrine Bodies, BADJ=Broncho-Alveolar Duct Junction, AT-I/II = Alveolar-Type I/II cells

Different alveolar progenitors and associating markers have been identified in response to lung injury and are summarized in figure 2b. AT-II cells expressing Sftpc are capable of self-renewal and a small fraction of mature type II cells can differentiate into AT-I cells in homeostasis and after injury [37, 38]. Besides the progenitor potential of AT-II cells, another progenitor subpopulation for alveolar epithelial cells has been identified. These cells co-express α6 andβ4 integrins, but lack expression of Scgb1a1 or Sftpc. They respond to lung injury and can differentiate into AT-II cells and club cells. These cells reside in the alveoli as well as in the BADJ and their differentiation potential in vivo is most likely restricted by their niches [39]. Furthermore, a distinct population of Sca1$^+$/Sftpc$^+$ AT-II cells appeared at the onset of repair after infection of the lung by Pseudomonas aeruginosa intratracheal instillation [40, 41]. Most of these cells were negative for β4 integrin, Trp63 and Scgb1a1, separating them from respectively other distal progenitor cells and BASCs [28, 35, 39, 41]. Lineage tracing experiments showed that Sca1$^+$ AT-II cells may arise from Sftpc$^+$/Scgb1a1$-$ cell and further differentiate into AT-I cell (fig. 2b). This conversion of Sca1$^+$ AT-II cells to AT-I cells depends on an active Wnt/β-catenin pathway [42]. Taken together, several populations are being marked as progenitor cells and the activity of subsets of progenitor

populations seems to depend on their niches and kind of epithelial damage. The current challenge is to elucidate whether the different progenitor cells are indeed different cells, or if these cells are variants of a single precursor cell that are induced by different damaging agents. Single-cell RNA sequencing of the developing distal lung epithelium has helped in defining more precisely the different types of (progenitor) cells in the distal region of the developing lung [12]. A similar approach during regeneration of the proximal and distal lung epithelium might provide additional clues on the heterogeneity of epithelial cells upon repair.

Plasticity of the lung

Further complexity and challenges in lung regeneration are generated by the plasticity of differentiated cells (Table 3). Independent studies have pointed at the potential of Scgb1a1$^+$ secretory cells to dedifferentiate into Trp63$^+$/Krt5$^+$ basal cells upon depletion of the basal cell lineage or after damage of the lung epithelium [14, 43]. These dedifferentiated basal cells have the full capacity to redifferentiate into ciliated or secretory cells (fig. 1c). The Hippo pathway and its down-stream effector Yap are required for the dedifferentiation of secretory cells [44]. Moreover, Yap has been shown to regulate stem cell proliferation and differentiation during normal epithelial homeostasis and regeneration upon injury in the adult lung [44, 45]. Further research showed that the nuclear-cytoplasmic distribution of Yap is important in the differentiation of adult lung epithelium and during development [16, 46]. Thus, Hippo signaling may be important in stimulating regeneration of the pseudostratified epithelium by controlling basal stem cell differentiation as well as luminal cell plasticity.

Table 3 Plasticity of Differentiated Cells

Cell type	Marker genes	Differentiation potential	Signaling Cues
Club cells	Scgb1a1$^+$, Cyp2f2$^+$	Basal	Hippo pathway [44]
		Ciliated	Unknown
		Goblet	IL-13 exposure [169]
AT-I	Hopx	AT-II	Modulated by TGF-β signaling [49] Proximal cell fate by overexpressing Sox2 [51]
AT-II cells	Sftpc$^+$, LysM	Proximal cells	Ectopic Sox2 expression [50]
Ciliated cells	TubIVa, Foxj1	Goblet	IL-13 exposure[47]

AT-I /AT-II = Alveolar type-I/II Cell

Differentiation of Foxj1$^+$ ciliated cells to mucus producing goblet cells was observed in human primary bronchial epithelial cell culture after exposure to IL-13, an important mediator in asthma [47]. Interestingly, this plasticity was not confirmed by a Foxj1$^+$ lineage tracing study in mice using an ovalbumin-induced injury model [48]. Either the difference of damage to the epithelium, smoke versus ovalbumin, or the use of different species could account for the different outcomes.

Previous lineage tracing studies using lysozyme M as marker for mature AT-II cells already demonstrated that AT-II cells can differentiate into AT-I cells [37]. More recently, a plasticity AT-I cells after pneumonectomy has been shown. To regenerate the alveoli, Hopx$^+$ AT-I cells

proliferate and differentiate into Sftpc$^+$ AT-II cells (Fig. 2b) [49]. The formation of AT-II cells from Hopx$^+$ AT-I cells in organoid culture seems to be modulated by TGF-β signaling [49]. These results suggest a bi-directional transition between the two types of mature alveolar cells. However, after pneumonectomy the contribution of AT-I cells to regenerate AT-II cells is small (~10 %). Vice versa, approximately 16% of regenerated AT-I cells are derived from Sftpc$^+$ ATII cells, indicating that other cell sources also contribute to re-alveolarization [49]. Thus, strategies for regeneration of lung epithelium in disease, includes targeting of progenitor cell populations and activating the plasticity or fate of differentiated lung cells. Signaling cues to induce endogenous lung regeneration are starting to be identified and might be targets for disease therapies in the future. In line with initiating differentiation through signaling, it has been demonstrated that conversion of a specific cell type can be induced by changing the expression of a single protein. Ectopic expression of Sox2 in AT-II cells changed its alveolar cell type to a more proximal cell fate expressing Scgb1a1 and Trp63, even though the cells remained in the niche for distal cells [50]. A similar approach was used to show the plasticity of AT-I cells, where overexpression of Sox2 was sufficient to reprogram AT-I cells towards a proximal airway cell fate with expression of Trp63 [51]. The differentiation potential and plasticity of the lung epithelial cells as described in the above sections are illustrated in figure 1 and 2 to show the complexity of the cells involved in regenerating the lung epithelium.

Regenerative medicine

Drugs to induce lung regeneration

Different signaling pathways are involved in either maintaining a quiescent homeostatic or inducing a proliferating regenerating epithelium [3]. Signaling consists of cross-talk and feedback loops between epithelial cells but also between epithelial and mesenchymal cells. Such interplay between mesenchymal and epithelial cells is for example important in Hedgehog (Hh) signaling. In the adult lung, Hh signaling balances between stimulating proliferation and quiescence. In the homeostatic lung Hh signaling is active to maintain quiescence, however upon injury Hh signaling is inhibited to stimulate epithelial proliferation [52]. A shift in the balance can lead to failure of repair but can also play a role in promoting tumorigenesis [52, 53]. Several pathways involved in lung development and regeneration are relevant in lung disease, and drugs that either inhibit or induce these pathways could have a beneficial effect for patients. Recently, it was shown that deletion of Notch3 leads to an expansion of basal cells, a hallmark of smokers and individuals with chronic obstructive pulmonary disease (COPD) [16, 54, 55]. Interestingly, Notch3 downregulation was observed in smokers and in COPD lung, making it a potential target for controlling the balance between basal and luminal cells [16, 56] Candidate pathways for targeting in COPD include Hedgehog signaling, Notch signaling, the retinoic acid pathway and the transforming growth factor-β (TGF-β) pathway [57]. The TGF-β pathway, as well as bone morphogenetic proteins (BMPs), growth differentiation factors and activins are also linked to asthma and these pathways could be potential drug targeting candidates [58]. In COPD there is mucus hypersecretion, and there are several ongoing studies that examine the effect of already marketed drugs on the production and secretion of mucus in COPD models [59]. Recently, it was shown that interference of Notch signaling with specific antibodies against the ligands Jag1 and Jag2 results in an increase in ciliated cells at the expense of club cells [60]. Moreover, jagged inhibition also reversed goblet cell hyperplasia, which could potentially be important in COPD patients to reduce the mucus production

and to increase clearance by the ciliated cells. Fibroblast growth factors (FGFs) also play a role in regeneration of several tissues including the lung [61]. FGF1 and FGF2 are thought to play a role in the protection of epithelial stem cells and lung maintenance, and are linked to pulmonary hypertension. FGF1 is also thought to play a role in idiopathic pulmonary fibrosis. FGF7 and FGF10 are involved in lung regeneration and several different injury models show that these FGFs are important for repair of the lung. Several recombinant FGFs (FGF1, FGF2) and truncated forms of FGFs (FGF7, FGF10) are already used in clinical applications, like angiogenic therapies, coronary heart disease and treatment of ulcers [61]. Although these therapies are not yet available for lung diseases, there may be some future perspectives, either in inducing or inhibiting pathways involved in disease or by activation of endogenous lung progenitor cells.

Stem cells

Stem cells are functionally characterized by their undifferentiated state and their properties of self-renewal and pluripotency to become specialized cells. Because of these characteristics, they are appealing to be used for the regeneration of damaged tissue. A distinction can be made between embryonic stem cells (ESCs) and adult stem cells. ESCs are derived from the inner cell mass of the blastocyst and these cells have the ability to differentiate into ectodermal, mesodermal and endodermal cell types. Human ESCs could be useful to study early embryonic development, for cell replacement therapy, to study disease pathways, and for drug discovery, although ethical and therapeutic issues hamper the use of these cells. Besides ESCs, several types of adult stem cells throughout the human body exist, like hematopoietic stem cells, intestinal stem cells, mammary stem cells, olfactory stem cells, mesenchymal stem cells, endothelial stem cells, and neural stem cells. Adult stem cells are also capable of self-renewal and may differentiate into several cell types, but their differentiation potential is more restricted [62–64]. As indicated, there is accumulating evidence that differentiated cells show more plasticity than previously thought. Moreover, the number of different progenitor cells in the lung is higher than previously expected, depending on the type of injury or disease.

Induced pluripotent stem cells

In 2006, the group of Yamanaka introduced a method to generate cells with properties similar to ESCs [65]. These so-called induced pluripotent stem cells (iPSCs) are somatic cells that are reprogrammed into a multipotent stem cell-like stage using only four different factors: Oct4, Sox2, cMyc and Klf4 (Yamanaka factors) [64]. Culturing these cells under distinct conditions induces several specialized cell types. iPSCs can be used for numerous applications, like disease modeling, regenerative medicine, drug discovery, and toxicity studies [64, 66].

The lung is a very complex organ that consists of many different specialized cell types, which makes it challenging to generate human airway and alveolar epithelial cells from iPSCs. First, definitive endoderm should be derived from human iPSCs (hiPSCs), followed by generation of anterior foregut endoderm [67]. From this anterior endoderm, lung endoderm can be derived, which can subsequently be guided towards bronchial progenitor cells ($Sox2^+$) or alveolar progenitor cells ($Sox9^+$), and finally towards bronchial or alveolar epithelial faith [64]. Several studies have shown the differentiation of ESCs and iPSCs into AT-II cells [68–73]. Other groups have shown the differentiation of iPSCs into multiciliated

cells [74], mature airway epithelium expressing functional CFTR protein [75], multipotent lung and airway progenitors [76], purified lung and thyroid progenitors [77], purified distal lung alveolar epithelium [78], lung and airway epithelial cells [79], and lung and airway progenitor cells [80]. An overview of these differentiation protocols is given by Ghaedi and co-workers, although optimization is clearly required before these cells may be used in clinical applications [64].

iPSCs may be used for the generation of patient specific disease models and (large scale) drug screening, as shown for example with cells derived from patients suffering from cystic fibrosis [81]. A more clinical use of iPSCs in lung disease therapy is not yet approved and more knowledge is necessary before this will be applicable [82].

Mesenchymal stem cells

Mesenchymal stem/stromal cells (MSCs) are adult stem cells that have the potential to differentiate into cells derived from the mesoderm lineage. MSCs were first derived from bone marrow, but many other sources are reported, including umbilical cord blood, placenta, skin, liver and brain [83, 84]. MSCs refer to a heterogeneous population of cells, making it difficult to isolate them. Therefore, MSCs are defined by a number of criteria based on the expression of specific cell surface antigens and their functionality. Cells should express CD75, CD90 and CD105, but not CD34, CD45, HLA-DR, CD11b, CD19 and CD14. MSCs should be capable to differentiate into chondrocytes, osteoblasts and adipocytes, and should adhere to plastic for stable cell culture [62, 83–85]. Recent studies have shown that MSCs may differentiate in other cell types, including lung cells, although this is still controversial [86, 87]. It has been reported that MSCs can also be isolated from the lung. Martin et al. reported the isolation of MSCs from tracheal aspirates of neonates and from adult broncho-alveolar lavage [88]. More recently, Gong and co-workers isolated lung resident MSCs and showed that these cells have the potential to differentiate into AT-II cells [89]. MSCs derived from other sources than the lung can also be differentiated into alveolar epithelium. These alveolar cells were generated from MSCs derived from human umbilical cord blood by culturing them in lung-specific differentiation media [87].

There are many completed and ongoing clinical trials using MSCs for applications in the nervous system, heart, liver and kidney. In lung disease, therapies with MSCs could be useful in bronchopulmonary dysplasia (BPD), COPD, acute respiratory distress syndrome and idiopathic pulmonary fibrosis [62, 83, 85, 90, 91]. However, given the low percentage of engraftment of the instilled MSCs as demonstrated in animal models, it is very likely that the beneficial effects of MSC therapy are not due to the differentiation potential of MSCs itself, but rather due to paracrine and immunomodulatory effects [83, 92–94].

Endothelial progenitor cells

There are two different subsets of endothelial progenitor cells (EPCs), proangiogenic hematopoietic cells and endothelial colony-forming cells (ECFCs) [95]. Proangiogenic hematopoietic cells are derived from the bone marrow and are involved in vascular repair. It is thought that these cells circulate to injury sites and there facilitate formation of new vessels using paracrine mechanisms, but lack direct vessel-forming ability. ECFCs are rare circulating blood cells that have the potential to generate cells that express genes from the endothelial lineage. They also have the potential to form blood vessels in vivo [95].

There is increasing evidence that EPCs are involved in several lung diseases, including COPD, BPD and pulmonary hypertension. Several lung injury animal models have shown (partial) reversal of the induced phenotype by systemic administration of EPCs, including improvement of pulmonary function and repair of the alveolar and vascular structure of the lung [96–98]. These therapeutic effects could be caused by structural conditions of the cells, by paracrine effects or by a combination of both [82]. The interaction between the pulmonary vasculature and the airways is important for proper growth and regeneration of the lung (reviewed in [99]). This was recently supported by the identification of endothelial derived angiocrine signals promoting alveolar regeneration after pneumonectomy [100, 101]. The interactions between the vasculature and epithelial cells upon repair are still elusive, but the identification of signaling molecules, like stromal cell-derived factor-1 (SDF-1), may be important for potential therapies. Systemic administration of EPCs has shown to be beneficial in patients with primary pulmonary hypertension [102, 103]. Several pre-clinical and clinical trials are ongoing to test the potential of using EPCs in lung disease therapies [82].

Besides the stem cells mentioned in this section, there are also endogenous lung progenitor cells that were discussed in previous sections. All these different stem/progenitor cells are potentially targets for therapeutic strategies. While MSCs and EPCs could be effective because of their paracrine effects, iPSCs could be useful in the development of lung mimics and tissue engineering. Pathways involved in differentiation of lung progenitor cells to other cell types and plasticity of these cells, could be induced or inhibited by medication to induce lung regeneration.

Lung mimics

Most studies on cell biology and tissue regulation are based on 2D cell-culture models. Although these models are valuable to answer specific scientific questions, it is clear that these models have limitations and fail to reconstitute the in vivo cellular microenvironment. Therefore, 3D cell-culture models were developed, which mimic a more realistic tissue and organ-specific micro-architecture, although some aspects, including tissue-tissue interfaces and a mechanically active microenvironment are still missing. However, these models are very useful in patient-specific disease models, drug-screening and as a source of cells for transplantation [104].

Air-liquid interface cultures

Air-liquid interface (ALI) cultures mimic a more realistic lung environment and make it possible for airway epithelial cells to proliferate and differentiate in vitro. Whitcutt et al. were the first to demonstrate mucociliary differentiation using ALI cultures [105]. Culturing human airway epithelial cells from patients, makes it possible to conduct patient-specific research and drug-screening, for example in cystic fibrosis and asthma [106, 107]. ALI cultures were also used to model the effects of smoke exposure on epithelial cells, which could be used to gain more insight in mechanisms involved in the pathogenesis of COPD [108, 109]. In 2015, a new computer-controlled ALI culture system was introduced in order to generate more stable and comparable cultures, which may be useful for large-scale toxicology studies [110].

Organoids

The concept of stem cell-derived organoids has already been discovered in the 1950's [111]. Organoid models use the pluri- or multi-potent properties of stem cells to differentiate into specialized cell types and to self-organize into a 3D structure with organor tissue-specific morphogenetic and histological properties [112–114]. Overviews of tissues and diseases modeled with organoids have been topics of recent reviews [113–115]. These tissues include intestinal buds, liver bud derivatives and retinal derivatives. In the intestine, single $Lgr5^+$ stem cells can be isolated and grow into intestinal organoids [116]. Generation of lung organoids from one single stem cell have not been reported yet, but several studies have reported the generation of lung organoids derived from human pluripotent stem cells (hPSCs), primary respiratory cells and cell lines (reviewed in [117]). These organoids include trachea/bronchospheres [15, 118–120], bronchiolar organoids [121], bronchioalveolar organoids [120, 121], alveolospheres [38, 120, 121], branching structures [122–124], alveolar spheroids [125] and multi-lineage organoids [126]. In 2015, Dye et al. established a protocol to successfully generate lung organoids derived from hPSCs (embryonic and induced). hPSCs were first differentiated into anterior foregut spheroids, using ActivinA, BMP and TGF-β inhibitors. This anterior foregut endoderm was subsequently induced into a lung lineage by modulating FGF and Hedgehog signaling. In this way, the foregut spheroids gave rise to lung organoids. These organoids possess both proximal airway-like structures and immature alveolar airwaylike structures and are globally similar to fetal human lung. These human lung organoids can be used to study lung development and regeneration [127]. Previously, tracheospheres were used to show the capacity of basal cells to self-renew and the potential to form secretory and ciliated cells [13]. Jain et al. used organoid cultures to show the potential of $Hopx^+$ AT-I cells to form AT-II cells [49]. Furthermore, application of the Clustered Regularly Interspaced Short Palindromic Repeats/Crispr associated protein (CRISPR/Cas) system in organoid culture might be a method to identify important players in epithelial cell differentiation. Recently, this approach was used to identify the role of transcription factor Grhl2 in the differentiation of ciliated cells [24]. In the future, the loss or gain of function by manipulation of genes in culture, will lead to more insight in potential stem cell populations in the lung. Organoids are very useful to answer specific questions about lung development and regeneration, but so far they are not exposed to air, resulting in incomplete differentiation of adult airway cells. Furthermore, it does not allow to expose organoids to air pollutants such as toxic gasses and micro- or nanoparticles, making it impossible to use them to study the effects of air pollutants on the airway epithelium.

Lung-on-a-Chip

Organs-on-chips refer to bioengineered devices that mimic tissue properties and functions in a well-controlled environment [112]. Additionally, there are also (acellular) lung-mimicking microfluidic devices not specifically to study lung biology, but as respiratory assist devices or oxygenators [128]. Over the past decade, several micro-engineered organ models have been developed to study liver, kidney, intestine, and heart, among others [129]. The first lung-on-a-chip was introduced by Huh and co-workers, which mimicked the vascular-alveolar structure by using lung epithelial cells exposed to air on one side and pulmonary vascular endothelial cells exposed to flowing culture medium on the other side of a permeable synthetic membrane (fig. 3, [130]). This model incorporated a microfluidics system and applied mechanical stress, and as such was capable of mimicking gas exchange.

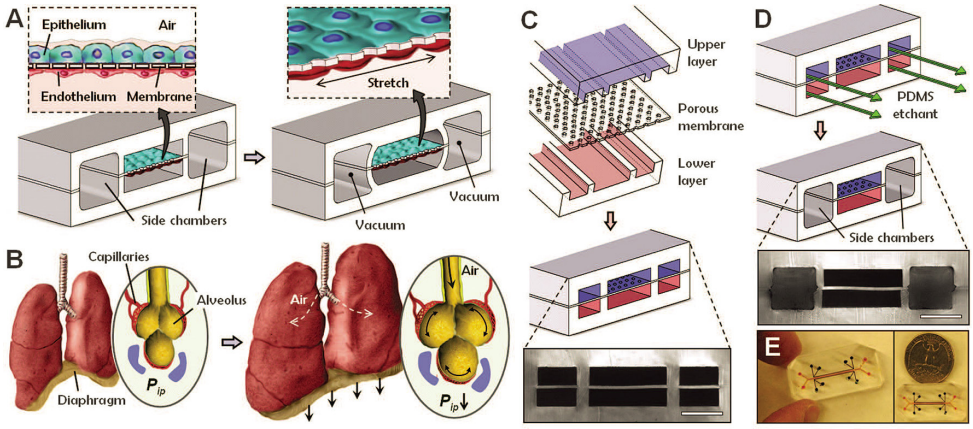

Figure 3. Example of a human breathing lung-on-a-chip microdevice. Lung-on-a-chip microfluidic device with compartmentalized microchannels to mimic a breathing lung (From Huh et al., "Reconstituting organ-level lung functions on a chip", Science 2010; 328:1662-8. Reprinted with permission from the AAAS [106]).See original reference for detailed description of the figure. In brief, A) indicates the creation of mechanical breathing movements causing mechanical stretch of the membrane, B) shows the physiology of the normal breathing human lung, C) and D) show the assembly and etching of the microdevice, and E) visualizes the actual size of the device.

However, it also has some limitations, since it uses a flat 2D membrane, cell lines instead of primary cells, and lacks interstitial fibroblasts and alveolar macrophages [130–132]. In 2015, Stucki and colleagues reported a lung-on-a-chip with an integrated, bio-inspired respiration mechanism. This model used primary human pulmonary alveolar epithelial cells, which were co-cultured with endothelial cells and exposed to a 3D cyclic mechanical strain to mimic respiration [133]. The group of Blume developed a 3D model, consisting of an air-liquid interface culture of human primary airway epithelial cells in a microfluidic culture system. This system had a continuous exchange of fluids and mediators, thereby simulating the interstitial flow in the lung [134]. The power of using the lung-on-a-chip approach includes the possibility of connecting multiple devices, thereby creating a more realistic lung mimic by integrating microfluidics, stretch, curvature and primary cells. In addition to air-liquid-interfaces and mimicking stretch during in- and exhalation, the microfluidic approach allows to apply pressure and shear flow profiles both in alveoli and attached blood capillaries. Compartmentalized microfluidic systems make bio-artificial/-engineered lung tissues also amenable for higher-throughput screening of the influence/impact of concentrations and mixtures of soluble factors in the blood/medium compartment, and of gases and particles in the air compartment

Tissue engineering

Although the above described systems are rapidly evolving, a huge hurdle is the generation of whole tissues and organs. There are three important demands to successfully create tissues and organs: the source of cells, the type of scaffold, and the composition of the extracellular matrix (ECM). An appropriate mixture of cells should be used for the recapitulation of cell-cell interactions [135]. Appropriate scaffolds are necessary to obtain a 3D structure and can be either synthetic or biological, and biodegradable or

non-biodegradable. In addition to the template three-dimensional structure, there is mechanical support and tissue instruction by engineered mechanical (e.g., through material or geometry-related matrix elasticity or stiffness), geometrical/topographical (e.g. through surface roughness or designed micro- or nanotextures) or (bio)chemical cues (e.g. RGD-adhesion moieties). An advantage of biodegradable scaffolds is that these are absorbed by the body. However, in the case of synthetic biodegradable scaffolds this may result in acidic degradation products causing inflammation in the surrounding tissue, e.g. when aliphatic polyesters like poly(lactic acid) are used [136]. Compared to synthetic scaffolds, biological scaffolds are more similar to the tissue or organ that they should substitute, although biological scaffolds may lack sufficient mechanical properties [137]. Different types of biological scaffolds can be used like collagen, Matrigel® and decellularized organs [137]. Decellularization of organs has to be done in a proper way to as much as possible preserve all components of the extracellular space/extracellular matrix components and their instructive properties. Several chemical, physical and enzymatical methods have been described to achieve this [62]. After decellularization, a process that does affect the extracellular matrix, the scaffold can be recellularized. Cells from different sources, as previously described, can be used for this purpose: embryonic, fetal or adult stem cells, autologous cells from the patient or iPSCs [62]. It is also possible to use allogeneic cells, e.g. in the case of transplantation of islets of Langerhans. There is also need for cells that are involved in vascularization and innervation, and cells with supportive, structural and barrier functions. Using autologous cells would be ideal to prevent rejection of the tissue-engineered organ in the patient, but could cause difficulties in the case of genetic or metabolic disorders [135]. Successful generation of tissue-engineered autologous bladders [138] and bio-engineered skin substitutes [139] have been reported as well as successful 3D bioprinting of several tissues and organs including multilayered skin, vascular grafts, heart tissue and tracheal splints [135, 140]. The structure and composition of the ECM should resemble that of embryonic organogenesis. It has been demonstrated that ECM signals are important to form pulmonary tissue structures in vitro [141]. Other signals, like cell-cell interactions, are also of importance to mimic the micro-environment of the organ [112, 142].

Tracheal bioengineering

In patients with a tracheal defect of 50 % of total length in adults or 30 % in children, artificial tracheal grafting is required [143]. Several approaches for tracheal epithelial differentiation have been tested, including co-culturing of tracheal epithelial cells with fibroblasts or adipose-derived stem cells [144–146] and cell sheet engineering with tracheal epithelial cells [147, 148]. In spite of the controversies and success rate, Macchiarini et al. were the first group that transplanted a tissue-engineered airway [149]. The group of Steinke produced a bio-artificial airway tissue using autologous primary cells to re-endothelialize and reseed a biological vascularized scaffold. After transplantation they observed complete airway healing and no evidence of tissue dedifferentiation [150]. Park and co-workers showed that human turbinated mesenchymal stromal cells cultured as intact sheets were able to differentiate into tracheal epithelium. These sheets were transplanted onto artificial grafts and tested in a rabbit model. After 1 month, regeneration of functional tracheal epithelium was observed [143]. Still, considerable problems are observed using tracheal grafts including failure to integrate and the formation of cartilaginous tissue [4, 62].

Vascular bioengineering

Interactions between epithelium, mesenchyme and endothelium are necessary for proper lung development and regeneration. Blood vessels secrete angiocrine factors that are involved in these processes including KLEIP, HIF-2α, VEGF, BMP-4, FGF, MMP14, EET and TSP-1. Angiogenesis, the process where vessels are formed from a pre-existing network, is important for adult vascular homeostasis, regeneration and adaption. Angiocrine signaling is necessary for this process [99]. The important role of the vasculature is also recognized in tissue engineering. Ren et al. attempted to generate transplantable rat lung grafts by seeding epithelial and endothelial cells into the airway and vascular compartments of a decellularized lung scaffold from the rat. The major problem was poor vascular performance, causing incomplete endothelial coverage of the scaffold vessels. They optimized their protocol by co-seeding endothelial and perivascular cells which resulted in an endothelial coverage of 75 % [151]. Even during decellularization of lung scaffolds, vascularization is important to preserve the integrity of the scaffold [152]. Orlova and coworkers showed that it is possible to generate endothelial cells and pericytes from human PSCs. This could provide a source of patient-specific vascular cells used in vascular bioengineering [153].

Whole lung bioengineering

Bioengineering of the whole lung is more complex than tracheal bioengineering due to the complexity of the lung. Lungs that are not suitable for transplantation can be decellularized and the scaffold can subsequently be used for seeding cells to regenerate the lung. It is still unknown which cell source is most suitable to repopulate the decellularized lung: MSCs, lung resident cells or a combination of both. Recently, it was shown that lung epithelial stem cells require co-culture with stromal cells to proliferate and differentiate. Fibroblasts have shown the highest efficiency in this support, and also the tissue origin of these cells gives varying patterns of support. Also, the use of FGFs and LIF-, ALK5- and ROCK-inhibitors activates proliferation and differentiation of quiescent lung stem cells [120]. Several methods were developed to decellularize lungs of rats, pigs, non-human primates and humans and to subsequently recellularize these scaffolds [154–160]. An overview of the currently available respiratory tract models, including the used cell sources and scaffolds, is reviewed by Nichols et al. [161].

Conclusions

Knowledge about potential stem cells in the lung has markedly increased through various recent developments. One of the challenges will be to merge all the data from different species and obtained with various techniques into a simplified model of lung stem cells and their role in the normal and diseased lung. Furthermore, a comprehensive view of all the (un)differentiated cells is still missing, because our repertoire of cell specific markers is still inadequate to identify the various cell types. One concern is that the use of different markers in individual studies might lead to the misconception that several subpopulations of progenitor cells exist, whereas there may possibly be only a few. In the future, the increase of cell-specific markers combined with single-cell lineage tracing should improve the definition of different (stem) cell populations in the lung. Additionally, a universal and unambiguous biological read out system to test the quality and purity of lung stem cells is also unavailable. So far, different systems, such as ALI cultures, organoids and explants, are successfully employed to fill this gap, but this makes it cumbersome to compare the various studies. Together with ESCs, iPSCs, MSCs and EPCs, local lung stem or progenitor

cells could be used for diverse clinical applications in the field of regenerative medicine. Current approaches to direct differentiation of stem cells, like iPSCs and MSCs, do generate lung-specific cells, but the specific lineages and the percentages of differentiated cells vary substantially. Therefore, optimization, improvement and expansion of the existing protocols is mandatory before clinical applications are possible. The manipulation of stem cells, like iPSCs, is required and useful for the development of lung mimics, for tissue engineering and for the generation of complete lung tissue. For tissue engineering applications, current scaffolds need to be improved or alternative suitable scaffolds need to be developed, which can be of synthetic and/or biological origin, and should contain appropriate ECM signals. Alternatively to bio-engineered lungs, specific pathways involved in differentiation of lung progenitor cells and plasticity of these cells may be targeted by novel compounds to induce their contribution to lung regeneration. Collectively, significant progress will be made through the interaction between very distinct scientific disciplines, such as developmental biology, biomedical engineering, and physics. These new and rapid developments in lung repair and regeneration offers a promising perspective for future patients with irreversible lung injury.

Competing interests
The authors declare that they have no competing interests

Authors' contributions
KAAS, EE, and RJR designed the concept and organized the review. KAAS, EE, SvR, AAP, DS, RT, PSH and RJR critically evaluated and improved the manuscript with significant additions. All authors read and approved the final manuscript.

Acknowledgements
This work was financially supported in part by the Lung Foundation Netherlands, project 6.1.14.010, the Sophia Foundation for Medical Research (SSWO) project numbers 641 (K.A.A.S.) and S14-12 (E.E) Pieter S. Hiemstra and Robbert J. Rottier: members of European Cooperation in Science and Technology (COST) action BM1201; "Developmental Origins of Chronic Lung Disease".

Author details [1]Department of Pediatric Surgery, Erasmus Medical Center-Sophia Children's Hospital, PO Box 20403000 CA Rotterdam, The Netherlands. [2]Department of Pulmonology, Leiden University Medical Center, PO Box 96002300 RC Leiden, The Netherlands. [3]Department of Biomaterials Science and Technology, University of Twente, MIRA Institute for Biomedical Technology and Technical Medicine, Faculty of Science and Technology, P.O Box 2177500 AE Enschede, The Netherlands. [4]Department of Complex Tissue Regeneration, Maastricht University, Faculty of Health, Medicine and Life Sciences, MERLN Institute for Technology-Inspired Regenerative Medicine, PO Box 6166200 MD Maastricht, The Netherlands.

Received: 22 December 2015 Accepted: 25 March 2016

References

1. Beers MF, Morrisey EE. The three R's of lung health and disease: repair, remodeling, and regeneration. J Clin Investig. 2011;121:2065–73.
2. Volckaert T, De Langhe S. Lung epithelial stem cells and their niches: Fgf10 takes center stage. Fibrogenesis Tissue Repair. 2014;7:8.
3. Kotton DN, Morrisey EE. Lung regeneration: mechanisms, applications and emerging stem cell populations. Nat Med. 2014;20:822–32.
4. Hogan BLM, Barkauskas CE, Chapman HA, Epstein JA, Jain R, Hsia CCW, et al. Repair and Regeneration of the Respiratory System: Complexity, Plasticity, and Mechanisms of Lung Stem Cell Function. Cell Stem Cell. 2014;15:123–38.
5. Lin C, Yao E, Chuang PT. A conserved MST1/2-YAP axis mediates Hippo signaling during lung growth. Dev Biol. 2015;403:101–13.
6. Rock JR, Hogan BLM. Epithelial Progenitor Cells in Lung Development, Maintenance, Repair, and Disease. Annu Rev Cell Dev Biol. 2011;27:493–512.
7. Boers JE, Ambergen AW, Thunnissen FB. Number and proliferation of basal and parabasal cells in normal human airway epithelium. Am J Respir Crit Care Med. 1998;157:2000–6.
8. Rock JR, Randell SH, Hogan BL. Airway basal stem cells: a perspective on their roles in epithelial homeostasis and remodeling. Dis Model Mech. 2010;3:545–56.
9. Morrisey EE, Hogan BL. Preparing for the first breath: genetic and cellular mechanisms in lung development. Dev Cell. 2010;18:8–23.
10. Guo M, Wang H, Potter SS, Whitsett JA, Xu Y. SINCERA: A Pipeline for Single-Cell RNA-Seq Profiling Analysis. PLoS Comput Biol. 2015;11, e1004575.
11. Du Y, Guo M, Whitsett JA, Xu Y. 'LungGENS': a web-based tool for mapping single-cell gene expression in the developing lung. Thorax. 2015;70:1092–4.
12. Treutlein B, Brownfield DG, Wu AR, Neff NF, Mantalas GL, Espinoza FH, et al. Reconstructing lineage hierarchies of the distal lung epithelium using single-cell RNA-seq. Nature. 2014;509:371–5.
13. Rock JR, Onaitis MW, Rawlins EL, Lu Y, Clark CP, Xue Y, et al. Basal cells as stem cells of the mouse trachea and human airway epithelium. Proc Natl Acad Sci U S A. 2009;106:12771–5.
14. Tata PR, Mou H, Pardo-Saganta A, Zhao R, Prabhu M, Law BM, et al. Dedifferentiation of committed epithelial cells into stem cells in vivo. Nature. 2013;503:218–23.
15. Rock JR, Gao X, Xue Y, Randell SH, Kong YY, Hogan BL. Notch-dependent differentiation of adult airway basal stem cells. Cell Stem Cell. 2011;8:639–48.
16. Mori M, Mahoney JE, Stupnikov MR, Paez-Cortez JR, Szymaniak AD, Varelas X, et al. Notch3-Jagged signaling controls the pool of undifferentiated airway progenitors. Development. 2015;142:258–67.
17. Tsao PN, Vasconcelos M, Izvolsky KI, Qian J, Lu JN, Cardoso WV. Notch signaling controls the balance of ciliated and secretory cell fates in developing airways. Development. 2009;136:2297–307.
18. Ghosh M, Helm KM, Smith RW, Giordanengo MS, Li B, Shen H, et al. A single cell functions as a tissue-specific stem cell and the in vitro niche-forming cell. Am J Respir Cell Mol Biol. 2011;45:459–69.
19. Cole BB, Smith RW, Jenkins KM, Graham BB, Reynolds PR, Reynolds SD. Tracheal Basal cells: a facultative progenitor cell pool. Am J Pathol. 2010;177:362–76.
20. Hong KU, Reynolds SD, Watkins S, Fuchs E, Stripp BR. In vivo differentiation potential of tracheal basal cells: evidence for multipotent and unipotent subpopulations. Am J Physiol Lung Cell Mol Physiol. 2004;286:L643–9.
21. Watson JK, Rulands S, Wilkinson AC, Wuidart A, Ousset M, Van Keymeulen A, Gottgens B, Blanpain C, Simons BD, Rawlins EL. Clonal Dynamics Reveal Two Distinct Populations of Basal Cells in Slow-Turnover Airway Epithelium. Cell Rep. 2015;12(1):90–101.
22. Teixeira VH, Nadarajan P, Graham TA, Pipinikas CP, Brown JM, Falzon M, et al. Stochastic homeostasis in human airway epithelium is achieved by neutral competition of basal cell progenitors. Elife. 2013;2, e00966.
23. Gao X, Vockley CM, Pauli F, Newberry KM, Xue Y, Randell SH, et al. Evidence for multiple roles for grainyhead-like 2 in the establishment and maintenance of human mucociliary airway epithelium.[corrected]. Proc Natl Acad Sci U S A. 2013;110:9356–61.
24. Gao X, Bali AS, Randell SH, Hogan BL. GRHL2 coordinates regeneration of a polarized mucociliary epithelium from basal stem cells. J Cell Biol. 2015; 211(3):669–682.
25. Paul MK, Bisht B, Darmawan DO, Chiou R, Ha VL, Wallace WD, et al. Dynamic changes in intracellular ROS levels regulate airway basal stem cell homeostasis through Nrf2-dependent Notch signaling. Cell Stem Cell. 2014;15:199–214.
26. Pardo-Saganta A, Law BM, Tata PR, Villoria J, Saez B, Mou H, et al. Injury induces direct lineage segregation of functionally distinct airway Basal stem/progenitor cell subpopulations. Cell Stem Cell. 2015;16:184–97.
27. Marshall CB, Mays DJ, Beeler JS, Rosenbluth JM, Boyd KL, Santos Guasch GL, Shaver TM, Tang LJ, Liu Q,

Shyr Y, et al. p73 Is Required for Multiciliogenesis and Regulates the Foxj1-Associated Gene Network. Cell Rep. 2016;14(10): 2289–2300.
28. Kumar PA, Hu Y, Yamamoto Y, Hoe NB, Wei TS, Mu D, et al. Distal airway stem cells yield alveoli in vitro and during lung regeneration following H1N1 influenza infection. Cell. 2011;147:525–38.
29. Zuo W, Zhang T, Wu DZ, Guan SP, Liew AA, Yamamoto Y, Wang X, Lim SJ, Vincent M, Lessard M, et al.. p63Krt5 distal airway stem cells are essential for lung regeneration. Nature. 2014;517(7536):616–620.
30. Rawlins EL. Stem cells: Emergency back-up for lung repair. Nature. 2015;517:556–7.
31. Vaughan AE, Brumwell AN, Xi Y, Gotts JE, Brownfield DG, Treutlein B, et al. Lineage-negative progenitors mobilize to regenerate lung epithelium after major injury. Nature. 2015;517:621–5.
32. Shaykhiev R. Multitasking basal cells: combining stem cell and innate immune duties. Eur Respir J. 2015;46:894–7. 33. Reynolds SD, Hong KU, Giangreco A, Mango GW, Guron C, Morimoto Y, et al. Conditional clara cell ablation reveals a self-renewing progenitor function of pulmonary neuroendocrine cells. Am J Physiol Lung Cell Mol Physiol. 2000;278:L1256–63.
34. Rawlins EL, Okubo T, Xue Y, Brass DM, Auten RL, Hasegawa H, et al. The role of Scgb1a1^{+} Clara cells in the long-term maintenance and repair of lung airway, but not alveolar, epithelium. Cell Stem Cell. 2009;4:525–34.
35. Kim CF, Jackson EL, Woolfenden AE, Lawrence S, Babar I, Vogel S, et al. Identification of bronchioalveolar stem cells in normal lung and lung cancer. Cell. 2005;121:823–35.
36. Zheng D, Limmon GV, Yin L, Leung NH, Yu H, Chow VT, et al. Regeneration of alveolar type I and II cells from Scgb1a1-expressing cells following severe pulmonary damage induced by bleomycin and influenza. PLoS One. 2012;7, e48451.
37. Desai TJ, Brownfield DG, Krasnow MA. Alveolar progenitor and stem cells in lung development, renewal and cancer. Nature. 2014;507:190–4.
38. Barkauskas CE, CronceMJ, Rackley CR,Bowie EJ, Keene DR,Stripp BR,et al. Type 2 alveolar cells are stem cells in adult lung. J Clin Invest. 2013;123:3025–36.
39. Chapman HA, Li X, Alexander JP, Brumwell A, Lorizio W, Tan K, et al. Integrin alpha6beta4 identifies an adult distal lung epithelial population with regenerative potential in mice. J Clin Invest. 2011;121:2855–62.
40. Liu Y, Sadikot RT, Adami GR, Kalinichenko VV, Pendyala S, Natarajan V, et al. FoxM1 mediates the progenitor function of type II epithelial cells in repairing alveolar injury induced by Pseudomonas aeruginosa. J Exp Med. 2011;208:1473–84.
41. Liu Y, Kumar VS, Zhang W, Rehman J, Malik AB. Activation of type II cells into regenerative stem cell antigen-1($^{+}$) cells during alveolar repair. Am J Respir Cell Mol Biol. 2015;53:113–24.
42. Xu W, Zhao Y, Zhang B, Xu B, Yang Y, Wang Y, Liu C. Resveratrol attenuates hyperoxia-induced oxidative stress, inflammation and fibrosis and suppresses Wnt/β-catenin signalling in lungs of neonatal rats. Clin Exp Pharmacol Physiol. 2015;42(10):1075–83.
43. Zheng D, Yin L, Chen J. Evidence for Scgb1a1($^{+}$) cells in the generation of p63($^{+}$) cells in the damaged lung parenchyma. Am J Respir Cell Mol Biol. 2014;50:595–604.
44. Zhao R, Fallon TR, Saladi SV, Pardo-Saganta A, Villoria J, Mou H, et al. Yap tunes airway epithelial size and architecture by regulating the identity, maintenance, and self-renewal of stem cells. Dev Cell. 2014;30:151–65.
45. Lange AW, Sridharan A, Xu Y, Stripp BR, Perl AK, Whitsett JA. Hippo/Yap signaling controls epithelial progenitor cell proliferation and differentiation in the embryonic and adult lung. J Mol Cell Biol. 2015;7:35–47.
46. Mahoney JE, Mori M, Szymaniak AD, Varelas X, Cardoso WV. The hippo pathway effector Yap controls patterning and differentiation of airway epithelial progenitors. Dev Cell. 2014;30:137–50.
47. Turner J, Roger J, Fitau J, Combe D, Giddings J, Heeke GV, et al. Goblet cells are derived from a FOXJ1-expressing progenitor in a human airway epithelium. Am J Respir Cell Mol Biol. 2011;44:276–84.
48. Pardo-Saganta A, Law BM, Gonzalez-Celeiro M, Vinarsky V, Rajagopal J. Ciliated cells of pseudostratified airway epithelium do not become mucous cells after ovalbumin challenge. Am J Respir Cell Mol Biol. 2013;48:364–73.
49. Jain R, Barkauskas CE, Takeda N, Bowie EJ, Aghajanian H, Wang Q, et al. Plasticity of Hopx($^{+}$) type I alveolar cells to regenerate type II cells in the lung. Nat Commun. 2015;6:6727.
50. Kapere Ochieng J, Schilders K, Kool H, Buscop-van Kempen M, Boerema-De Munck A, Grosveld F, et al. Differentiated Type II Pneumocytes Can Be Reprogrammed by Ectopic Sox2 Expression. PLoS One. 2014;9, e107248. 51. Yang J, Hernandez BJ, Martinez Alanis D, Narvaez Del Pilar O, Vila-Ellis L, Akiyama H, et al. The development and plasticity of alveolar type 1 cells. Development. 2016;143:54–65.
52. Peng T, Frank DB, Kadzik RS, Morley MP, Rathi KS, Wang T, et al. Hedgehog actively maintains adult lung quiescence and regulates repair and regeneration. Nature. 2015;526:578–82.
53. Kugler MC, Joyner AL, Loomis CA, Munger JS. Sonic hedgehog signaling in the lung. From development to disease. Am J Respir Cell Mol Biol. 2015;52:1–13.
54. Khuri FR, Lee JS, Lippman SM, Lee JJ, Kalapurakal S, Yu R, et al. Modulation of proliferating cell nuclear antigen in the bronchial epithelium of smokers. Cancer Epidemiol Biomarkers Prev. 2001;10:311–8.

55. Snitow ME, Li SR, Morley MP, Rathi K, Lu MM, Kadzik RS, et al. Ezh2 represses the basal cell lineage during lung endoderm development. Development. 2015;142:108–17.
56. Tilley AE, Harvey BG, Heguy A, Hackett NR, Wang R, O'Connor TP, et al. Down-regulation of the notch pathway in human airway epithelium in association with smoking and chronic obstructive pulmonary disease. Am J Respir Crit Care Med. 2009;179:457–66.
57. Shi W, Chen F, Cardoso WV. Mechanisms of lung development: contribution to adult lung disease and relevance to chronic obstructive pulmonary disease. Proc Am Thorac Soc. 2009;6:558–63.
58. Verhamme FM, Bracke KR, Joos GF, Brusselle GG. Transforming Growth Factor-beta Superfamily in Obstructive Lung Diseases. Am J Respir Cell Mol Biol. 2015;52:653–62.
59. Martin C, Frija-Masson J, Burgel PR. Targeting mucus hypersecretion: new therapeutic opportunities for COPD? Drugs. 2014;74:1073–89.
60. Lafkas D, Shelton A, Chiu C, de Leon BG, Chen Y, Stawicki SS, et al. Therapeutic antibodies reveal Notch control of transdifferentiation in the adult lung. Nature. 2015;528:127–31.
61. El Agha E, Kosanovic D, Schermuly RT, Bellusci S. Role of fibroblast growth factors in organ regeneration and repair. Semin Cell Dev Biol. 2015.
62. Stoltz JF, de Isla N, Li YP, Bensoussan D, Zhang L, Huselstein C, Chen Y, Decot V, Magdalou J, Li N, et al. Stem Cells and Regenerative Medicine: Myth or Reality of the 21th Century. Stem Cells International. 2015;734731.
63. Quan Y, Wang D. Clinical potentials of human pluripotent stem cells in lung diseases. Clin Transl Med. 2014;3:15. 64. Ghaedi M, Niklason LE, Williams J. Development of Lung Epithelium from Induced Pluripotent Stem Cells. Curr Transplant Rep. 2015;2:81–9.
65. Takahashi K, Yamanaka S. Induction of pluripotent stem cells from mouse embryonic and adult fibroblast cultures by defined factors. Cell. 2006;126:663–76.
66. Singh VK, Kumar N, Kalsan M, Saini A, Chandra R. Mechanism of Induction: Induced Pluripotent Stem Cells (iPSCs). J Stem Cells. 2015;10:43–62.
67. Green MD, Chen A, Nostro MC, d'Souza SL, Schaniel C, Lemischka IR, et al. Generation of anterior foregut endoderm from human embryonic and induced pluripotent stem cells. Nat Biotechnol. 2011;29:267–U153.
68. Ali NN, Edgar AJ, Samadikuchaksaraei A, Timson CM, Romanska HM, Polak JM, et al. Derivation of type II alveolar epithelial cells from murine embryonic stem cells. Tissue Eng. 2002;8:541–50.
69. Van Haute L, De Block G, Liebaers I, Sermon K, De Rycke M. Generation of lung epithelial-like tissue from human embryonic stem cells. Respir Res. 2009;10:105.
70. Banerjee ER, Laflamme MA, Papayannopoulou T, Kahn M, Murry CE, Henderson Jr WR. Human embryonic stem cells differentiated to lung lineage-specific cells ameliorate pulmonary fibrosis in a xenograft transplant mouse model. PLoS One. 2012;7, e33165.
71. Samadikuchaksaraei A, Cohen S, Isaac K, Rippon HJ, Polak JM, Bielby RC, et al. Derivation of distal airway epithelium from human embryonic stem cells. Tissue Eng. 2006;12:867–75.
72. Wang D, Haviland DL, Burns AR, Zsigmond E, Wetsel RA. A pure population of lung alveolar epithelial type II cells derived from human embryonic stem cells. Proc Natl Acad Sci U S A. 2007;104:4449–54.
73. Rippon HJ, Polak JM, Qin M, Bishop AE. Derivation of distal lung epithelial progenitors from murine embryonic stem cells using a novel three-step differentiation protocol. Stem Cells. 2006;24:1389–98.
74. Firth AL, Dargitz CT, Qualls SJ, Menon T, Wright R, Singer O, et al. Generation of multiciliated cells in functional airway epithelia from human induced pluripotent stem cells. Proc Natl Acad Sci U S A. 2014;111:E1723–30.
75. Wong AP, Bear CE, Chin S, Pasceri P, Thompson TO, Huan LJ, et al. Directed differentiation of human pluripotent stem cells into mature airway epithelia expressing functional CFTR protein. Nat Biotechnol. 2012;30:876–82.
76. Mou H, Zhao R, Sherwood R, Ahfeldt T, Lapey A, Wain J, et al. Generation of multipotent lung and airway progenitors from mouse ESCs and patientspecific cystic fibrosis iPSCs. Cell Stem Cell. 2012;10:385–97.
77. Longmire TA, Ikonomou L, Hawkins F, Christodoulou C, Cao Y, Jean JC, et al. Efficient derivation of purified lung and thyroid progenitors from embryonic stem cells. Cell Stem Cell. 2012;10:398–411.
78. Ghaedi M, Calle EA, Mendez JJ, Gard AL, Balestrini J, Booth A, et al. Human iPS cell-derived alveolar epithelium repopulates lung extracellular matrix. J Clin Invest. 2013;123:4950–62.
79. Huang SX, Islam MN, O'Neill J, Hu Z, Yang YG, Chen YW, et al. Efficient generation of lung and airway epithelial cells from human pluripotent stem cells. Nat Biotechnol. 2014;32:84–91.
80. Huang SXL, Green MD, de Carvalho AT, Mumau M, Chen YW, D'Souza SL, Snoeck HW. The in vitro generation of lung and airway progenitor cells from human pluripotent stem cells. Nature Protocols 2015;10(3):413–425.
81. Martin U. Pluripotent stem cells for disease modeling and drug screening: new perspectives for treatment of cystic fibrosis? Mol Cell Pediatr. 2015;2:15.
82. Weiss DJ. Concise review: current status of stem cells and regenerative medicine in lung biology and diseases. Stem Cells. 2014;32:16–25.
83. D'souza N, Rossignoli F, Golinelli G, Grisendi G, Spano C, Candini O, Osturu S, Catani F, Paolucci P, Horwitz EM,

Dominici M. Mesenchymal stem/stromal cells as a delivery platform in cell and gene therapies. BMC Medicine. 2015. 13 12;13:186.
84. Neofytou E, Deuse T, Beygui RE, Schrepfer S. Mesenchymal stromal cell therapy: different sources exhibit different immunobiological properties. Transplantation. 2015;99:1113–8.
85. Mobius MA, Thebaud B. Stem Cells and Their Mediators - Next Generation Therapy for Bronchopulmonary Dysplasia. Front Med (Lausanne). 2015;2:50.
86. Dominici M, Le Blanc K, Mueller I, Slaper-Cortenbach I, Marini F, Krause D, et al. Minimal criteria for defining multipotent mesenchymal stromal cells. The International Society for Cellular Therapy position statement. Cytotherapy. 2006;8:315–7.
87. Sueblinvong V, Loi R, Eisenhauer PL, Bernstein IM, Suratt BT, Spees JL, et al. Derivation of lung epithelium from human cord blood-derived mesenchymal stem cells. Am J Respir Crit Care Med. 2008;177:701–11.
88. Martin J, Helm K, Ruegg P, Varella-Garcia M, Burnham E, Majka S. Adult lung side population cells have mesenchymal stem cell potential. Cytotherapy. 2008;10:140–51.
89. Gong X, Sun Z, Cui D, Xu X, Zhu H, Wang L, Qian W, Han X. Isolation and characterization of lungresidentmesenchymal stem cells capable of differentiatingintoalveolar epithelial type II cells.Cell Biol Int.2014;38(4):405–11.
90. Stabler CT, Lecht S, Lazarovici P, Lelkes PI. Mesenchymal stem cells for therapeutic applications in pulmonary medicine. Br Med Bull. 2015;115:45–56.
91. Weiss DJ, Casaburi R, Flannery R, LeRoux-Williams M, Tashkin DP. A Placebo-Controlled, Randomized Trial of Mesenchymal Stem Cells in COPD. Chest. 2013;143:1590–8.
92. Petrella F, Rizzo S, Borri A, Casiraghi M, Spaggiari L. Current Perspectives in Mesenchymal Stromal Cell Therapies for Airway Tissue Defects. Stem Cells Int. 2015;2015:746392.
93. Rosen C, Shezen E, Aronovich A, Klionsky YZ, Yaakov Y, Assayag M, et al. Preconditioning allows engraftment of mouse and human embryonic lung cells, enabling lung repair in mice. Nat Med. 2015;21:869–79.
94. Li Q, Wang Y, Deng Z. Pre-conditioned mesenchymal stem cells: a better way for cell-based therapy. Stem Cell Res Ther. 2013;4:63.
95. Weiss DJ, Chambers D, Giangreco A, Keating A, Kotton D, Lelkes PI, et al. An official American Thoracic Society workshop report: stem cells and cell therapies in lung biology and diseases. Ann Am Thorac Soc. 2015;12:S79–97.
96. Zhao YD, Courtman DW, Deng Y, Kugathasan L, Zhang Q, Stewart DJ. Rescue of monocrotaline-induced pulmonary arterial hypertension using bone marrow-derived endothelial-like progenitor cells: efficacy of combined cell and eNOS gene therapy in established disease. Circ Res. 2005;96:442–50.
97. Lam CF, Roan JN, Lee CH, Chang PJ, Huang CC, Liu YC, et al. Transplantation of endothelial progenitor cells improves pulmonary endothelial function and gas exchange in rabbits with endotoxin-induced acute lung injury. Anesth Analg. 2011;112:620–7.
98. Balasubramaniam V, Ryan SL, Seedorf GJ, Roth EV, Heumann TR, Yoder MC, et al. Bone marrow-derived angiogenic cells restore lung alveolar and vascular structure after neonatal hyperoxia in infant mice. Am J Physiol Lung Cell Mol Physiol. 2010;298:L315–23.
99. Woik N, Kroll J. Regulation of lung development and regeneration by the vascular system. Cell Mol Life Sci. 2015;72:2709–18.
100. Ding BS, Nolan DJ, Guo P, Babazadeh AO, Cao Z, Rosenwaks Z, et al. Endothelial-derived angiocrine signals induce and sustain regenerative lung alveolarization. Cell. 2011;147:539–53.
101. Rafii S, Cao Z, Lis R, Siempos II, Chavez D, Shido K, et al. Platelet-derived SDF-1 primes the pulmonary capillary vascular niche to drive lung alveolar regeneration. Nat Cell Biol. 2015;17:123–36.
102. Wang XX, Zhang FR, Shang YP, Zhu JH, Xie XD, Tao QM, et al. Transplantation of autologous endothelial progenitor cells may be beneficial in patients with idiopathic pulmonary arterial hypertension: a pilot randomized controlled trial. J Am Coll Cardiol. 2007;49:1566–71.
103. Zhu JH, Wang XX, Zhang FR, Shang YP, Tao QM, Zhu JH, et al. Safety and efficacy of autologous endothelial progenitor cells transplantation in children with idiopathic pulmonary arterial hypertension: open-label pilot study. Pediatr Transplant. 2008;12:650–5.
104. Huh D, Hamilton GA, Ingber DE. From 3D cell culture to organs-on-chips. Trends Cell Biol. 2011;21:745–54.
105. Whitcutt MJ, Adler KB, Wu R. A biphasic chamber system for maintaining polarity of differentiation of cultured respiratory tract epithelial cells. In Vitro Cell Dev Biol. 1988;24:420–8.
106. Randell SH, Fulcher ML, O'Neal W, Olsen JC. Primary epithelial cell models for cystic fibrosis research. Methods Mol Biol. 2011;742:285–310.
107. Wark PA, Johnston SL, Bucchieri F, Powell R, Puddicombe S, Laza-Stanca V, et al. Asthmatic bronchial epithelial cells have a deficient innate immune response to infection with rhinovirus. J Exp Med. 2005;201:937–47.
108. Herr C, Beisswenger C, Hess C, Kandler K, Suttorp N, Welte T, et al. Suppression of pulmonary innate host defence in smokers. Thorax. 2009;64:144–9.

109. Amatngalim GD, van Wijck Y, de Mooij-Eijk Y, Verhoosel RM, Harder J, Lekkerkerker AN, et al. Basal cells contribute to innate immunity of the airway epithelium through production of the antimicrobial protein RNase 7. J Immunol. 2015;194:3340–50.
110. Aufderheide M, Forster C, Beschay M, Branscheid D, Emura M. A new computer-controlled air-liquid interface cultivation system for the generation of differentiated cell cultures of the airway epithelium. Exp Toxicol Pathol. 2015;68(1):77–87.
111. Ranga A, Gjorevski N, Lutolf MP. Drug discovery through stem cell-based organoid models. Adv Drug Deliv Rev. 2014;69:19–28.
112. Gjorevski N, Ranga A, Lutolf MP. Bioengineering approaches to guide stem cell-based organogenesis. Development. 2014;141:1794–804.
113. Huch M, Koo BK. Modeling mouse and human development using organoid cultures. Development. 2015;142:3113–25.
114. Yin X, Mead BE, Safaee H, Langer R, Karp JM, Levy O. Engineering Stem Cell Organoids. Cell Stem Cell. 2016;18:25–38.
115. Willyard C. The boom in mini stomachs, brains, breasts, kidneys and more. Nature. 2015;523:520–2.
116. Sato T, Clevers H. Growing self-organizing mini-guts from a single intestinal stem cell: mechanism and applications. Science. 2013;340:1190–4.
117. Nadkarni RR, Abed S, Draper JS. Organoids as a model system for studying human lung development and disease. Biochem Biophys Res Commun. 2015;S0006-291X(15)31096-2
118. Schoch KG, Lori A, Burns KA, Eldred T, Olsen JC, Randell SH. A subset of mouse tracheal epithelial basal cells generates large colonies in vitro. Am J Physiol Lung Cell Mol Physiol. 2004;286(4):L631–42.
119. Danahay H, Pessotti AD, Coote J, Montgomery BE, Xia D, Wilson A, et al. Notch2 is required for inflammatory cytokine-driven goblet cell metaplasia in the lung. Cell Rep. 2015;10:239–52.
120. Hegab AE, Arai D, Gao J, Kuroda A, Yasuda H, Ishii M, et al. Mimicking the niche of lung epithelial stem cells and characterization of several effectors of their in vitro behavior. Stem Cell Res. 2015;15:109–21.
121. Lee JH, Bhang DH, Beede A, Huang TL, Stripp BR, Bloch KD, et al. Lung stem cell differentiation in mice directed by endothelial cells via a BMP4-NFATc1-thrombospondin-1 axis. Cell. 2014;156:440–55.
122. Delgado O, Kaisani AA, Spinola M, Xie XJ, Batten KG, Minna JD, et al. Multipotent capacity of immortalized human bronchial epithelial cells. PLoS One. 2011;6, e22023.
123. Franzdottir SR, Axelsson IT, Arason AJ, Baldursson O, Gudjonsson T, Magnusson MK. Airway branching morphogenesis in three dimensional culture. Respir Res. 2010;11:162.
124. Kaisani A, Delgado O, Fasciani G, Kim SB, Wright WE, Minna JD, et al. Branching morphogenesis of immortalized human bronchial epithelial cells in three-dimensional culture. Differentiation. 2014;87:119–26.
125. Gotoh S, Ito I, Nagasaki T, Yamamoto Y, Konishi S, Korogi Y, et al. Generation of alveolar epithelial spheroids via isolated progenitor cells from human pluripotent stem cells. Stem Cell Reports. 2014;3:394–403.
126. Dye BR, Hill DR, Ferguson MA, Tsai YH, Nagy MS, Dyal R, et al. In vitro generation of human pluripotent stem cell derived lung organoids. Elife. 2015;4. doi:10.7554/eLife.05098.001.
127. Dye BR, Hill DR, Ferguson MAH, Tsai YH, Nagy MS, Dyal R, Wells JM, Mayhew CN, Nattiv R, Klein OD, et al. In vitro generation of human pluripotent stem cell derived lung organoids. Elife. 2015;4. doi:10.7554/eLife.05098.
128. Kniazeva T, Hsiao JC, Charest JL, Borenstein JT. A microfluidic respiratory assist device with high gas permeance for artificial lung applications. Biomed Microdevices. 2011;13:315–23.
129. Bhatia SN, Ingber DE. Microfluidic organs-on-chips. Nat Biotechnol. 2014;32:760–72.
130. Huh D, Matthews BD, Mammoto A, Montoya-Zavala M, Hsin HY, Ingber DE. Reconstituting Organ-Level Lung Functions on a Chip. Science. 2010;328:1662–8.
131. Huh D, Leslie DC, Matthews BD, Fraser JP, Jurek S, Hamilton GA, Thorneloe KS, McAlexander MA, Ingber DE. A Human Disease Model of Drug Toxicity-Induced Pulmonary Edema in a Lung-on-a-Chip Microdevice. Sci Transl Med. 2012;4(159):159ra147.
132. Fukumoto J, Kolliputi N. Human lung on a chip: innovative approach for understanding disease processes and effective drug testing. Front Pharmacol. 2012;3:205.
133. Stucki AO, Stucki JD, Hall SRR, Felder M, Mermoud Y, Schmid RA, et al. A lung-on-a-chip array with an integrated bio-inspired respiration mechanism. Lab Chip. 2015;15:1302–10.
134. Blume C, Reale R, Held M, Millar TM, Collins JE, Davies DE, Morgan H, Swindle EJ. Temporal Monitoring of Differentiated Human Airway Epithelial Cells Using Microfluidics. PLoS ONE. 2015;10(10):e0139872.
135. Murphy SV, Atala A. 3D bioprinting of tissues and organs. Nat Biotechnol. 2014;32:773–85.
136. Patel M, Fisher JP. Biomaterial scaffolds in pediatric tissue engineering. Pediatr Res. 2008;63:497–501.
137. Li Q, Uygun BE, Geerts S, Ozer S, Scalf M, Gilpin SE, Ott HC, Yarmush ML, Smith LM, Welham NV, Frey BL. Proteomic Analysis of Naturally-Sourced Biological Scaffolds. Biomaterials. 2016;75:37–46.
138. Atala A, Bauer SB, Soker S, Yoo JJ, Retik AB. Tissue-engineered autologous bladders for patients needing

cystoplasty. Lancet. 2006;367:1241–6.
139. Pham C, Greenwood J, Cleland H, Woodruff P, Maddern G. Bioengineered skin substitutes for the management of burns: a systematic review. Burns. 2007;33:946–57.
140. Zopf DA, Hollister SJ, Nelson ME, Ohye RG, Green GE. Bioresorbable airway splint created with a three-dimensional printer. N Engl J Med. 2013;368:2043–5.
141. Mondrinos MJ, Jones PL, Finck CM, Lelkes PI. Engineering De Novo Assembly of Fetal Pulmonary Organoids. Tissue Eng A. 2014;20:2892–907.
142. Ranga A, Lutolf MP. High-throughput approaches for the analysis of extrinsic regulators of stem cell fate. Curr Opin Cell Biol. 2012;24:236–44.
143. Park JH, Park JY, Nam IC, Hwang SH, Kim CS, Jung JW, et al. Human turbinate mesenchymal stromal cell sheets with bellows graft for rapid tracheal epithelial regeneration. Acta Biomater. 2015;25:56–64.
144. Kobayashi K, Nomoto Y, Suzuki T, Tada Y, Miyake M, Hazama A, et al. Effect of fibroblasts on tracheal epithelial regeneration in vitro. Tissue Eng. 2006;12:2619–28.
145. Kobayashi K, Suzuki T, Nomoto Y, Tada Y, Miyake M, Hazama A, et al. A tissue-engineered trachea derived from a framed collagen scaffold, gingival fibroblasts and adipose-derived stem cells. Biomaterials. 2010;31:4855–63.
146. Okano W, Nomoto Y, Wada I, Kobayashi K, Miyake M, Nakamura T, et al. Bioengineered trachea with fibroblasts in a rabbit model. Ann Otol Rhinol Laryngol. 2009;118:796–804.
147. Yang J, Yamato M, Shimizu T, Sekine H, Ohashi K, Kanzaki M, et al. Reconstruction of functional tissues with cell sheet engineering. Biomaterials. 2007;28:5033–43.
148. Kanzaki M, Yamato M, Hatakeyama H, Kohno C, Yang J, Umemoto T, et al. Tissue engineered epithelial cell sheets for the creation of a bioartificial trachea. Tissue Eng. 2006;12:1275–83.
149. Macchiarini P, Jungebluth P, Go T, Asnaghi MA, Rees LE, Cogan TA, et al. Clinical transplantation of a tissue-engineered airway. Lancet. 2008;372:2023–30.
150. Steinke M, Dally I, Friedel G, Walles H, Walles T. Host-Integration of a Tissue-Engineered Airway Patch: Two-Year Follow-Up in a Single Patient. Tissue Eng A. 2015;21:573–9.
151. Ren X, Moser PT, Gilpin SE, Okamoto T, Wu T, Tapias L, et al. Engineering pulmonary vasculature in decellularized rat and human lungs. Nature Biotechnology. 2015;1097
152. da Palma RK, Campillo N, Uriarte JJ, Oliveira LVF, Navajas D, Farre R. Pressure- and flow-controlled media perfusion differently modify vascular mechanics in lung decellularization. J Mech Behav Biomed Mater. 2015;49:69–79.
153. Orlova VV, van den Hil FE, Petrus-Reurer S, Drabsch Y, Ten Dijke P, Mummery CL. Generation, expansion and functional analysis of endothelial cells and pericytes derived from human pluripotent stem cells. Nat Protoc. 2014;9:1514–31.
154. Ott HC, Clippinger B, Conrad C, Schuetz C, Pomerantseva I, Ikonomou L, et al. Regeneration and orthotopic transplantation of a bioartificial lung. Nat Med. 2010;16:927–33.
155. Petersen TH, Calle EA, Colehour MB, Niklason LE. Bioreactor for the long-term culture of lung tissue. Cell Transplant. 2011;20:1117–26.
156. Price AP, England KA, Matson AM, Blazar BR, Panoskaltsis-Mortari A. Development of a decellularized lung bioreactor system for bioengineering the lung: the matrix reloaded. Tissue Eng Part A. 2010;16:2581–91.
157. Wallis JM, Borg ZD, Daly AB, Deng B, Ballif BA, Allen GB, et al. Comparative assessment of detergent-based protocols for mouse lung de-cellularization and re-cellularization. Tissue Eng Part C Methods. 2012;18:420–32.
158. Booth AJ, Hadley R, Cornett AM, Dreffs AA, Matthes SA, Tsui JL, et al. Acellular normal and fibrotic human lung matrices as a culture system for in vitro investigation. Am J Respir Crit Care Med. 2012;186:866–76. 159. Nichols JE, Niles J, Riddle M, Vargas G, Schilagard T, Ma L, et al. Production and assessment of decellularized pi g and human lung scaffolds. Tissue Eng Part A. 2013;19:2045–62.
160. Wagner DE, Bonenfant NR, Sokocevic D, DeSarno MJ, Borg ZD, Parsons CS, et al. Three-dimensional scaffolds of acellular human and porcine lungs for high throughput studies of lung disease and regeneration. Biomaterials. 2014;35:2664–79.
161. Nichols JE, Niles JA, Vega SP, Argueta LB, Eastaway A, Cortiella J. Modeling the lung: Design and development of tissue engineered macro- and microphysiologic lung models for research use. Exp Biol Med. 2014;239:1135–69.
162. Song H, Yao E, Lin C, Gacayan R, Chen MH, Chuang PT. Functional characterization of pulmonary neuroendocrine cells in lung development, injury, and tumorigenesis. Proc Natl Acad Sci U S A. 2012;109:17531–6.
163. Chen G, Korfhagen TR, Xu Y, Kitzmiller J, Wert SE, Maeda Y, et al. SPDEF is required for mouse pulmonary goblet cell differentiation and regulates a network of genes associated with mucus production. J Clin Invest. 2009;119:2914–24.
164. Morimoto M, Nishinakamura R, Saga Y, Kopan R. Different assemblies of Notch receptors coordinate the

distribution of the major bronchial Clara, ciliated and neuroendocrine cells. Development. 2012;139:4365–73.
165. Shan L, Aster JC, Sklar J, Sunday ME. Notch-1 regulates pulmonary neuroendocrine cell differentiation in cell lines and in transgenic mice. Am J Physiol Lung Cell Mol Physiol. 2007;292:L500–9.
166. Ito T, Udaka N, Yazawa T, Okudela K, Hayashi H, Sudo T, et al. Basic helixloop-helix transcription factors regulate the neuroendocrine differentiation of fetal mouse pulmonary epithelium. Development. 2000;127:3913–21.
167. Xing Y, Li A, Borok Z, Li C, Minoo P. NOTCH1 is required for regeneration of Clara cells during repair of airway injury. Stem Cells. 2012;30:946–55.
168. Zhang Y, Goss AM, Cohen ED, Kadzik R, Lepore JJ, Muthukumaraswamy K, et al. A Gata6-Wnt pathway required for epithelial stem cell development and airway regeneration. Nat Genet. 2008;40:862–70.
169. Park KS, Korfhagen TR, Bruno MD, Kitzmiller JA, Wan H, Wert SE, et al. SPDEF regulates goblet cell hyperplasia in the airway epithelium. J Clin Invest. 2007;117:978–88.

Chapter 7.
General discussion

General discussion

Sox2 in cell fate determination

The lung consists of different subsets of epithelial cells along the proximal-distal axis. Basal cells (which are the stem cells of the upper airways), secretory cells (club cells and goblet cells) and ciliated cells and some neuroendocrine cells make up the airways of the human lung. In mice, the trachea and main stem bronchi have a similar structure. The smallest respiratory bronchioles of human and the intralobular airways of mice are aligned by club, ciliated and neuroendocrine cells and the alveoli of both human and mice consist of alveolar type I (AT-I) and type II cells (AT-II) (1). Differentiation of the proximal epithelial cells already starts at the pseudoglandular phase (embryonic day (E) 11.5-16.6 in mice/ week (wk) 5-15 in human), while alveolar differentiation starts during the canalicular phase (E16.6-17.4 in mice/wk16-25 in human) (2). The anterior foregut endoderm starts to express the earliest lung endoderm marker Nkx2.1 around E9 (comparable with wk3 in human) . The Wnt signaling pathway components Wnt2 and Wnt2b, which are expressed in the mesoderm surrounding the Nkx2.1^{+} endoderm, are necessary for this expression. Deletion of both Wnt2 and Wnt2b results in loss of Nkx2.1, while activation of Wnt results in expansion of Nkx2.1 (3, 4). Bmp signaling is also involved in this regulation process by repressing the expression of Sox2, which allows Nkx2.1 expression (5). Nkx2.1^{+} endoderm cells give rise to both the proximal and distal epithelial cells lining the airways. Sox2 marks the proximal progenitor cells, while the distal progenitor cells are characterized by Sox9 and Id2 expression (fig. 1A) (6). Neuroendocrine cells, secretory cells, ciliated cells and goblet cells are all differentiated from these Sox2^{+} progenitor cells, while the Id2^{+}/Sox9^{+} cells give rise the AT-1 and AT-II cells (fig. 1B) (6). In the distal cells, Fgf10 activates β-catenin signaling which results in the inhibition of Sox2 expression, thereby preventing differentiation of these cells into a proximal cell type (7).

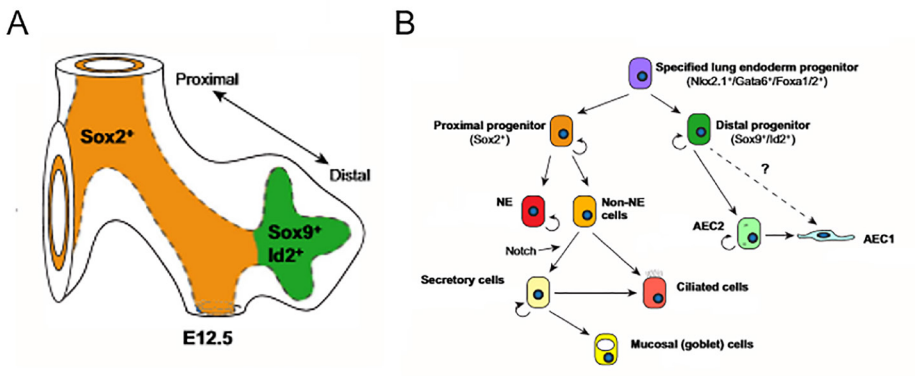

Figure 1. A) During lung development the epithelial cells in the proximal airways are characterized by Sox2 expression while the distal epithelial cells are marked by Id2/Sox9 expression (1). B) Sox2^{+} progenitor cells give rise to neuroendocrine, secretory, ciliated and goblet cells while the Id2^{+}/Sox9^{+} cells give rise to AT-I and AT-II cells (1). Figure is adapted from Herriges and Morrisey, Development 2014.

Several groups showed that loss of Sox2 results in reduction of ciliated and secretory cells in the lung epithelium (table 1) (8, 9). One of these studies used a Nkx2.5-Cre;Sox2$^{COND/+}$ mouse model in which Sox2 is conditionally deleted from the ventral foregut epithelium (8). The tracheal epithelium of these mice contained a reduced number of basal cells, Club cells and ciliated cells and more mucus-producing cells than wild type mice (8). A second mouse model used the Scgb1a1 promoter to express Sox2 in the respiratory epithelial Club cells. Expression of Sox2 resulted in cell proliferation and hyperplasia of the alveolar cells. Furthermore, an increase of markers of Club cells (*Scgb1a1, Car3, Cyp2f2*), ciliated cells (*Tubb3, Foxj1*) and basal cells (*Trp63*) was observed, which are all proximal epithelial cells (9). A mouse model in which the Notch signaling pathway, which is also involved in regulation of the airway epithelium, is affected also shows abnormalities in the composition of the airways epithelium. When the Notch signaling pathway is inhibited by blocking Jag1 and Jag2, a decrease in club cells and an increase in ciliated cells is observed, as well as a reverse in goblet cell hyperplasia (10). The Notch ligand Jag1 is also a target gene of Sox2, so deletion or overexpression of Sox2 directly affect Jag1 expression, resulting in similar changes of the airway epithelium as described by Que et al. (8). Ectopic Sox2 expression on the other hand resulted in the aberrant emergence of basal cells and neuroendocrine cells (11). This resulted in lungs with enlarged airspaces, abnormal alveolar formation and a decrease in the number of airways (11).

Table 1. Mouse models that show an effect on the airway epithelium.

Mouse model		Effect on airway epithelium
Nkx2.5-Cre;Sox2$^{COND/+}$ (8)	Conditional deletion of Sox2 from the ventral foregut epithelium	Decrease basal cells, Club cells and ciliated cells; increase mucus-producing cells
rCCSP-rtTA$^{tg/wt}$, (tetO)7CMVSox2$^{tg/wt}$ (9)	Ectopic Sox2 expression in the respiratory epithelial cells (driven by Scgb1a1 promoter)	Increase (markers) of basal cells, Club cells and ciliated cells
Scgb1a1-CreERT2^{GNE} (10)	Inhibition of Notch signaling by blocking its ligands Jag1 and Jag2	Increase ciliated cells; decrease club cells
iSox2$^{SPC\text{-}rtTA}$ (11)	Ectopic Sox2 expression in the epithelial cells of the developing lung (driven by the SPC promoter)	Increase basal cells and neuroendocrine cells

In chapter 2 we showed that the size of these cyst-like structures depended on the timing of Sox2 expression. The ectopic expression of Sox2 in the distal epithelial cells forced these cells to become proximal cells unresponsive to Fgf10 signaling. This proximalization of the epithelial cells caused the lungs to have reduced branching with large cysts. We also showed that Sox2 directly regulates the Trp63 and Gata6 genes, which may explain the emergence of Trp63^{+} basal cells and Gata6^{+} bronchoalveolar stem cells. Previous microarray data showed that levels of the ΔN Trp63 were increased in the lungs of iSox2$^{SPC\text{-}rtTA}$ mice. We now showed that Sox2 directly binds to the ΔN Trp63 promoter *in vivo*, thereby directly regulating its expression. Trp63 is a regulator of basal cells and these cells can form ciliated and secretory cells and are capable of self-renewal(12-14). Besides regulation of Trp63, Sox2 also directly regulates Gata6 transcription. During lung development Gata6 is expressed in the proximal bronchiolar epithelium and is also involved in branching morphogenesis and epithelial cell differentiation (15). Gata6 is involved in the regulation

of BASCs in the lung and when Gata6 is deleted from the lung epithelium, this results in premature appearance of BASCs (16). The fact that Sox2 directly regulates Trp63 and Gata6 expression and thereby regulating the emergence of basal cells and BASCs, showing the importance of Sox2 in proximal cell fate determination.

Sox2 and lung plasticity

An important issue in lung epithelial cell differentiation and regeneration is the plasticity of the different epithelial cells. In chapter 3, we describe the reprogramming of AT-II cells by ectopic Sox2 expression. This showed that the cell fate of fully differentiated distal epithelial cells can be changed to a proximal cell fate by the expression of a single transcription factor. Previously it has been shown that by inducing Sox2 expression, several cell cycle genes were upregulated and that there was induction of proliferation (17). In chapter 3, we also detected expression of phospo-histone H3 and cyclinD1 in cells where Sox2 was ectopically expressed, showing the proliferation of these cells. When Sox2 expression was induced in these cells, proliferation and formation of cuboidal cell clusters was observed. These cells were positive for both Sca1 and Ssea1, which are stem cell markers, and Sox2 directly regulated expression of Sca1. We also observed co-expression of Spc and Cc10, which all together mark the BASC, and Trp63. This showed that it is possible to change cell fate of distal lung cell types into proximal lung cell types, by expressing just one transcription factor. Recently, it was shown that ectopic Sox2 expression in AT-I cells has a similar effect (18). Other studies also showed the plasticity of AT-I and AT-II cells. Alveolar type II (AT-II) cells have the capability to differentiate into alveolar type I (AT-I) cells and more recently it was also shown that $Hopx^+$ AT-I cells can differentiate into $Sftpc^+$ AT-II cells. This was shown using pneumonectomy (19, 20). More epithelial cells in the lung have shown plasticity under selective conditions. Lineage tracing experiments showed that after damage of the lung epithelium (by ablation of the basal cells), $Scgb1a1^+$ cells are able to dedifferentiate into $Trp63^+/Krt5^+$ basal cells, which subsequently differentiate into secretory and ciliated cells (13) (21). The transcription factor Yes-associated protein (Yap1) is involved in this dedifferentiation process (22). Yap1, a member of the Hippo signaling pathway is involved in stem cell self-renewal and tissue regeneration (23). Deletion of Yap1 from airway basal cells resulted in a columnar epithelium with a reduced number of basal cells. Overexpression of Yap1 on the other hand, results in a thickened stratified epithelium (22). In the basal cells there is interaction of Yap1 and ΔN Trp63, resulting in the regulation of common target genes (22). Ciliated cells have also shown plasticity. A asthma model in which human primary bronchial epithelial cells were exposed to IL-13, showed that $Foxj1^+$ ciliated cells have to ability to differentiate into goblet cells (24). This is in line with the goblet cell hyperplasia that is observed in patients with mild and moderate asthma(25). The plasticity or transdifferentiation of epithelial cells is very rare under homeostatic conditions, but due to damage and injury these processes are observed. Knowledge of the plasticity of these lung epithelial cells and how the cell fate of these cells can be changed could be used in regenerative medicine and therapies for diseases like asthma and chronic obstructive pulmonary disease (COPD), although damage models in mice that were used to show these transdifferentiation effects are very extreme, so it remains unclear how comparable this is with transdifferentiation effects in the human lung after lung injury and disease. When it is known which pathways are involved in lung regeneration and lung disease, therapies in diseases could be based on drugs that either induce or inhibit these pathways. For example, the Notch signaling pathway would be a

good target for patients with COPD, since it has been shown that Notch3 is down-regulated in the lungs of COPD patients (26, 27). Furthermore, deletion of Notch3 results in basal cell expansion, which is characteristic for patients with COPD (28, 29). As previously described, Notch signaling interference also results in an increase in ciliated cells and reversed goblet cell hyperplasia (10). This could be used in COPD patients to reduce the production of mucus and to increase mucus clearance.

Knowledge of factors involved in cell fate determination of different lung epithelial cells opens possibilities to mimic these processes *in vitro*. Since the introduction of induced pluripotent stem cells in 2006, many studies have been published in which the differentiation of (induced pluripotent) stem cells into human airway and alveolar epithelial is described (30-43). These protocols still require optimization before they can be used as standard practice in clinical applications. Since Sox2 is one of the transcription factors involved in epithelial differentiation, knowledge of its partners could help to optimize these differentiation protocols. Differentiation of stem cells into lung cells is necessary for the development of lung mimics, such as air-liquid interfaces and organoids, and for the generation of lung tissue. In the future this will offer new perspectives for patients suffering from lung injury and disease.

Sox2 interaction networks and its clinical relevance

Anophthalmia-/esophageal-Genital (AEG) syndrome is associated with eye disorders (anopthalmia/microphthalmia), oesophageal atresia (with or without trachea-oesophageal fistula) and anomalies of the urogenital tract (44). Comparable abnormalities are also present in yet another syndrome that displays multiple syndromes, CHARGE syndrome (coloboma, heart defects, atresia of the choanac, retarded growth, genital hypoplasia and ear abnormalities) (45). Due to the large variability in phenotypes of AEG syndrome and CHARGE syndrome, it is very difficult to distinguish these two syndromes clinically (44, 45). SOX2 is linked to AEG syndrome, while CHD7 is involved in CHARGE syndrome (44, 46, 47). The finding that SOX2 and CHD7 are interacting partners suggested a molecular link between the two syndromes. Moreover, the SOX2-CHD7 complex was shown to regulate genes that are implicated in other syndromes that share features associated with AEG and CHARGE, such as Feingold syndrome (MYCN), Alagille syndrome (JAG1) and Pallister-Hall syndrome (GLI3) (48). This may suggest that the molecular pathways involved in these syndromes are similar (48). Furthermore, we also showed interaction of Sox2 with Exportin 4 (Xpo4) (49), which is involved in nuclear import of Sox2. Importantly, we showed that Sry, which has 85% overlap in HMG domain with Sox2, is also imported by Xpo4 (49). Some mutations have been shown to cause defects in nuclear localization of SRY in XY females (50). Our group showed that these mutations disrupted the interaction with Xpo4 and thus the nuclear import, providing a molecular explanation for the sex reversal (49). The interactions of Sox2 with Chd7 and Xpo4, show the importance of Sox2 interaction partners in a clinical context.

Several studies have identified Sox2 interaction partners *in vitro* using different cell lines (48, 51-53). There is quite some variability between the different datasets in these studies, which may reflect the cell-specificity of the Sox2 interaction partners. We aimed to identify Sox2 partners isolated directly from lung tissue during development. Since Sox2 expression is both temporally and spatially regulated, we expected to detect a dynamic change in

partners during the different stages of lung development. In chapter 4 we describe the biotinylated-Sox2 mouse model we generated for this purpose. This mouse model contains a biotinylatable tag at the N-terminus of the endogenous Sox2 gene (bioSox2). This tag can be biotinylated by the bacterial birA proteins resulting in a fully functional bioSox2 protein. The biotinylation and subsequent purification by streptavidin of transcription factors has been previously described (54). The BioSox2/birA mice were used to purify bioSox2 complexes from both lung and brain tissue. As validation we also identified several partners that were previously identified in embryonic stem cells and neural stem cells. Several of the partners identified in lung tissue could be linked to respiratory phenotypes. The overlap between the partners identified in the bioSox2 purifications with lung tissue and brain tissue is very low, showing that interaction between Sox2 and its partners is tissue-specific. This makes it difficult to extrapolate our findings in lung tissue to other tissues.

We also performed a large scale purification in a human lung adenocarcinoma cell line stably expressing a FLAG-Sox2 transgene. This is a more homogenous cell population, which might give less background. This construct has also been used to identify Sox2 partners in ES cell, which showed that the FLAG tagged Sox2 was fully functional (48, 49). We found 28 putative binding partners that were also identified in the lung tissue purifications. Naturally, we also detected some differences, which are probably caused by the fact that A549 cells are a carcinoma cell line. Additionally, the cell line may not reflect the normal cellular microenvironment of the lung. Despite the disadvantage, we could still link some of the identified target genes to a respiratory phenotype. Although the data derived from the A549 cells provides less insight in partners involved in lung development, they may provide more insight in the Sox2 partner complexes in lung cancer. The A549 cell line is an adenocarcinoma lung cell line, isolated from cancerous lung tissue (55). All types of lung cancer tissue show an increased expression of Sox2, including lung adenocarcinoma. In approximately 20 percent of patients suffering from lung adenocarcinoma an amplification of Sox2 was found which was also associated with a poor prognosis and shorter overall survival (56-58). The partners identified in the A549 cell line may be involved in the pathogenesis of lung adenocarcinoma and could provide more inside in the pathways behind this disease. These pathways may then serve as therapeutic targets, thereby increasing the survival rate of these patients.

To identify the Sox2 interactome of the lung that is more comparable to the *in vivo* Sox2 interactome, it would be a better option to use primary human bronchial epithelial cells. Several groups have shown the differentiation of embryonic stem cells and induced pluripotent stem cells into different types of lung cells, including AT-II cells, multiciliated cells and lung and airway progenitor cells (31) (32, 34-43). Optimization of these differentiation methods is required but the ability of generating a specific lung cell type also provides perspectives for the identification of Sox2 partners since this would give the opportunity to identify partners in a specific cell type.

Interaction of Sox2 with Chd4, FoxP2/4 and Cux1 in the developing lung

In chapter 5 we describe the interaction of Sox2 with Chd4, FoxP2/4 and Cux1 in the developing lung (fig. 2). These partners were identified with bioSox2 purification in E18 lungs (table 2). We and others found Chd4 as a potential interaction partner, but this interaction

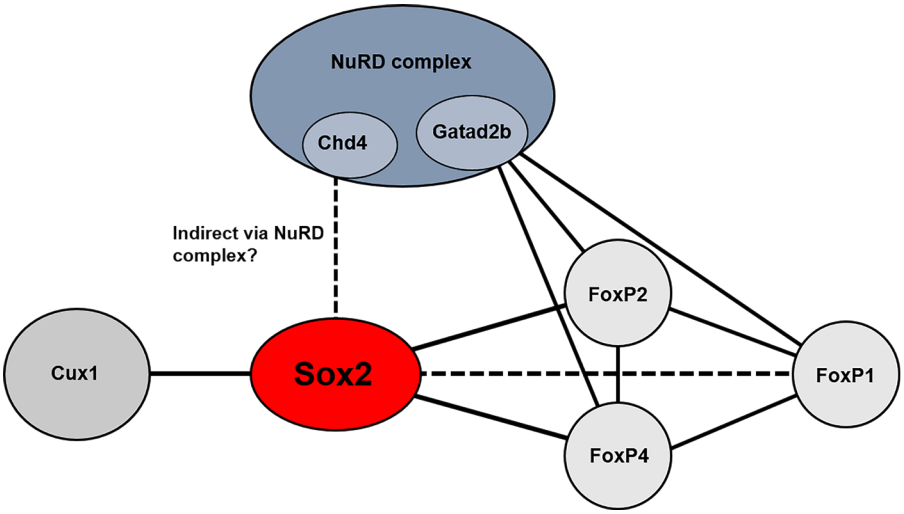

Figure 2. Schematic representation of the interaction between Sox2 and partners identified in chapter 5 during lung development. Black lines represent validated interactions, while dashed lines give expected interactions.

has not been validated nor has the functionality been examined (Gontan, unpublished data) (48). During the canalicular and saccular phase of lung development, co-localization of Sox2 and Chd4 was detected in the epithelial cells of the proximal airways, suggesting that interaction between Sox2 and Chd4 is possible in these cells. We also validated interaction between Chd4 and Sox2, although we could not detect this interaction with GST-fusion proteins. This could be explained by the physiological conditions of the experiments. While the lung develops under relative hypoxic circumstances, the interaction assays were performed under normoxic conditions. Hypoxia causes stabilization and activation of Hif1α, which regulates the expression of Chd4. Therefore, there is upregulation of Chd4 under hypoxic circumstances, and this higher expression of Chd4 could be the reason why we detect interaction with Sox2 *in vivo* but no direct interaction in the normoxic *in vitro* assays (59).

Table 2. Identification of Chd4, FoxP1/2/4 and Cux1 as Sox2 candidate binding partners in lung tissue using mass spectrometry analysis.

	BioSox purification lung tissue		BioSox2 purification trachea tissue	
Symbol	Mascot[a]	Peptides[b]	Mascot[a]	Peptides[b]
Chd4	1343 (939)	26 (21)	319 (N.A.)	7 (0)
Cux1	476 (N.A.)	8 (0)	N.A.	N.A.
FoxP1	146 (N.A.)	3 (0)	N.A.	N.A.
FoxP2	61 (N.A.)	2 (0)	N.A.	N.A.
FoxP4	86 (N.A.)	2 (0)	N.A.	N.A.

[a] Mascot score of the identified binding partner, mascot score of the control is between brackets.
[b] Number of unique proteins for the identified binding partner, mascot score of the control is between brackets.

Another possible explanation for not detecting a direct interaction between Sox2 and Chd4 is the involvement of other factors in the interaction complex. Likely candidates are components of the nucleosome remodeling and deacetylase (NuRD) complex, from which Chd4 is one of the subunits. Other components of this complex are histone deacetylases Hdac1/2, Gatad2a/b, retinoblastoma-binding proteins Mta1/2/3 and the non-enzymatic proteins Mbd2/3 (60). It was previously shown by Cox et al. that Hdac1/2 are direct interaction partners of Sox2 (51). Other partners of the NuRD complex were also identified as putative partners in several studies. FLAG-Sox2 purifications in neural stem cells, suggested possible interaction between Sox2 and Mta1/2, Gatad2a/b and Hdac1/2, while in the medulloblastoma cell line DAOY, Mta1/3, Gatad2a, Hdac1/2 and Mbd2 were identified as putative Sox2 partners (48, 52). Previous FLAG-Sox2 purifications in embryonic stem cells performed by our group, also identified several components of the NuRD complex as putative interactors of Sox2 (unpublished data). In the same large scale bioSox2 purification in which Chd4 was detected, we also detected Gatad2a/b and Hdac2 (enriched in both lung and trachea), and Hdac1 and Mta1/2 (enriched in trachea). This suggests that the Sox2-Chd4 interaction could be mediated by one of these factors. This could be validated by determining which factors are capable of direct physical interaction with Sox2. Hdac1/2 could be interesting potential partners since these histone deacetylases are bot involved in regeneration of $Sox2^+$ lung endoderm progenitors (61). Deletion of Hdac1/2 leads to a decrease in Sox2 expression which results in loss of branching morphogenesis and enlarged airspaces (61). Bmp4, which is a direct target of Hdac1/2, is inhibited when Hdac1/2 is deleted, which causes a decrease in $Sox2^+$ progenitor cells while there is an expansion of $Sox9^+/Id2^+$ progenitor cells, resulting in abnormal formation of the proximal airways in the developing lung (61). Another histone deacetylase, Hdac3, has recently be shown to be involved in remodeling of lung alveolar epithelial cells (62). They observed increased thickening of the alveolar wall and more compact distal airspaces when Hdac3 was deleted from the lung. Hdac3 is also important for the spreading of the AT-I cells(62). Several studies have linked the NuRD complex to repression of genes involved in lymphoma, hematopoiesis and prostate and breast cancer (63-66). This is regulated by direct or indirect interaction with a DNA-binding protein (60). For example, in glioblastoma cells, there is interaction between ZFHX4 and the NuRD complex via CHD4 to regulate the tumor-initiating cell state (67). Sox2 is also a DNA-binding protein, suggesting that this is one of the proteins that regulates the ability of the NuRD complex to regulate gene transcription. It should first be determined which of the components of the NuRD complex are interacting with Sox2 in the lung. This could provide more insight in the functionality of the complex during lung development.

Previous studies have identified target genes of Sox2 in neural stem cells and Chd4 in endothelial cells (48, 68). Comparison of these targets showed some overlap although it has not been studied if they both bind in the same region. One of these common target genes is Id2, a distal epithelial cell marker. When Chd4 is deleted, an upregulation of Id2 expression is observed (68). Since Id2 is also a target of Sox2, it might by that Id2 expression is repressed by both Sox2 and Chd4, thereby preventing cells from a distal cell fate to differentiate into proximal cells. To gain more insight in the role of Chd4 in distal-proximal cell lineage specification in the lung, it would be interesting to study the effect of selective ablation of either Chd4 or Sox2 on the expression of Id2 and Sox9. Schwann cells with an inactivated Chd4, showed an upregulation of Sox2(69). To identify target genes of Chd4,

we performed chromatin immunoprecipitations (ChIP). In chapter 5 we showed that we detected an enrichment of Sox2 in the single cross-linked Chd4 ChIP. This suggests that Chd4 is rather a direct interactor of Sox2 transcriptional activity than a direct interaction partner. It would also be interesting to study the effect of Chd4 on Sox2 regulation.

In chapter 5 we also showed that FoxP2 and FoxP4 are Sox2 interaction partners. FoxP1/2/4 expression overlap in the developing tissues and by forming specific dimer combinations, the expression of different target gene subsets is regulated (70). Deletion of FoxP1 and FoxP4 is embryonic lethal preventing detailed lung analysis, but FoxP2$^{-/-}$ mice showed lung alveolarization defects (71). Interplay between FoxP1 and FoxP2 is involved in esophagus development and morphogenesis of the airways and both of these factors are able to repress the promoters of the human surfactant protein C and the CC10 genes, which are markers of differentiated epithelial cells (72, 73). In chapter 3, we observed an increase in expression of CC10 after ectopic Sox2 expression in fully differentiated AT-II cells, suggesting opposite roles for Sox2 and FoxP1/2 in the regulation of these two genes. Conditionally deletion of FoxP1/4 resulted in a decrease of secretory cells, which suggest the involvement of Foxp1/4 in secretory cell fate (74). Secretory cells are derived from Sox2^{+} progenitor cells, so interaction between Sox2 and FoxP1/4 could be involved in cell fate regulation of these cells. This may provide more insights in the role of the Sox2-FoxP2 partner complex during early lung development.

In chapter 5, we also showed that Sox2 expression is restricted to the proximal airways during the late pseudoglandular, canalicular and saccular phases of lung development, while FoxP2 is restricted to the distal airways. However, during the embryonic and early pseudoglandular phase, we did detect co-localization of Sox2 and FoxP2 in the cells localized at the branching site between the proximal and distal region. This broncho-alveolar duct junction contains BASCs, which are characterized by the expression of Scgb1a1 and Spc (75). In this area, a change of the subcellular localization of Yap1 is observed (76). While Yap1 in the upper airway epithelium is expressed in the cytoplasm, expression in the distal tips is nuclear (76). At this same region where localization of Yap is switched, cells start to express Sox2. In this region, both the expression of Sox2 and Yap1 are nuclear (76). Since it is previously shown that Yap1 can regulate Sox2 expression, this data suggests that Sox2 is regulated by Yap1 in the broncho-alveolar duct (76-78). In chapter 2 we describe that Sox2 directly regulated Gata6 in the lung, and thereby the emergence of BASC cells. It would be interesting to further study if and how FoxP2 is involved in this process. Stainings for BASC specific markers should be done to ascertain that the cells that do co-express FoxP2 and Sox2 are indeed BASCs. Furthermore, it would be interesting to study if FoxP2 is also involved in the regulation of Gata6. FoxP2 was also identified as Sox2 interactor in one of the bioSox2 purifications with brain tissue, suggesting that the Sox2-FoxP2 complex could be involved in other organs besides the lung.

FoxP1/2/4 also interacts with the NuRD complex via its component Gatad2b and this interaction complex is involved in lung injury as well as in repair and regeneration (79). This mechanism acts as a response to hyperoxic injury, which is often seen in premature babies. Worldwide many of these babies are mechanically ventilated after birth and thereby exposed to high levels of oxygen which may cause lung injury (80). This type of lung injury is defined as the old bronchopulmonary dysplasia (BPD). Characteristics of this disorder

include disruption of the lung structure, smooth-muscle hypertrophy and diffuse airway damage as well as a loss of pulmonary vessels (80). Nowadays, the old definition of BPD is largely replaced by new BPD which is caused by very preterm birth, resulting in under-developed alveoli at the moment of birth (80, 81). Exposure of mice to hyperoxia results in damage of the AT-I cells (79). After such damage AT-II cells start to differentiate into AT-I cells to repopulate the alveolar epithelium (82, 83). The NuRD complex together with the FoxP factors is involved in this response to hyperoxic injury by directly relating cytokine IL-6, leading to higher resistance to hyperoxic lung injury (79). Since we and others suggested an interaction between Sox2 and the NuRD complex, it would be interestingly to study if the Sox2-NuRD complex association is involved in similar injury responses in the bronchial epithelium.

Cut-Like Homeobox1 (Cux1) was also identified as a Sox2 interaction partner. This transcription factor was previously identified as a putative Sox2 interaction partner in neural stem cells and DAOY cells, but interaction had not been validated yet (48, 52). Several Cux1 mouse models have been described, showing roles for Cux1 in development of hair follicles, skin, bones, kidneys and the reproductive system (84-87). Cux1 mutants that carry a deletion of the cut repeat 1 region have lactation defects and wavy hair and curly whiskers (84). When these mice were crossed with a mice strain that develops cysts in their kidneys, this results in larger cysts, indicating that defects in Cux1 accelerate the growth of these cysts (85). Mice in which the C-terminus of Cux1 was deleted also showed abnormalities in their fur and whiskers, and these mice also suffered from hematopoietic defects as well as defects of lymphoid and myeloid development (86). These same morphological abnormalities were observed in another strain in which the C-terminus was deleted. Besides these defects, these mice also had a reduced male fertility (87). A mouse model in which an inactive Cux1 protein is expressed, suggests a role for Cux1 in lung development (88). These mice have a thick, non-functional epithelium and die of respiratory distress shortly after birth (88). Looking at the morphology of these lungs, enlargement of the airways was observed. In chapter 2, we observed a similar lung morphology in the iSox2$^{SPC\text{-}rtTA}$ mice, in which we ectopically expressed Sox2 in the epithelial cells of the developing airways. In chapter 5, we noticed that the formation of Cux1 isoforms was inhibited when Sox2 was expressed in high extents. It could be that in the iSox2$^{SPC\text{-}rtTA}$ mice, formation of Cux1 isoforms is also inhibited, contributing to a similar phenotype as seen in the mice that express an inactive Sox2 protein.

Sox2 and Cux1 co-localize in subsets of the proximal airway epithelium in the developing lung. Sox2^{+} progenitor cells give rise to neuroendocrine cells, secretory cells, ciliated cells and goblet cells in the upper airways of the developing lung (6). Since Cux1 expression is not detected in all the proximal epithelial cells, this suggest that the Sox2-Cux1 partner complex could be involved in the differentiation of one of these subsets of cells. Stainings for specific cell markers should clarify which subset of cells is involved. Cux1 homologue Cut expression studies in *Drosophila* showed that during early development, Cut is expressed in multipotent progenitor cells of the airways, while later only some subsets of cells express Cut (89). This could be similar in lung development in mice. These Cut positive cells are possibly involved in cell proliferation (89). In the cells of the developing and adult central nervous system, Cux1 expression is also linked to proliferation of cells. Proliferation of stem cells and progenitor cells in the central nervous system is regulated by Sox2 in a

dose-dependent manner. In stem cells, high levels of Sox2, repress proliferative genes, thereby preventing cell cycle progression (90). When these cells start to differentiate, they lose expression of Sox2 and start to express Cux1 (90). This suggests that high levels of Sox2 prevent post-translationally processing of Cux1 (90). We detected a similar influence of the level of Sox2 expression on the processing of Cux1 isoforms. When Sox2 was robustly expressed, only the full length isoform p200 was detected, while at low Sox2 expression also the p150, p110 and p75 isoforms were detected. The different Cux1 isoforms are products of different mRNA transcripts and the result of proteolytic cleavage and the different isoforms show different DNA binding properties (91, 92). Binding to DNA of the p200 isoform is very rapid and unstable, suggesting very low transcriptional activity of Cux1 when only this isoform is expressed, as seen in cells with high Sox2 expression. This would mean that high Sox2 expression could prevent stable binding of Cux1 to DNA, thereby causing low transcription Cux1 activity. One of the molecular pathways involved in this mechanism could be Wnt signaling. Previous research suggested that high levels of Wnt signaling has no effect on development of the alveoli but does affect differentiation of bronchiolar cell lines (93). By activating β-catenin in the endoderm of the developing lung, levels of canonical Wnt signaling are remained high. This resulted in an expansion of $Sox9^+$ cells in the larger airways (93). A similar effect was seen in the lungs of conditional Sox2-null mutants. These $Sox9^+$ cells were unable to differentiate into normal airway epithelium (93). These results showed that Wnt downregulation is required for expression of Sox2 and the generation of the epithelial cells in the proximal airways. They also found that ectopic Wnt activation resulted in loss of Trp63, which is in line with our findings that Sox2 directly regulates the transcription of Trp63 (93), Cux1 can activate the Wnt signaling pathway by stimulating the activity of β-catenin, which is shown in breast cancers where Cux1 cooperates with Glis1 to activate β-catenin (94). Specifically the p110 Cux1 isoform is responsible for this activation (94). This suggests that the p110 isoform can indirectly down-regulate the expression of Sox2 by activating the Wnt signaling pathway.

It was previously shown that multiple domains are involved in the interaction of Sox2 with its associating partners (51). This was shown by comparing the interaction of partners with full length Sox2 and different Sox2 mutant proteins, either lacking the HMG domain or the C-terminal transcription domain or only expression the HMG domain (51). Only the HMG domain of Sox2is required for interaction with Hdac2, while multiple Sox2 domains are involved in the interaction with Hdac1 (51). For interaction between Sox2 and Sall4, the C-terminal part is important for interaction since binding is observed in much lower extends when this part is missing (51). In chapter 5, we describe a similar assay to determine interaction between Sox2 and Cux1 and particular interaction depends on the DNA-binding domain and N-terminus of Sox2. Our lab previously showed the importance of conserved residues in the HMG box of Sox2 in the interaction with Xpo4 (49). For Cux1, these conserved residues are also necessary for interaction. When there is a mutation of one of these residues, interaction is no longer detected. Since not all domains of Sox2 are involved in interaction with Sox2, other proteins could, together with Cux1, interact with Sox2, forming a complex of different transcription factors.

In the FlagSox2 purification in A549 cells in chapter 4, we also identified Cux1 as Sox2 partner. A549 cells are a adenocarcinomic alveolar basal epithelial cell line, so our findings could suggest a role for the Sox2-Cux1 partner complex in lung cancer. Several

studies have shown overexpression of Sox2 in cancer, including non-small cell lung cancer (NSCLC) and small cell lung cancer (SCLC) and in all types of lung cancer, overexpression of Sox2 is described (95-97) (56). In lung adenocarcinomas, Sox2 might be part of the activating pathway to develop this cancer (98). Although no studies have linked Cux1 to lung cancer yet, it has been shown that Cux1 can be involved in both the suppression and progression of tumors (92). In some breast tumors, there is an overexpression of the p75 and p110 isoforms. Transgene mice that express these isoforms in mammary epithelial cells, developed mammary tumors (99). In chapter 5 we showed that these isoforms are also expressed in A549 cells. Performing Sox2 immunoprecipitations in these cells could provide insight in the specific Cux1 isoform interacting with Sox2 in A549 cells, thereby providing more insight in the tumorigenicity of the Sox2-Cux1 complex and the potential role in lung cancer.

Regulation of Sox2 target genes

In Chapter 4, we identified target genes of SOX2 in NCCIT cells by performing chromatin immunoprecipitations (ChIPs) followed by sequencing. Single and double cross-linked ChIPs were performed to evaluate direct protein-DNA interactions and to identify protein-protein-DNA interactions respectively. In both the single and double cross-linked SOX2 ChIP several targets could be linked to lung and respiratory tube development including GLI2 and GLI3. GLI2 and 3 have previously been identified as SOX2 target genes in neural stem cells (48). Other targets involved in lung development are HOPX, HHIP, PDPN (T1-α), BMPR1A and TNS3. Interestingly, most of these targets are distal cell markers, while Sox2 is only expressed in the epithelial cells of the proximal airways. If Sox2 is repressing the expression of these genes, that would explain why there is no expression of these genes in the proximal epithelial cells. This would also mean that when Sox2 is expressed in AT-I and AT-II cells, expression of these distal markers is inhibited, contributing to dedifferentiation of these cells in proximal epithelial cells. As mentioned earlier, interaction partners of Sox2 are tissue-specific. This means that target genes that are regulated by the Sox2-partner complex are also tissue-specific. In chapter 4 and 5 we used NCCIT cells for the ChIPs, due to the high expression of Sox2 and its partners in this cell line. Since the NCCIT cells are an embryonic carcinomic cell line, and not a lung cell line, the Sox2 interactome in these cells, and thereby the regulated target genes will differ from the *in vivo* interactome in the lung. This could explain why we identified targets with our ChIP that are not expressed in the Sox2 expressing regions of the lung. ChIPs using streptavidin should be performed on lung tissue from bioSox2/birA mice, to identify Sox2 targets that are specific during lung development.

Another interesting direct target identified is β-catenin, a component of the canonical Wnt signaling pathway. During early lung development β-catenin is inducing Wnt2 and Wnt2b which results in the specification of lung progenitors in the foregut endoderm (3, 4). Later during development, β-catenin is required for proper proximal-distal lung patterning (100). When β-catenin is deleted from the epithelial cells of the developing lung during early stages of development, the epithelium primarily consists of proximal epithelial cells suggesting a role for β-catenin in distal cell fate (101). Our data identified β-catenin as a direct target of Sox2, which could suggest that expression of β-catenin is downregulated by Sox2 in proximal epithelial cells, thereby preventing these cells to obtain a distal cell fate. Previously it was shown that β-catenin is an interaction partner of Sox2 and that β-catenin

can also inhibit Sox2 transcriptional activity (102).

In the double cross-linked SOX2 ChIP, GRHL2 was identified as a target gene. This suggests that Sox2 indirectly regulates expression of Grhl2 by interacting with a partner and not by direct DNA binding. In the airway epithelium of the human lung, GRHL2 is expressed in $Trp63^{+}/KRT5^{+}$ basal cells where it functions as a regulator for several processes including cell morphogenesis (103). Grhl2 is necessary for establishment and maintenance of the epithelial barrier and knock-down of Grhl2 results in the inability for basal cells to differentiate. Grhl2 is a direct regulator of ΔN Trp63 (104). In chapter 2 we showed that Sox2 is also directly regulating the same Trp63 isoform and that there is induction of Trp63 expression when Sox2 is ectopically expressed. It would be interesting to study how ectopic Sox2 expression influences the expression of Grhl2, which could be done by selective ablation of Sox2.

Conclusion

Through new techniques like lineage-tracing experiments, the knowledge about lung stem and progenitor cells and the markers they are characterized by has markedly increased. Targeting progenitor cell populations or activating the plasticity of differentiated lung cells could be used for novel strategies for lung epithelium regeneration in lung diseases and congenital anomalies. We have shown that Sox2 is directly involved in the emergence of basal cells and BASCs by directly regulating Trp63 and Gata6 (chapter 2). Furthermore, we showed that Sox2 induced transdifferentiation of AT-II cells into proximal cells (chapter 3). These data contribute to show that Sox2 is important in epithelial cell differentiation in lung development and repair. To gain more insight in the role of Sox2 during lung development we generated a biotinylated Sox2 mouse model, from which we could successfully purify bioSox2-partner complexes *in vivo* (chapter 4). Interaction with putative partners Chd4, FoxP2/4 and Cux1 was validated and expression patterns of these partners showed co-localization with Sox2 in the developing lung (chapter 5). Furthermore we found that SOX2 and CHD4 could be involved in co-regulation of genes involved in the respiratory system (chapter 5). Knowledge about the development of the healthy lung will contribute to unraveling the molecular pathways behind congenital diseases of the newborn.

References

1. Volckaert T, De Langhe S. Lung epithelial stem cells and their niches: Fgf10 takes center stage. Fibrogenesis Tissue Repair. 2014;7:8.
2. Volckaert T, De Langhe SP. Wnt and FGF Mediated Epithelial-Mesenchymal Crosstalk During Lung Development. Dev Dynam. 2015;244(3):342-66.
3. Goss AM, Tian Y, Tsukiyama T, Cohen ED, Zhou D, Lu MM, et al. Wnt2/2b and beta-catenin signaling are necessary and sufficient to specify lung progenitors in the foregut. Dev Cell. 2009;17(2):290-8.
4. Harris-Johnson KS, Domyan ET, Vezina CM, Sun X. beta-Catenin promotes respiratory progenitor identity in mouse foregut. Proc Natl Acad Sci U S A. 2009;106(38):16287-92.
5. Domyan ET, Ferretti E, Throckmorton K, Mishina Y, Nicolis SK, Sun X. Signaling through BMP receptors promotes respiratory identity in the foregut via repression of Sox2. Development. 2011;138(5):971-81.
6. Herriges M, Morrisey EE. Lung development: orchestrating the generation and regeneration of a complex organ. Development. 2014;141(3):502-13.
7. Volckaert T, Campbell A, Dill E, Li C, Minoo P, De Langhe S. Localized Fgf10 expression is not required for lung branching morphogenesis but prevents differentiation of epithelial progenitors. Development. 2013;140(18):3731-42.
8. Que J, Luo X, Schwartz RJ, Hogan BL. Multiple roles for Sox2 in the developing and adult mouse trachea. Development. 2009;136(11):1899-907.
9. Tompkins DH, Besnard V, Lange AW, Keiser AR, Wert SE, Bruno MD, et al. Sox2 Activates Cell Proliferation and Differentiation in the Respiratory Epithelium. Am J Resp Cell Mol. 2011;45(1):101-10.
10. Lafkas D, Shelton A, Chiu C, de Leon Boenig G, Chen Y, Stawicki SS, et al. Therapeutic antibodies reveal Notch control of transdifferentiation in the adult lung. Nature. 2015;528(7580):127-31.
11. Gontan C, de Munck A, Vermeij M, Grosveld F, Tibboel D, Rottier R. Sox2 is important for two crucial processes in lung development: branching morphogenesis and epithelial cell differentiation. Dev Biol. 2008;317(1):296-309.
12. Rock JR, Onaitis MW, Rawlins EL, Lu Y, Clark CP, Xue Y, et al. Basal cells as stem cells of the mouse trachea and human airway epithelium. P Natl Acad Sci USA. 2009;106(31):12771-5.
13. Tata PR, Mou HM, Pardo-Saganta A, Zhao R, Prabhu M, Law BM, et al. Dedifferentiation of committed epithelial cells into stem cells in vivo. Nature. 2013;503(7475):218-+.
14. Rock JR, Gao X, Xue Y, Randell SH, Kong YY, Hogan BLM. Notch-Dependent Differentiation of Adult Airway Basal Stem Cells. Cell Stem Cell. 2011;8(6):639-48.
15. Koutsourakis M, Keijzer R, Visser P, Post M, Tibboel D, Grosveld F. Branching and differentiation defects in pulmonary epithelium with elevated Gata6 expression. Mech Dev. 2001;105(1-2):105-14.
16. Zhang Y, Goss AM, Cohen ED, Kadzik R, Lepore JJ, Muthukumaraswamy K, et al. A Gata6-Wnt pathway required for epithelial stem cell development and airway regeneration. Nat Genet. 2008;40(7):862-70.
17. Tompkins DH, Besnard V, Lange AW, Keiser AR, Wert SE, Bruno MD, et al. Sox2 activates cell proliferation and differentiation in the respiratory epithelium. Am J Respir Cell Mol Biol. 2011;45(1):101-10.
18. Yang J, Hernandez BJ, Martinez Alanis D, Narvaez Del Pilar O, Vila-Ellis L, Akiyama H, et al. The development and plasticity of alveolar type 1 cells. Development. 2016;143(1):54-65.
19. Desai TJ, Brownfield DG, Krasnow MA. Alveolar progenitor and stem cells in lung development, renewal and cancer. Nature. 2014;507(7491):190-+.
20. Jain R, Barkauskas CE, Takeda N, Bowie EJ, Aghajanian H, Wang QH, et al. Plasticity of Hopx(+) type I alveolar cells to regenerate type II cells in the lung. Nat Commun. 2015;6.
21. Zheng D, Yin L, Chen J. Evidence for Scgb1a1(+) cells in the generation of p63(+) cells in the damaged lung parenchyma. Am J Respir Cell Mol Biol. 2014;50(3):595-604.
22. Zhao R, Fallon TR, Saladi SV, Pardo-Saganta A, Villoria J, Mou HM, et al. Yap Tunes Airway Epithelial Size and Architecture by Regulating the Identity, Maintenance, and Self-Renewal of Stem Cells. Developmental Cell. 2014;30(2):151-65.
23. Zhao B, Tumaneng K, Guan KL. The Hippo pathway in organ size control, tissue regeneration and stem cell self-renewal. Nat Cell Biol. 2011;13(8):877-83.
24. Turner J, Roger J, Fitau J, Combe D, Giddings J, Heeke GV, et al. Goblet cells are derived from a FOXJ1-expressing progenitor in a human airway epithelium. Am J Respir Cell Mol Biol. 2011;44(3):276-84.
25. Ordonez CL, Khashayar R, Wong HH, Ferrando R, Wu R, Hyde DM, et al. Mild and moderate asthma is associated with airway goblet cell hyperplasia and abnormalities in mucin gene expression. Am J Respir Crit Care Med. 2001;163(2):517-23.
26. Tilley AE, Harvey BG, Heguy A, Hackett NR, Wang R, O'Connor TP, et al. Down-regulation of the notch pathway in human airway epithelium in association with smoking and chronic obstructive pulmonary disease. Am J Respir Crit Care Med. 2009;179(6):457-66.
27. Mori M, Mahoney JE, Stupnikov MR, Paez-Cortez JR, Szymaniak AD, Varelas X, et al. Notch3-Jagged signaling

controls the pool of undifferentiated airway progenitors. Development. 2015;142(2):258-67.
28. Khuri FR, Kim ES, Lee JJ, Winn RJ, Benner SE, Lippman SM, et al. The impact of smoking status, disease stage, and index tumor site on second primary tumor incidence and tumor recurrence in the head and neck retinoid chemoprevention trial. Cancer Epidemiol Biomarkers Prev. 2001;10(8):823-9.
29. Snitow ME, Li SR, Morley MP, Rathi K, Lu MM, Kadzik RS, et al. Ezh2 represses the basal cell lineage during lung endoderm development. Development. 2015;142(1):108-17.
30. Takahashi K, Yamanaka S. Induction of pluripotent stem cells from mouse embryonic and adult fibroblast cultures by defined factors. Cell. 2006;126(4):663-76.
31. Ali NN, Edgar AJ, Samadikuchaksaraei A, Timson CM, Romanska HM, Polak JM, et al. Derivation of type II alveolar epithelial cells from murine embryonic stem cells. Tissue Eng. 2002;8(4):541-50.
32. Van Haute L, De Block G, Liebaers I, Sermon K, De Rycke M. Generation of lung epithelial-like tissue from human embryonic stem cells. Respir Res. 2009;10:105.
33. Banerjee ER, Laflamme MA, Papayannopoulou T, Kahn M, Murry CE, Henderson WR, Jr. Human embryonic stem cells differentiated to lung lineage-specific cells ameliorate pulmonary fibrosis in a xenograft transplant mouse model. Plos One. 2012;7(3):e33165.
34. Samadikuchaksaraei A, Cohen S, Isaac K, Rippon HJ, Polak JM, Bielby RC, et al. Derivation of distal airway epithelium from human embryonic stem cells. Tissue Eng. 2006;12(4):867-75.
35. Wang D, Haviland DL, Burns AR, Zsigmond E, Wetsel RA. A pure population of lung alveolar epithelial type II cells derived from human embryonic stem cells. Proc Natl Acad Sci U S A. 2007;104(11):4449-54.
36. Rippon HJ, Polak JM, Qin M, Bishop AE. Derivation of distal lung epithelial progenitors from murine embryonic stem cells using a novel three-step differentiation protocol. Stem Cells. 2006;24(5):1389-98.
37. Firth AL, Dargitz CT, Qualls SJ, Menon T, Wright R, Singer O, et al. Generation of multiciliated cells in functional airway epithelia from human induced pluripotent stem cells. P Natl Acad Sci USA. 2014;111(17):E1723-E30.
38. Wong AP, Bear CE, Chin S, Pasceri P, Thompson TO, Huan LJ, et al. Directed differentiation of human pluripotent stem cells into mature airway epithelia expressing functional CFTR protein. Nat Biotechnol. 2012;30(9):876-U108.
39. Mou HM, Zhao R, Sherwood R, Ahfeldt T, Lapey A, Wain J, et al. Generation of Multipotent Lung and Airway Progenitors from Mouse ESCs and Patient-Specific Cystic Fibrosis iPSCs. Cell Stem Cell. 2012;10(4):385-97.
40. Longmire TA, Ikonomou L, Hawkins F, Christodoulou C, Cao YX, Jean JC, et al. Efficient Derivation of Purified Lung and Thyroid Progenitors from Embryonic Stem Cells. Cell Stem Cell. 2012;10(4):398-411.
41. Ghaedi M, Calle EA, Mendez JJ, Gard AL, Balestrini J, Booth A, et al. Human iPS cell-derived alveolar epithelium repopulates lung extracellular matrix. J Clin Invest. 2013;123(11):4950-62.
42. Huang SX, Islam MN, O'Neill J, Hu Z, Yang YG, Chen YW, et al. Efficient generation of lung and airway epithelial cells from human pluripotent stem cells. Nat Biotechnol. 2014;32(1):84-91.
43. Huang SXL, Green MD, de Carvalho AT, Mumau M, Chen YW, D'Souza SL, et al. The in vitro generation of lung and airway progenitor cells from human pluripotent stem cells. Nat Protoc. 2015;10(3).
44. Williamson KA, Hever AM, Rainger J, Rogers RC, Magee A, Fiedler Z, et al. Mutations in SOX2 cause anophthalmia-esophageal-genital (AEG) syndrome. Hum Mol Genet. 2006;15(9):1413-22.
45. Schulz Y, Freese L, Manz J, Zoll B, Volter C, Brockmann K, et al. CHARGE and Kabuki syndromes: a phenotypic and molecular link. Human Molecular Genetics. 2014;23(16):4396-405.
46. Vissers LE, van Ravenswaaij CM, Admiraal R, Hurst JA, de Vries BB, Janssen IM, et al. Mutations in a new member of the chromodomain gene family cause CHARGE syndrome. Nat Genet. 2004;36(9):955-7.
47. Zentner GE, Layman WS, Martin DM, Scacheri PC. Molecular and phenotypic aspects of CHD7 mutation in CHARGE syndrome. Am J Med Genet A. 2010;152A(3):674-86.
48. Engelen E, Akinci U, Bryne JC, Hou J, Gontan C, Moen M, et al. Sox2 cooperates with Chd7 to regulate genes that are mutated in human syndromes. Nat Genet. 2011;43(6):607-U153.
49. Gontan C, Guttler T, Engelen E, Demmers J, Fornerod M, Grosveld FG, et al. Exportin 4 mediates a novel nuclear import pathway for Sox family transcription factors. J Cell Biol. 2009;185(1):27-34.
50. Harley VR, Layfield S, Mitchell CL, Forwood JK, John AP, Briggs LJ, et al. Defective importin beta recognition and nuclear import of the sex-determining factor SRY are associated with XY sex-reversing mutations. Proc Natl Acad Sci U S A. 2003;100(12):7045-50.
51. Cox JL, Mallanna SK, Luo X, Rizzino A. Sox2 Uses Multiple Domains to Associate with Proteins Present in Sox2-Protein Complexes. Plos One. 2010;5(11).
52. Cox JL, Wilder PJ, Gilmore JM, Wuebben EL, Washburn MP, Rizzino A. The SOX2-Interactome in Brain Cancer Cells Identifies the Requirement of MSI2 and USP9X for the Growth of Brain Tumor Cells. Plos One. 2013;8(5).
53. Fang XF, Yoon JG, Li LS, Tsai YSS, Zheng S, Hood L, et al. Landscape of the SOX2 protein-protein interactome. Proteomics. 2011;11(5):921-34.
54. de Boer E, Rodriguez P, Bonte E, Krijgsveld J, Katsantoni E, Heck A, et al. Efficient biotinylation and single-step purification of tagged transcription factors in mammalian cells and transgenic mice. Proc Natl Acad Sci U S A.

2003;100(13):7480-5.
55. Giard DJ, Aaronson SA, Todaro GJ, Arnstein P, Kersey JH, Dosik H, et al. In vitro cultivation of human tumors: establishment of cell lines derived from a series of solid tumors. J Natl Cancer Inst. 1973;51(5):1417-23.
56. Karachaliou N, Rosell R, Viteri S. The role of SOX2 in small cell lung cancer, lung adenocarcinoma and squamous cell carcinoma of the lung. Transl Lung Cancer Res. 2013;2(3):172-9.
57. Sholl LM, Barletta JA, Yeap BY, Chirieac LR, Hornick JL. Sox2 protein expression is an independent poor prognostic indicator in stage I lung adenocarcinoma. Am J Surg Pathol. 2010;34(8):1193-8.
58. Cai YR, Zhang HQ, Zhang ZD, Mu J, Li ZH. Detection of MET and SOX2 amplification by quantitative real-time PCR in non-small cell lung carcinoma. Oncol Lett. 2011;2(2):257-64.
59. Ayrapetov MK, Xu C, Sun YL, Zhu KY, Parmar K, D'Andrea AD, et al. Activation of Hif1 alpha by the Prolylhydroxylase Inhibitor Dimethyoxalyglycine Decreases Radiosensitivity. Plos One. 2011;6(10).
60. Allen HF, Wade PA, Kutateladze TG. The NuRD architecture. Cell Mol Life Sci. 2013;70(19):3513-24.
61. Wang Y, Tian Y, Morley MP, Lu MM, DeMayo FJ, Olson EN, et al. Development and Regeneration of Sox2+ Endoderm Progenitors Are Regulated by a HDAC1/2-Bmp4/Rb1 Regulatory Pathway. Developmental Cell. 2013;24(4):345-58.
62. Wang Y, Frank DB, Morley MP, Zhou S, Wang X, Lu MM, et al. HDAC3-Dependent Epigenetic Pathway Controls Lung Alveolar Epithelial Cell Remodeling and Spreading via miR-17-92 and TGF-beta Signaling Regulation. Dev Cell. 2016;36(3):303-15.
63. Fujita N, Jaye DL, Kajita M, Geigerman C, Moreno CS, Wade PA. MTA3, a Mi-2/NuRD complex subunit, regulates an invasive growth pathway in breast cancer. Cell. 2003;113(2):207-19.
64. Hong W, Nakazawa M, Chen YY, Kori R, Vakoc CR, Rakowski C, et al. FOG-1 recruits the NuRD repressor complex to mediate transcriptional repression by GATA-1. Embo J. 2005;24(13):2367-78.
65. Gao Z, Huang Z, Olivey HE, Gurbuxani S, Crispino JD, Svensson EC. FOG-1-mediated recruitment of NuRD is required for cell lineage re-enforcement during haematopoiesis. Embo J. 2010;29(2):457-68.
66. Srinivasan R, Mager GM, Ward RM, Mayer J, Svaren J. NAB2 represses transcription by interacting with the CHD4 subunit of the nucleosome remodeling and deacetylase (NuRD) complex. J Biol Chem. 2006;281(22):15129-37.
67. Chudnovsky Y, Kim D, Zheng SY, Whyte WA, Bansal M, Bray MA, et al. ZFHX4 Interacts with the NuRD Core Member CHD4 and Regulates the Glioblastoma Tumor-Initiating Cell State. Cell Rep. 2014;6(2):313-24.
68. Curtis CD, Griffin CT. The Chromatin-Remodeling Enzymes BRG1 and CHD4 Antagonistically Regulate Vascular Wnt Signaling. Molecular and Cellular Biology. 2012;32(7):1312-20.
69. Hung H, Kohnken R, Svaren J. The Nucleosome Remodeling and Deacetylase Chromatin Remodeling (NuRD) Complex Is Required for Peripheral Nerve Myelination. J Neurosci. 2012;32(5):1517-27.
70. Sin C, Li HY, Crawford DA. Transcriptional Regulation by FOXP1, FOXP2, and FOXP4 Dimerization. J Mol Neurosci. 2015;55(2):437-48.
71. Shu WG, Lu MM, Zhang YZ, Tucker PW, Zhou DY, Morrisey EE. Foxp2 and Foxp1 cooperatively regulate lung and esophagus development. Development. 2007;134(10):1991-2000.
72. Shu WG, Yang HH, Zhang LL, Lu MM, Morrisey EE. Characterization of a new subfamily of winged-helix/forkhead (Fox) genes that are expressed in the lung and act as transcriptional repressors. Journal of Biological Chemistry. 2001;276(29):27488-97.
73. Yang Z, Hikosaka K, Sharkar MTK, Tamakoshi T, Chandra A, Wang B, et al. The mouse forkhead gene Foxp2 modulates expression of the lung genes. Life Sci. 2010;87(1-2):17-25.
74. Li SR, Wang Y, Zhang YZ, Lu MM, DeMayo FJ, Dekker JD, et al. Foxp1/4 control epithelial cell fate during lung development and regeneration through regulation of anterior gradient 2. Development. 2012;139(14):2500-9.
75. Kim CF, Jackson EL, Woolfenden AE, Lawrence S, Babar I, Vogel S, et al. Identification of bronchioalveolar stem cells in normal lung and lung cancer. Cell. 2005;121(6):823-35.
76. Mahoney JE, Mori M, Szymaniak AD, Varelas X, Cardoso WV. The hippo pathway effector Yap controls patterning and differentiation of airway epithelial progenitors. Dev Cell. 2014;30(2):137-50.
77. Lian I, Kim J, Okazawa H, Zhao J, Zhao B, Yu J, et al. The role of YAP transcription coactivator in regulating stem cell self-renewal and differentiation. Genes Dev. 2010;24(11):1106-18.
78. Cao X, Pfaff SL, Gage FH. YAP regulates neural progenitor cell number via the TEA domain transcription factor. Genes Dev. 2008;22(23):3320-34.
79. Chokas AL, Trivedi CM, Lu MM, Tucker PW, Li SR, Epstein JA, et al. Foxp1/2/4-NuRD Interactions Regulate Gene Expression and Epithelial Injury Response in the Lung via Regulation of Interleukin-6. Journal of Biological Chemistry. 2010;285(17):13304-13.
80. Baraldi E, Filippone M. Current concepts: Chronic lung disease after premature birth. New Engl J Med. 2007;357(19):1946-55.
81. Jobe AJ. The new BPD: an arrest of lung development. Pediatr Res. 1999;46(6):641-3.

82. Adamson IY, Bowden DH. The type 2 cell as progenitor of alveolar epithelial regeneration. A cytodynamic study in mice after exposure to oxygen. Lab Invest. 1974;30(1):35-42.
83. Evans MJ, Cabral LJ, Stephens RJ, Freeman G. Cell division of alveolar macrophages in rat lung following exposure to NO2. Am J Pathol. 1973;70(2):199-208.
84. Tufarelli C, Fujiwara Y, Zappulla DC, Neufeld EJ. Hair defects and pup loss in mice with targeted deletion of the first cut repeat domain of the Cux/CDP homeoprotein gene. Dev Biol. 1998;200(1):69-81.
85. Alcalay NI, Sharma M, Vassmer D, Chapman B, Paul B, Zhou J, et al. Acceleration of polycystic kidney disease progression in cpk mice carrying a deletion in the homeodomain protein Cux1. Am J Physiol Renal Physiol. 2008;295(6):F1725-34.
86. Sinclair AM, Lee JA, Goldstein A, Xing D, Liu S, Ju R, et al. Lymphoid apoptosis and myeloid hyperplasia in CCAAT displacement protein mutant mice. Blood. 2001;98(13):3658-67.
87. Luong MX, van der Meijden CM, Xing D, Hesselton R, Monuki ES, Jones SN, et al. Genetic ablation of the CDP/Cux protein C terminus results in hair cycle defects and reduced male fertility. Mol Cell Biol. 2002;22(5):1424-37.
88. Ellis T, Gambardella L, Horcher M, Tschanz S, Capol J, Bertram P, et al. The transcriptional repressor CDP (Cutl1) is essential for epithelial cell differentiation of the lung and the hair follicle. Gene Dev. 2001;15(17):2307-19.
89. Pitsouli C, Perrimon N. The homeobox transcription factor cut coordinates patterning and growth during Drosophila airway remodeling. Sci Signal. 2013;6(263):ra12.
90. Hagey DW, Muhr J. Sox2 Acts in a Dose-Dependent Fashion to Regulate Proliferation of Cortical Progenitors. Cell Rep. 2014;9(5):1908-20.
91. Sansregret L, Nepveu A. The multiple roles of CUX1: Insights from mouse models and cell-based assays. Gene. 2008;412(1-2):84-94.
92. Ramdzan ZM, Nepveu A. CUX1, a haploinsufficient tumour suppressor gene overexpressed in advanced cancers. Nat Rev Cancer. 2014;14(10):673-82.
93. Hashimoto S, Chen H, Que J, Brockway BL, Drake JA, Snyder JC, et al. beta-Catenin-SOX2 signaling regulates the fate of developing airway epithelium. J Cell Sci. 2012;125(Pt 4):932-42.
94. Vadnais C, Shooshtarizadeh P, Rajadurai CV, Lesurf R, Hulea L, Davoudi S, et al. Autocrine Activation of the Wnt/beta-Catenin Pathway by CUX1 and GLIS1 in Breast Cancers. Biol Open. 2014;3(10):937-46.
95. Lu Y, Futtner C, Rock JR, Xu X, Whitworth W, Hogan BLM, et al. Evidence That SOX2 Overexpression Is Oncogenic in the Lung. Plos One. 2010;5(6).
96. Leung EL, Fiscus RR, Tung JW, Tin VP, Cheng LC, Sihoe AD, et al. Non-small cell lung cancer cells expressing CD44 are enriched for stem cell-like properties. Plos One. 2010;5(11):e14062.
97. Rudin CM, Durinck S, Stawiski EW, Poirier JT, Modrusan Z, Shames DS, et al. Comprehensive genomic analysis identifies SOX2 as a frequently amplified gene in small-cell lung cancer. Nat Genet. 2012;44(10):1111-6.
98. Cai YR, Zhang HQ, Qu Y, Mu J, Zhao D, Zhou LJ, et al. Expression of MET and SOX2 genes in non-small cell lung carcinoma with EGFR mutation. Oncol Rep. 2011;26(4):877-85.
99. Cadieux C, Kedinger V, Yao L, Vadnais C, Drossos M, Paquet M, et al. Mouse Mammary Tumor Virus p75 and p110 CUX1 Transgenic Mice Develop Mammary Tumors of Various Histologic Types. Cancer Res. 2009;69(18):7188-97.
100. Shu W, Guttentag S, Wang Z, Andl T, Ballard P, Lu MM, et al. Wnt/beta-catenin signaling acts upstream of N-myc, BMP4, and FGF signaling to regulate proximal-distal patterning in the lung. Dev Biol. 2005;283(1):226-39.
101. Mucenski ML, Wert SE, Nation JM, Loudy DE, Huelsken J, Birchmeier W, et al. beta-Catenin is required for specification of proximal/distal cell fate during lung morphogenesis. J Biol Chem. 2003;278(41):40231-8.
102. Ye XX, Wu F, Wu CS, Wang P, Jung KR, Gopal K, et al. beta-Catenin, a Sox2 binding partner, regulates the DNA binding and transcriptional activity of Sox2 in breast cancer cells. Cell Signal. 2014;26(3):492-501.
103. Gao X, Vockley CM, Pauli F, Newberry KM, Xue Y, Randell SH, et al. Evidence for multiple roles for grainyheadlike 2 in the establishment and maintenance of human mucociliary airway epithelium. P Natl Acad Sci USA. 2013;110(23):9356-61.
104. Mehrazarin S, Chen W, Oh JE, Liu ZX, Kang KL, Yi JK, et al. The p63 Gene Is Regulated by Grainyhead-like 2 (GRHL2) through Reciprocal Feedback and Determines the Epithelial Phenotype in Human Keratinocytes. Journal of Biological Chemistry. 2015;290(32):19999-20008.

Chapter 8.
Summary/Samenvatting

Summary

Sry-related HMG box 2 (SOX2) is a member of the SOX family of transcription factors. SOX genes are highly conserved across species and are dynamically expressed during embryogenesis. The expression of SOX2 is spatially and temporally regulated during development and involved in the morphogenesis of several organs, including the brain, eyes and lung. During the embryonic phase of lung development, Sox2 expression is restricted to the epithelial cells of the foregut. Expression remains restricted to the epithelial cells of the non-branching airways during the canalicular and saccular phase and after birth Sox2 is exclusively expressed in the epithelium of the conducting airways. We and other groups have shown that Sox2 is required for proper branching morphogenesis of the lung and for differentiation of lung epithelial. Gene ablation of sox2 specifically in the early foregut results in shortening of the trachea and abnormal cell differentiation with an increase in secretory cells at the expense of basal, Club and ciliated cells. On the other hand, conditional overexpression of Sox2 in virtually all epithelial cells of the developing lung results in the formation of cyst-like structures with increased numbers of basal cells and neuroendocrine cells, also in the distal part of the lung.

In chapter 2, we first studied the effects of timed Sox2 expression on these cyst-like structures during lung development. This showed that ectopic Sox2 results in variable cyst sizes, depending on the duration of ectopic Sox2 expression. We also detected the emergence of basal cells in the respiratory epithelium after Sox2 expression, characterized by the expression of Trp63 which is a master regulator of basal cells. We showed that Sox2 directly binds to the ΔN Trp63 promoter region and activates its transcription, indicating that Sox2 directly regulates the basal cell specific ΔN Trp63. Besides an increase of Trp63 after ectopic Sox2 expression, we also detected an increase of Gata6 expression, which is involved in the emergence of bronchoalveolar stem cells (BASCs). We also showed that Sox2 directly regulates Gata6 transcription. Collectively, our data showed that ectopic Sox2 expression leads to differentiation into proximal epithelial cell types and induced proliferation, resulting in the development of cyst-like structures in the lung. Moreover, we showed that Sox2 may be a master regulator of two important genes involved in the formation of two progenitor cells in the lung, the basal cells and the BASCs.

In chapter 3, we describe that the expression of a single gene, Sox2, can induce transdifferentiation. Induced expression of Sox2 in alveolar type II cells resulted in the gradual dedifferentiation and subsequent differentiation of this distal cell type into proximal cells. The cellular changes induced by ectopic expression of Sox2 in fully differentiated alveolar type II (AT-II) cells *in vivo* also induced an emphysema-like phenotype with enlarged airspaces and destruction of the alveolar architecture. Expression of Sox2 in AT-II cells both *in vivo* and *in vitro* resulted in an increase of proliferation markers phosphohistone H3 and cyclin D1, showing that Sox2 induces proliferation in these cells. We also detected expression of Sca1 and Ssea1, both markers for progenitor cells, suggesting that dedifferentiation of the AT-II cells occurs through an intermediate progenitor cell type. Furthermore, the cells started to express Trp63 and Cc10, markers for basal cells and Club cells which are both proximal epithelial cells. These Cc10 positive cells also expressed Spc, a AT-II marker, which indicated the emergence of BASCs. Our data showed that Sox2 can change cell fate of fully differentiated AT-II cells, which could be useful for implications in regenerative medicine.

The transcriptional activity of Sox2 always depends on its interaction with other proteins. To gain more insight in the role of Sox2 during lung development, we therefore wanted to identify specific partners during lung development. In chapter 4 we describe the generation of the bioSox2/birA mouse model that we used for this purpose. This model contains a biotin-tagged Sox2 allele, which can be biotinylated by the bacterial birA ligase, resulting in a fully functional bioSox2 protein. BioSox2 protein complexes were isolated from embryonic day 18 lung and brain tissue using streptavidin in a single-step approach followed by MALDI-ToF mass spectrometry. We isolated and identified multiple putative partners, and several of these proteins had been described to be involved in respiratory functions. To validate our procedure, we used two proteins, Wdr5, a known Sox2 partner, and Tcf3, which was not a validated partner protein yet. Subsequent ChIP-seq analysis to identify Sox2 specific target genes revealed a number of potential interesting genes, such as β-catenin and Grhl2 that could be linked to lung and respiratory tube development. Identification of these partners and target genes could provide us more insight in the molecular pathways involved in lung development.

In chapter 5, we further analyzed several of the interaction partners of Sox2 in the developing lung identified with the screen described in chapter 4. Putative partners we identified were Chromodomain Helicase DNA-binding protein 4 (Chd4), Forkhead box transcription factors FoxP2 and FoxP4 and Cut-Like Homeobox1 (Cux1). We examined the expression pattern of these partners and detected co-localization of Sox2 with Chd4 during the saccular phase of lung development and co-localization of Sox2 and Cux1 during the canalicular and saccular phase. FoxP2 and Sox2 only showed co-localization in cells located at the bronchioalveolar duct junction during the embryonic and early pseudoglandular phase, suggesting a role for the Sox2-FoxP2 partner complex in these cells. Co-immunoprecipitations showed interaction of Sox2 with FoxP2, FoxP4, Chd4 and Cux1, although interaction with Chd4 did not seem to be a direct binding. We also showed that the level of Sox2 expression influenced the formation of Cux1 isoforms and it appeared that high extends of Sox2 expression prevents this formation. ChIP data indicated that that Sox2 and Chd4 could be involved in co-regulation of genes, such as Jag1 and Id2 involved in the respiratory system. These partners could provide more insight in the molecular pathways involved in lung development and congenital lung disease.

In chapter 6 we review the different populations of stem cells and progenitor cells in the lung and the plasticity of different lung cell types. By using new techniques such as lineage-tracing experiments, knowledge behind the mechanisms of cell differentiation an plasticity is increasing. This knowledge could be used in regenerative medicine and the generation of lung mimics such as organoids and lung-on-a-chip.

In chapter 7, our findings were discussed in a broader perspective and in chapter 8 we summarize our findings.

In conclusion, we showed that Sox2 directly regulates genes involved in differentiation of the proximal airway epithelium. Furthermore, we showed that Sox2 has the ability to dedifferentiate fully differentiated AT-II cells into cells with a proximal cell fate. These findings could be used in regenerative medicine and therapies for lung disease. We also identified several Sox2 interaction partners which gives more insight in the molecular pathways behind lung development.

Samenvatting

Sry-related HMG box 2 (Sox2) behoort tot de SOX familie van transcriptiefactoren. Deze genen zijn goed geconserveerd in de evolutie en worden tijdens de embryogenese dynamisch tot expressie gebracht. Tijdens de embryonale ontwikkeling is de expressie van SOX2 afhankelijk van tijd en plaats. SOX2 is betrokken bij de vorming van verschillende organen waaronder de hersenen, ogen en longen. Tijdens de longontwikkeling komt Sox2 enkel tot expressie in de niet vertakte, proximale delen van de luchtwegen. Wij en andere groepen hebben aangetoond dat Sox2 essentieel is voor een normaal vertakkingsproces van de longen en voor de differentiatie van het longepitheel. Wanneer Sox2 expressie wordt verwijderd in een vroeg stadium van de longontwikkeling, resulteert dit in een verkorte trachea en abnormale differentiatie van het longepitheel. Wanneer Sox2 tot expressie wordt gebracht in de distale epitheelcellen van de long, dan resulteert dit in de vorming van cyste-achtige structuren waarbij er een verhoogd aantal basale cellen en neuro-endocrine cellen worden gevonden.

In hoofdstuk 2 beschrijven we de effecten van de duur van de expressie van Sox2 in het distale epitheel van de long op de vorming van deze cyste-achtige structuren. Hieruit bleek dat er een correlatie is tussen de duur van Sox2 expressie en het tijdspunt waarop Sox2 tot expressie gebracht wordt en de grootte van de cystes. Ook zagen we basale cellen in het distale epitheel, gekenmerkt door de expressie van Trp63, een belangrijke regulator van basale cellen. We hebben aangetoond dat Sox2 rechtstreeks kan binden aan de ΔN Trp63 promoter, en hierdoor direct de transcriptie van ΔN Trp63 kan activeren. Behalve een verhoogde expressie van Trp63, hebben we ook een verhoogde expressie van Gata6 gevonden, wat wijst op inductie van bronchoalveolaire stamcellen. We hebben laten zien dat de transcriptie van Gata6 ook rechtstreeks gereguleerd kan worden door Sox2. Afwijkende Sox2 expressie leidt tot differentiatie van proximale celtypes en proliferatie, wat leidt tot vorming van cyste-achtige structuren. Ook hebben we aangetoond dat Sox2 de transcriptie van twee belangrijke genen betrokken bij de vorming van basale cellen en bronchioalveolaire stamcellen direct kan reguleren.

In hoofdstuk 3 beschrijven we dat expressie van Sox2 kan leiden tot transdifferentiatie van volledig gedifferentieerde alveolaire type II (AT-II) cellen. Zowel *in vivo* als *in vitro* zagen we een verhoogde expressie van de proliferatiemarkers phospho-histon H3 en cycline D1, wat aantoont dat proliferatie van deze cellen geïnduceerd wordt door Sox2. Ook zagen we expressie van Sca1 en Ssea1, beide stamcelachtige markers, hetgeen aantoont dat dedifferentiatie van AT-II cellen via een intermediair cel type gebeurt. De cellen beginnen ook Trp63 en Cc10 tot expressie te brengen, wat markers zijn voor basale cellen en Club cellen, beide proximale epitheelcellen. De cellen die Cc10 tot expressie brengen, brengen daarnaast ook Spc tot expressie, een AT-II marker, wat duidt op het ontstaan van bronchioalveolaire stamcellen. Met andere woorden, Sox2 kan volledig gedifferentieerde AT-II cellen transdifferentiëren, wat gebruikt zou kan worden voor regeneratieve therapie.

De transcriptionele activiteit van Sox2 is afhankelijk van interactie met andere factoren en om meer inzicht te krijgen in de rol van Sox2 tijdens de longontwikkeling, hadden we als doel de specifieke partners tijdens de longontwikkeling te identificeren. In hoofdstuk 4 beschrijven we het bioSox2/birA muismodel. Dit model bevat een Sox2 allel met daaraan aan korte peptide, een biotin-tag, die gebiotinyleerd kan worden door de bacteriële birA

ligase. Dit resulteert in een volledig functioneel bioSox2 eiwit dat we met streptavidine geïsoleerd hebben uit extracten van embryonaal 18 dagen oud long- en hersenweefsel en vervolgens geanalyseerd hebben met MALDI-ToF massa spectrometrie. We hebben verschillende partners geïdentificeerd waarvan bekend is dat ze een rol spelen in de luchtwegen. Om onze resultaten te valideren, hebben we twee eiwitten gebruikt, Wdr5, waarvan interactie met Sox2 bekend is, en Tcf3, waarvan interactie nog niet gevalideerd was. Om genen te identificeren die door Sox2 gereguleerd worden, hebben we ChIP-seq analyse uitgevoerd. Hierbij kwamen enkele interessante genen naar voren, waaronder β-catenin en Grhl2, die ook betrokken zijn bij longontwikkeling. Het identificeren van partners en genen die door Sox2 gereguleerd worden, kan meer inzicht geven in de moleculaire mechanismen van de longontwikkeling.

In hoofdstuk 5 zijn we verder gegaan met de analyse van enkele van de geïdentificeerde Sox2 partners, namelijk Chromodomain Helicase DNA-binding protein 4 (Chd4), Forkhead box transcription factors FoxP2 en FoxP4 en Cut-Like Homeobox1 (Cux1). We hebben het expressiepatroon van deze partners onderzocht en co-lokalisatie van Chd4 en Sox2 gedetecteerd gedurende de sacculaire fase van de longontwikkeling en co-lokalisatie tussen Cux1 en Sox2 gedurende de canaliculaire en sacculaire fase. Gedurende de embryonale en vroege pseudoglandulaire fase, zagen we ook co-lokalisatie van FoxP2 en Sox2 in de cellen in het bronchioalveolaire verbindingsgebied, wat zou kunnen betekenen dat het FoxP2-Sox2 complex een rol speelt in deze cellen. Met behulp van co-immunoprecipitaties hebben we de interacties tussen Chd4, FoP2, FoxP4 en Cux1 met Sox2 gevalideerd. Verder zagen we ook dat het niveau van Sox2 expressie van invloed is op de vorming van Cux1 isovormen en het lijkt dat een hogere expressie van Sox2 deze vorming remt. ChIP data heeft aangetoond dat Sox2 en Chd4 een overlap hebben in de genen die ze reguleren, waaronder Jag1 en Id2, beiden betrokken bij de longontwikkeling. Verder onderzoek naar deze partners kan meer inzicht geven in de moleculaire processen die een rol spelen in de ontwikkeling van de longen en het ontstaan van aangeboren longafwijkingen.

In hoofdstuk 6 geven we een overzicht van de verschillende stam cellen en voorloper cellen in de long en de plasticiteit van de verschillende celtypes in de long. Het gebruik van nieuwe technieken, zorgt voor stijgende kennis op het gebied van cel differentiatie en cel plasticiteit. Deze kennis kan gebruikt worden voor regeneratieve therapieën en voor het ontwikkelen van systemen als organoide kweekjes en long-op-een-chip.

In hoofdstuk 7 worden onze bevindingen bediscussieerd in een breder perspectief en in hoofdstuk 8 geven we een samenvatting van onze bevindingen.

Samenvattend hebben we aangetoond dat Sox2 rechtstreeks genen kan reguleren die betrokken zijn bij de differentiatie van het proximale longepitheel en dat Sox2 kan zorgen voor dedifferentiatie van volledig gedifferentieerde AT-II cellen. Deze bevindingen kunnen mogelijk gebruikt worden voor de behandeling van longziekten. Ook hebben we een aantal partners van Sox2 geïdentificeerd in de long, wat meer inzicht geeft in de moleculaire mechanismen die betrokken zijn bij de ontwikkeling van de longen.

Appendices

Curriculum Vitae
List of Publications
PhD Portfolio
Dankwoord

Curriculum Vitae

Personal information

Name: Kim Albertina Adriana Schilders
Date of birth: January 30, 1984
Place of birth: Hoogeloon, Hapert en Casteren, the Netherlands

Education

2002 – 2011 Biomedical Engineering
Technical University of Eindhoven, the Netherlands

1996 – 2002 VWO
Pius X College Bladel, the Netherlands

Research

2011 – 2015 PhD research
Department of Pediatric Surgery/Cell Biology, Erasmus MC, Rotterdam, the Netherlands
(Prof.dr. D. Tibboel and Dr. R.J. Rottier)

2010 – 2011 Internship
Department of experimental therapy, The Netherlands Cancer Institute – Antoni van Leeuwenhoek, Amsterdam, the Netherlands
(Prof.dr. J.H.M. Schellens and Dick Pluim, BSc)

2009 – 2010 Master thesis project
Molecular Biology, Catharina Hospital, Eindhoven, the Netherlands
(Dr. B.A.L.M. Deiman)

2008 Internship
Clinical Laboratory, Maxima Medical Center Veldhoven/ Eindhoven, the Netherlands
(Prof.dr. Ir. H.L. Vader)

List of publications

Kim A.A. Schilders, Evelien Eenjes, Sander van Riet, André A. Poot, Dimitrios Stamatialis, Roman Truckenmüller, Pieter S. Hiemstra and Robbert J. Rottier; *Regeneration of the lung: Lung stem cells and the development of lung mimicking devices;* Respiratory Research 2016; 17:44

Kim Schilders, Joshua K. Ochieng, Cornelis P van de Ven, Cristina Gontan, Dick Tibboel, Robbert J. Rottier; *Role of SOX2 in foregut development in relation to congenital abnormalities*; World Journal of Medical Genetics 2014; 4(4)

Joshua Kapere Ochieng, **Kim Schilders**, Heleen Kool, Marjon Buscop-van Kempen, Anne Boerema-De Munck, Frank Grosveld, Rene Wijnen, Dick Tibboel, Robbert J Rottier; *Differentiated Type II Pneumocytes Can Be Reprogrammed by Ectopic Sox2 Expression*; PLoS ONE 2014; 9(9)

Joshua K Ochieng, **Kim Schilders**, Heleen Kool, Anne Boerema-de Munck, Marjon Buscop-van Kempen, Cristina Gontan, Ron Smits, Frank G Grosveld, Rene Mh Wijnen, Dick Tibboel, Robbert J Rottier; *SOX2 REGULATES THE EMERGENCE OF LUNG BASAL CELLS BY DIRECTLY ACTIVATING THE TRANSCRIPTION OF TRP63*; American Journal of Respiratory Cell and Molecular Biology 2014; 51(2)

Dick Pluim, **Kim A A Schilders**, Bart A W Jacobs, Daniëlle Vaartjes, Jos H Beijnen, Jan H M Schellens; *Pharmacodynamic assay of thymidylate synthase activity in peripheral blood mononuclear cells*; Analytical and Bioanalytical Chemistry 2013; 405(8)

Erasmus MC
Universitair Medisch Centrum Rotterdam

PhD Portfolio

Summary of PhD training and teaching

Name PhD student: Kim Albertina Adriana Schilders Erasmus MC Department: Pediatric Surgery/Cell Biology Research School: Medical Genetics Center (MGC)	PhD period: August 2011 – December 2015 Promotor(s): Prof. Dr. Dick Tibboel Supervisor: Dr. Robbert Rottier

1. PhD training	
	Year
General courses	
- Safety working at the Laboratory	2011
- Biochemistry and Biophysics	2011
- Laboratory animal science	2012
- Genetics	2012
- Cell and Developmental Biology	2013
- Biostatistical methods I: Basic Principles Part A	2014
- Biomedical English Writing	2015
Specific courses (e.g. Research school, Medical Training)	
- Literature course	2012
- Technology Facilities	2012
Seminars and workshops	
- 18th MCG PhD workshop, Dusseldorf, Germany	2012
- 19th MGC PhD workshop, Luxembourg, Luxembourg **Poster presentation**	2013
- Sophia Onderzoeksdag **Poster presentation**	2013
- NRS symposium, Utrecht, the Netherlands	2011, 2013
- MGC symposium	2012, 2013, 2014
- NRS 6th Young Investigator Symposium, Amsterdam, the Netherlands **Oral presentation**	2014
- Longdagen	2015
Presentations	
- Monday Morning Meeting	2011-2015
- Work discussions (Dr. Rottiers' group)	2011-2015
- Literature discussions	2011-2015
(Inter)national conferences	
- ERS Lung Science Conference, Estoril, Portugal **Oral presentation**	2013
- International CDH workshop, Rotterdam, the Netherlands **Oral Presentation**	2013
- 26th International Symposium on Paediatric Surgical Research, Cape Town, South Africa **Oral presentation**	2013
- Gordon Research Seminar on Lung Development, Injury & Repair, Andover NH, United States **Poster presentation**	2015

2. Teaching	
	Year
Supervising students	
- Student supervision (Bianca Oresta)	2013-2014
- Student supervision (Sheren Elizabeth)	2015
- Student supervision (Francesca Triani)	2015
- Student supervision (Judith Birckhoff)	2015

Dankwoord

Na bijna vijf jaar is het nu tijd om mijn periode als PhD student af te ronden. Ik had dit niet kunnen doen zonder de hulp en steun van de mensen om mij heen.

Allereerst wil ik mijn promoter prof.dr. Dick Tibboel bedanken. Beste professor Tibboel, bedankt dat u me de kans hebt gegeven om mijn promotieonderzoek te doen bij de afdeling kinderchirurgie. Bedankt voor uw interesse en suggesties en uw hulp bij het afronden van mijn onderzoek.

Verder wil ik mijn co-promoter en supervisor dr. Robbert Rottier bedanken. Beste Robbert, bedankt voor alle adviezen en steun tijdens mijn promotieonderzoek, en voor de fijne sfeer op het lab. Je was altijd beschikbaar om mijn vragen te beantwoorden en om te helpen daar waar het nodig was. Mede hierdoor kan ik terugkijken op een erg leerzame en leuke periode.

Dank aan dr. Annelies de Klein, dr. Raymond Poot en dr. Machteld Hylkema voor het lezen en beoordelen van mijn proefschrift. Raymond, ook hartelijk dank voor je input en suggesties die je gegeven hebt op de momenten dat wij even vastliepen met onze experimenten. Verder dank aan dr. Niels Galjart, prof.dr. Danny Huylebroeck en prof.dr. Irwin Reiss voor het deelnemen in de grote promotiecommissie.

Beste prof.dr. René Wijnen, bedankt voor je interesse in mijn onderzoek en natuurlijk voor de leuke tijd in Kaapstad. Beste prof.dr. Frank Grosveld, bedankt voor je adviezen tijdens de (altijd erg gezellige) donderdag meetings.

Thanks to all colleagues and former colleagues of lab 1034: Anne, Marjon, Heleen, Evelien, Daphne, Petra, Mieke, Bob, Marta, Joshua, Yadi, Lalini and Ilona. Anne en Marjon, bedankt voor jullie hulp en inzet bij het afronden van mijn experimenten. Daphne en Heleen, succes met het afronden van jullie promotieonderzoek. Evelien, bedankt dat je mijn paranimf wilt zijn. Het was fijn om met je samen te werken en ik wens je veel succes met het afronden van je onderzoek. Lieve Mieke, we zijn ongeveer rond dezelfde tijd op het lab gekomen en het klikte eigenlijk meteen. Bedankt voor je steun de afgelopen 4 jaar, ik ben blij dat je mijn paranimf wilt zijn. Ik weet zeker dat we elkaar nog regelmatig zullen zien!

During my project I supervised several students and I would especially like to thank Bianca and Judith for their commitment. Dear Bianca, thanks for your hard work on the lab and all the stainings that you performed. I wish you all the best for the future. Beste Judith, bedankt voor je inzet en harde werk en alle experimenten die je nog voor me gedaan hebt toen ik druk bezig was met schrijven. De resultaten waren soms wat frustrerend maar je bleef volhouden en uiteindelijk is het allemaal goed gekomen. Heel veel succes met het afronden van je studie en ik weet zeker dat je een hele goede PhD student zal zijn.

Thanks to all colleagues and former colleagues from the department of Cell biology who I met during the lat few years. Thanks for the fun and support. Guillaume, thanks for your help with the ChIP protocol. Petros, thanks for your help with analyzing the ChIP-seq data. Ook hartelijk dank aan de secretaresses, de mensen van de inkoopafdeling, de dames van de spoelkeuken en de IT afdeling. Veel dank ook aan de mensen van de afdelingen

Proteomics en Biomics voor de analyse van de large scale IPs en ChIPs.

Danny, you always showed interest in my research and personal life when we ran into each other. I wish you all the best for the future, good luck with finishing your PhD! Erwin, bedankt voor je input tijdens de werk- en literatuurbesprekingen. Het was altijd weer gezellig om je tegen te komen.

Alle mensen van Scouting Oud Best en dan met name de gidsen, heel erg bedankt voor alle gezellige zaterdagen de afgelopen vier jaar. Het was fijn om die ene middag in de week even niet met mijn onderzoek bezig te zijn.

Lieve Bastiaan, Maarten, Yvette, Moniek, Monique, Marloes, Jeroen, Mark, Joris en Rob, we hebben elkaar niet heel veel gezien de afgelopen jaren maar als we elkaar zagen was het altijd meteen weer erg gezellig als vanouds. Bedankt voor jullie begrip als ik weer eens een afspraak moest afzeggen vanwege werk of een deadline.

Natuurlijk ook heel veel dank aan mijn (schoon)familie en hun steun en begrip. Lieve Evert en Pauline, bedankt dat jullie altijd klaar staan om ons te helpen als dat nodig is.

Lieve Ruud, Agata en natuurlijk Bryan, het is een drukke periode geweest maar gelukkig was er toch altijd tijd om even af te spreken. Bedankt dat jullie altijd voor me klaar staan!

Lieve papa en mama, bedankt voor alles wat jullie voor me gedaan hebben. Jullie staan altijd voor me klaar en zonder jullie steun had ik dit niet gekund. Voor jullie was het ook niet altijd makkelijk maar gelukkig zit het er nu op. Bedankt voor alles, ik hou van jullie.

Lieve Sebastiaan, bedankt voor al je liefde en steun tijdens de afgelopen jaren, zonder jou had ik het niet gekund. Het was niet altijd makkelijk maar samen hebben we ons er doorheen geslagen. Gelukkig hebben we nu weer wat meer tijd voor ons samen en vanaf november natuurlijk voor ons drietjes. Ik hou van je.

Kim